
Energy Efficiency and Interference Management in Long Term Evolution-Advanced Networks

PhD Thesis

Armeline Dembo Mafuta

A thesis submitted in fulfilment of the requirement for the
degree of

**DOCTOR OF PHILOSOPHY IN ENGINEERING
(ELECTRONIC)**



School of Electrical, Electronic & Computer Engineering

Durban

South Africa

Thesis submitted March, 2019

As the candidate's supervisor, I have approved this thesis for submission.

Signed.....Date.....

Name: Dr. Tom Mmbasu Walingo

Declaration 1 - Plagiarism

I, **Armeline Dembo Mafuta**, declare that;

1. The research reported in this thesis, except where otherwise indicated, is my original research.
2. This thesis has not been submitted for any degree or examination at any other university.
3. This thesis does not contain other persons' data, pictures, graphs or other information, unless specifically acknowledged as being sourced from other persons.
4. This thesis does not contain other persons' writing, unless specifically acknowledged as being sourced from other researchers. Where other written sources have been quoted, then:
 - (a) Their words have been re-written but the general information attributed to them has been referenced,
 - (b) Where their exact words have been used, then their writing has been placed in italics and inside quotation marks, and referenced.
5. This thesis does not contain text, graphics or tables copied and pasted from the Internet, unless specifically acknowledged, and the source being detailed in the thesis and in the references sections.

Signed.....Date.....

Declaration 2 - Publication

The following journal papers emanating from this work have been published or are under review:

1. **Armeline Dembo Mafuta, Tom Walingo and Telex M.N. Ngatched**, "Energy Efficient Coverage Extension Relay Node Placement in LTE-A Networks", *IEEE Communications Letters*, April, 2017, pp.1617 - 1620.
2. **Armeline Dembo Mafuta, Tom Walingo and Fambirai Takawira**, "Interference Management in LTE-Advanced Cooperative Relay Networks: Decentralized Transceiver Design with Channel Estimation", *IEEE Transaction on wireless communications*, 2018 (*Under review*).
3. **Armeline Dembo Mafuta, Tom Walingo and Fambirai Takawira**, "Energy Efficient Transceiver Design for Cooperative Multi-User MIMO Systems", *IEEE Transactions on Communications Journal*, 2018, (*Under review*)

The following conference papers were published during the doctoral research:

1. **Armeline Dembo Mafuta and Tom Walingo**, "Interference Alignment for Transceiver Design in Multi-User MIMO Relay System", in *Proc. 88th IEEE Vehicular Technology Conference (VTC Fall)*, August 2018, Chicago, USA.
2. **Armeline Dembo Mafuta and Tom Walingo**, "Power Consumption Minimization in the Downlink MU-MIMO Systems with Optimal and Heuristic Linear Pre-coding techniques", in *Proc. SATNAC Conference*, Barcelona, Spain, 3 - 10 September, 2017.
3. **Armeline Dembo Mafuta and Tom Walingo**, "Spatial Relay Node Placement in Wireless Sensor Networks", in *Proc. 83rd IEEE Vehicular Technology Conference (VTC Spring)*, July 2016, Nanjing, China
4. **Armeline Dembo Mafuta and Tom Walingo**, "Comparison of Multi-User Interference Cancellation Techniques on LTE Femtocell networks", in *Proc. of SATNAC 2015 Conference*, Hermanus, South Africa, 6 – 9 September 2015.

Dedication

Above all, I thank the almighty God for his love, blessing and protection. To my future *husband and children*, I pray that one day we will all enjoy the product of this hard work.

Acknowledgements

Firstly, I wish to express my most sincere gratitude to Dr. Tom Walingo for his supervision and for believing in me even when I thought I was in my doldrums, thank you for your encouragement and support. Secondly, I would like to thank Prof. Fambirai Takawira, Prof. Telex M.N. Ngatched and Prof. Jules-Raymond Tapamo for their support throughout my doctorate degree.

To my parent, Arthur and Petronnelle Mafuta, all the words in the world could not express the tremendous love I have for you and the deep gratitude that I testify to you for all the sacrifices and efforts you have never ceased to consent for my well-being, health and education. It is through your support that I opted for this noble study and it is through your criticism that I have been able to make it. By this modest work, I am showing you my eternal gratitude and infinite love. To my brothers and sisters, despite the distance, you have always been a great support during this long journey. I thank you for your encouragement and sincere affection. I acknowledge you all in this work and I wish you my best wishes for success, health and happiness. To all my aunts, uncles, cousins and entire family, you have been a real support in my education especially in my life. By this work, I thank you for being there throughout my life and my studies. To my grandmothers, I acknowledge you in this work. In the memory of my grandfathers, any dedication could explain the love and respect I always had for you. This work is the results of your support and advice invested in my education and training. I wish that you shall see the rewards of your efforts.

To all my friends, you have been my joy and confidence when I needed the most. You were the best advisers and friends during this achievement. Through this work, receive my sincere gratitude. I cannot forget Assionvi Hove Kouevi, you have always been there since the beginning of this challenge. Without your love, encouragement and advices, this work could not be achieved. Find in this work, a testimony of my deep affection and sincere gratitude. To my pastors Timothee and Joelle Kabasele, pastor Serge and Tanya Kambanga, my church (A.E.N.A), winners chapel Durban, your prayers and faith upon me helped me achieve this research. Thank you.

To all who participated from near or far, all my students, colleagues and staff at University of KwaZulu-Natal (UKZN). By this great achievement which is my Ph.D. work, I strongly thank you.

Contents

| | |
|--|-------------|
| Declaration 1 - Plagiarism | ii |
| Declaration 2 - Publication | iii |
| Dedication | iv |
| Acknowledgements | v |
| List of Figures | x |
| List of Tables | xii |
| List of Acronyms | xiii |
| Abstract | xix |
| Preface | xxi |
| | |
| I Introduction | 1 |
| | |
| Introduction and Research Background | 2 |
| 1 Mobile Network Evolution | 2 |
| 2 Long Term Evolution-Advanced Standard | 4 |
| 2.1 LTE and LTE-Advanced | 4 |
| 2.2 LTE-Advanced Architecture | 5 |
| 2.3 LTE-Advanced Multiple Access Schemes | 7 |
| 3 Features of the LTE-Advanced network | 9 |
| 3.1 Enhanced Multi-Antenna Support | 9 |
| 3.1.1 SU-MIMO System | 10 |
| 3.1.2 Cooperative-MIMO System | 10 |

| | | |
|-------|--|----|
| 3.1.3 | MU-MIMO System | 11 |
| 3.2 | Macrocell and Small-cells Networks | 12 |
| 3.2.1 | Macrocell Networks | 14 |
| 3.2.2 | Microcell Networks | 14 |
| 3.2.3 | Picocell Networks | 15 |
| 3.2.4 | Femtocell Networks | 15 |
| 3.3 | Cooperative Relaying Communication | 17 |
| 4 | Challenges of LTE-Advanced System and Mitigation Approaches | 18 |
| 4.1 | Challenges Description | 18 |
| 4.1.1 | Effective Coverage Extension in LTE-Advanced Network | 18 |
| 4.1.2 | Interference Challenge and Mitigation Approaches | 19 |
| 4.1.3 | Energy Efficiency in LTE-Advanced Network | 24 |
| 4.2 | Approaches to Manage the LTE-Advanced Challenges | 26 |
| 4.2.1 | Optimal and Energy Efficient RNs Placement with Greedy Algorithm | 26 |
| 4.2.2 | Pre-coding and Decoding Design | 27 |
| 4.2.3 | Pilot-Assisted Channel Estimation | 28 |
| 5 | Research Motivation | 29 |
| 6 | Objectives of the Research | 30 |
| 7 | Research Methodology: Analytical Tools | 31 |
| 7.1 | Sub-modularity, Monotonicity Optimisation and Matroid | 31 |
| 7.1.1 | Sub-modularity and Monotonicity | 32 |
| 7.1.2 | Matroid | 32 |
| 7.2 | Convex Optimisation | 33 |
| 7.3 | Lagrange Duality | 33 |
| 7.3.1 | Lagrange Multiplier | 34 |
| 7.3.2 | Karush-Kuhn-Tucker | 34 |
| 8 | Main Contributions | 35 |
| 8.1 | PAPER A: Energy Efficient Coverage Extension Relay Node Placement in LTE-A Networks | 35 |
| 8.2 | PAPER B: Interference Management in LTE-Advanced Cooperative Relay Networks: Decentralized Transceiver Design with Channel Estimation | 35 |
| 8.3 | PAPER C: Energy Efficient Transceiver Design for Cooperative Multi-User MIMO Systems | 36 |
| | References | 37 |

| | | |
|-----------|---|-----------|
| II | Papers | 47 |
| A | Energy Efficient Coverage Extension Relay Node Placement in LTE-A Networks | 48 |
| 1 | Introduction and Related Works | 49 |
| 2 | System Model and Problem Formulation | 50 |
| 3 | Network Coverage with Energy Efficient and Optimal RN Placement | 52 |
| 3.1 | Sub-modularity, monotonicity optimisation and matroid | 52 |
| 3.2 | The Energy Efficient and Optimal RN Placement (EEORNP) Algorithm | 54 |
| 4 | Performance Evaluation | 56 |
| 5 | Conclusion | 59 |
| | References | 60 |
| B | Interference Management in LTE-Advanced Cooperative Relay Networks: Decentralized Transceiver Design with Channel Estimation | 62 |
| 1 | Introduction | 63 |
| 1.1 | Related Research | 65 |
| 1.2 | Main Contributions | 66 |
| 1.3 | Organisation and Notations | 67 |
| 2 | System Model and Problem Formulation | 68 |
| 2.1 | The Network Architecture | 68 |
| 2.2 | Uplink Training and Channel Estimation | 69 |
| 2.2.1 | LS Channel Estimator | 70 |
| 2.2.2 | MMSE Channel Estimator | 71 |
| 2.3 | Uplink Transmission Design | 71 |
| 3 | Decentralised Algorithms for Linear Transceiver Designs | 75 |
| 3.1 | Coordinated MMSE Approach for Femtocell and MUEs Pre-coders and Decoders during the First Time Slot | 75 |
| 3.1.1 | Optimisation of the FAPs Pre-coding and Decoding Vectors | 75 |
| 3.1.2 | Optimisation of the MUEs pre-coding and decoding matrices | 78 |
| 3.2 | Coordinated MMSE approach for UEs (CUEs and MUEs) during the second time slot | 80 |
| 3.2.1 | Design of the RN pre-coding matrix | 82 |
| 3.2.2 | Design of the pre-coding and decoding matrices | 83 |
| 4 | Performance Evaluation | 85 |
| 5 | Conclusion | 95 |

| | |
|---|------------|
| References | 96 |
| C Energy Efficient Transceiver Design for Cooperative Multi-User MIMO Systems | 99 |
| 1 Introduction and Related Works | 100 |
| 2 System Model | 103 |
| 2.1 Network architecture | 103 |
| 2.2 The total power consumption design | 110 |
| 3 EE Maximisation and Transceiver Optimisation for FUEs and MUEs | 111 |
| 3.1 EE problem formulation for FUEs and MUEs | 111 |
| 3.2 Optimisation of the pre-coders $\mathbf{w}_{j,i}^{\text{FAP}}$, $\mathbf{w}_{o,m}^{\text{MUE}}$ and decoders $\mathbf{d}_{j,i}^{\text{FAP}}$, $\mathbf{d}_{o,m}^{\text{MUE}}$ | 112 |
| 3.3 EE Maximisation Algorithms | 118 |
| 4 EE Maximisation and Transceiver Optimisation for CUEs through RN and MUEs during the second time slot | 119 |
| 4.1 EE problem formulation for UEs | 120 |
| 4.2 Optimisation of RN pre-coder and Receiver decoder | 121 |
| 4.3 EE Maximisation Algorithm for the UEs | 125 |
| 5 Performance Evaluation | 126 |
| 6 Conclusion | 130 |
| References | 131 |
| | |
| III Thesis Conclusion | 135 |
| | |
| Conclusion and Future Works | 136 |
| 1 Summary of the Research Contributions | 136 |
| 2 Future Works | 137 |

List of Figures

| | | |
|-----|--|----|
| 1 | Network architecture of LTE/LTE-Advanced systems [12] | 6 |
| 2 | Block diagram of OFDMA | 8 |
| 3 | Block diagram of SC-FDMA | 9 |
| 4 | SU-MIMO operating mode | 10 |
| 5 | Co-MIMO operating mode | 11 |
| 6 | MU-MIMO operating mode | 12 |
| 7 | LTE-Advanced networks with macrocell, microcell, picocell, femtocell, cooperative RN and potential technologies to be deployed for 5G [44] | 13 |
| A.1 | The system model with a single MBS, FAP clusters and RN placement. | 51 |
| A.2 | Different Relay Nodes Placement algorithms | 57 |
| A.3 | Comparison of Random vs Greedy vs EEORNP | 58 |
| A.4 | Coverage percentage of RNs | 59 |
| B.1 | The network architecture with a single MBS, MUEs, RNs clusters with CUEs, FAPs with FUEs | 68 |
| B.2 | Simulation scenario with fixed MBS, FAPs with their FUEs, MUEs and CUEs randomly distributed with a certain distance. | 86 |
| B.3 | BER performance of the proposed schemes for MUEs with different values of σ_{ϵ}^2 , SNR= 15 dB | 88 |
| B.4 | BER performance of the proposed schemes for FAP with different values of σ_{ϵ}^2 , SNR= 15 dB | 89 |
| B.5 | BER performance versus SNR for the FAP during the first time slot | 90 |
| B.6 | BER performance versus different values σ_{ϵ}^2 for the CUEs with and without the RN | 91 |
| B.7 | BER evaluation as function of the SNR for the CUEs with and without the RN during the first time slot, for $\sigma_{\epsilon}^2 = 0.05$ and $\sigma_{\epsilon}^2 = 0.06$ | 92 |

| | | |
|-----|--|-----|
| B.8 | BER performance of the proposed schemes for UEs with different values of σ_ε^2 , SNR= 15 dB | 93 |
| B.9 | BER performance of the proposed schemes for the UEs during the second time slot, for $\sigma_\varepsilon^2 = 0.03$ | 94 |
| C.1 | Illustration of an uplink MU-MIMO relay system with several CUEs, MUEs, RN and femtocells under MBS coverage. | 104 |
| C.2 | Average EE versus the maximum UEs transmit powers for $N_s = 2, N_R = 2, 4$ | 126 |
| C.3 | Average EE versus the different value of $\sigma_{\Delta_e}^2$ for the UEs with $N_s = 2, N_R = 2$ | 127 |
| C.4 | Average EE versus the maximum RN transmit power for $N_s = 2, N_R = 2, 4$ | 128 |
| C.5 | Average EE versus the number of iteration for $N_s = 2, N_R = 2, 4$ | 129 |
| C.6 | Average EE versus the different value of $\sigma_{\Delta_e}^2$ for the MUEs and FAPs. | 130 |

List of Tables

| | | |
|-----|---|----|
| 1 | Comparison between LTE and LTE-Advanced standards | 5 |
| 2 | Charateritics and specifications of macrocell and small-cells networks [44] | 13 |
| 3 | Different interfeence scenarios in two-tier architecture femtocell networks | 21 |
| A.1 | Results illustration from Fig. A.2 | 56 |
| B.1 | Coordinate Parameters | 87 |
| B.2 | Simulation Parameters | 88 |

List of Acronyms

| | |
|-----------------|--------------------------------------|
| 1G | First Generation |
| 2G | Second Generation |
| 3G | Third Generation |
| 3GPP | Third Generation Partnership Project |
| 4G | Fourth Generation |
| 5G | Fifth Generation |
| AF | Amplify-and-Forward |
| AMPS | Advanced Mobile Phone System |
| BER | Bit Error Rate |
| CA | Carrier Aggregation |
| CDMA | Code Division Multiple Access |
| cdma2000 | Code Division Multiple Access 2000 |
| CF | Compress-and-Forward |
| CoMP | Cooperative Multi-Point |
| CP | Cyclic Prefix |
| CS | Circuit-Switched |
| CSI | Channel State Information |
| CUE | Cell-edge macrocell User Equipment |
| DF | Decode-and-Forward |

| | |
|----------------------|---|
| DFT | Discrete Fourier Transform |
| DL | Downlink |
| DoF | Degrees of Freedom |
| EE | Energy Efficiency |
| E-UTRAN | Evolved Universal Terrestrial Radio Access Networks |
| EDGE | Enhanced Data rates for GSM Evolution |
| EEORNP | Energy Efficient and Optimal Relay Node placement |
| eNBs | evolved Node Base Station |
| enhanced ICIC | enhanced Inter-cell Interference Coordination |
| enhanced MIMO | enhanced Multiple Input Multiple Output |
| EPC | Evolved Packet Core |
| FAP | Femtocell Access Point |
| FDD | Frequency Division Duplexing |
| FDMA | Frequency-Division Multiple Access |
| FFR | Fractional Frequency Reuse |
| FFT | Fast Fourier Transform |
| FRF | Frequency Reuse Factor |
| FUE | Femtocell User Equipment |
| GPRS | General Packet radio service |
| GSM | Global System for Mobility |
| HeNB | Home eNodeB |
| HetNets | Heterogeneous Networks |
| HIC | Hybrid Interference Cancellation |
| HSDPA | High-Speed Downlink Packet Access |

| | |
|---------------------|---|
| HSPA+ | evolved High Speed Packet Access |
| HSS | Home Subscriber Server |
| IA | Interference Alignment |
| IC | Interference Cancellation |
| ICI | Inter-Cell Interference |
| ICT | Information and Communications Technology |
| i.i.d. | independent identically distributed |
| IDFT | Inverse Discrete Fourier Transform |
| IEEE | Institute of Electrical and Electronics Engineers |
| IFFT | Inverse Fast Fourier Transform |
| IMS | Internet protocol Multimedia Subsystem |
| IMT-U | International Mobile Telecommunication-Union |
| IP | Internet Protocol |
| IS-95 | Interim Standard 95 |
| LP-OFDMA | Linearly Precoded Orthogonal Frequency-Division Multiple Access |
| LSAS | Large Scale Antenna Systems |
| LS | Least Square |
| LTE | Long Term Evolution |
| LTE-Advanced | Long Term Evolution-Advanced |
| MBS | Macrocell Base Station |
| MIMO | Multiple-Input Multiple-Output |
| MME | Mobility Management Entity |
| MMUE | Marginalized Macrocell User Equipment |
| MMSE | Minimum Mean Square Error |

| | |
|----------------|---|
| MSE | Mean Square Error |
| MTC | Machine Type Communication |
| MUE | Macrocell User Equipment |
| MU-MIMO | Multi-User Multiple-Input Multiple-Output |
| NGWNs | Next Generation Wireless Networks |
| NMT | Nordic Mobile Telephone |
| NTT | Nippon Telegraph and Telephone |
| OFDM | Orthogonal Frequency-Division Multiplexing |
| OFDMA | Orthogonal Frequency-Division Multiple Access |
| OSIC | Ordered Successive Interference Cancellation |
| PAPR | Peak-to-Average Ratio |
| PDN GW | Packet Data Network Gateway |
| PFR | Partial Frequency Reuse |
| PIC | Parallel Interference Cancellation |
| PL | Path Loss |
| PS | Packet-Switched |
| PSTN | Public Switched Telephone Networks |
| QAM | Quadrature Amplitude Modulation |
| QoS | Quality of Service |
| QPSK | Quadrature Phase Shift Keying |
| RATs | Radio Access Technologies |
| RF | Radio Frequency |
| RN | Relay Node |
| SA | Simulated Annealing |

| | |
|----------------|--|
| SAGE | Space-Alternating Generalized Expectation-maximization |
| SC-FDMA | Single-Carrier Frequency-Division Multiple Access |
| SDMA | Space-Division Multiple Access |
| SDN | Software Defined Networks |
| SE | Spectral Efficiency |
| SER | Symbol Error Rate |
| SFR | Soft Frequency Reuse |
| SIC | Successive Interference Cancellation |
| SINR | Signal-to-Interference Noise Ratio |
| SIR | Signal-to-Interference Ratio |
| SISO | Single Input Single Output |
| SGW | Serving Gateway |
| SNR | Signal-to-Noise Ratio |
| SU-MIMO | Single-User Multiple-Input Multiple-Output |
| TACS | Total Access Communications System |
| TDD | Time Division Duplexing |
| TDMA | Time Division Multiple Access |
| UE | User Equipment |
| UMTS | Universal Terrestrial Mobile System |
| UP | Uplink |
| W-CDMA | Wideband Common Radio Resource Management |
| WLANs | Wireless Local Area Networks |
| WMMSE | Weighted Minimum Mean Square Error |
| Wi-Fi | Wireless Fidelity |

WiMAX Worldwide Interoperability for Microwave Access

WSN Wireless Sensor Networks

ZF Zero-Forcing

Abstract

Cellular networks are continuously undergoing fast extraordinary evolution to overcome technological challenges. The fourth generation (4G) or Long Term Evolution-Advanced (LTE-Advanced) networks offer improvements in performance through increase in network density, while allowing self-organisation and self-healing. The LTE-Advanced architecture is heterogeneous, consisting of different radio access technologies (RATs), such as macrocell, smallcells, cooperative relay nodes (RNs), having various capabilities, and coexisting in the same geographical coverage area. These network improvements come with different challenges that affect users' quality of service (QoS) and network performance. These challenges include; interference management, high energy consumption and poor coverage of marginal users. Hence, developing mitigation schemes for these identified challenges is the focus of this thesis.

The exponential growth of mobile broadband data usage and poor networks' performance along the cell edges, result in a large increase of the energy consumption for both base stations (BSs) and users. This due to improper RN placement or deployment that creates severe inter-cell and intra-cell interferences in the networks. It is therefore, necessary to investigate appropriate RN placement techniques which offer efficient coverage extension while reducing energy consumption and mitigating interference in LTE-Advanced femtocell networks. This work proposes energy efficient and optimal RN placement (EEORNP) algorithm based on greedy algorithm to assure improved and effective coverage extension. The performance of the proposed algorithm is investigated in terms of coverage percentage and number of RN needed to cover marginalised users and found to outperform other RN placement schemes.

Transceiver design has gained importance as one of the effective tools of interference management. Centralised transceiver design techniques have been used to improve network performance for LTE-Advanced networks in terms of mean square error (MSE), bit error rate (BER) and sum-rate. The centralised transceiver design techniques are not effective and computationally feasible for distributed cooperative heterogeneous networks, the systems considered in this thesis. This work proposes decentralised transceivers design based on the least-square (LS) and minimum

MSE (MMSE) pilot-aided channel estimations for interference management in uplink LTE-Advanced femtocell networks. The decentralised transceiver algorithms are designed for the femtocells, the macrocell user equipments (MUEs), RNs and the cell edge macrocell UEs (CUEs) in the half-duplex cooperative relaying systems. The BER performances of the proposed algorithms with the effect of channel estimation are investigated.

Finally, the EE optimisation is investigated in half-duplex multi-user multiple-input multiple-output (MU-MIMO) relay systems. The EE optimisation is divided into sub-optimal EE problems due to the distributed architecture of the MU-MIMO relay systems. The decentralised approach is employed to design the transceivers such as MUEs, CUEs, RN and femtocells for the different sub-optimal EE problems. The EE objective functions are formulated as convex optimisation problems subject to the QoS and transmit powers constraints in case of perfect channel state information (CSI). The non-convexity of the formulated EE optimisation problems is surmounted by introducing the EE parameter subtractive function into each proposed algorithms. These EE parameters are updated using the Dinkelbach's algorithm. The EE optimisation of the proposed algorithms is achieved after finding the optimal transceivers where the unknown interference terms in the transmit signals are designed with the zero-forcing (ZF) assumption and estimation errors are added to improve the EE performances. With the aid of simulation results, the performance of the proposed decentralised schemes are derived in terms of average EE evaluation and found to be better than existing algorithms.

Preface

"However difficult life may seem, there is always something you do and succeed at."

— Professor Stephen Hawking

Armeline Dembo Mafuta

University of KwaZulu-Natal, March 15, 2019

Part I

Introduction

Introduction and Research Background

In the last decade, mobile communication networks have significantly evolved in terms of transmitted information, increased number of users and mobile applications. The evolution of mobile networks includes mobile internet, smartphones, data traffic, wireless services and high demand of quality of services (QoS) for users required at any time. Transmission reliability and overall throughput are also among the essential measures of service quality in mobile networks. Such measures are mainly subjected to multiple challenges such as interference management constraint in a multi-user network, energy efficiency (EE), optimal relay node (RN) placement for effective coverage extension and others. Therefore, this work is focused on the study and design of algorithms that optimise the RN placement for coverage extension, the interference management and EE optimisation in the long term evolution-advanced (LTE-Advanced) femtocell network. The background informations, challenges, motivation, and contributions of this research are widely discussed in the following sections.

1 Mobile Network Evolution

In 1979, the first generation (1G) of cellular system was launched in Japan by nippon telegraph and telephone (NTT) and later several countries followed such as European countries with the nordic mobile telephone (NMT) standard in 1981, the USA with the advanced mobile phone system (AMPS) in 1983, UK with total access communications system (TACS) and Canada. The 1G standard is an analogue cellular system using frequency-division multiple access (FDMA) in multiple cell sites. It has the ability to transfer voice calls from one cell to an other as the user travels between cells. However, 1G had a limitation such that, it did not have data service to convert the voice into digital signals, low capacity, no global roaming services, poor voice quality, unreliable hand off [1]. These were due to the fact that 1G data can only use one channel from source to destination.

As the network expanded and neared capacity, the ability to reduce transmission power of mobile phones enabled new cells to be added, resulting in much smaller cells and thus more capacity. Then, the second generation (2G) mobile phone system emerged in 1987 as a digital cellular standard primarily using the global system mobile (GSM) communication. The 2G improves the modulation,

voice codes and security service as compared to the 1G analogue voice system [2]. Moreover, GSM adopted the time division multiple access (TDMA) to serve several subscribers. Code-division multiple access (CDMA) technology was also used in the Interim standard 95 developed by Qualcomm [3] which was considered as part of the 2G in Korea and North America. However, the strong digital signals and proper networks coverage in specific areas are required in the 2G to make the mobile phones work. The family of this generation includes 2G, 2.5G and 2.75G, among which we have the general packet radio service (GPRS) providing data rate from 56 Kbps to 384 Kbps, enhanced data rates for GSM evolution (EDGE) with data rate up to 236,8 Kbits/s [4].

The third generation (3G) were developed based on CDMA by groups of telecommunication associations in 1989 called the third generation partnership project (3GPP) and 3GPP2. The 3G combines the internet protocol (IP)-based services and the high speed mobile access. The 3GPP and 3GPP2 worked on the standardisation based on GSM and interim standard 95 (IS-95) networks respectively, resulting into wideband CDMA (W-CDMA) for 3GPP and cdma2000 for 3GPP2 [5]. In 2000, the universal mobile telecommunication system (UMTS) was released by the 3GPP as the first version of the standard and continued its evolution up to the high-speed downlink packet access (HSDPA) and evolved high-speed packet access (HSDP+) known as 3.5G. These provided a smooth evolutionary path for the UMTS-based 3G networks allowing for higher data transfer speeds. However, the data rate in 3G depends on the area in which the call is being made, with 144 Kbps for calls in the satellite and rural outdoor areas, 384 Kbps in urban outdoor while in indoor and low range outdoor is 2 Mbps. The higher bandwidth requirement is one of the limitations in this cellular generation; the cost for the mobile phones is high and their size too large. Moreover, it was difficult to implement a 3G infrastructure due to its high power consumption [6].

With the increasing demand for wireless data rates, CDMA reached its limit and could no longer accommodate the user's demand; then a standard based new access technology was developed by the 3GPP called long term evolution (LTE). Instead of using the CDMA as multiple access technology, LTE employed the orthogonal frequency division multiplexing (OFDM) to efficiently support wideband transmission [7], [8]. 3GPP finalised the LTE standard and yielded release 9 as its final version. According to Ericson [9] and Cisco [10], the expected growth of the world-wide mobile broadband user subscriptions and global mobile data traffic were up to 3.5 billion by 2015 and 11.2 Exabyte per month by 2017, respectively. Hence, the 3GPP release 10 presented an advanced standard of LTE known as LTE-Advanced capable of accommodating this tremendous growth. It offers new features such as the cooperative multi-point (CoMP) communication, heterogeneous networks (HetNets), carrier aggregation (CA), enhanced inter-cell interference coordination (enhanced ICIC), enhanced multiple input multiple output (enhanced MIMO), uplink and downlink

MIMO, relaying technology [11]. Moreover, the LTE-Advanced networks have the ability, as HetNets technologies, to overlay smallcells with low power level such as picocell, femtocell, relay node (RN), microcell etc, within macrocell coverage area operating at higher power levels. These HetNets provide and achieve significant capacity gain for the global mobile data traffic. However, they bring different challenges especially to cell-edge users including severe interferences, energy consumption, design of the security mechanism [12]. Some challenges and terms related to the LTE-Advanced networks are summarised in [13]. An overview and survey on the interference management techniques in 3GPP LTE-Advanced was studied in [14]. Among the key facilities of 4G includes high spectral efficiency, easy access to the internet, high voice quality, streaming media, video calling, very low latency, simple protocol architecture and efficient multicast/broadcast [15]. However, the basic drawbacks of 4G are the higher data prices for consumers, high energy consumption, complex hardware, high expense and the difficulty to implement [6].

The fifth generation (5G) is the name given to the next mobile telecommunication standard still under construction. It is expected to be probably finalised by 2021 and take over from the actual LTE-Advanced networks. It is supposed to provide very high speeds to the users and an efficient use of the bandwidth. It is assumed to achieve perfection level of the wireless communication in the mobile technology. Although, it still has a long way to go, 5G will be an amazing product that is bound to emerge in future years to come where the services and applications are expected to be improved in order to meet the users' demands.

2 Long Term Evolution-Advanced Standard

2.1 LTE and LTE-Advanced

LTE is an improved standard of UMTS mobile system developed by the 3GPP [16]. It goes a long way in fulfilling the user expectations to meet and cope with future requirements. LTE also allows operators to use a new and a much wider spectrum when compared to previous standard [17]. It supports peak data rates exceeding 300 Mbps in the downlink (DL) and 75 Mbps in the uplink (UL). To further enhance this and to meet the constraints set by the international mobile telecommunication-union (IMT-U), 3GPP has been investigated on different aspects of the LTE-Advanced technology. It aims to provide peak data rate that can be up to 1 Gbps for low mobility, 100 Mbps for high mobility in the downlink (DL) and 500 Mbps in uplink (UP). A comparison of the LTE and LTE-Advanced standards is given in Table 1. There is a set of targets and requirements for LTE-Advanced that includes reduced latency, peak data rate, bandwidth flexibility, reinforcement for HetNets deployment, architecture simplification and improved QoS. The authors in [18] investigated the research challenges

on deploying smallcell networks and these include the self-organisation of smallcells deployment and the related standardisation support in LTE-Advanced networks.

Table 1: Comparison between LTE and LTE-Advanced standards

| Specifications | LTE | LTE-Advanced |
|-----------------------------------|--|--|
| Standard | 3GPP Release 9 | 3GPP Release 10 |
| Upload rate | 5-50 Mbps | 10-70 Mbps |
| Download rate | 10-100 Mbps | 100 -300 Mbps |
| Bandwidth | supports 20MHz, 15MHz, 10MHz, 5MHz and < 5MHz | 70 MHz in DL and 40 MHz in UL |
| Throughput | about 100 Mbps for single chain | 2 times less than LTE |
| Latency (Delay) | in user plan < 5ms in control plan < 5ms | from idle to connected in less than 50 ms and then shorter than 5 ms |
| Modulation schemes supported | quadrature phase shift keying (QPSK), 16 quadrature amplitude modulation (16QAM), 64QAM | QPSK, 16QAM, 64QAM |
| DL peak data rate | 300 Mbps | 1 Gbps |
| UL peak data rate | 75 Mbps | 500 Mbps |
| Spectral Efficiency (peak,b/s/Hz) | 16.3 for 4 × 4 MIMO in the DL, 4.32 for 64QAM single input single output (SISO) case in the UL | 30 for 8 × 8 MIMO in the DL, 15 for 4 × 4 MIMO in the UL |
| Relay node | not supported | supported |
| Carrier aggregation | not supported | supported |

2.2 LTE-Advanced Architecture

The LTE-Advanced architecture is usually sub-divided into four main sub-systems; evolved universal terrestrial radio access networks (E-UTRAN), evolved packet core (EPC), user equipments (UEs) and the service domain. The EPC consists of a mobility management entry (MME) and a serving gateway (SGW), a packet data network gateway (PDN GW) together with home subscriber server

(HSS). The IP multimedia subsystem (IMS) network handles the voice service that is traditionally known as circuit-switched (CS) network service [19]. When a UE connects to the EPC, the MME represents the EPC to perform a mutual authentication with the UE. The E-UTRAN includes the E-UTRAN base stations (BSs), named eNodeBs (eNB) that communicates with UEs. The networks architecture of this cellular network is clearly illustrated in Figure 1. The LTE and LTE-Advanced

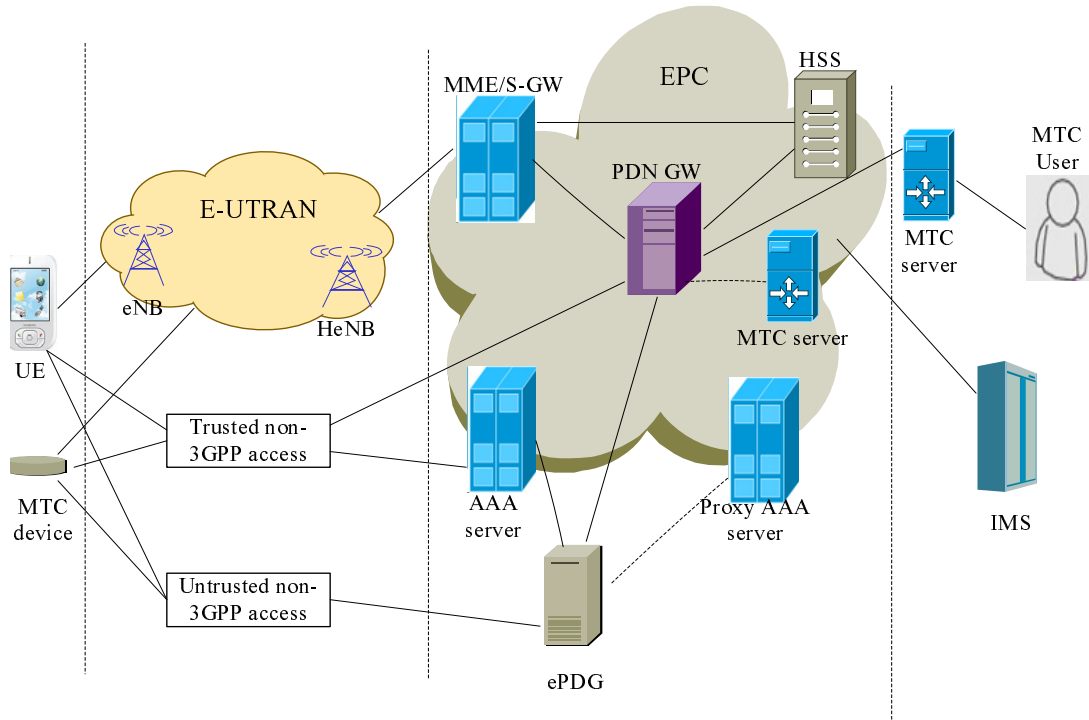


Figure 1: Network architecture of LTE/LTE-Advanced systems [12]

systems present new entities and functions compared to the 3G cellular networks which are:

- (i) The 3GPP committee suggested a new form of access point, named Home eNodeB to improve indoor coverage and network capacity, referred to as femtocell access points (FAPs). They are low-power access points that are typically installed by end users in small offices or residences to increase the indoor coverage for high speed data and voice service. The femtocell networks connect to the EPC over the Internet via a broadband backhaul [20].
- (ii) In addition to the E-UTRAN systems, the LTE-Advanced system supports other access systems called non-3GPP access networks, some of them are the cdma2000 systems, worldwide interoperability for microwave access (WiMAX) systems and wireless local area networks (WLAN) connected to the EPC system [21]. There exist two types of non-3GPP access networks, the trusted non-3GPP access networks and the untrusted non-3GPP access

networks [22]. However, the characteristic of the access networks does not depend on whether a non-3GPP access networks is trusted or untrusted but on the decision of the network operators. For an untrusted non-3GPP access network, an UE needs to pass a trusted evolved packet data gateway (ePDG) which is connected to the EPC.

- (iii) The machine type communication (MTC) is a new form of data communication between different entities that LTE-Advanced standard supports [23]. It has the ability to share and exchange the data with no requirement on any type of human mediation.

2.3 LTE-Advanced Multiple Access Schemes

The multiple access scheme for downlink communication in 3GPP LTE-Advanced is the orthogonal frequency-division multiple access (OFDMA) and the single-carrier FDMA (SC-FDMA) for uplink communication [24]. OFDMA is a multi-user version of the popular orthogonal frequency-division multiplexing (OFDM) digital modulation scheme. It is possible to achieve multiple access in OFDMA by allocating subsets of sub-carriers to single users. SC-FDMA, on the other hand, is known as linearly precoded OFDMA (LP-OFDMA). The OFDMA and SC-FDMA schemes are both similar, apart from the additional discrete Fourier transform (DFT) processing step following the conventional OFDMA processing [25]. This additional processing transforms the transmission logic to a large extent as well as the data symbols distribution over different sub-carriers. In practice, DFT and inverse DFT (IDFT) processes are useful for implementing the orthogonal signals. It is worth mentioning that DFT and IDFT can be implemented efficiently by using fast Fourier transform (FFT) and inverse FFT (IFFT), respectively. SC-FDMA has been found as a great alternative to OFDMA in the uplink communication due to its peak-to-average ratio (PAPR), being sufficiently lower than OFDMA and benefits the user terminals in terms of reduced cost of the power amplifier and power consumption [26]. Apart from supporting the wide range of data rates, SC-FDMA is also able to enhance uplink system throughput. The details of these multiple access schemes are given as follows:

1. *OFDMA in the Downlink* is a multi-user multi-access multiplexing scheme where a different numbers of sub-carriers can be assigned to different users. Different users are provided with multiple channels and their data symbols are distributed over the entire frequency band. It is known that in the OFDMA, the sub-carriers are orthogonal to each other and carry the data symbols of one user. In the TDMA, the time domain symbols for each user are transmitted in serial; compared with OFDMA, it is done in parallel which implies that each user has only some portion of the frequency band and the duration of the symbol becomes longer. Thus, an OFDMA is a robust system protected against time delays caused by multipath fading.

However, the orthogonality of the sub-carrier must be ensured in order to mitigate the inter-symbol-interference [25].

In order to mitigate the high signal distortion of high energy consumption, it is essential for the PAPR to be reduced to some extent. When the system throughput and PAPR are considered, SC-FDMA becomes more advantageous in the uplink instead of using OFDMA for both downlink and uplink for full downlink-uplink commonality [25]. The PAPR ratio is defined as follows:

$$PAPR = \frac{P_{t,peak}}{P_{avg}}, \quad (1)$$

where P_{avg} and $P_{t,peak}$ are respectively the average power of the transmit symbols and the transmit symbols power with the peak amplitude value. The PAPR ratio of the OFDMA system is high due to the independent identically distributed (i.i.d.) complex symbols that are directly assigned to each sub-carrier and a linear IDFT operation is performed over these sub-carriers. The block diagram of the OFDMA system is illustrated in Figure 2. The OFDMA process is considered as a linear transform over a great number of i.i.d. complex symbols using the quadrature amplitude modulation (QAM). This results in a direct dependency of the transmit symbols amplitudes to the constellation points of the QAM modulation method. The time domain OFDMA signal is considered as an approximation of the Gaussian waveform when the central limit theorem is employed. It is worth mentioning that this Gaussian waveform has a property of keeping great variations in the amplitudes of each transmit symbol leading to high PAPR.

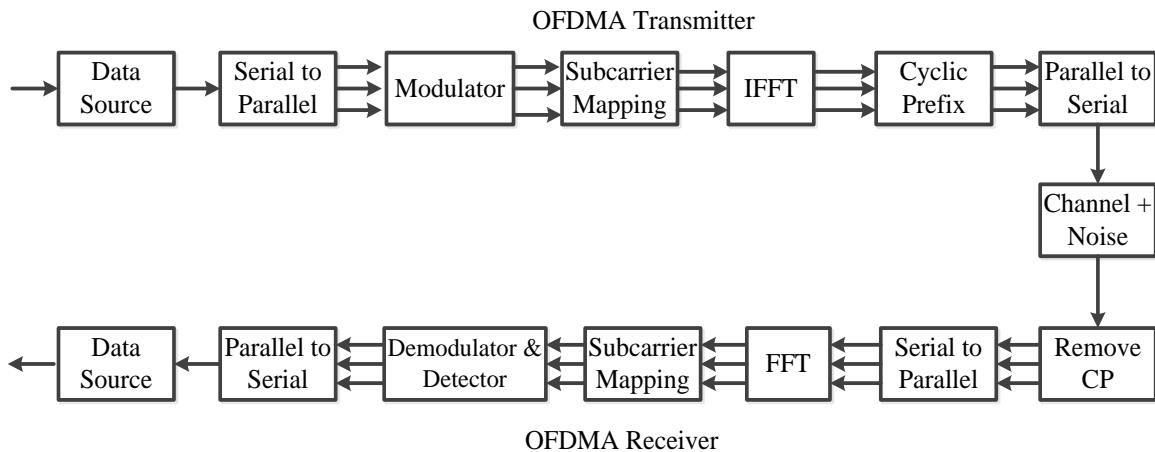


Figure 2: Block diagram of OFDMA

2. *SC-FDMA in the Uplink* has similarities with OFDMA such that the transmission bandwidth is divided into multiple parallel sub-carriers. The sub-carriers are orthogonally maintained by

adding the cyclic prefix (CP) as a guard interval. In SC-FDMA, the signal attributed to each sub-carrier is the linear combination of all data symbols that have been modulated and transmitted at the same time while in OFDMA, the data symbols are directly and independently assigned to each sub-carrier. Figure 3 illustrates the difference between the OFDMA and SC-FDMA transmission where one can see the additional DFT block before the sub-carrier mapping. This shows that the SC-FDMA system is single-carrier and not multi-carrier like OFDMA.

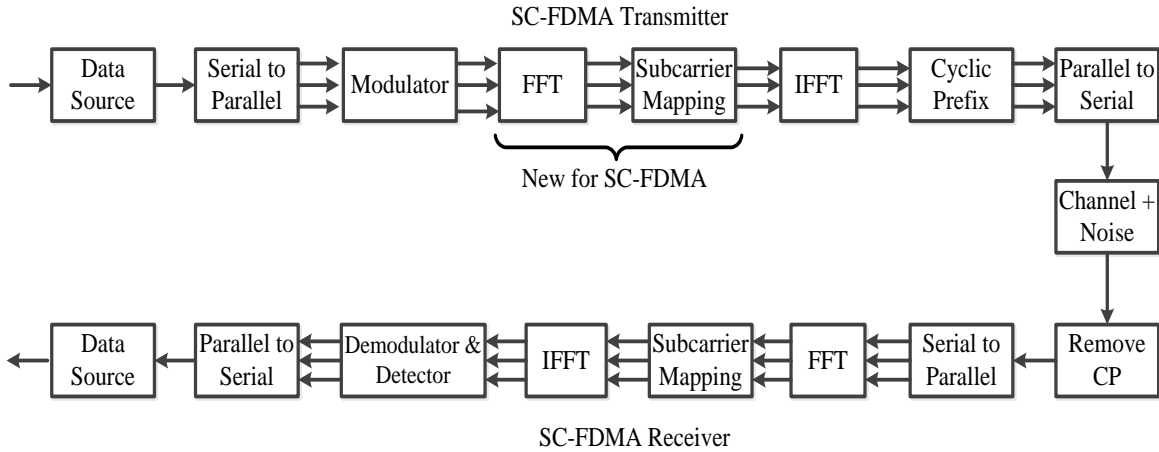


Figure 3: Block diagram of SC-FDMA

3 Features of the LTE-Advanced network

3.1 Enhanced Multi-Antenna Support

As a major enhancement technique, MIMO uses multiple antennas at the transmitter and receiver sides which increases the system performance. The multi-antenna support is one of the most important component of achieving the goals of the LTE-Advanced system as it is crucial in driving the increased data rates and system level performance. MIMO is an important technology for meeting the system performance requirements which include the cell-edge users throughput and spectral efficiency. Some of the fundamental schemes of the MIMO system used in LTE network are also vital in the LTE-Advanced system which are the spatial diversity, spatial multiplexing and beam-forming. The configuration of the multi-antenna support in enhanced MIMO system is extended for up to 4×4 in the uplink and 8×8 in the downlink [27]. The spatial multiplexing and transmission diversity are most preferred in actualising the enhancements for an improved coverage and absolute peak data rate in the LTE-Advanced targets. The main operating modes in the MIMO systems are single-user MIMO (SU-MIMO), cooperative-MIMO and MU-MIMO systems, and their

details are given in this subsection. This thesis considers the cooperative MU-MIMO system due to its complexity performance and its ability to manage interferences.

3.1.1 SU-MIMO System

The main aspect of the SU-MIMO operating mode is that the BS communicates only with a single user as illustrated in Figure 4. It has the advantage of no interference, no channel state information (CSI), data rate increases for the single user and the throughput is high at low signal-to-noise ratio (SNR) [28]. The beam-forming technique in SU-MIMO is combined with a selection of the spatial multiplexing and the transmit diversity techniques. This gives the possibility for substantial higher data by using higher order MIMO.

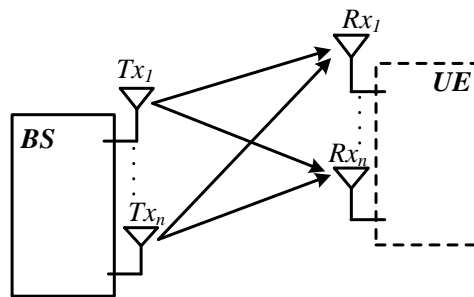


Figure 4: SU-MIMO operating mode

3.1.2 Cooperative-MIMO System

Cooperative-MIMO system is a form of MIMO with cooperation between the BSs [29] as illustrated in Figure 5. They are also known as distributed or virtual MIMO systems that utilise distributed antennas on multiple mobile or radio devices in order to achieve similar benefits provided by the MIMO systems [30]. The overall technique involved is known as the CoMP transmission and reception, where the signals transmission and reception from different BSs are coordinated; this helps to reduce the inter-carrier interference [31]. Cooperative-MIMO operating mode improves the system capacity, the network coverage, the cell edges throughput and the group mobility of the wireless communication network. Apart those advantages, this system provides high data rates coupled with an excellent network throughput in high load scenarios. However, the increased system complexity and the large signalling overload required for supporting device cooperation are the main disadvantages of this communication system. A study of this technique has been done in [32] where a deep examination and review on the fundamental theory of the cooperative-MIMO were provided. The authors showed that the multi-cell cooperative-MIMO can dramatically improve the performance

of the networks when the interference problem is properly addressed. Energy consumption has also been an attractive research focus in cooperative-MIMO systems. The authors in [33] investigated the EE in cooperative-MIMO networks to show that these systems can provide an efficient and reliable energy transmission. Moreover, new relay selection policy and power allocation based on opportunistic relaying scheme have been proposed in [34].

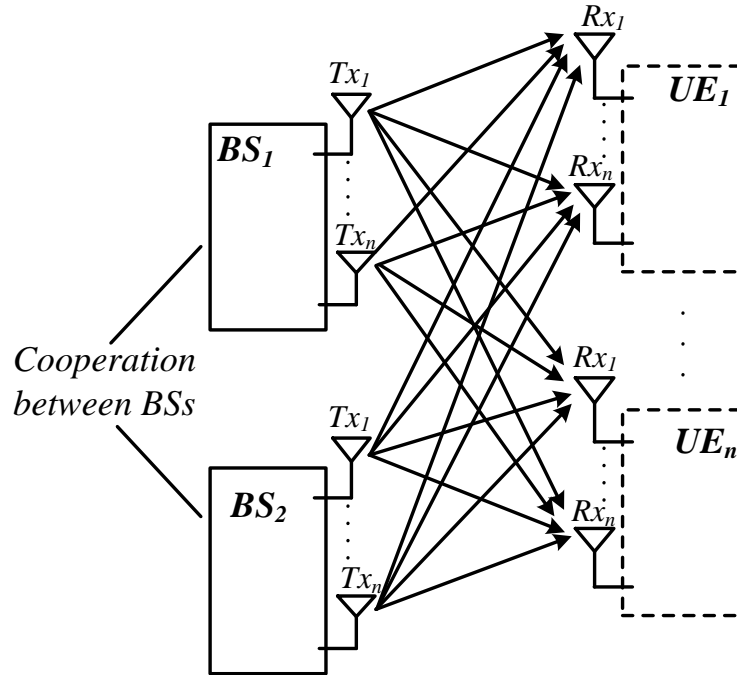


Figure 5: Co-MIMO operating mode

3.1.3 MU-MIMO System

MU-MIMO system is an advanced form of MIMO communication system that has gained enormous attention due to its potential in improving the WLANs performance. It is a system in which the multiple users can have the same allocated resources and can transmit signals simultaneously. However, these transmitted signals are separated in the spatial domain at the receiver side [35]. Figure 6 illustrates the MU-MIMO system operating mode. This system exploits the spatial resource to improve the system performance. Furthermore, it can obtain a significant throughput gain for user in the center of a cell while guaranteeing the throughput improvement at the cell edges [36]. MU-MIMO system is capable of combining the space-division multiple access (SDMA) with the high capacity achievable with MIMO network. It is known that SDMA uses spatial multiplexing and can support multiple connections on a single conventional channel where different users are identified by spatial signatures [28]. One of the interesting benefits brought by the SDMA is the

mitigation and management of the interference effect coming from adjacent cells. Several researches have been done in MU-MIMO systems in past years [37], [38]. A survey on key requirements of MU-MIMO design was investigated in [37] with the background information on multiple access channel (MAC) scheme of IEEE 802.11 standards and amendments. Moreover, the benefits and challenges of MU-MIMO system are also detailed in [28]. A complete introduction to the downlink MU-MIMO is given in [39]. Aside of these works, some addressed the interference management [40], [41] and/or EE optimisation in MU-MIMO systems [42], [43].

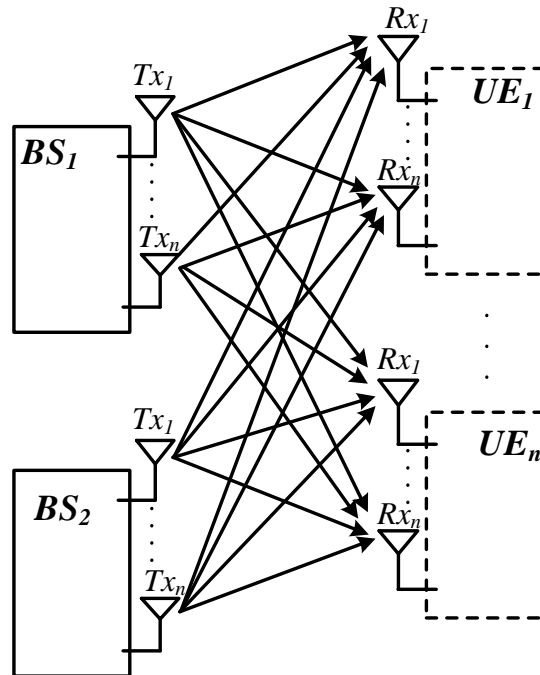


Figure 6: MU-MIMO operating mode

3.2 Macrocell and Small-cells Networks

Small-cell networks are deployed into the coverage of macrocell network and are mainly categorised based on their cell size (coverage area) and power level. The most common small-cells are the microcell (metrocell), picocell and femtocell networks as illustrated in Figure 7. Table 2 illustrates the specifications and characteristics of the macrocell and small-cells networks based on transmission power, cell radius, access mode, back-haul connectivity, installation deployment location, number of users and cost.

3. FEATURES OF THE LTE-ADVANCED NETWORK

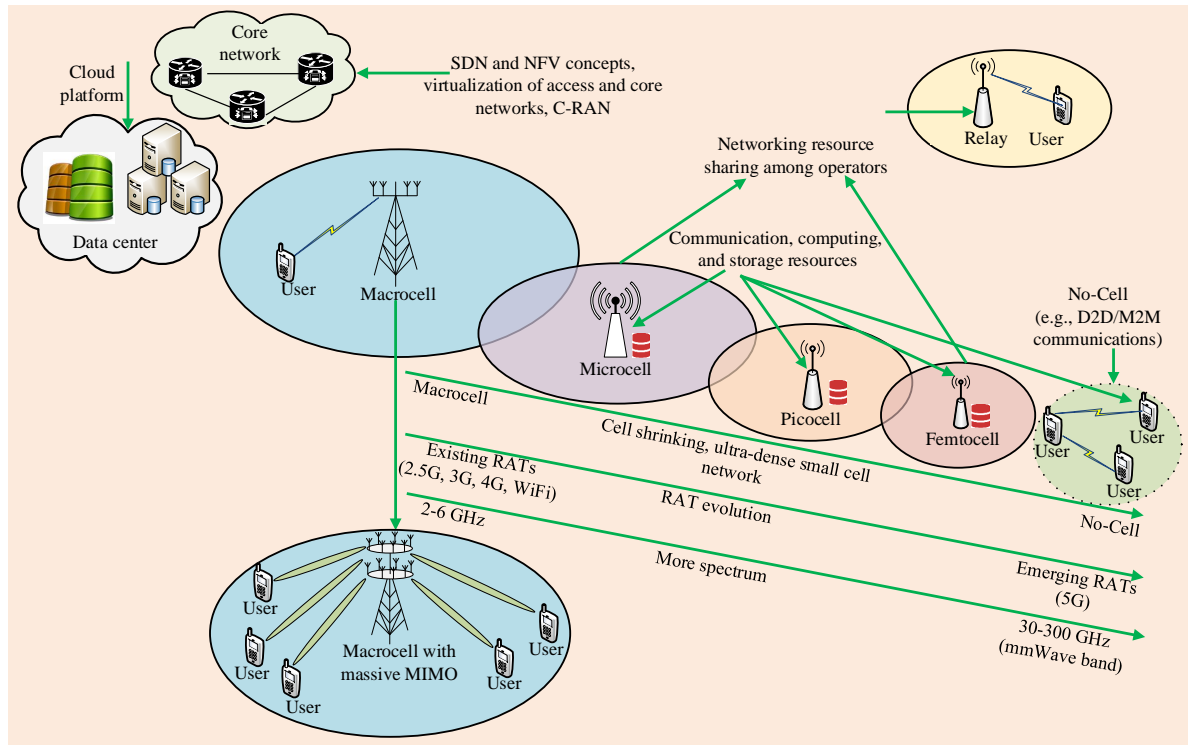


Figure 7: LTE-Advanced networks with macrocell, microcell, picocell, femtocell, cooperative RN and potential technologies to be deployed for 5G [44]

Table 2: Characteristics and specifications of macrocell and small-cells networks [44]

| Specifications | Femtocell | Picocell | Microcell | Macrocell |
|------------------------|-------------------|-------------------|-------------------|-------------------|
| Typical cell radius | 10-30m | 100m-300m | 250m-1km | > 1km |
| Transmission power | 0.1 Watt | 1 Watt | 5 Watt | Up to 40 Watt |
| Access mode | close/open/hybrid | open to all users | open to all users | open to all users |
| Back-haul connectivity | Broadband | X2 interface | X2 interface | X2 interface |
| Deployment location | indoor | indoor/ outdoor | outdoor | outdoor |
| Installation | user | operator | operator | operator |
| Number of users | Up to 30 | 30 to 100 | 100 to 200 | > 2000 |
| Cost | very cheap | cheap | expensive | very expensive |

3.2.1 Macrocell Networks

Macrocell or eNB is a big cell in a cellular network that provides radio coverage served by a high power cellular BS. Usually, it provides a larger coverage area than any other technology e.g. microcells, femtocells, relay nodes, picocells. This is because, the macrocells' antennas are mounted on the ground-based masts, rooftops and other existing structures, at a height that provides a clear view over the surrounding terrain and buildings. It also has a power output of typical 10 Watts and its performance can be increased by increasing the effectiveness of the transceiver [45]. Macrocell BSs (MBSs) locations and settings are respectively chosen through network planning and configured to control the interference and to optimise the coverage area. As the traffic demand grows and the radio frequency (RF) environment changes, the system relies on the splitting of the cell or additional carriers in order to overcome capacity and transmission link limitations while maintaining UEs QoS [46]. However, this deployment process is difficult and inefficient. Moreover, the site acquisition for MBSs with towers becomes more difficult in dense urban areas. Another severe issue for macrocells in LTE-Advanced networks is the high penetration loss in indoor environment, which has in itself a negative impact on the transmitted and received signals [47], [48]. Therefore, femtocells technology has been incorporated into the LTE-Advanced network in order to improve UEs broadband experience in a ubiquitous and cost-effective way. These small-cells are seen as the future of next generation networks as they are more reachable and cost-effective than any other technologies as shown in this research.

3.2.2 Microcell Networks

Microcells are one of the small-cell networks used to enhance the capacity of GSM networks as the popularity of mobile services exploded in the mid-90s. They are difficult to differentiate from picocells and their coverage zone is the first delineator. Microcells coverage area can be less than a certain mile in diameter where the power control is used to limit the radius [49]. They are temporarily deployed to anticipate the high-traffic within a limited area like a sport or athletic event, but can also be installed as a permanent feature of mobile networks. Moreover, they allow network operators to increase the frequency re-use and spectral efficiency of their networks dramatically and it was also easier to find sites for the smaller BSs [50], and their associated antennas, compared with traditional macrocell sites. One of its main disadvantage is the difficulty of connecting the microcell BSs with the cellular networks [51].

3.2.3 Picocell Networks

Picocell networks are simple low-cost devices with great capacities and coverage areas, capable to support 30 to 100 users over a cell radius of 100 to 300m. Picocells are often deployed indoors in order to improve poor cellular and wireless coverage within a residential building or offices. Their designs appear to be small enough to be installed by only one technician. Like any smallcells, picocells extend the macrocell coverage area where the wireless signal appears to be poor or where they can serve a large number of users on behalf of the macrocell [52]. Picocells have benefits of data throughput improvement, alleviating capacity issues in the mobile networks or challenges such as interference or energy consumption [53]. The authors in [54] investigated the effect of EE when deploying picocell into macrocell coverage in LTE-Advanced networks. The performance and capacity results of their work showed that picocells are beneficial addition to the existing macrocell LTE-Advanced networks. The EE issues of picocells, relays and macrocells is investigated in [55], and simulations results showed that the relays and picocells both provide positive EE gains in the uplink, but not for the downlink scenario. For downlink, the RN produce similar throughput and energy consumption as macrocell deployments.

3.2.4 Femtocell Networks

Femtocells are lower power access points than picocells and their decreased cell size increases the capacity of the wireless networks. The femtocell deployment inside the macrocell networks improves the poor indoor coverage and fills the holes in the coverage networks by providing excellent signal quality where the coverage area is deficient of the optimal strength to make calls. Moreover, they provide high data rates for next generation of wireless networks in rural areas [56] but mostly suffer from interferences. These interferences can be generated either between macrocell and femtocells (cross-tier) or among femtocells (co-tier).

The femtocell network has several advantages such as increasing capacity and system coverage by making the macrocell's resources available for more users. They are energy efficient due to the distance between the FAP and its users which is very small i.e. 5m-20m [57] and this may reduce the battery consumption of the devices. Femtocells can be purchased from resellers or through the mobile operator. Contrary to microcells and picocells, femtocells support merely a handful of users and are capable of handling only few calls at the same time.

3.2.4.1 Characteristic of Femtocell Networks

The femtocells can support all major cellular standards protocols standardised by 3GPP, 3GPP2 and the IEEE/WiMAX forum, e.g. GSM, CDMA, W-CDMA, LTE, LTE-A, WiMAX. They are

characterised by the following features [58]:

- The femtocells work in a licensed spectrum that exclusively reserves the resources to the subscribed users.
- They have higher density, lower power and lower cost than other small-cells, such as picocells.
- As specified above, the femtocells coverage is very small such that the transmitting power is approximatively around 0.1 Watt. This results to an excellent quality of signal for their users within the coverage range.
- They also enable end users to install and start the devices without any technical support.

3.2.4.2 Types of Access in Femtocell networks

The types of access in a network could reduce, control or increase the interference in the networks. There are different access methods for femtocell networks which include [59]:

- *Closed access method:* allows only the femtocell subscribed users to connect to its BS. This method is mostly deployed by private owners in offices or homes and leads to high cross-tier interference. Only the users listed in the permitted access list of a femtocell are given access to this particular femtocell [60]. The prime reason for this type of access is to guarantee users knowledge once they are inside the femtocell coverage. However, problems arise with this access type once an unregistered user accesses the femtocell coverage when the user is not on the permitted access list. This access method is considered throughout this study to maintain the communication performance of the subscribed users. Although this method decreases the performance of the non-subscriber users, this thesis consider RN to manage and improve their communication with their base stations, which solves the communication performance problem of the non-subscribed users.
- *Open access method:* is the opposite of the closed access method where both subscribed and non-subscribed users can access the femtocell resources without any restriction. The deployment is done in open areas like airports, shopping malls or hospitals [61]. Apparently, this method is profitable to mobile operators, by providing an inexpensive way to expand their capacities through influencing third-party back-haul for free. However, it increases the number of hand-overs for multiple mobile users accessing and leaving that femtocell which causes a noticeable QoS decrease [62].
- *Hybrid access method:* is a combination of closed and open access approaches by giving a limited amount of femtocell resources to all users as the open access method while the rest

operate as the closed access method [63]. Deploying the subscribers group of the closed access method into femtocell networks makes the interference management problem more complex to solve. However, hybrid access approach aligns the level of granted access of non-subscribers and the performance impact of the subscribers [64]. Thus, the share of femtocell resources between non-subscribers and subscribers needs to be exquisitely fixed. Otherwise, the subscribers might feel that they are paying for services that is exploited by others. In this case, OFDMA scheme can be used in femtocell networks to manage the shared resources over frequency and time between subscribers and non-subscribers as well as to define the available resources for each [65].

3.3 Cooperative Relaying Communication

Cooperative relaying is a promising technology for wireless communication that provides throughput and capacity gains in the networks. The classical relay channel model was first introduced in [66] by Van Der Meulen. According to the 3GPP committee, cooperative RN systems provide the following improvements to the LTE-Advanced networks: group mobility, cell-edge throughput improvement, temporary network deployment, coverage of high data rate, coverage in new areas, power consumption reduction and cost reduction. In this study, the cooperative relaying system is employed to improve reliability and the coverage extension of the system with optimal and energy efficient RNs placement. An efficient RN placement is necessary in LTE-Advanced networks such as to minimise the energy consumption between the source and the destination [67]. An energy efficient of RN placement for the coverage extension is proposed in the study. Moreover, the the design of transceiver for the cooperative RN system is proposed to manage the interferences and optimise the energy consumption.

There are three types of communication protocol in cooperative relaying system, decode-and-forward (DF), amplify-and-forward (AF) and compress-and-forward (CF). The description of these cooperative communication techniques is given as follows:

1. *AF cooperative communication protocol* is referred to as non-regenerative or analogue relaying. The AF relay nodes amplify the received signal and re-transmit to the destination. Since the AF relay nodes do not require front-end processing, demodulation, and decoding, they have less complexity than the DF relay nodes. However, since the AF relay nodes do not perform any decision operation on the received signal, noise along the transmission path can be accumulated and propagated [68]. AF is employed in this thesis over DF due to its simplicity and its low complexity.
2. *DF cooperative communication protocol*, contrary to AF, It is referred to as regenerative or

digital relaying. During the first phase of cooperative communication, the DF relays protocol can decode the received signal, re-encode it, and then re-transmit it to the destination. The DF relay advantage is that the RNs can prevent error propagation, if the relay can successfully decode the source signal [69]. According to whether error detection is employed or not, the DF relays can be categorised into two schemes: fixed DF relays and selection DF relays. The fixed DF relays do not use the error detection, and re-transmit the relayed signal although it has errors; thus, full diversity order cannot be achieved [70]. While the fixed DF relays always forwards the signals received at the RN to the destination, the selection DF relays only retransmit the successfully decoded signals.

3. *CF cooperative communication* is known to be an efficient forwarding technique where the RNs compress the received signal and then forwards an estimation of it to the destination. This scheme has good performance only when the RN is close to the destination, for instance when there is no obstacle or shadow in the RN-destination link [71].

4 Challenges of LTE-Advanced System and Mitigation Approaches

This section describes some challenges investigated throughout this thesis as well as the approaches considered to mitigate these challenges. There are several challenges in the LTE-Advanced networks including interference management, energy efficiency (EE), network architecture security, effective coverage extension, resource scheduling [18], [28]. Due to different requirement and dense deployment of femtocells in the LTE-Advanced networks, this research focuses on the effective coverage extension, the interference management and EE optimisation challenges.

4.1 Challenges Description

4.1.1 Effective Coverage Extension in LTE-Advanced Network

With the increasing number of cellular subscribers, wireless networks are facing difficulties in providing satisfactory signal-to-interference-plus-noise ratio (SINR) level to users especially at the cell edges of the systems. In LTE-Advanced network, most wireless services provide enhancement in data service by employing technologies such as OFDM and by adopting MIMO antennas. Nevertheless, in practice there are still issues such as coverage holes due to shadowing, and poor SINR for users that are far away from the BS. One of many solutions to support the ever increasing number of subscribers per cell is to decrease the cell radius. However, this requires more BSs per area with a small size coverage area, thus increasing cost, especially when there are few users to be

served (e.g., in rural areas) and causing higher inter-cell interference between the BSs. An alternative to adding more BSs, is deploying low-cost RNs that provide a cost-effective way to overcome the costly problem. The optimal RNs are a simplified version of a full BSs requiring lower cost than the normal BSs. Moreover, RNs do not require backhaul connections, thus reducing operating costs. The effective coverage extension depends on the radial position of RNs in the cell. This is because the location of a RN affects the SINR of the received signal on the MBS to RN and RN to UEs links. The RNs placement problem can be seen as a sub-case of the well studied facility location problem, which has been proved to be NP-hard [72]. Therefore, it deserves some attention because the objective functions and the interdependence between transmitting stations through interference make it very specific. The authors in [73] investigated the optimal RN placement problem in a single WLAN cell, based on Lagrangian relaxation, a discretisation of possible RN placement and an iterative algorithm. In [74], the authors addressed the optimality placement of relay in a LTE-Advanced network with the aim of maximising the cell capacity and thus the coverage extension.

4.1.2 Interference Challenge and Mitigation Approaches

According to [75], interference can be described as any unwanted signals or symbols entering the receiving signal or system. It is also illustrated as any noise or signal that modifies, disrupts a transmit signal as it travels along a channel between a source and a receiver. In local area networks (LAN) or cellular networks, interference occurs whenever there is identical channel sharing between different access points or sharing of the same carrier frequency between BSs due to frequency reuse [76]. Similarly, neighbouring nodes in a dense mobile networks can also interfere with each other when they share the same frequency resources at the same time. Communication in the presence of interference is often analysed using an abstraction known as the interference channel. There are other sources of interference such as self-interference resulting from non-linearities in the radio frequency components or jamming in military networks, those sources are not captured in the basic interference channel; are not a concern of this thesis. Traditional methods for managing the interference in wireless networks often revolve around giving an exclusive access to each user in order to fraction the communication resources. For example, in FDMA, the system bandwidth is partitioned among the transmitters while in TDMA, transmitters take turns to transmit on a periodic set of transmission intervals [77]. As an inevitable challenge in wireless networks, interference has always been an important concern in designing communication systems, particularly in LTE-Advanced networks. It reduces the data rates throughout of the cells and causes outages at the cell edges [76].

This study is particularly interested in multi-tier LTE-Advanced femtocell networks deployed

into macrocell coverage area where there are multiple radio access technologies (RATs) or network infrastructures that back-haul the data traffic of the mobile users to the core of mobile operators. This leads to two types of interference scenarios, namely the cross-tier (cross-layer) and co-tier (co-layer) interference. Due to the vast degree of freedom (DoF) and the need of optimising some parameters depending on the network performance requirement, it is necessary to categorise the type of interference for an effective deployment of interference management approach. The system performance requirement can either be the achievable throughput maximisation, or the area spectral efficiency maximisation in each layer of the cellular network. The description of cross-layer and co-layer interference are detailed as follows:

- *The cross-layer interference* happens among network elements that belong to different layers or cell-types located in the same geographical area of a network. The network entity that causes the interference is called aggressor while the victim is the network entity suffering from the interference coming from the aggressor. It is worth mentioning that the contribution level of this type of interference commonly depends on the aggressors transmit power on the adjacent or shared spectrum resource and their density in a geographical area [78].
- *The co-layer interference* occurs between the network entities belonging to the same tier of the network. As result, the interference occurs from the transmitting and receiving activities of both mobile UEs and the BSs connected to the same network infrastructure type (e.g. macrocells or femtocells) of a mobile operator in a geographical region. Femtocell to femtocell co-tier interference can happen because of low isolation between the residences in which femtocells deployment is done through the overall low transmission power of femtocells and high likelihood of attenuation [78].

The different interference scenarios that occurs between macrocells and femtocells are summarised in Table 3.

Several interference management schemes have been proposed in the past works to mitigate the interference and some of them are mentioned for literature review purpose [79], [80]. These techniques are interference alignment (IA), interference cancellation (IC) and interference avoidance. In the IA scheme, signals are constrained into the same subspaces at the unintended receivers and the desired signal is retrieved at each receiver by eliminating the aligned interferences using decoding matrix [81]. In the interference avoidance, on the other hand, the allocation of various system resources to users is controlled to ensure that the interference remains within acceptable limits [82]. IC is the technique in which the suppression of the interference is done at the transmitter or receiver side. The important note about the IC approaches is that when using them conventionally, the sum-capacity

Table 3: Different interference scenarios in two-tier architecture femtocell networks

| Aggressors | Victims | Interference types | Transmission mode |
|--------------------|--------------------|---------------------------|--------------------------|
| macrocell UE (MUE) | FAP | cross-layer | Uplink |
| MBS | femtocell UE (FUE) | cross-layer | Downlink |
| FUE | MBS | cross-layer | Uplink |
| FAP | MUE | cross-layer | Downlink |
| FUE | FAP | co-layer | Uplink |
| FAP | FUE | co-layer | Downlink |

of the network is still limited by interference unless they are improved or combine with techniques like transceiver design, optimisation techniques or other efficient mitigation techniques. However, the IA is an approach in which the sum-capacity of the time-varying interference networks using limited resources, i.e. time, frequency, can be increased linearly with the number of users [83].

1. *IA Technique:* is a remarkable interference management strategy that improves the spectral efficiency and reduces the impact of interference. The main idea of IA is to coordinate multiple transmitters so that their mutual interference aligns at the receivers, facilitating simple interference mitigation. Researchers have investigated its performance and proposed several improvements [38], [84]. Research efforts have been primarily focused on verifying IA's ability in order to achieve the maximum DoF [85]. In [86], authors also considered as an approximation of sum-rate capacity, developing algorithms to determine proper alignment solutions, and designing transmission strategies that release the need for perfect alignment but yield better performance. A centralised efficient sub-channel allocation algorithm based on IA was proposed in [87] to maximise the number of QoS guaranteed UEs performing IA. Its strategy ensures that the interference is properly aligned into a given subspace and leaves a residual subspace free from the desired signal [88].

IA, in its simplest form, is a pre-coding technique for the interference channel. Like IC, IA helps to develop transceiver design with or without channel estimation in order to mitigate inter-cell and inter-user interference. A robust transceiver design based on the IA is proposed in [89] to minimise the interference leakage and maximise the EE. IA is also known to be a cooperative interference mitigation technique exploiting the available multiple dimensions such as antennas, frequency blocks, or time slots [76]. By coding over multiple signalling dimensions, transmissions are designed to align the interference observed at each receiver into a low-dimensional subspace. This maximises the number of non-interfering signals that can be

simultaneously communicated over the interference channel, known as the multiplexing gain. EE optimisation is addressed in [90] where a IA technique is proposed to achieve maximal EE in multi-cell MIMO interfering broadcast channels.

2. *Interference Avoidance Technique* is a common technique of inter-cell interference coordination (ICIC) [82]. It is a technique that improves the system performance by having each cell allocate its resources so that interference experienced in the system is minimised, while maximising spatial reuse [91], [92]. The conventional frequency reuse (FR) methods are the inheritance schemes of interference avoidance in the cellular systems. The frequency resource is divided into different blocks which are assigned to each cell in the system. The interference avoidance in the network is improved when employing the non-overlapping frequencies blocks; this also decreases the trunking capacity of each cells. The FR factor (FRF) is defined as the number of adjacent cells which cannot use the same frequencies for transmission. The fractional FR (FFR) improves the inheritance of the FR technique by splitting each cell into sub-areas before using a FRF greater than the unity in some areas or before using the FRF of unity in other areas. This results to an improvement of trunking capacity while the mitigation of the interference is maintained. There are various variants of interference avoidance techniques [93] and some of these are further discussed in the following subsection.

- *The FFR* is defined as a sub-carrier reuse technique that allocates only a part of the total bandwidth which is subset of sub-carriers to each cell. The authors in [94] proposed a FFR interference avoidance scheme and power control for a standard cellular network deployment. The key idea of this method is the cell's bandwidth partition, for the following reason: First, it avoids any interference between the cell edge users located in the adjacent cells. Secondly, it reduces the interference created by the interior users. Finally, it allows more use of total spectrum than the conventional FR. The cell space is also partitioned into two different regions, the inner and outer regions. The inner region appears to be close to the BS while the outer is located at the cell borders. Furthermore, in the FFR, the entire frequency band is divided into multiple sub-bands where each sub-band is allocated either to outer or inner region of the cell. An evaluation and comparison of three state-of-art FFR deployment schemes with a proposed optimal FFR were investigated in [93] for OFDMA based two-tier HetNets networks. The results show a higher performance in spectral efficiency of the proposed scheme compared to the others schemes. The authors in [95] proposed a hybrid dynamic frequency reuse and CoMP technique for interference management that is able to enhance the adjacent sector transmission and the cell edges

performance.

- *The soft frequency reuse (SFR)* employs similar frequency allocation procedure to that of the FFR. The term of soft reuse comes from the fact that the efficient reuse of the technique can be adjusted by dividing the powers among the frequencies used in edge and centre bands. SFR is an effective frequency reuse technique for inter-cell interference (ICI) coordination and can maintain the spectrum efficiency. Performance of this was investigated in [96] with issues of various traffic loads and different power ratio configurations constraints, and results confirmed the effectiveness of SFR scheme. In SFR, the centre region MUE devices are allocated the sub-bands being used by other MUEs at the cell edge area of neighbouring cells within the cluster. For a cluster of I -cells, the total number of available sub-channels in a cell is divided into I sub-bands with one sub-band allocated to each of the edge areas [97]. Femtocells to be overlaid on the existing macrocell infrastructure are assigned resources that are orthogonal to that of the macrocell in both the cell edge area and cell centre of the cell. SFR was first proposed in [98] in order to find a balance between the FFR and the partial FR (PFR) schemes [99]. As mentioned by the authors in [82], SFR can avoid high ICI levels when associated with the unity FFR configurations and can provide more flexibility to the PFR scheme as well.
3. *IC Technique*; among the interference management schemes, IC appears to be one of the oldest technique proposed. In order to cancel interferences from adjacent cells, it is required to detect the interfering signals first and then cancel them from the received signal. It is usually difficult to detect the interfering signals from adjacent cells in a practical situation. However, spatial characteristics are used to suppress interference when multiple antennas are available at the receiver [100]. IC scheme has widely been studied in last decade and different schemes have been proposed. There are two well known categories of IC techniques called parallel IC (PIC) [101] and successive IC (SIC) [102] that are mostly mentioned and improved in the literature. PIC processes all signals in parallel and then starts the cancellation of the signals' interference after all signals have independently been decoded. SIC method, on the other hand, processes each signal successively by cancelling the previously decoded signals [103]. Other schemes have been derived from these two techniques such as ordered SIC (OSIC) and hybrid IC (HIP), which is a combination of the advantages of both PIC and SIC. Most of these techniques for interference management were proven to perform well depending on the scenarios considered. IC techniques are also used with others schemes such as in channel estimation, to improve the network performance, to achieve effective results and particularly to design transceivers in

LTE-Advanced networks. Authors in [104] combined the channel estimation and IC technique for MIMO LTE-Advanced networks to improve the symbol detection. Similar combination is proposed in [105] where a prediction method characterising the Turbo SIC performance and deriving an approximate post detection SINR for each layer with channel estimation error statistic are investigated. Aside from channel estimation, transceiver design is also used with IC [106]. The authors in [107] proposed a transceiver architecture for full duplex eNodeB and the UEs transceiver; the SIC with optimal ordering is used in the uplink to decouple the UEs signals operating in the same sub-carriers.

4.1.3 Energy Efficiency in LTE-Advanced Network

The progress of 4G and the design of the future 5G wireless technologies requires meeting huge service expectations, among which EE is an important design criterion to enable operations at virtually affordable energy consumption levels. It was suggested in [108] that the mobile information and communications technology (ICT) sector would emit more than 300 million tons of greenhouse gases per annum by ≈ 2020 [109]. Hence energy consumption remains a crucial challenge to optimise due to the contribution of mobile networks towards significant stake in the global carbon footprint [108], approximately $> 2\%$ of the worldwide energy consumption.

Moreover, the deployment of smallcells enhances the cellular coverage and potentially solves the poor received signal strength experienced by the mobile users that are located in cellular coverage holes. However, this deployment solution increases overall networks' energy consumption, leading to the trade-off between power consumption and system throughput [110]. As a result, existing schemes are proposed to improve EE and fulfil the increasing demand on capacity in a cost-efficient way. According to [111], strong interference caused by the spectrum reuse and dense deployment can degrade the EE and QoS in the wireless network to the extent that the cell edge UEs have to increase their transmission power to meet the QoS requirement. As a result, UEs with limited battery capacity will quickly run out of battery power without careful energy optimisation and interference management design. Hence, EE algorithms can also be designed with interference management schemes to immediately decrease the nodes transmit power that make up the system leading to improved system performance and throughput. The authors in [112] used EE approach to address the issue of interference by adjusting the transmitting power in each access point in order to optimise energy consumption. EE schemes are frequently time embedded in other algorithms to increase the network capacity, to prolong the battery life by conserving the energy and to support the QoS by power requirement adaptation to match the variation of the channel condition [113]. EE schemes are also deployed for both co-layer and cross-layer interference management as described in [114] and

their application is extensively practised and applied to the system management with a view of increasing system capacity as well [115].

According to the survey in [116], EE approaches to mitigate the interference are grouped into two categories, assistance or non-assistance. The assistance based techniques employ the coordination between the Home eNodeB and the eNB [117], while the non-assistance based techniques do not use such coordination. Moreover, the EE approaches are also grouped based on the conceptual architecture such as distributed and centralised EE. The distributed EE scheme performs a localised interference management at the nodes of each tier of the network [118]. The centralised EE, on the other side, needs a central controller that employs the universal information of all the link gains in order to avoid the interference. However, this method results in a high latency and heavy signalling in the system [116]. Therefore, this thesis considers the distributed EE approach.

A key design parameter in the LTE-Advanced networks is the bit-per-joule EE, defined as [111]:

$$EE = \frac{\text{Throughput (bits/s)}}{\text{Power consumption (Joule/s)}} [\text{bits/Joule}] \quad (2)$$

As observed from (2), the EE is measured in bits/Joule to represent the effectiveness with which the energy in Joule is employed for information transmission. It is also observed from the same equation, that the EE of a wireless network can be increased by using methods which maximise the system throughput or minimise energy consumption, or both. The EE equation (2) is referred to a single communication link, but the expression becomes more involved in a communication network based on the advantages and cost incurred by each single link and/or the proposed multiple network-wide performance functions. In [111], the authors identified two formulation approaches for EE problem called network benefit-cost ratio and multi-objective approach. The network benefit-cost ratio approach, also known as the global EE, is represented by a ratio between the sum of all single advantages of different links and the overall power consumption in the networks [119]. The multi-objective approach, on the other hand, regards each single node as a different EE objective function to optimise, leading to a multiple objective resource allocation [120]. In addition, the EE maximisation problem can also be executed subject to all practical constraints that are characteristically enforced in the communications networks. Those practical constraints can be the following: QoS constraints, maximum power constraint, minimum delay constraints [121], minimum rate guarantees [122], interference temperature constraints [123] and maximal delay bound constraints [124].

4.2 Approaches to Manage the LTE-Advanced Challenges

In this sub-section, we present the focused approaches in this thesis to manage the aforementioned challenges, which are the efficient coverage extension, the interference management and EE optimisation challenges. These approaches are the optimal and energy efficient RNs placement for effective coverage extension, the pre-coding and decoding design (transceivers), and pilot-assisted channel estimation.

4.2.1 Optimal and Energy Efficient RNs Placement with Greedy Algorithm

The RNs help increase the cell coverage or cell radius for the same cell capacity and provide higher cell capacity in a given cell area because of the link diversity. Moreover, deploying RN is advantageous such that it reduces the infrastructure cost of deploying more base stations. Hence, the coverage extension is achieved through the RN placement since the RNs provide better SINR to the cell edge users, compared to the normal BSs due to their proximity to the users. However, the RNs need to be placed at a right location to ensure an effective coverage and optimise the energy consumption of the cell edge users. Thus, in this thesis, an optimal and energy efficient RNs placement approach is considered to place the RNs in the LTE-Advanced networks, subject to the energy consumption constraint, in order to improve the communication and reliability between the users and the BSs. The greedy algorithm is improved to design an optimal and energy efficient algorithm for the RNs placement that maximises the system coverage subject to the energy cost constraint while maintaining the signal-to-interference-ratio (SIR). This improvement in the greedy algorithm can enable an effective RN placement, only if the Matroid rank function of the effective coverage extension problem is submodular and monotonic.

Many problems using greedy approach to find the near optimal solution can be defined as a problem consisting of finding a maximum-weight independent subset in weighted Matroid. So a weighted Matroid $\mathcal{M} = (E, \mathcal{I})$ is a Matroid which is associated to weight function w that assigns a positive weight $w(e)$ to each element $e \in E$. For a given weighted Matroid $\mathcal{M} = (E, \mathcal{I}, w)$, we need to find an independent subset A such that $A \in \mathcal{I}$ and $w(A)$ is maximised. That means, the algorithm works for any weighted Matroid with the guarantee of finding a near-optimal solution. In general, the greedy algorithm is formulated for a given weighted Matroids $\mathcal{M} = (E, \mathcal{I}, w)$ as: the input will be $\mathcal{M} = (E, \mathcal{I}, w)$ with a weight function w (such that w is positive), the output will be an independent subset $A \in \mathcal{I}$ called optimal subset of Matroid. Algorithm 1 illustrates the greedy algorithm [125].

Algorithm 1 Greedy (\mathcal{M}, w)

- 1: $A := \emptyset$
 - 2: Sort E into monotonically decreasing order by weight w
 - 3: **for** each $e \in E$, taken in monotonically decreasing order by weight $w(e)$ **do**
 - 4: **if** $A \cup e \in \mathcal{I}$ **then**
 - 5: $A := A \cup e$
 - 6: **Return** A
-

4.2.2 Pre-coding and Decoding Design

Pre-coding and decoding design, also known as transceivers design, is a technique commonly used in recent research [126], [127] to manage the interferences and retrieve the intended signal at the receiver side. The pre-coding and decoding concept works as follows: the transmitted signals from the different antennas are weighted pre-coding matrices to maximise the received SNR. At the receiver, the pre-coded signals are decoded using decoding matrices. This method is mainly considered in this thesis due to its great impact on the performance of the whole network and the improvement of the range data rate and for its effectiveness in the mitigation of interference.

In this thesis, the decentralised pre-coding and decoding matrices are designed for the femtocells, the MUEs and the cell-edge MUEs (CUEs) based on MMSE criteria in a cooperative MU-MIMO relay system. The transceivers are iteratively updated to minimise the MSE, subject to the total transmit power. These MMSE pre-coders and decoders are designed with the pilot-assisted channel estimators for more realistic scenarios which improve the accuracy of the the CSI. The information received from the channel after estimation is used to generate the optimal pre-coders and decoders in order to minimise the MSE that improves the performance of the system. In the algorithms, the MSE problem is bounded below zero and decreases at each iteration while the pre-coders and decoders are updating until the optimal values that minimises the MSE are reached.

Furthermore, the decentralised pre-coders and decoders are also designed to optimise the EE of the femtocells, RNs, MUEs and CUEs based on the WMMSE in a half-duplex MU-MIMO relay system. CUEs are grouped into clusters and transmit to the MBS through the RN in two time slots. The EE optimisation problems are also formulated as convex optimisation for each FAPs, CUEs and MUEs depending on the time slot they are transmitting. The WMMSE is employed to optimally and iteratively determine the pre-coders and decoders and is based on the relationship between the SINR and the MSE.

4.2.3 Pilot-Assisted Channel Estimation

Channel estimation received an enormous attention in past years because of its importance in wireless communications. Without a good channel estimator, the throughput and coverage of the a wireless system is severely limited. The transmit pilot multiplexes the known symbols with information bearing the data. These transmit pilot symbols are assumed to be known at the receiver side and are exploited for the channel estimation and the optimal decoding. In this work, the pilot-assisted channel estimation is considered where some of the channel bandwidth is reserved for transmitting pilot (training) signals to the receiver and using them to estimate the channel. By sacrificing some bandwidth efficiency to transmit pilot signals, the pilot-assisted channel estimators can typically make fast and accurate measurements of the channel. There are two main pilot patterns, the comb-type and block-type patterns. The block-type pattern reserves periodically one symbol for just pilot transmission. The comb-type pattern allocates few sub-carriers for pilot transmission in every OFDM symbol. The comb-type arrangement is considered in this thesis due to its ability to track the variation of the channel caused by Doppler frequency. There are different types of channel estimators such as maximum likelihood (ML) estimator [128], minimum mean-squared error (MMSE) estimator [129], the least-squares (LS) estimator [130], space-alternating generalised expectation-maximisation (SAGE) estimator [131] and others. Due to their simplicity and complexity performance, the two common estimators particularly used in this research for performing estimation at the pilot sub-carriers are the MMSE estimator and the LS estimator. Both channel estimators are considered in the design of transceivers and are compared in the second research paper of this thesis.

1. *The LS channel estimator* is a simple, low-complexity alternative to the MMSE, but cannot achieve the level of performance of the MMSE estimator. The aim of LS channel estimator is minimising the square distance between the original signal and the received signal [132]. The channel estimates are simply found by multiplying the received pilot by the inverse of the known transmitted pilot [130], i.e. consider the following received pilot signal Y_p expressed as [133]:

$$Y_p = \mathbf{H}_p X_p + z_p, \quad (3)$$

where $(\cdot)_p$ is the positions where reference signals are transmitted. \mathbf{H}_p and X_p are the channel frequency response and the matrix containing the transmitted elements on its diagonals, respectively. z_p denotes the noise vector whose entries have the i.i.d. complex Gaussian distribution with zero mean and variance σ^2 and it is assumed that z_p is uncorrelated with the channel \mathbf{H}_p [132]. From (3), the LS estimates of the channel at the pilot sub-carriers is

obtained as

$$\hat{\mathbf{H}}_p^{\text{LS}} = \frac{Y_p}{X_p}, \quad (4)$$

where $\hat{\mathbf{H}}_p^{\text{LS}}$ is the LS estimates obtained over the pilot sub-carriers. The LS estimator performs well at high SNR but quickly degrades as the noise level increases and suffers from high mean-square error (MSE) [134].

2. *The MMSE channel estimator* predicts more current channel estimate from the delayed LS estimates as the coefficient is adjusted depending on the delay of the LS estimate. It is designed to minimise the MSE estimation. Considering the equation (3), the MMSE estimates the channel responses as follows:

$$\mathbf{H}_p^{\text{MMSE}} = \mathbf{R}_{HH_p} \left(\mathbf{R}_{H_p H_p} + \sigma_{z_p}^2 (X X_p)^{-1} \right)^{-1} \hat{\mathbf{H}}_p^{\text{LS}}, \quad (5)$$

where \mathbf{R}_{HH_p} denotes the cross-correlation matrix between all sub-carriers and the sub-carriers with the reference signals while $\mathbf{R}_{H_p H_p}$, on the other hand, is the autocorrelation matrix of the sub-carriers with reference signals. It depends on second-order channel statistics and can produce a very accurate estimate when the channel statistics are known. Hence, this estimator can be computationally complex because it depends on a matrix inversion in equation (5) and requires knowledge of the channel to be effective. This complexity, however, can be reduced by averaging the transmitted data [132]. Therefore, $(X X_p)^{-1}$ in (5) is replaced with its expectation $\mathbb{E}[(X X_p)^{-1}]$. The simplified form of MMSE channel estimator is expressed as [135]:

$$\hat{\mathbf{H}}_p^{\text{MMSE}} = \mathbf{R}_{HH_p} \left(\mathbf{R}_{H_p H_p} + \frac{\beta}{SNR} \mathbf{I}_p \right)^{-1} \tilde{\mathbf{H}}_p^{\text{LS}}, \quad (6)$$

where β represents the scaling factor which depends on the signal constellation like QPSK ($\beta = 1$) and 16QAM ($\beta = 17/9$) and \mathbf{I}_p denotes the identity matrix.

5 Research Motivation

In the next generation of wireless communication network, HetNets architecture with macrocells, small-cells and relays offers numerous advantages such as higher spectrum efficiency, better fairness in resource allocation and energy efficient usage as well as effective coverage extension. However, these approaches encounter various network management challenges such as coverage extension, EE and interference management. These challenges are critical factors in the LTE-Advanced networks that need to be properly addressed to improve the throughput and capacity of the overall networks. It is worth specifying that the macrocell coverage could not meet the demand set of the mobile data rate

growth at high rate level. Due to the spatial, financial and regulatory constraints, setting up macrocell everywhere needed, is not feasible.

The solution to this issue was to break the large macrocell into smaller low-powered cells and to assure a cooperative communication between the MBS and these small-cells inside macrocell coverage. Although the deployment of small-cells solved the coverage problem, they increased the handoff rate of mobiles users among the adjacent cells and degraded the EE of the whole network. Moreover, this deployment increases or creates new interference challenges known as cross-tier and co-tier interferences. The users located at the cell-edge of the network still suffer from system performance degradation, due to high energy consumption and inter-cell interference. The high energy consumption is attributed to the long distance between the cell-edge users and the BS with limited transmit power antennas. The inter-cell interference is generated when the transmission from one cell to neighbouring cells occurs at the same time and same frequency. The addition of RNs to the MU-MIMO system further enhances the transmission between the cell-edge users and the BS. Furthermore, processing technology of RNs helps reduce the effect of interference. However, the placement of RN at the right position is important to achieve better system performance for cell-edge users and effective coverage extension. The small-cells considered throughout this study are femtocells and RNs such that the femtocells provide better cellular connectivity to the mobile users compared to other femtocells and the RNs improve the network reliability. Mobiles users have more tendency to shift from mobile voice traffic to mobile data traffic like social video services, when it comes to use the mobile networks. This results in a enormous use of data bandwidth and energy. Therefore, the effective coverage extension, interference management and EE optimisation are among the great challenges in LTE-Advanced networks, due to the enormous growth of mobile networks and the increase of the data volume transferred by users. Managing the interference, efficiently extending the network coverage and optimising the EE are the challenges that can be solved together so that when optimising one, it also affect the others and vice versa. These are the challenges that this work aims to solve.

6 Objectives of the Research

The purpose of this research is summarised as follows:

- To investigate the effective coverage extension in LTE-Advanced network where energy efficient and optimal algorithm for the RN placement is proposed in order to improve the nodes energy consumption. This is achieved by introducing and combining the concept of Matroids, submodularity and monotonicity optimisation in the design of an improved greedy algorithm

for optimal RN placement.

- To manage the interferences in cooperative LTE-Advanced networks, particularly the cross-tier interference by designing decentralised pre-coders and decoders (transceivers) algorithms with pilot-aided channel estimators.
- To optimise the EE using proposed decentralised transceiver design for the CUEs, MUEs and FAPs during both the first and second time slots. The EE problem is formulated as a convex optimisation problem where the transceivers are designed using the WMMSE and Lagrange duality.

7 Research Methodology: Analytical Tools

In order to contribute to the knowledge, apart from the simulations, the following analytical tools have been considered throughout this work; Sub-modularity, monotonicity optimisation, Matroid, convex optimisation and Lagrange Duality. Sub-modularity, monotonicity optimisation, Matroid are widely used in wireless sensor networks [74] and are also be considered in LTE-Advanced networks due to their ability to find a near optimal solution. When used altogether, they can offer optimal solution, hence are considered in this thesis for energy efficient and optimal placement of RN in a LTE-Advanced networks in order to achieve effective coverage extension. Convex optimisation and Lagrange duality are considered to formulate the optimisation problem for interference management and EE in a cooperative LTE-Advanced system where a RN placement is assumed to be properly done. Convex optimisation has been mostly used in LTE-Advanced networks. Today, it serves as a new indispensable computational tool, which increases the ability to solve problems such as linear programming and LS to a much richer and larger class of problems. In this thesis, we use the Python and Matlab programming languages for simulations. Furthermore, to efficiently solve the convex optimisation problems, we use the widely-adopted software toolbox named CVX.

7.1 Sub-modularity, Monotonicity Optimisation and Matroid

Sub-modularity is defined as a property of set function with deep theoretical consequences and far reaching applications. In one way, sub-modularity appears to be similar to concavity and in other ways it resembles to convexity. Sub-modularity is used in various computer science applications such as image segmentation, information gathering, sensors deployment and RN deployment. Sub-modularity, monotonicity optimisation and Matroid methods are considered in this thesis to improve the greedy algorithm for an energy efficient RN placement in a LTE-Advanced networks. Greedy

algorithm is defined as an algorithm that iteratively makes the optimal choice at the moment, the choice that seems the best until the near-optimal solution is found.

7.1.1 Sub-modularity and Monotonicity

The notion of sub-modularity is defined as follows; let \mathcal{S} be a set of possible locations. The function $F : 2^{\mathcal{S}} \rightarrow \mathbb{R}$ is sub-modular if:

1. $\forall \mathcal{A} \subseteq \mathcal{B} \subseteq \mathcal{S}$ and $\forall x \in \mathcal{S} \setminus \mathcal{B}$:

$$F(\mathcal{A} \cup \{x\}) - F(\mathcal{A}) \geq F(\mathcal{B} \cup \{x\}) - F(\mathcal{B}). \quad (7)$$

2. Equivalently, $\forall \mathcal{A}, \mathcal{B} \subseteq \mathcal{S}$, we have:

$$F(\mathcal{A}) + F(\mathcal{B}) \geq F(\mathcal{A} \cap \mathcal{B}) + F(\mathcal{A} \cup \mathcal{B}). \quad (8)$$

Considering the set of possible locations \mathcal{S} and all subsets \mathcal{A}, \mathcal{B} such that $\mathcal{A} \subseteq \mathcal{B}$, the monotonicity concept is commonly defined as follows

$$F(\mathcal{A}) \leq F(\mathcal{B}). \quad (9)$$

The reason to consider sub-modularity is that if F is sub-modular and monotone, then a greedy approach for RN placement is not far from being optimal.

7.1.2 Matroid

We consider the notion of Matroid to guarantee optimal and energy efficient placement of the RN once the rank function of the Matroid is found to be both monotonic and sub-modular. To properly define the Matroid in this thesis, we need to consider a finite set E , named a ground set and \mathcal{I} , a family or set of subset of $E, \mathcal{I} \subseteq P(E)$ named independent set.

The pair (E, \mathcal{I}) is considered to be a Matroid \mathcal{M} , if and only if, the following properties are satisfied by the Matroid \mathcal{M} .

1. \mathcal{I} is non-empty set of subsets of E where if $\mathcal{B} \subseteq \mathcal{A}$ and $\mathcal{A} \in \mathcal{I}$ then $\mathcal{B} \in \mathcal{I}$. The family \mathcal{I} is sometimes said to be *hereditary*.
2. If $\mathcal{A}, \mathcal{B} \in \mathcal{I}$ and $|\mathcal{A}| > |\mathcal{B}|$, then there is an element $\{x\} \in \mathcal{A} \setminus \mathcal{B}$ such that $(\mathcal{B} \cup \{x\}) \in \mathcal{I}$. That is called the *exchange property*.

The dependent sets are defined as the subset of the ground E that are not in \mathcal{I} . We denote B as a maximal independent set B that is a subset of finite set E in Matroid $\mathcal{M} = (E, \mathcal{I})$ becomes dependent,

if for any $\{x\} \in E \setminus \mathcal{B}$, we have $\{x\} \cup \mathcal{B}$ then a maximal independent set is called base of Matroid \mathcal{M} . The rank function of a Matroid $\mathcal{M} = (E, \mathcal{I})$ is a function $r : 2^E \rightarrow \mathbb{N}$ satisfying:

1. $\forall \mathcal{A} \subseteq E, r(\mathcal{A}) \leq |\mathcal{A}|$ (cardinality bound). (10)

2. If \mathcal{A}, \mathcal{B} are subsets of E , with $\mathcal{A} \subseteq \mathcal{B}$, then $r(\mathcal{A}) \leq r(\mathcal{B})$. This is monotonicity. (11)

3. $\forall \mathcal{A}, \mathcal{B} \subseteq E$, we have $r(\mathcal{A}) + r(\mathcal{B}) \geq r(\mathcal{A} \cup \mathcal{B}) + r(\mathcal{A} \cap \mathcal{B})$. This is sub-modularity. (12)

By the equations (11) and (12), we can say that the Matroid rank function is a sub-modular and monotone function.

7.2 Convex Optimisation

Convex optimisation is described as a fusion of three different disciplines, convex analysis [136], optimisation [137] and numerical computation [138]. It has recently become a tool of central importance in wireless communication and networking, enabling the solution of large problems. Formulating and converting communication problems into convex optimisation problems facilitate their analytic and numerical solutions. In this thesis, the convex optimisation technique is considered to design and formulate the sum-MSE and EE optimisation problems. This technique is utilised because the optimal solution can be verified with the existing rigorous optimality conditions and duality theory. It means that when the designed optimisation problems are converted into convex forms, the structure of the optimal solution can efficiently be identified [139].

In general, the mathematical optimisation problem has the following form

$$\min_{x \in Z \subseteq \mathbb{R}^n} f(x) \tag{13}$$

where x describes a vector known as the optimisation variable, $f : \mathbb{R}^n \rightarrow \mathbb{R}$ denotes a convex function which needs to be minimise, and Z is a convex set describing the set of feasible solutions. From a computational perspective, convex optimisation problems are interesting in the sense that any locally optimal solution will always be guaranteed to be globally optimal. One of the effective concepts of convex optimisation considered in this thesis, is called Lagrange Duality. More particularly, the Karush-Kuhn-Tucker (KKT) conditions and Lagrange multipliers which are part of Lagrange duality. These two methods provide important and efficient optimality conditions for convex optimisation problems.

7.3 Lagrange Duality

It is known that the theory of Lagrange duality is the study of optimal solutions to convex optimisation problems. In the more general setting of the convex optimisation problem with constraints, however,

this simple optimality condition does not work. One primary goal of duality theory is to characterise the optimal points of convex programs in a mathematically rigorous way.

To explain and define the Lagrange duality and Lagrange multiplier, we consider a generic differentiable convex optimisation problems of the following form;

$$\begin{aligned} \min_{x \in Z \subseteq \mathbb{R}^n} f(x) \\ \text{s. t. } g_i(x) \leq 0, i = 1, \dots, j, \\ h_i(x) = 0, i = 1, \dots, k, \end{aligned} \quad (14)$$

where $g_i, h_i : \mathbb{R}^n \rightarrow \mathbb{R}$ represent differentiable convex functions and the affine functions, respectively.

7.3.1 Lagrange Multiplier

This study considers the artificial looking construct known as the '*Lagrange multiplier or Lagrangian*'. This method is considered as the Lagrange duality basis. Considering the above constrained convex optimisation problem in (14), the generalised Lagrange multiplier is a function $\mathcal{L} : \mathbb{R}^n \times \mathbb{R}^j \times \mathbb{R}^k \rightarrow \mathbb{R}$, expressed as

$$\mathcal{L}(x, \alpha, \beta) = f(x) + \sum_{i=1}^j \alpha_i g_i(x) + \sum_{i=1}^k \beta_i h_i(x), \quad (15)$$

where the first term is the vector $x \in \mathbb{R}^n$ which has the same dimension as the optimisation variable in the problem (14), by convention, the vector x is referred as the prime variable of the Lagrange multiplier. The second term of the Lagrange multiplier is the $\alpha \in \mathbb{R}^j$ with a variable α_i for each of the j convex inequality constraints in (14). The third term in (15) is a vector $\beta \in \mathbb{R}^k$ with a variable β_i for each of the k affine equality constraints in (14). These variables of α and β are globally referred as the Lagrange multipliers of the dual variables. When associated with different violating constraints, the Lagrangian dual variables α_i and β_i can be thought as *costs*.

7.3.2 Karush-Kuhn-Tucker

Incidentally, the KKT theorem was originally derived by Karush in 1939 but did not catch any attention until it was rediscovered in 1950 by Kuhn and Tucker [140]. A variant of essentially the same result was also derived by John in 1948. Finally, given everything so far, we can now characterise the optimal conditions for a primal dual optimisation pair. We have the following theorem:

Theorem 1. Assume that $x^* \in \mathbb{R}^n, \alpha^* \in \mathbb{R}^j$ and $\beta^* \in \mathbb{R}^k$ satisfy the following conditions:

1. The primal feasibility: $g_i(x^*) \leq 0, i = 1, \dots, j$ and $h_i(x^*) = 0, i = 1, \dots, k,$
2. The dual feasibility: $\alpha^* \geq 0, i = 1, \dots, j,$

3. *The complementary slackness:* $\alpha_i^* g_i(x^*) = 0, i = 1, \dots, j$, and
4. *The Lagrange multiplier stationarity:* $\nabla_x \mathcal{L}(x^*, \alpha^*, \beta^*) = \mathbf{0}$.

where x^* and (α^*, β^*) is primal and the dual optimal, respectively. Moreover, in a case where the strong duality holds, any primal optimal x^* and dual optimal (α^*, β^*) must satisfy all the 4 conditions. These conditions are known as the KKT conditions. These analytical tools help to find the optimal solutions and are employed in the design of optimal transceivers to solve the EE maximisation problems and the sum-MSE problem, which manages the interference in the MU-MIMO relay systems.

8 Main Contributions

The main contributions of this research are described as follows:

8.1 PAPER A: Energy Efficient Coverage Extension Relay Node Placement in LTE-A Networks

Deployed Long Term Evolution-Advanced (LTE-A) infrastructure may need coverage extension due to exponential growth of mobile broadband data usages as well as poor network performance along the cell edges. A proper installation of Relay Nodes (RN) extends the network coverage in LTE-A networks. In this paper, we propose an energy efficient and optimal RN placement (EEORNP) algorithm that maximises the network coverage under the energy constraint, while maintaining the signal-to-interference ratio (SIR). The proposed algorithm is based on an improved greedy algorithm where an effective and optimal RN placement is guaranteed when the Matroid rank function of the energy efficient coverage extension optimisation is sub-modular and monotonic. The performance is investigated in terms of coverage percentage and number of RN needed to cover users. Simulation results show that the proposed EEORNP outperforms both greedy and random placement algorithms.

8.2 PAPER B: Interference Management in LTE-Advanced Cooperative Relay Networks: Decentralized Transceiver Design with Channel Estimation

Wireless networks improve indoor communications by deploying femtocell networks into the macrocell coverage. This results in spectrum sharing with the consequences of cross-tier interference from the macrocell user equipments (MUEs) to the femtocell access points (FAPs). This work considers the uplink cross-tier interference management for the cell-edge MUEs (CUEs) in cooperative multi-user multiple input multiple output (MU-MIMO) systems. For better interference

management, the CUEs are grouped into clusters and communicate to the macrocell base station (MBS) through a relay node (RN). The linear pre-coders and decoders algorithms for the FAPs, MUEs and CUEs are proposed for effective interference management to minimize the sum mean square error (MSE), subject to the total transmit power constraints. The designed pre-coders and decoders use the pilot-assisted channel estimation to improve the accuracy of the acquired channel state information (CSI). The least square (LS) and minimum MSE (MMSE) channel estimators are considered. The performance of the system is investigated in terms of the bit error rate (BER) for the linear pre-coders and decoders algorithms with the pilot-assisted channel estimators.

8.3 PAPER C: Energy Efficient Transceiver Design for Cooperative Multi-User MIMO Systems

This work undertakes an efficient transceivers design that optimises energy efficiency (EE) in multi-user multiple-input multiple-output (MU-MIMO) relay systems. In this system, cell-edge macrocell user equipments (CUEs) are grouped into clusters and communicate with the macrocell base station (MBS) through a relay node (RN). The macrocell UEs (MUEs), on the other hand, communicate directly with the MBS. The femtocell UEs (FUEs) communicate with their respective femtocell access points (FAPs). The centralised transceiver design for such a system is not trivial. This work proposes decentralised algorithms with perfect channel state information (CSI) to optimise the linear transceivers for the multi-users and the RN. This is done under the quality of service (QoS) and transmit power constraints to achieve the EE maximisation. The weighted minimum mean square error (WMMSE) is employed in the design of the decentralised algorithms. Parameter subtractive functions are introduced into each proposed schemes to surmount the non-convexity of the formulated EE optimisation problem. These parameters are updated by the Dinkelbach's algorithm. The performance investigation demonstrates the superiority of the proposed over existing scheme in terms of the average EE and convergence.

References

- [1] L. J. Vora, "Evolution of mobile generation technology: 1G to 5G and review of upcoming wireless technology 5G," 2015.
- [2] M. Mouly, M.-B. Pautet, and T. Foreword By-Haug, *The GSM system for mobile communications*. Telecom publishing, 1992.
- [3] J. S. Lee and L. E. Miller, *CDMA systems engineering handbook*. Artech House, Inc., 1998.
- [4] M. Mir and S. Kumar, "Evolution of mobile wireless technology from OG to 5G," *International Journal of Computer Science and Information Technologies*, vol. 6, no. 3, pp. 2545–2551, 2015.
- [5] T. Ojanpera and R. Prasad, "WCDMA: Towards IP mobility and mobile internet, artech house," *Inc., Norwood, MA*, 2001.
- [6] J. Agrawal, R. Patel, P. Mor, P. Dubey, and J. Keller, "Evolution of mobile communication network: From 1G to 4G," *International Journal of Multidisciplinary and Current Research*, vol. 3, pp. 1100–1103, 2015.
- [7] I. Poole, "LTE OFDM, OFDMA SC-FDMA and modulation," *Radio electronics (Online)*. Available: www.radio-electronics.com/cellulartelecomms/long-term-evolution. Accessed, vol. 10, 2015.
- [8] O. Oshin, M. Luka, and A. Atayero, "From 3GPP LTE to 5G: An evolution," in *Springer Trans. Engineering Technol.*, 2016, pp. 485–502.
- [9] E. W. paper, "Differentiated mobile broadband," 2011.
- [10] C. W. paper, "Cisco visual networking index: Global mobile data traffic forecast update," 2012.
- [11] A. Gosh and R. Ratasuk, *Essentials of LTE and LTE-A*. Cambridge University Press, 2011.
- [12] J. Cao, M. Ma, H. Li, Y. Zhang, and Z. Luo, "A survey on security aspects for LTE and LTE-A networks," *IEEE Commun. Surveys Tuts*, vol. 16, no. 1, pp. 283–302, 2014.
- [13] A. Yahya, "Opportunities, challenges, and terms related to LTE-A cellular networks," in *Springer LTE-A Cellular Netw.*, 2017, pp. 5–40.
- [14] M. S. Ali, "An overview on interference management in 3GPP LTE-advanced heterogeneous networks," *International Journal of Future Generation Communication and Networking*, vol. 8, no. 1, pp. 55–68, 2015.
- [15] I. F. Akyildiz, D. M. Gutierrez-Estevez, and E. C. Reyes, "The evolution to 4G cellular systems: LTE-Advanced," *Physical communication*, vol. 3, no. 4, pp. 217–244, 2010.
- [16] S. Sesia, M. Baker, and I. Toufik, *LTE-the UMTS long term evolution: from theory to practice*. John Wiley & Sons, 2011.
- [17] K. R. Rao, Z. S. Bojkovic, and B. M. Bakmaz, *Wireless multimedia communication systems: design, analysis, and implementation*. CRC Press, 2017.

REFERENCES

- [18] Z. Bharucha, E. Calvanese, J. Chen, X. Chu, A. Feki, A. De Domenico, A. Galindo-Serrano, W. Guo, R. Kwan, J. Liu *et al.*, “Small cell deployments: Recent advances and research challenges,” *arXiv preprint arXiv:1211.0575*, 2012.
- [19] “3rd Generation Partnership Project; Technical Specification Group Services and System Aspects; IP Multimedia Subsystem (IMS); (Rel 11), 3GPP TS 23.228 V11.6.0,” Sep. 2012.
- [20] “3rd Generation Partnership Project; Technical Specification Group Services and System Aspects; Service requirements for Home Node B (HNB) and Home eNode B (HeNB) (Rel 11) , 3GPP TS 22.220 V11.6.0,” Sep. 2012.
- [21] “3rd Generation Partnership Project; Technical Specification Group Services and System Aspects; Service requirements for the Evolved Packet System (EPS) (Rel 12), 3GPP TS 22.278 V12.1.0,” June 2012.
- [22] “3rd Generation Partnership Project; Technical Specification Group Core Network and Terminals; Access to the 3GPP Evolved Packet Core (EPC) via non-3GPP access networks (Rel 11), 3GPP TS 24.302 V11.4.0,” Sep. 2012.
- [23] “3rd Generation Partnership Project; Technical Specification Group Services and System Aspects; Service requirements for Machine-Type Communications (MTC) (Rel 12), 3GPP TS 22.368 V12.0.0,” Sep. 2012.
- [24] M. Jamal, B. Horia, K. Maria, and I. Alexandru, “Study of multiple access schemes in 3GPP LTE OFDMA vs. SC-FDMA,” in *Proc. IEEE Int. Conf. Applied Electronics (AE)*, 2011, pp. 1–4.
- [25] B. Hanta, “SC-FDMA and LTE uplink physical layer design,” *Siminar LTE: Der Mobilfunk der Zukunft, University of Erlangen-Nuremberg, LMK*, 2009.
- [26] S. Hanchate, S. Borsune, and S. Nema, “Comparative study of PAPR performances for different subcarrier mapping techniques in SC-FDMA,” *International Journal of Electronics, Communication Instrumentation Engineering Research and Development (IJECIERD)*, vol. 5, no. 1, 2015.
- [27] K. Meik, “LTE-Advanced technology introduction white paper,” *Rhode & Schwarz*, pp. 3–22, 2010.
- [28] B. Z. Maha and R. Kosai, “Multi user MIMO communication: Basic aspects, benefits and challenges,” in *Recent Trends in Multi-user MIMO Commun.* InTech, 2013.
- [29] M. B. Zid, K. Raouf, and A. Bouallegue, “MIMO systems and cooperative networks performances,” *Advanced Cognitive RadioNetwork*, 2012.
- [30] C.-X. Wang, X. Hong, X. Ge, X. Cheng, G. Zhang, and J. Thompson, “Cooperative mimo channel models: A survey,” *IEEE Commun. Mag.*, vol. 48, no. 2, 2010.
- [31] D. Lee, H. Seo, B. Clerckx, E. Hardouin, D. Mazzaresse, S. Nagata, and K. Sayana, “Coordinated multipoint transmission and reception in LTE-Advanced: deployment scenarios and operational challenges,” *IEEE Commun. Mag.*, vol. 50, no. 2, 2012.

- [32] D. Gesbert, S. Hanly, H. Huang, S. S. Shitz, O. Simeone, and W. Yu, "Multi-cell MIMO cooperative networks: A new look at interference," *IEEE Journal on Sel. Areas in Commun.*, vol. 28, no. 9, pp. 1380–1408, 2010.
- [33] H. Y. Shen, H. Yang, and S. Kalyanaraman, "Energy efficient cooperative mimo systems," in *Proc. of INFOCOM*, 2008, pp. 1–9.
- [34] Z. Bai, Y. Xu, D. Yuan, and K. Kwak, "Performance analysis of cooperative MIMO system with relay selection and power allocation," in *Proc. IEEE Int. Conf. Commun. (ICC)*, 2010, pp. 1–5.
- [35] L. Nagel, S. Pratschner, S. Schwarz, and M. Rupp, "Efficient multi-user mimo transmission in the LTE-A uplink," in *Link-and System Level Simulations (IWSLS), International Workshop on.* IEEE, 2016, pp. 1–6.
- [36] L. Liu, R. Chen, S. Geirhofer, K. Sayana, Z. Shi, and Y. Zhou, "Downlink MIMO in LTE-Advanced: SU-MIMO vs. MU-MIMO," *IEEE Commun. Mag.*, vol. 50, no. 2, 2012.
- [37] R. Liao, B. Bellalta, M. Oliver, and Z. Niu, "MU-MIMO MAC protocols for wireless local area networks: A survey," *IEEE Commun. Surveys & Tuts*, vol. 18, no. 1, pp. 162–183, 2016.
- [38] C. Le, S. Moghaddamnia, and J. K. Peissig, "A hybrid optimization approach for interference alignment in multi-user MIMO relay networks under different CSI," *IEEE Trans. Wireless Commun.*, vol. 16, no. 12, pp. 7834–7847, 2017.
- [39] Q. H. Spencer, C. B. Peel, A. L. Swindlehurst, and M. Haardt, "An introduction to the multi-user MIMO downlink," *IEEE Commun. Mag.*, vol. 42, no. 10, pp. 60–67, 2004.
- [40] Y. Hayashi, I. Shubhi, and H. Murata, "User collaboration for interference cancellation on multi-user mimo communication systems," in *Proc. 82nd IEEE Veh. Technol. Conf. (VTC Fall)*, 2015, pp. 1–5.
- [41] T. T. Vu, H. H. Kha, and T. Q. Duong, "Interference alignment designs for secure multiuser mimo systems: Rank constrained rank minimization approach," in *Proc. IEEE Int. Conf. Commun., Management and Telecommun.s (ComManTel)*, 2015, pp. 116–121.
- [42] E. Björnson, L. Sanguinetti, J. Hoydis, and M. Debbah, "Optimal design of energy-efficient multi-user MIMO systems: Is massive MIMO the answer?" *IEEE Trans. Wireless Commun.*, vol. 14, no. 6, pp. 3059–3075, 2015.
- [43] H. Q. Ngo, E. G. Larsson, and T. L. Marzetta, "Energy and spectral efficiency of very large multiuser MIMO systems," *IEEE Trans. Commun.*, vol. 61, no. 4, pp. 1436–1449, 2013.
- [44] N. C. Luong, P. Wang, D. Niyato, Y.-C. Liang, F. Hou, and Z. Han, "Applications of economic and pricing models for resource management in 5G wireless networks: A survey," *arXiv preprint arXiv:1710.04771*, 2017.
- [45] A. Jhansi ran and N. Venkatesan, "Typical heterogeneous network deployment in green cellular networks," *Int. Journal of Computer Science and Engineering Commun.*, vol. 5, no. 1, 2017.

- [46] A. A. Jasim and S. A. Mawjoud, "LTE heterogeneous network: a case study," *International Journal of Computer Applications*, vol. 61, no. 8, 2013.
- [47] M. Reardon, "Cisco predicts wireless data explosion," *Press release*, 9th Feb, 2010.
- [48] P. Sambanthan and T. Muthu, "Interference avoidance through pilot-based spectrum sensing algorithm in overlaid femtocell networks," *ETRI Journal*, vol. 38, no. 1, pp. 30–40, 2016.
- [49] S. Rajanandhini and R. Suganya, "An improved M- layer architecture to minimize energy in heterogeneous wireless networks," *Int. Journal of Adv. Research in Computer and Commun. Engineering (IJARCCE)*, vol. 5, no. 11, pp. 112–116, 2016.
- [50] A. Rustako, N. Amitay, G. Owens, and R. Roman, "Radio propagation at microwave frequencies for line-of-sight microcellular mobile and personal commun." *IEEE Trans. Veh. Technol.*, vol. 40, no. 1, pp. 203–210, 1991.
- [51] R. Coombs and R. Steele, "Introducing microcells into macrocellular networks: A case study," *IEEE Trans. Commun.*, vol. 47, no. 4, pp. 568–576, 1999.
- [52] A. S. Bhosle, "Emerging trends in small-cell technology," in *Proc. IEEE Int. Conf. Electrical, Instrumentation and Commun. Engineering (ICEICE)*, 2017, pp. 1–4.
- [53] D. Lopez-Perez, I. Guvenc, G. De la Roche, M. Kountouris, T. Q. Quek, and J. Zhang, "Enhanced intercell interference coordination challenges in heterogeneous networks," *IEEE Wireless Commun.*, vol. 18, no. 3, 2011.
- [54] L. Saker, S.-E. Elayoubi, L. Rong, and T. Chahed, "Capacity and energy efficiency of picocell deployment in LTE-A networks," in *Proc. 73rd IEEE Veh. Technol. Conf. (VTC Spring)*, 2011, pp. 1–5.
- [55] A. B. Saleh, Ö. Bulakci, S. Redana, B. Raaf, and J. Hämäläinen, "Evaluating the energy efficiency of LTE-Advanced relay and picocell deployments," in *Wireless Commun. and Networking Conference (WCNC), 2012 IEEE*. IEEE, 2012, pp. 2335–2340.
- [56] P. Sambanthan and t. Muthu, "Why femtocell networks?" *Global Journal of research In Engineering*, 2017.
- [57] K. R. Chaudhary and R. Arya, "Comparison of SINR in Femtocell & Macrocell network in macrocell environment," *International Journal of Engineering And Computer Science*, vol. 2, no. 08, 2013.
- [58] V. Chandrasekhar, J. G. Andrews, and A. Gatherer, "Femtocell networks: a survey," *IEEE Commun. Mag.*, vol. 46, no. 9, 2008.
- [59] P. Xia, V. Chandrasekhar, and J. G. Andrews, "Open vs. closed access femtocells in the uplink," *IEEE Trans. Wireless Commun.*, vol. 9, no. 12, pp. 3798–3809, 2010.
- [60] S. Padmapriya and M. Tamilarasi, "A case study on femtocell access modes," *Elsevier Int. Journal Engineering Science and Technol.*, vol. 19, no. 3, pp. 1534–1542, 2016.

- [61] A. Al-Dulaimi, *Self-organization and Green Applications in Cognitive radio networks*. IGI Global, 2013.
- [62] P. Xia, V. Chandrasekhar, and J. Andrews, "Open vs. closed access femtocells in the uplink," in *IEEE Trans. Wireless Commun.*, vol. 9, no. 12, 2010, pp. 3798 – 3809.
- [63] S. Mahmud, G. Khan, H. Zafar, K. Ahmad, and N. Behtani, "A survey on femtocells: Benefits deployment models and proposed solutions," *Journal of applied research and technology*, vol. 11, no. 5, pp. 733–754, 2013.
- [64] A. U. Ahmed, M. T. Islam, M. Ismail, and M. Ghanbarisabagh, "Dynamic resource allocation in hybrid access femtocell network," *Hindawi Scientific World Journal*, vol. 2014, 2014.
- [65] S. I. Rubaye, A. Al-Dulaimi, and C. J. "Cognitive femtocells: Future wireless networks for indoor applications," in *IEEE Veh. Technol. Mag.*, vol. 6, no. 1, 2011, pp. 44 – 51.
- [66] E. C. Van Der Meulen, "Three-terminal communication channels," *Advances in applied Probability*, vol. 3, no. 1, pp. 120–154, 1971.
- [67] O. Waqar, M. A. Imran, M. Dianati, and R. Tafazolli, "Energy consumption analysis and optimization of BER-constrained amplify-and-forward relay networks," *IEEE Trans. Veh. Technol.*, vol. 63, no. 3, pp. 1256–1269, 2014.
- [68] J. Garg, P. Mehta, and K. Gupta, "A review on cooperative communication protocols in wireless world," *International Journal of Wireless & Mobile Networks*, vol. 5, no. 2, 2013.
- [69] D. Liang, S. Xin Ng, and L. Hanzo, "Relay-induced error propagation reduction for decode-and-forward cooperative communications," in *Proc. IEEE Global Telecommun. Conf. (GLOBECOM)*, 2010.
- [70] A. B. Saleh, S. Redana, B. Raaf, T. Riihonen, J. Hamalainen, and R. Wichman, "Performance of amplify-and-forward and decode-and-forward relays in LTE-Advanced," in *Proc. 70th IEEE Veh. Technol. Conf. (VTC-Fall)*, 2009, pp. 1–5.
- [71] C.-H. Yeh, Y.-L. Lin, C.-C. Liu, and W.-J. Huang, "Compressed-and-forward: Compressive sensing for cooperative communication," in *Proc. IEEE Int. Symposium Intelligent Signal Process. and Commun. Systems (ISPACS)*, 2012, pp. 319–322.
- [72] Z. Drezner and H. W. Hamacher, *Facility location: applications and theory*. Springer Science & Business Media, 2004.
- [73] A. So and B. Liang, "Enhancing WLAN capacity by strategic placement of tetherless relay points," *IEEE Trans. Mobile Computing*, vol. 6, no. 5, pp. 522–535, 2007.
- [74] M. Minelli, M. Ma, M. Coupechoux, J.-M. Kelif, M. Sigelle, and P. Godlewski, "Optimal relay placement in cellular networks," *IEEE Trans. Wireless Commun.*, vol. 13, no. 2, pp. 998–1009, Jan. 2014.
- [75] J. Geier, *Designing and Deploying 802.11 Wireless Networks: A Practical Guide to Implementing 802.11 n and 802.11 ac Wireless Networks for Enterprise-based Applications*. Cisco Press, 2015.

- [76] O. El Ayach, S. W. Peters, and R. W. Heath, "The practical challenges of interference alignment," *IEEE Wireless Commun.*, vol. 20, no. 1, pp. 35–42, 2013.
- [77] A. W. Scott and R. Frobenius, *RF measurements for cellular phones and wireless data systems*. John Wiley & Sons, 2011.
- [78] J. Zhang and G. De la Roche, *Femtocells: technologies and deployment*. John Wiley & Sons, 2011.
- [79] Y. Zhou, L. Liu, H. Du, L. Tian, X. Wang, and J. Shi, "An overview on intercell interference management in mobile cellular networks: From 2G to 5G," in *Proc. IEEE Int. Conf. Commun. Systems (ICCS)*. IEEE, 2014, pp. 217–221.
- [80] Y. Adediran, H. Lasisi, and O. Okedere, "Interference management techniques in cellular networks: A review," *Cogent Engineering*, vol. 4, no. 1, p. 1294133, 2017.
- [81] N. Zhao, F. R. Yu, M. Jin, Q. Yan, and V. C. Leung, "Interference alignment and its applications: A survey, research issues, and challenges," *IEEE Commun. Surveys & Tutorials*, vol. 18, no. 3, pp. 1779–1803, 2016.
- [82] A. S. Hamza, S. S. Khalifa, H. S. Hamza, and K. Elsayed, "A survey on inter-cell interference coordination techniques in OFDMA-based cellular networks," *IEEE Commun. Surveys Tuts*, vol. 15, no. 4, pp. 1642–1670, 2013.
- [83] F. Talebi, "A tutorial on interference alignment," 2012.
- [84] S.-Y. Huang, K.-M. Lin, and J.-H. Deng, "Interference alignment with efficient dynamic information selection for LTE-A uplink coordinated multipoint systems," in *Proc. IEEE Asia Pacific Conf. Wireless and Mobile*, 2014, pp. 72–77.
- [85] A. A. Naguib, K. Elsayed, and M. Nafie, "Achievable degrees of freedom of the K-user interference channel with partial cooperation," in *Proc. 45th IEEE Asilomar Conf. Signals, Systems and Computers (ASILOMAR)*, 2011, pp. 1363–1367.
- [86] V. S. Annapureddy, A. El Gamal, and V. V. Veeravalli, "Degrees of freedom of interference channels with CoMP transmission and reception," *IEEE Trans. Inf. Theory*, vol. 58, no. 9, pp. 5740–5760, 2012.
- [87] H. Zhang, H. Li, J. H. Lee, and H. Dai, "QoS-based interference alignment with similarity clustering for efficient subchannel allocation in dense small cell networks," *IEEE Trans. Commun.*, vol. 65, no. 11, pp. 5054–5066, 2017.
- [88] A. Dong, H. Zhang, D. Yuan, and X. Zhou, "Interference alignment transceiver design by minimizing the maximum mean square error for MIMO interfering broadcast channel," *IEEE Trans. Veh. Technol.*, vol. 65, no. 8, pp. 6024–6037, 2016.
- [89] X. Xie, H. Yang, and A. V. Vasilakos, "Robust transceiver design based on interference alignment for multi-user multi-cell MIMO networks with channel uncertainty," *IEEE Access*, vol. 5, pp. 5121–5134, 2017.

- [90] J. Tang, D. K. So, E. Alsusa, K. A. Hamdi, and A. Shojaeifard, "Energy efficiency optimization with interference alignment in multi-cell MIMO interfering broadcast channels," *IEEE Trans. Commun.*, vol. 63, no. 7, pp. 2486–2499, 2015.
- [91] T. D. Novlan, R. K. Ganti, A. Ghosh, and J. G. Andrews, "Analytical evaluation of fractional frequency reuse for OFDMA cellular networks," *IEEE Trans. Wireless Commun.*, vol. 10, no. 12, pp. 4294–4305, 2011.
- [92] —, "Analytical evaluation of fractional frequency reuse for heterogeneous cellular networks," *IEEE Trans. Commun.*, vol. 60, no. 7, pp. 2029–2039, 2012.
- [93] N. Saquib, E. Hossain, and D. I. Kim, "Fractional frequency reuse for interference management in LTE-Advanced hetnets," *IEEE Wireless Commun.*, vol. 20, no. 2, pp. 113–122, 2013.
- [94] N. Himayat, S. Talwar, A. Rao, and R. Soni, "Interference management for 4G cellular standards [WIMAX/LTE UPDATE]," *IEEE Commun. Mag.*, vol. 48, no. 8, 2010.
- [95] H.-C. Jang and W.-D. Wend, "Interference management using frequency reuse and CoMP for LTE-Advanced networks," in *Proc. 17th IEEE Int. Conf. Ubiquitous and Future Networks (ICUFN)*, 2015, pp. 740–745.
- [96] Y. Yu, E. Dutkiewicz, X. Huang, M. Mueck, and G. Fang, "Performance analysis of soft frequency reuse for inter-cell interference coordination in LTE networks," in *Proc. IEEE Int. Symposium Commun. Inf. Technol. (ISCIT)*, 2010, pp. 504–509.
- [97] E. Hossain, L. B. Le, and D. Niyato, *Radio resource management in multi-tier cellular wireless networks*. John Wiley & Sons, 2013.
- [98] 3GPP and Huawei, "Soft frequency reuse scheme for UTRAN LTE," *R1-050507, TSG RAN WG1 Meeting41, Athens, Greece*, 2015.
- [99] X. Mao, A. Maaref, and K. H. Teo, "Adaptive soft frequency reuse for inter-cell interference coordination in SC-FDMA based 3GPP LTE uplinks," in *Proc. IEEE GLOBECOM*, 2008, pp. 1–6.
- [100] Y. S. Cho, J. Kim, W. Y. Yang, and C. G. Kang, *MIMO-OFDM wireless communications with MATLAB*. John Wiley & Sons, 2010.
- [101] M. Mondin, B. Melis, I. Collotta, M. Caretti, I. Bari, and F. Daneshgaran, "Simulation and complexity analysis of iterative interference cancellation receivers for LTE/LTE-advanced," in *Proc. WTC*, 2014, pp. 1–6.
- [102] J. Axnäs, Y.-P. E. Wang, M. Kamuf, and N. Andgart, "Successive interference cancellation techniques for LTE downlink," in *Proc. 22nd IEEE Int. Symposium Pers. Indoor and mobile radio Commun. (PIMRC)*, 2011, pp. 1793–1797.
- [103] S. Ahmadi, *LTE-Advanced: a practical systems approach to understanding 3GPP LTE releases 10 and 11 radio access technologies*. Academic Press, 2013.

- [104] P. Sridhar and M. Sumalatha, "Interference cancellation and channel estimation for MIMO-LTE-A networks," in *Proc. IEEE Int. Conf. Wireless Commun., Signal Process, and Netw. (WiSPNET)*, 2016, pp. 2098–2103.
- [105] M. Jiang, G. Yue, N. Prasad, and S. Rangarajan, "Link adaptation in LTE-A uplink with turbo SIC receivers and imperfect channel estimation," in *Proc. 45th IEEE Annual Conf. Inf. Sciences and Systems (CISS)*, 2011, pp. 1–6.
- [106] O. Sahin, J. Li, E. Lu, Y. Li, and P. J. Pietraski, "Interference mitigation through successive cancellation in heterogeneous networks," *ISRN Commun. and Networking*, vol. 2013, 2013.
- [107] C. Pradhan and G. R. Murthy, "Full-duplex transceiver for future cellular network: A smart antenna approach," in *Proc. IEEE Int. Conf. Adv. Netws. and Telecommun. Systems (ANTS)*, 2015, pp. 1–6.
- [108] Ericsson, "Ericsson energy and carbon report: Including results from the first-ever national assessment of the environmental impact of ICT," 2014.
- [109] M. Webb *et al.*, "Smart 2020: Enabling the low carbon economy in the information age," *The Climate Group. London*, vol. 1, no. 1, pp. 1–87, 2008.
- [110] J.-H. Chu, K.-T. Feng, and T.-S. Chang, "Energy-efficient cell selection and resource allocation in LTE-A heterogeneous networks," in *Proc. 25th IEEE Annual Int. Symposium Pers., Indoor, and Mobile Radio Commun. (PIMRC)*, 2014, pp. 976–980.
- [111] S. Buzzi, I. Chih-Lin, T. E. Klein, H. V. Poor, C. Yang, and A. Zappone, "A survey of energy-efficient techniques for 5G networks and challenges ahead," *IEEE Journal on Sel. Areas in Commun.*, vol. 34, no. 4, pp. 697–709, 2016.
- [112] B. Katz, M. Völker, and D. Wagner, "Energy efficient scheduling with power control for wireless networks," in *Proc. 8th IEEE Int. Symposium Modeling and Optimization in Mobile, Ad Hoc and Wireless Networks (WiOpt)*, 2010, pp. 160–169.
- [113] V. G. Douros and G. C. Polyzos, "Review of some fundamental approaches for power control in wireless networks," *Elsevier Computer Commun.*, vol. 34, no. 13, pp. 1580–1592, 2011.
- [114] D. Liu, W. Zheng, H. Zhang, W. Ma, and X. Wen, "Energy efficient power optimization in two-tier femtocell networks with interference pricing," in *Proc. 8th IEEE Int. Conf. Computing and Networking Technology (ICCNT)*, 2012, pp. 247–252.
- [115] M. Adedoyin and O. Falowo, "Joint optimization of energy efficiency and spectrum efficiency in 5G ultra-dense networks," in *Proc. IEEE European Conf. Netw. and Commun. (EuCNC)*, 2017, pp. 1–6.
- [116] S. A. Saad, M. Ismail, and R. Nordin, "A survey on power control techniques in femtocell networks." *JCM*, vol. 8, no. 12, pp. 845–854, 2013.
- [117] N. Saquib, E. Hossain, L. B. Le, and D. I. Kim, "Interference management in OFDMA femtocell networks: Issues and approaches," *IEEE Wireless Commun.*, vol. 19, no. 3, pp. 86–95, 2012.

REFERENCES

- [118] B. Du, C. Pan, W. Zhang, and M. Chen, "Distributed energy-efficient power optimization for CoMP systems with max-min fairness," *IEEE Commun. Lett.*, vol. 18, no. 6, pp. 999–1002, 2014.
- [119] A. Zappone, L. Sanguinetti, G. Bacci, E. Jorswieck, and M. Debbah, "Energy-efficient power control: A look at 5G wireless technologies," *IEEE Trans. Signal Process.*, vol. 64, no. 7, pp. 1668–1683, 2016.
- [120] L. Venturino, A. Zappone, C. Risi, and S. Buzzi, "Energy-efficient scheduling and power allocation in downlink OFDMA networks with base station coordination," *IEEE Trans. wireless Commun.*, vol. 14, no. 1, pp. 1–14, 2015.
- [121] F. Meshkati, A. J. Goldsmith, H. V. Poor, and S. C. Schwartz, "A game-theoretic approach to energy-efficient modulation in CDMA networks with delay QoS constraints," *IEEE Journal Sel. Areas in Commun.*, vol. 25, no. 6, 2007.
- [122] G. Bacci, E. V. Belmega, P. Mertikopoulos, and L. Sanguinetti, "Energy-aware competitive power allocation for heterogeneous networks under QoS constraints," *IEEE Trans. Wireless Commun.*, vol. 14, no. 9, pp. 4728–4742, 2015.
- [123] J. Lv, A. Zappone, and E. A. Jorswieck, "Energy-efficient MIMO underlay spectrum sharing with rate splitting," in *Proc. 15th IEEE Int. Workshop Signal Process. Adv. Wireless Commun. (SPAWC)*, 2014, pp. 174–178.
- [124] C. She, C. Yang, and L. Liu, "Energy-efficient resource allocation for MIMO-OFDM systems serving random sources with statistical QoS requirement," *IEEE Trans. Commun.*, vol. 63, no. 11, pp. 4125–4141, 2015.
- [125] T. H. Cormen, C. E. Leiserson, R. L. Rivest, and C. Stein, "Introduction to algorithms, second edition," 2001.
- [126] H. Zhi, L. Yang, and H. Zhu, "Precoding and decoding design for two-way MIMO AF multiple-relay system," *Springer Journal of Electronics (China)*, vol. 29, no. 3-4, pp. 177–189, 2012.
- [127] W. Wang, R. Wang, W. Duan, R. Feng, and G. Zhang, "Optimal transceiver designs for wireless-powered full-duplex two-way relay networks with SWIPT," *IEEE Access*, vol. 5, pp. 22 329–22 343, 2017.
- [128] F. A. Dietrich and W. Utschick, "Pilot-assisted channel estimation based on second-order statistics," *IEEE Trans. Signal Process.*, vol. 53, no. 3, pp. 1178–1193, 2005.
- [129] A. K. Shrivastava, "A comparative analysis of LS and MMSE channel estimation techniques for MIMO-OFDM system," *International Journal for Scientific Research and Development*, vol. 1, no. 8, pp. 44–48, 2015.
- [130] L. Kewen *et al.*, "Research of MMSE and LS channel estimation in OFDM systems," in *Proc. 2nd IEEE Int. Conf. Inf. Science and Engineering (ICISE)*, 2010, pp. 2308–2311.
- [131] J. A. Fessler and A. O. Hero, "Space-alternating generalized expectation-maximization algorithm," *IEEE Trans. Signal Process.*, vol. 42, no. 10, pp. 2664–2677, 1994.

REFERENCES

- [132] A. Khelifi and R. Bouallegue, “Performance analysis of LS and LMMSE channel estimation techniques for LTE downlink systems,” *arXiv preprint arXiv:1111.1666*, 2011.
- [133] J.-J. Van De Beek, O. Edfors, M. Sandell, S. K. Wilson, and P. O. Borjesson, “On channel estimation in OFDM systems,” in *Proc. 45th IEEE Veh. Technol. Conf. (VTC)*, vol. 2, 1995, pp. 815–819.
- [134] J.-C. Lin, “Least-squares channel estimation for mobile OFDM communication on time-varying frequency-selective fading channels,” *IEEE Trans. Veh. Technol.*, vol. 57, no. 6, pp. 3538–3550, 2008.
- [135] O. Edfors, M. Sandell, J.-J. Van de Beek, S. K. Wilson, and P. O. Borjesson, “OFDM channel estimation by singular value decomposition,” *IEEE Trans. Commun.*, vol. 46, no. 7, pp. 931–939, 1998.
- [136] J. v. Tiel, *Convex analysis*. John Wiley, 1984.
- [137] M. S. Bazaraa, H. D. Sherali, and C. M. Shetty, *Nonlinear programming: theory and algorithms*. John Wiley & Sons, 2013.
- [138] J. W. Demmel, *Applied numerical linear algebra*. Siam, 1997, vol. 56.
- [139] Z.-Q. Luo and W. Yu, “An introduction to convex optimization for communications and signal processing,” *IEEE Journal on selected areas in commun.*, vol. 24, no. 8, pp. 1426–1438, 2006.
- [140] C. B. Do, “Convex optimization overview (cnt’d),” 2009.

Part II

Papers

Paper A

Energy Efficient Coverage Extension Relay Node Placement in LTE-A Networks

Armeline Dembo Mafuta, Tom Walingo and T. N.M. Ngatched *Member IEEE*

IEEE communication Letters, 2017

© 2017

The layout has been revised.

Abstract

Deployed Long Term Evolution-Advanced (LTE-A) infrastructure may need coverage extension due to exponential growth of mobile broadband data usages as well as poor network performance along the cell edges. A proper installation of Relay Nodes (RN) extends the network coverage in LTE-A networks. In this paper, we propose an energy efficient and optimal RN placement (EEORNP) algorithm that maximises the network coverage under the energy constraint, while maintaining the signal-to-interference ratio (SIR). The proposed algorithm is based on an improved greedy algorithm where an effective and optimal RN placement is guaranteed when the matroid rank function of the energy efficient coverage extension optimisation is sub-modular and monotonic. The performance is investigated in terms of coverage percentage and number of RN needed to cover users. Simulation results show that the proposed EEORNP outperforms both greedy and random placement algorithms.

1 Introduction and Related Works

To keep up with the exponential growth of mobile broadband data usages and improve the network capacity, the Third Generation Partnership Project (3GPP) LTE-Advanced (LTE-A) has recently been standardized. In LTE-A, wireless relaying, where small relay nodes (RNs) are placed within the coverage area of a macrocell base station (MBS), is a promising technique to extend cell coverage and improve spectral efficiency [1]. The RN relays data to the users having unfavourable channel conditions and low data rates (e.g., at the cell-edge), by mitigating high pathloss and fading channel impairments. Moreover, they increase the users experience indoor and extends the network coverage to users in shadowed zones. Because they are relatively small nodes with low power consumption, RNs also offer deployment flexibility and eliminate the need for high cost site selection, planning, acquisition and installation. It helps alleviate the problem of poor network planning and unforeseen infrastructural changes.

Needless to say, wireless relaying has some technical challenges and limitations such as RN placement and energy consumption. The proper placement of RNs is very crucial, as this can aggravate the interference problem. The network coverage should be extended keeping the energy consumption of the network low and, at the same time, maintaining the interference levels of the whole network at acceptable levels. This work presents an energy efficient solution, in term of power consumption, optimal RN placement in Macrocell/ Femtocell networks where Femtocell Access Points (FAP), and users are grouped into clusters. This has partially been studied separately in wireless sensor networks (WSN) [2], Software Defined Networks (SDN) [3] and/or LTE

networks [4]. However, the joint network coverage, energy efficient optimisation, and RNs placement problem in LTE-A networks has not been fully investigated in the literature. The authors in [5] minimised the total energy consumption from RNs and eNodeBS (eNBs), but did not consider the network coverage and users' data rates. On the other hand, in [6] the coverage extension, interference cell capacity in LTE-A networks is investigated and a suboptimal RN placement heuristic is proposed, but the energy consumption was not totally considered among the RN placement constraints. In [7], the authors proposed a Simulated Annealing (SA) algorithm based on signal-plus-interference-to-noise ratio (SINR) calculations for RN placement where energy cost of a candidate configuration is considered as an inverse of its related cell capacity. However, the complexity of the proposed SA algorithm is not calculated and it turns out to be high when finding a near-optimal solution. In [4], considering RNs placement based only on the distance and aiming at achieving maximum rate to users at the cell edge region, an algorithm that reduces the transmitted power of moving RNs is proposed. The energy is not directly modelled in this work.

In this paper, using sub-modularity and monotonicity optimisation, we propose an energy efficient and optimal RN placement (EEORNP) algorithm that maximises the networks coverage under the energy cost constraint. The algorithm is designed as an improved optimal greedy algorithm where the network coverage and connectivity are guaranteed. Maximising coverage in the networks is modelled with a sub-modular set function. The scheme solves the combinatorial problem where improvement is achieved when the matroid rank function is sub-modular and monotonic. It is well known that for a sub-modular and monotone maximisation problem, an improved greedy algorithm provides a $1 - 1/e$ approximation [8]. For networks with large number of users and FAPs, the proposed algorithm is very effective and efficient for its low computational complexity and near-optimality.

2 System Model and Problem Formulation

Consider an LTE-A network with MBS, FAPs, RNs and users (Marginalised Macrocell User Equipment as MMUE). Let $G = (V, E)$ be a graph with the vertices $V = X \cup Y \cup b_o$, where $X = \{x_1, x_2, \dots, x_i\}$ is the set of MMUE in the network, $Y = \{y_1, y_2, \dots, y_j\}$, the set of RN and b_o is the MBS. The edges E represent all communication link, $e \in E$, i.e. $e(x_i, y_j)$ is the communication link between x_i and y_j . Let \mathcal{S} be a finite set of all locations in the network, the FAPs are grouped into clusters \mathcal{L} for effective RN placement management and energy efficiency. Let p denote a RN possible position, $p \in \mathcal{A}$ where \mathcal{A} is the set of possible positions in cluster \mathcal{L} . Network coverage is achieved in a given cluster by placing RNs y_j at optimal position p^* . Fig A.1 illustrates the system model where the MMUE, a MUE that needs coverage extension, wants to communicate with the MBS.

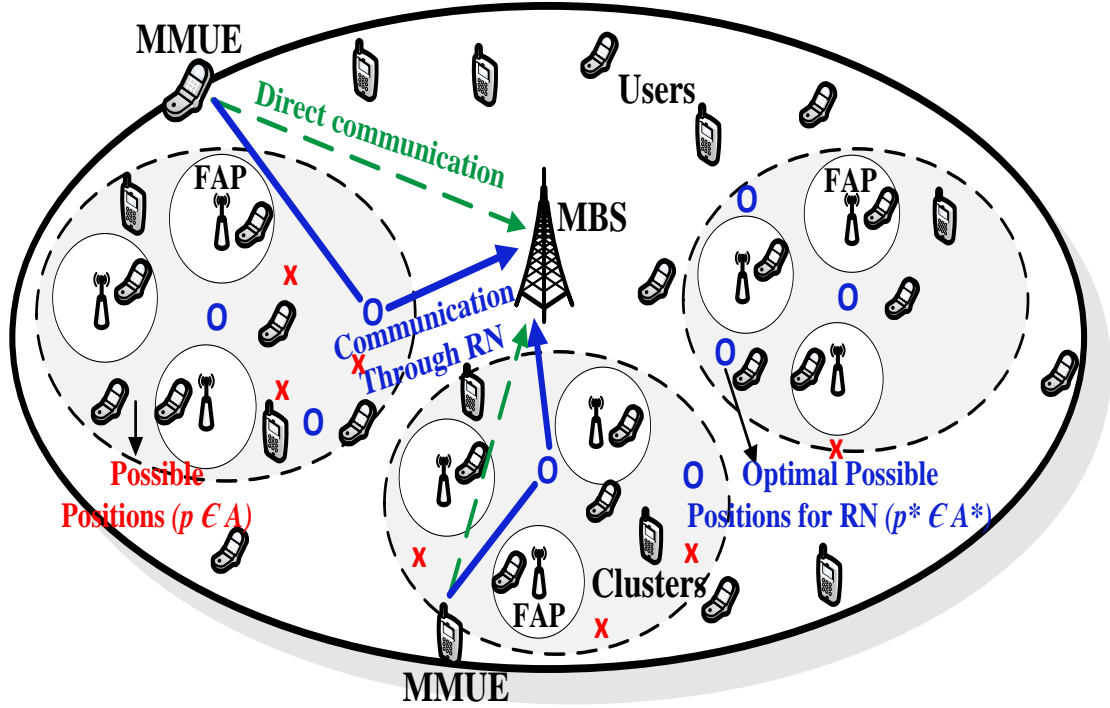


Figure A.1: The system model with a single MBS, FAP clusters and RN placement.

Objective. Our objective is to maximise the network coverage subject to minimising the energy consumption at manageable interference. This means reducing the energy cost in the each cluster \mathcal{L} . Let $f : 2^{\mathcal{S}} \rightarrow \mathbb{R}$ be the network coverage optimisation function, where the coverage quality in cluster \mathcal{L} is denoted as $f(\mathcal{A})$ and \mathcal{A}^* is the set of location where $f(\mathcal{A})$ is maximised, $\mathcal{A} \subseteq \mathcal{S}$. The coverage quality is achieved by placing RN y_j at the optimal possible position p^* in each cluster. The restricted optimisation problem is defined as:

$$\mathcal{A}^* \in \{\mathcal{A} \subseteq \mathcal{S} \mid f(\mathcal{A}) \text{ is maximum and } j \geq |\mathcal{A}|\} \quad (\text{A.1})$$

The network coverage optimisation function $f(\mathcal{S})$ is given as

$$\text{maximise}_{\mathcal{A} \subseteq \mathcal{S}} f(\mathcal{S}) = \sum_{\mathcal{L}} \sum_{p \in \mathcal{A}} f(\mathcal{A}). \quad (\text{A.2})$$

Subject to: Energy constraint: Let $\mathcal{E} : V \rightarrow \mathbb{R}^+$ denotes the energy cost function, where $\mathcal{E}(\mathcal{A})$ is the energy cost of all edges in the set of location \mathcal{A} . $\mathcal{E}(e)$ represents the energy cost for a certain communication link e . The placement should satisfy the following constraint:

$$\sum_{\mathcal{L}} \mathcal{E}(\mathcal{A}) \leq K, \quad (\text{A.3})$$

where K is constant threshold representing the maximum allowable interference. The total energy cost in the set of location \mathcal{A} after placing RN at p^* in the cluster \mathcal{L} is given as

$$\mathcal{E}(\mathcal{A}^*) = \sum_{(x_i, y_j) \in \mathcal{A}^*} \mathcal{E}(x_i, y_j). \quad (\text{A.4})$$

The energy cost $\mathcal{E}(x_i)$ from a i^{th} user to MBS b_o or to MBS through y_j is formulated as follows

$$\mathcal{E}(x_i) = \operatorname{argmin}(\mathbf{P}_{rx}) \cup \left[\operatorname{arg} \|x_i, (y_j \cup b_o)\| \quad \operatorname{argmin}_{e_{(y_k, b_o)} \in (Y \cup b_o)} \|x_i, e_{(y_k, b_o)}\| \right], \quad (\text{A.5})$$

where \mathbf{P}_{rx} is the received power of the node (RN, MBS), $e_{(y_k, b_o)} \in (Y \cup b_o)$ represents the communication link through RN y_k to the MBS, $y_k \in Y$ and $\|\cdot\|$ is the Euclidean distance of two nodes. The received power is expressed as [9], [10]

$$\mathbf{P}_{rx} = \mathbf{G}_{rx} + \mathbf{G}_{tx} + \mathbf{P}_{tx} - \mathbf{L}_{FM} - \mathbf{PL}, \quad (\text{A.6})$$

where \mathbf{G}_{tx} and \mathbf{G}_{rx} are the transmitting and receiving gain antenna in dBi , respectively. \mathbf{P}_{tx} is the transmit power in dBm , \mathbf{L}_{FM} is considered fading margin in dB , and \mathbf{PL} is the path loss in dB in the location \mathcal{A} .

Coverage constraint: To assure an optimal connectivity and coverage, we need the RN placement to respect some quota $Q \geq 0$, which denotes the required amount of certainty achieved by any RN placement:

$$f(\mathcal{A}) \geq Q. \quad (\text{A.7})$$

The possible positions are retained in \mathcal{A} if the distance between the two vertices are less than or equal to a certain transmission range or communication range.

$$\{p \mid \|x_i, p\| \leq r, \forall p \in \mathcal{A}\}, \quad (\text{A.8})$$

where r is the communication range.

$$c_p = 1 \iff \mathbf{P}_{rx} \geq \mathbf{R}_{sens}, c_p \in \{0, 1\}, \quad (\text{A.9})$$

c_p is the coverage guaranteed with the chosen p and \mathbf{R}_{sens} is the receiver sensitivity. c_p indicates that RN y_j should be placed at the selected $p = p^*$ such that if the \mathbf{P}_{rx} is greater or equal to \mathbf{R}_{sens} , the coverage c_p is guaranteed with $c_p = 1$ or $c_p = 0$, otherwise.

3 Network Coverage with Energy Efficient and Optimal RN Placement

3.1 Sub-modularity, monotonicity optimisation and matroid

The coverage maximisation function $f : 2^S \rightarrow \mathbb{R}$ is sub-modular if it satisfies one of the following two equivalent properties:

- 1) $f(\mathcal{A} \cup \{a\}) - f(\mathcal{A}) \geq f(\mathcal{B} \cup \{a\}) - f(\mathcal{B}), \forall \mathcal{A} \subseteq \mathcal{B} \subseteq \mathcal{S}$ and $a \in \mathcal{S} \setminus \mathcal{B}$,
- 2) $f(\mathcal{A}) + f(\mathcal{B}) \geq f(\mathcal{A} \cup \mathcal{B}) + f(\mathcal{A} \cap \mathcal{B}), \forall \mathcal{A}, \mathcal{B} \subseteq \mathcal{S}$.

The common concept of monotonicity is defined for all subsets \mathcal{A}, \mathcal{B} of \mathcal{S} as $f(\mathcal{A}) \leq f(\mathcal{B})$ where $\mathcal{A} \subseteq \mathcal{B}$. The following lemma is a direct result of the above properties.

Lemma 1. *If f is a sub-modular set function on the set of subset of \mathcal{S} , then*

$$\sum_{i=1}^m f(\mathcal{A}_i) \geq f\left(\bigcup_{i=1}^m \mathcal{A}_i\right), \forall \mathcal{A}_i \subseteq \mathcal{S}, m \geq 1.$$

Proof: Sub-modularity is a generalization of sub-additivity such that the set function f is sub-additive if for all $\mathcal{A} \cap \mathcal{B} = \emptyset$ with $\mathcal{A}, \mathcal{B} \subseteq \mathcal{S}$ implies $f(\mathcal{A}) + f(\mathcal{B}) \geq f(\mathcal{A} \cup \mathcal{B}) + f(\emptyset)$. Consider a set of subsets $\mathcal{T}_1, \mathcal{T}_2, \dots, \mathcal{T}_i \subseteq \mathcal{S}, i \geq 1$, we have:

$$\begin{aligned} f(\mathcal{T}_1 \cup \{a\}) - f(\mathcal{T}_1) + \dots + f(\mathcal{T}_{i-1} \cup \{a\}) - f(\mathcal{T}_{i-1}) &\geq f(\mathcal{T}_i \cup \{a\}) - f(\mathcal{T}_i) + f(\emptyset) \\ f(\mathcal{T}_1 \cup \{a\}) - f(\mathcal{T}_1) + \dots + f(\mathcal{T}_{i-1} \cup \{a\}) - f(\mathcal{T}_{i-1}) &\geq f(\mathcal{T}_i \cup \{a\}) - f(\mathcal{T}_i) + f(\mathcal{T}_1 \cap \dots \\ &\quad \dots \cap (\mathcal{T}_{i-1} - \{a\}) \cap \mathcal{T}_i) \\ f(\mathcal{T}_1 \cup \{a\}) + \dots + f(\mathcal{T}_{i-1} \cup \{a\}) + f(\mathcal{T}_i) &\geq f(\mathcal{T}_1) + \dots + f(\mathcal{T}_{i-1}) + f(\mathcal{T}_i \cup \{a\}) + \\ &\quad + \dots + f(\emptyset) \\ f(\mathcal{T}_1 \cup \dots \cup (\mathcal{T}_{i-1} \cup \{a\}) \cup \mathcal{T}_i) &\geq f(\mathcal{T}_1 \cup \dots \cup (\mathcal{T}_{i-1} \cup \{a\}) \cup \mathcal{T}_i) \\ &\quad + f(\mathcal{T}_1 \cap \dots \cap (\mathcal{T}_{i-1} \cup \{a\}) \cap \mathcal{T}_i) \end{aligned}$$

Assume $\mathcal{T}_1 = \mathcal{A}_1, \mathcal{T}_{i-1} \cup \{a\} = \mathcal{A}_{i-1}$ and $\mathcal{T}_i = \mathcal{A}_i$, we have:

$$\begin{aligned} f(\mathcal{A}_1 \cup \dots \cup \mathcal{A}_{i-1} \cup \mathcal{A}_i) &\geq f(\mathcal{A}_1 \cup \dots \cup \mathcal{A}_{i-1} \cup \mathcal{A}_i) + f(\mathcal{A}_1 \cap \dots \cap \mathcal{A}_{i-1} \cap \mathcal{A}_i) \\ f(\mathcal{A}_1) + \dots + f(\mathcal{A}_{i-1}) + f(\mathcal{A}_i) &\geq f(\mathcal{A}_1 \cup \dots \cup \mathcal{A}_{i-1} \cup \mathcal{A}_i) + f(\mathcal{A}_1 \cap \dots \cap \mathcal{A}_{i-1} \cap \mathcal{A}_i). \end{aligned}$$

We pose that $f(\mathcal{A}_1 \cap \dots \cap \mathcal{A}_{i-1} \cap \mathcal{A}_i) = \emptyset$ based on the sub-additivity of the sub-modularity. Thus,

$$f(\mathcal{A}_1) + \dots + f(\mathcal{A}_{i-1}) + f(\mathcal{A}_i) \geq f(\mathcal{A}_1 \cup \dots \cup \mathcal{A}_{i-1} \cup \mathcal{A}_i).$$

$$\text{Therefore, } \sum_{i=1}^m f(\mathcal{A}_i) \geq f\left(\bigcup_{i=1}^m \mathcal{A}_i\right), \forall \mathcal{A}_i \subseteq \mathcal{S} \text{ and } m \geq 1.$$

Let $G = (V, E)$, a vertex-weighted graph with the energy cost function \mathcal{E} , a monotone and sub-modular function f on the set of subset of \mathcal{S} ($f(\emptyset) = 0$) and the maximum allowable interference threshold K . The network coverage with the energy constraint asks for a subset $\mathcal{S} \subseteq V$ where \mathcal{S} is connected with respect to G , the energy cost of \mathcal{S} is less than K and $f(\mathcal{S})$ is maximised. Given a matroid $\mathcal{M} = (V, \mathcal{I})$, we denote by $r_{\mathcal{M}}$ the rank function of \mathcal{M} where $r_{\mathcal{M}}(\mathcal{S}) = \max\{|\mathcal{A}| : \mathcal{A} \subseteq \mathcal{S}, \mathcal{A} \in \mathcal{I}\}$. It is well known that the rank function is monotone and sub-modular. A weighted matroid $\mathcal{M} = (E, \mathcal{I})$ is a matroid which is associated to a weight function w that computes and

assigns a positive weight $w(e)$ to each element $e \in E$. The goal of the EEORNP algorithm is to find a maximum-weight independent subset in a weighted matroid. This involves working for any weighted matroid with the guarantee of finding an optimal solution. For a given weighted matroid $\mathcal{M} = (E, \mathcal{I}, w)$, we need to find an independent subset \mathcal{A} such that $\mathcal{A} \in \mathcal{I}$ and $w(\mathcal{A})$ is maximised. The weight function w is the energy cost function with $w(e) = \mathcal{E}(e)$ in this work. The EEORNP finds the optimal solution for the optimisation problem when \mathcal{M} is a matroid with $f(\mathcal{S})$ as sub-modular and monotone function.

Theorem 1. Given a set V , let $f(\mathcal{S}) = \sum_{i=1}^m r_i(\mathcal{S})$ where $r_i, \dots, r_m: 2^N \rightarrow \mathbb{R}^+$ are the weighted rank function. r_i defined by the matroid $\mathcal{M}_i = (V, \mathcal{I}_i)$ and the weight energy cost function $\mathcal{E}_i: V \rightarrow \mathbb{R}^+$. Given another matroid $\mathcal{M} = (V, \mathcal{A})$ and membership oracles for $\mathcal{M}_1, \mathcal{M}_2, \dots, \mathcal{M}_m$ and \mathcal{M} , there is a polynomial time $(1 - 1/e)$ - approximation for the problem $\max_{\mathcal{S} \in \mathcal{I}} f(\mathcal{S})$ [11].

The functions are generated from a fairly rich subclass of monotone sub-modular functions. The sums of weighted rank function $r_i(\mathcal{S})$ generalise sub-modular functions arising from coverage systems. A uniform matroid with $\mathcal{I} = \{\mathcal{A} \subseteq V \mid |\mathcal{A}| \leq n\}$ helps to obtain the coverage sub-modular. Considering a ground set $[m]$ as a collection of weights on V with a set of subsets $\{\mathcal{A}_j\}_{j \in V}$, the energy cost weight $\mathcal{E}_{(i,j)} > 0$, if \mathcal{A}_j^* contains an optimal p_j^* (Y contains a RN y_j) and equal to 0 otherwise. Then the weighted rank function $r_i(\mathcal{S})$ is an indicator of whether $\bigcup_{j \in \mathcal{S}} \mathcal{A}_j$ covers x_i users. Therefore the sum of $r_i(\mathcal{S})$ gives exactly the sizes of this union $f(\mathcal{S}) = \sum_{i=1}^m r_i(\mathcal{S}) = |\bigcup_{j \in \mathcal{S}} \mathcal{A}_j|$. Generalization to the weighted case is straightforward from Theorem 1.

3.2 The Energy Efficient and Optimal RN Placement (EEORNP) Algorithm

The EEORNP algorithm generates randomly all possible positions p to place RN in each cluster \mathcal{L} . After computing the path loss and Euclidean distance between the MMUE x_i and all the generated possible positions of RN, the algorithm retains the possible positions that satisfies $\|x_i, p_j\| \leq r$. For each e satisfying the previous condition, the edges are sorted monotonically in decreasing order based on the Euclidean distance and path loss. The EEORNP starts with sets of empties possible positions $\mathcal{A} = \emptyset, \mathcal{A}^* = \emptyset$ and in the i^{th} iteration it adds the possible position p_j that satisfies the condition $\mathcal{A} \cup \{p_j\} \in \mathcal{I}$ where $f(\mathcal{A})$ is the objective function. The energy cost is calculated only for the MMUE and the set of possible position RN in \mathcal{A} . The RN y_j is placed at the optimal possible position selected based on the minimum energy cost that maximises the network coverage function $f(\mathcal{A})$. The complete details of the EEORNP algorithm is presented as Algorithm 2. The computational complexity of Algorithm 2 is dependent on the number of users in each cluster \mathcal{L} . Computing the path loss and Euclidean distance $\|k, p\|$ requires a complexity of $O(N)$. Sorting the edges into decreasing order

Algorithm 2 EEORNP algorithm

- 1: **Input:** A set of users nodes $X = \{x_1, x_2, \dots, x_i\}$, $r > 0$
 - 2: **Output:** Set of optimal possible location \mathcal{A}^* , a set of RN placed at the optimal possible positions
 $Y^* = \{y_1, y_2, \dots, y_j\}$
 - 3: **Initialize:** $\mathcal{A}, \mathcal{A}^*, Y^* = \emptyset$
 - 4: Consider $G = (V, E)$
 - 5: **for** $l = 1 : \mathcal{L}$ **do**
 - 6: Generate all possible positions in the network.
 - 7: Compute the path loss and $\|x_i, p_j\| \leq r$, eq. A.8
 - 8: **for each** $e = 1 : |E|$ **do**
 - 9: Sort the edges $E(x_i, p_j)$ into monotonically decreasing order based on Euclidean distance and path loss.
 - 10: **if** $\mathcal{A} \cup p_j \in \mathcal{I}$ **then**
 - 11: compute $\{(x_i, p_j)\} = f(\{(x_i, p_j)\} \cup \mathcal{A}) - f(\mathcal{A})$ section 3.
 - 12: $\mathcal{A} = \mathcal{A} \cup \{p_j\}$
 - 13: **for each** $p_j \in \mathcal{A}$ **do**
 - 14: compute the energy cost $\mathcal{E}(x_i)$ passing through p_j as given in eqs. (A.5, A.6)
 - 15: **for each** $\mathcal{E}(x_i)$ **do** eqs. (A.3, A.4)
 - 16: **if** $\mathcal{E}(x_i) \leq K$ **then**
 - 17: select p_j that maximise $f(\mathcal{A})$ in cluster \mathcal{L} with minimum energy cost \mathcal{E} .
 - 18: $p^* = p_j$, one of the optimal position for a RN.
 - 19: $\mathcal{A}^* = \mathcal{A}^* \cup \{p^*\}$
 - 20: $\mathcal{A}^* \in \{\mathcal{A} \subseteq \mathcal{S} | f(\mathcal{A}) \text{ is max. and } n \geq |\mathcal{A}|\}$ eq. (A.1)
 - 21: Place the y_j at the optimal position p^* , eq. (A.9)
 - 22: **if** $f(\mathcal{A}) \geq Q$ **then**
 - 23: $Y^* = Y^* \cup y_j$, eqs. (A.7, A.2)
 - 24: **Return** Y, \mathcal{A}^*
-

and finding all possible position for RNs involves a complexity of $O(|E|^2 \log|E|)$. Computing the energy cost before returning the optimal set of location \mathcal{A}^* involves a complexity of $O(N^2)$. Placing the RN at the \mathcal{A}^* involves a complexity of $O(1)$. Note that N is at most $|V|$. Thus, the complexity of EEORNP is $O(|V|^2 + |E|^2 \log|E|)$.

4 Performance Evaluation

In this model, the FAP close to each other are grouped into a cluster and placed uniformly within the MBS coverage area. The users are also placed according to a uniform random distribution into the clusters. We considered a maximum of 100 RNs for the all networks with 20 RNs per cells and 500 users. The transmission range r is 40 m while P_{tx} of users, RN and MBS are 30, 23 and 43 dBm, respectively.

The EEORNP method is compared to the random and greedy methods. The chosen environment or cluster is divided into a grid cells where the users are represented by "O" and RN by *squares* as illustrated in Fig. A.2.

The results are explained in Table A.1 where the EEORNP utilises 12 RN to cover 17 users as compared to the others.

Table A.1: Results illustration from Fig. A.2

| Comparison | | | |
|--------------------------|-------------------------------------|-------------------------------------|-------------------------------------|
| | Fig. 1a Random algorithm | Fig. 1b Greedy algorithm | Fig. 1c EEORNP algorithm |
| Utilised RN | 15 | 15 | 12 |
| Users covered | 9 | 17 | 17 |
| Users not covered | 9 | 1 | 1 |
| RN wasted | ≈ 8 | ≈ 3 | none |

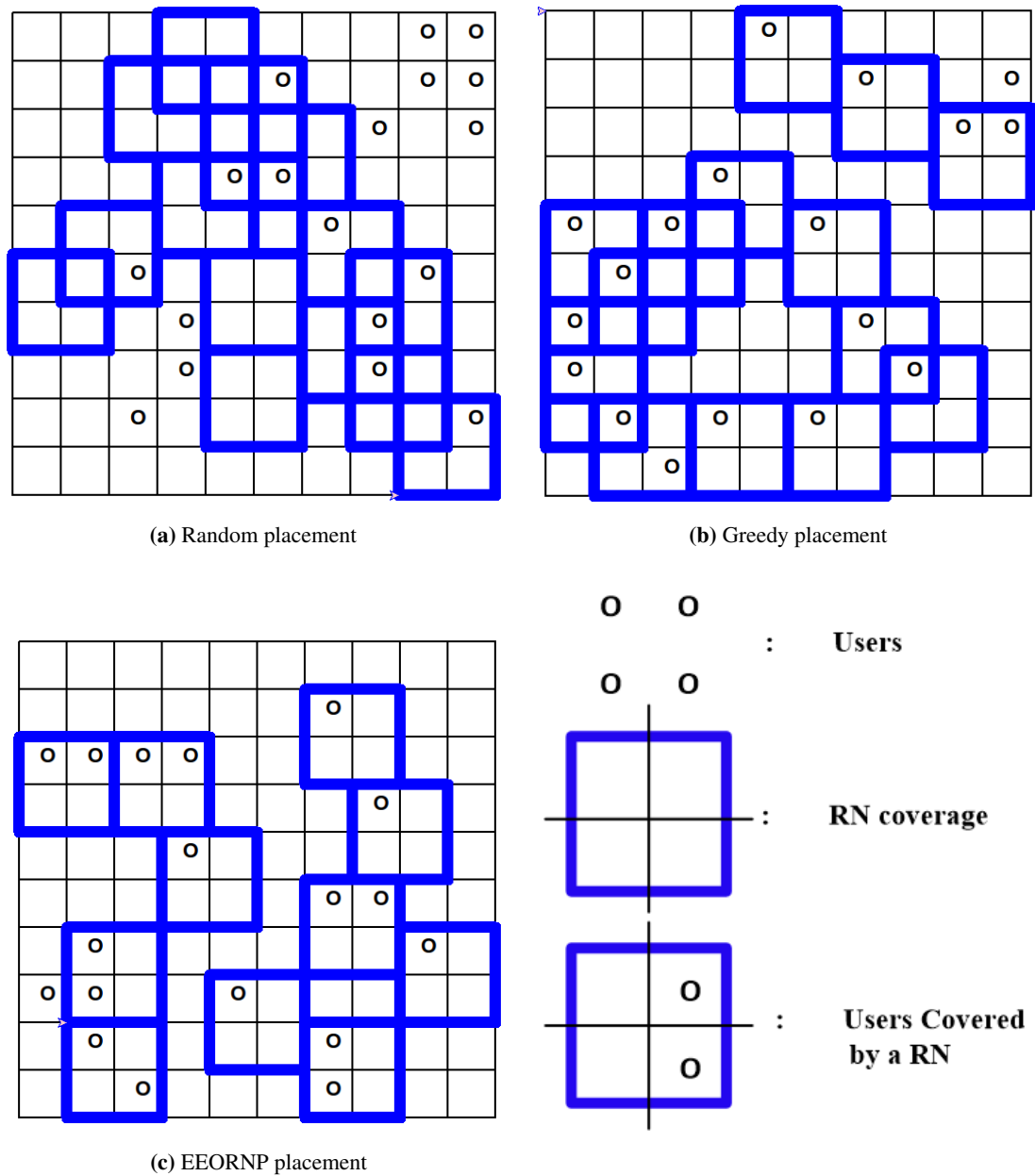


Figure A.2: Different Relay Nodes Placement algorithms

The comparison of the three methods, random, greedy and EEORNP is given in Fig. A.3 in terms of the number of RN used to cover users. Results shows that the proposed algorithm EEORNP performs better than the other placement algorithms by using fewer RN with the same number of users.

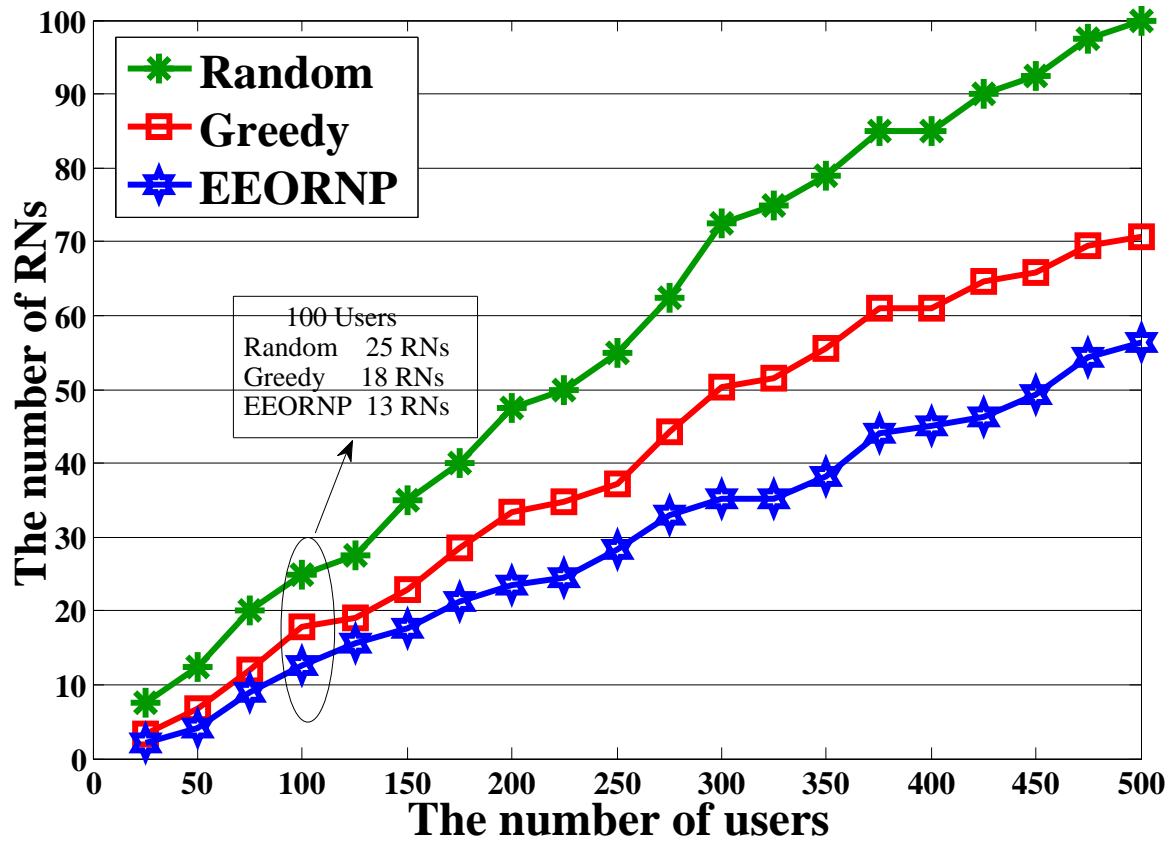


Figure A.3: Comparison of Random vs Greedy vs EEORNP

The coverage percentage based on energy cost minimisation is illustrated in Fig. A.4 for the different methods. As shown, the EEORNP algorithm achieves better coverage than the other methods which means better connectivity with minimum energy consumption and minimum number of RN, $\approx 0.80\%$ while the random and greedy algorithm achieve $\approx 0.49\%$ and $\approx 0.63\%$, respectively.

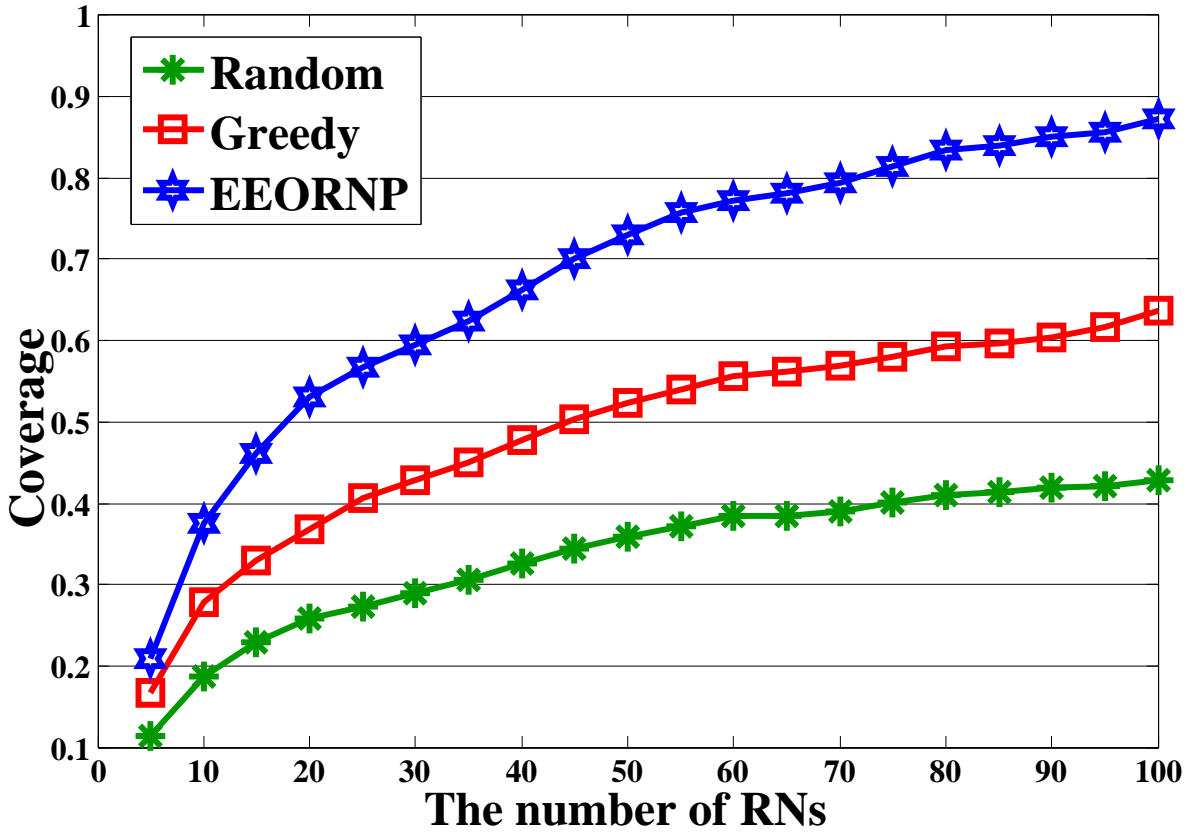


Figure A.4: Coverage percentage of RNs

5 Conclusion

This work investigated the RN placement in LTE-A networks for coverage extension under an energy efficient constraints. The proposed EEORNP algorithm gives a better improvement due to the matroid rank function constraint considered. The sub-modularity and monotonicity properties were considered in EEORNP algorithm which achieved an optimal solution compared to a random and greedy algorithms. Results have shown that the proposed algorithm performs better than the other algorithms in term of coverage percentage and number of RNs used with low computational time.

References

- [1] M. Minelli, M. Maode, M. Coupechoux, J.-M. Kelif, M. Sigelle, and P. Godlewski, "Uplink energy-delay trade-off under optimized relay placement in cellular networks," *IEEE Transactions on Mobile Computing*, vol. 15, no. 9, pp. 2376–2387, Aug. 2016.
- [2] C. Ma, W. Liang, and M. Zheng, "Set-covering-based algorithm for delay constrained relay node placement in wireless sensor networks," in *IEEE ICC*, May 2016, pp. 1–6.
- [3] T. Han, Y. Han, X. Ge, Q. Li, J. Zhang, Z. bai, and L. Wang, "Small cell offloading through cooperative communication in software-defined heterogeneous networks," *IEEE Sensors Journal*, vol. 16, no. 20, pp. 7381–7392, Jun. 2016.
- [4] J. A. Aldhaibani, A. Yahya, and R. B. Ahmad, "Coverage extension and balancing the transmitted power of the moving relay node at LTE-A cellular network," *The Scientific World Journal*, vol. 2014, pp. 1–10, Jan. 2014.
- [5] H. Y. Lateef, C. F. Chiasserini, T. ElBatt, A. Mohamed, and M. Guizani, "Towards energy efficient relay placement and load balancing in future wireless networks," in *IEEE 25th PIMRC*, Sep. 2014, pp. 1397 – 1402.
- [6] M. Minelli, M. Ma, M. Coupechoux, and P. Godlewski, "Scheduling impact on the performance of relay-enhanced LTE-A networks," *IEEE Transactions on Vehicular Technology*, vol. 65, no. 4, pp. 2496–2508, Apr. 2016.
- [7] M. Minelli, M. Ma, M. Coupechoux, J.-M. Kelif, M. Sigelle, and P. Godlewski, "Optimal relay placement in cellular networks," *IEEE Transactions on Wireless Communications*, vol. 13, no. 2, pp. 998–1009, Jan. 2014.
- [8] S. Fujishige, *Submodular Functions and Optimization, 2nd Edition*. Philadelphia, Pa, USA: Elsevier Science, 2005.
- [9] A. Alsayyari, I. Kostanic, C. Otero, M. Almeer, and K. Rukieh, "An empirical path loss model for wireless sensor network deployment in a sand terrain environment," in *IEEE WF-IoT*, Mar. 2014, pp. 218–223.
- [10] D. Puccinelli and M. Haenggi, "Multipath fading in wireless sensor networks: Measurements and interpretation," in *Proceedings of the IWCMC'06*, Jul. 2006, pp. 1039–1044.

REFERENCES

- [11] G. Calinescu, C. Chekuri, M. Pål, and J. Vondrák, “Maximizing a submodular set function subject to a matroid constraint (extended abstract),” in *Proceedings of the 12th IPCO*, vol. 4513, Jun. 2007, pp. 182–196.

Paper B

Interference Management in LTE-Advanced Cooperative Relay Networks: Decentralized Transceiver Design with Channel Estimation

Armeline Dembo Mafuta, Tom Walingo and Fambirai Takawira

The paper is under review at the
IEEE Transaction on wireless communications, 2018

© 2018

The layout has been revised.

Abstract

Wireless networks improve indoor communications by deploying femtocell networks into the macrocell coverage. This results in spectrum sharing with the consequences of cross-tier interference from the macrocell user equipments (MUEs) to the femtocell access points (FAPs). This work considers the uplink cross-tier interference management for the cell-edge MUEs (CUEs) in cooperative multi-user multiple input multiple output (MU-MIMO) systems. For better interference management, the CUEs are grouped into clusters and communicate to the macrocell base station (MBS) through a relay node (RN). The linear pre-coders and decoders algorithms for the FAPs, MUEs and CUEs are proposed for effective interference management to minimize the sum mean square error (MSE), subject to the total transmit power constraints. The designed pre-coders and decoders use the pilot-assisted channel estimation to improve the accuracy of the acquired channel state information (CSI). The least square (LS) and minimum MSE (MMSE) channel estimators are considered. The performance of the system is investigated in terms of the bit error rate (BER) for the linear pre-coders and decoders algorithms with the pilot-assisted channel estimators.

1 Introduction

Femtocell networks are deployed into macrocell networks to improve the indoor coverage and to provide high data rates to end users while reducing their load. Femtocells do not require specific infrastructure as they are easily installed by the end users. They operate in the licensed band of the macrocell and in some cases, they are imposed to use the same frequency spectrum [1]. This results in the challenge of cross-tier interference between macrocell and femtocells when both transmit on the same frequency band simultaneously. Furthermore, the macrocell users located at the cell-edge, referred in this paper, as cell-edge macrocell user equipments (CUEs), experience performance degradation due to the long distance between the CUEs and the macrocell base station (MBS). The management of cross-tier interference from CUEs to the femtocell access point (FAPs) is of paramount importance and is part of the focus of this work.

Several techniques have been employed to mitigate this interference. They include; interference alignment, where the signals are constrained into the same subspaces at the unintended receivers and the desired signals are retrieved at each receiver by eliminating the aligned interferences, using a decoding matrix [2]; interference avoidance, where the allocation of various system resources to users is controlled to ensure that the interference remains within acceptable limits [3]; and interference cancellation, where the suppression of the interference can be done at the transmitter or

receiver side [4]. Another effective interference management technique is the pre-coding approach, which provides reliable high data rate communication in multi-user multiple input multiple output (MU-MIMO) systems. A linear pre-coder and decoder design, also known as transceiver design, is an effective way to reduce or mitigate multi-user interferences in femtocell networks while improving the performance [5]. It can be employed to enhance the bit error rate (BER) performance and increase the information rate of spatial multiplexed MU-MIMO systems. Moreover, minimum mean square error (MMSE) or zero-forcing (ZF) can be used to design the pre-coder at the source and decoder at the destination to estimate the transmitted signal. In this paper, MMSE is employed in the transceiver design, due to its simplicity and effectiveness [6]. It is also known that MMSE mitigates both interference and noise compared to other linear detectors such as ZF, which cancels interference but enhances noise power [7].

The performance of the linear pre-coder and decoder is heavily dependent on the availability of timely channel state information (CSI) at both transmitter and receiver [8]. Although, a non-linear pre-coder and decoder can provide good performance, it is at expense of complex design [6]. At the receiver, the channel is estimated using known pilot symbols. Channel estimation techniques can either be least square (LS) based, minimum mean square error (MMSE) based or maximum likelihood (ML) based [9]. The pilot-assisted LS and MMSE channel estimators are employed in the MU-MIMO networks, due to their inherent advantages of low complexity and good mean square error (MSE) performance. MMSE receiver and detection are also considered for their simplicity and effectiveness in terms of BER performance that strongly depends on the MSEs of all the symbols.

To further improve the coverage area and reliability of the link in a MU-MIMO system [6], cooperative relays are incorporated to the system as one of the interference management techniques. With this technique, the relay node (RN) acts as a bridge that facilitates the cooperative communication and retransmits the signal received from a CUE to the MBS, interference-free. The CUE's high signal power causes interference to the neighbouring FAPs. Hence, an effective interference management is required to optimise the network lifetime. The RNs improve the transmit signal of the CUEs and maintain good communication to the MBS within the cluster by relaying their signals to the MBS. They should mitigate the cross-tier interference to the FAPs. This enhances the performance of the CUEs and FAPs in the MU-MIMO relay systems. Cooperative technique enables a FAP to gather information about its neighbouring femtocells and performs its allocation by considering its effects on the neighbours. This increases the average femtocells' throughput and quality of services (QoS) as well as its global performance, which are locally optimised. The MU-MIMO relay networks are heterogeneous featuring FAP, RN and MBS networks with their respective users, the half-duplex communication network with the CUEs, RNs, FUEs, MUEs in

multi-slot transmission. For such a distributed network, a centralised or joint pre-coder and decoder design is not appropriate or feasible. Therefore, decentralised algorithms for the FAPs, MUEs, RNs and CUEs are considered in the design optimal pre-coders and decoders based on pilot-assisted channel estimation. Each FAP manages its own sub-channels for suitable performance. The pre-coder for the RNs is also designed based on the channel estimation for the MU-MIMO relay networks considering amplify-and-forward (A-F) technique at the RN in this work.

1.1 Related Research

Different techniques for interference mitigation in femtocells have been proposed. The authors in [10] studied the interference mitigation techniques in femtocells/macrocell networks where a frequency reuse mechanism that increases overall system performance was proposed. Clustering and cooperative relay schemes have been used in multiple interference management schemes for a better radio resource allocation, interference management or power control [11]. The authors in [12], [13] investigated a management of cross-tier interference, where a novel femtocell clustering based on interference cancellation (IC) was introduced. A distributed antenna system was also used to mitigate cross-tier interference between macrocell and femocells. The authors in [14] proposed a scheme called IC-Relay-TDMA, which allows multi-user concurrent transmission in the source relay link. They aimed to cancel interference at the multi-antenna relay by linear IC techniques. A MIMO relaying system with fixed relay networks was introduced in [15] for IC. Authors in [16] analysed and designed an A-F, decode-forward and demodulation-forward relay protocol and discussed IC in the MU-MIMO environment.

Several pilot-aided schemes have been investigated to enhance the channel estimation accuracy in the MU-MIMO systems. This guarantees the performance of linear pre-coder and decoder designs. However, pilot contamination is one of the limitations of this technique. Authors in [17] provided an explicit expression of the massive MIMO user capacity in the pilot contaminated regime where the number of users is larger than the pilot sequence length. Authors in [18] proposed a channel estimation scheme for a massive MIMO which does not require the knowledge of the inter-cell large fading coefficient, thus no overload. An iterative soft decision IC has been investigated in multi-cell multi-user massive MIMO with pilot contamination. However, the algorithm is based only on MMSE estimation [19] while we consider two channel estimators for comparison purpose. Authors in [20] designed a pilot contamination pre-coding which maximizes the minimum SINR subject to the network sum power constraint for interference reduction. Most of these works assumed the perfect CSI at the transceiver side, whereas in practice CSI is prone to errors due to different factors. In [21] and [22], the authors did not only consider perfect CSI, but also the channel uncertainty and/or Imperfect

CSI. This work considers imperfect CSI for a more realistic scenario and, the pilot-aided scheme is also considered for synchronisation and channel estimation purposes to design the transceivers.

The linear pre-coder and decoder designs have also been considered as interference management techniques. In [23], with the assumption of perfect CSI, the authors employed an optimisation technique for the design of optimal source, relay and receiver in uplink MU-MIMO relay communication systems in order to minimize the MSE of the estimated signal at the destination. The pilot-aided channel estimation is not done in [23]. Channel uncertainties were considered in [24], where a robust transceiver design for a general MU-MIMO relay were studied in the presence of statistical CSI errors. Imperfect CSI was also considered in [25], where proposed joint linear pre-coder and decoder designs for downlink and uplink were compared to a conventional joint linear pre-coder and decoder design in MU-MIMO systems. The authors in [26] and [27] designed algorithms that converge to the optimum pre-coders and decoders for users in a MU-MIMO system. Moreover, the authors in [27] introduced interference alignment to help the femtocell user equipments (FUEs) to eliminate the cross-tier interference by aligning the MUE interference signal, subject to individual SINR constraints at their MBS. Interference alignment transceiver is designed in [28] to minimize the maximum MSE for multicell MU-MIMO wireless communication systems where a robust Min-Max MSE algorithm is proposed to counter the channel uncertainty. Transceiver designs with imperfect CSI were addressed in [29] for a MIMO relaying system where a near-optimal closed-form solution is provided for the source-to-relay-destination transceiver designs with imperfect CSI at all nodes. However, in the aforementioned research works, clustering, relaying and decentralised algorithms for the pre-coders and decoders design are not considered together. In this paper, the advantages of the aspect is employed to achieve a better interference management transceiver for the proposed distributed system and well instigated.

1.2 Main Contributions

In this paper, we present a cooperative relay interference management technique where decentralised algorithms for linear pre-coders and decoders design based on pilot-assisted channel estimation are employed. The main contributions of this paper are summarized as follows:

- This paper extends the system model presented in [27] by introducing cooperative RN systems to manage the cross-tier interference caused by the CUEs to FAPs, while providing further performance enhancements for the CUEs as well as increasing the coverage of macrocell networks. Numerical evaluations are provided to prove the benefit of this cooperative RN extension over a simple MU-MIMO system.

- This work presents a comparison performance of the LS and MMSE channel estimations in the MU-MIMO relay systems. Knowledge of channel autocorrelation matrix and SNR (covariance channel) are required for this channel estimation. Unlike [30] [29], which considered imperfect CSI, the pilot-assisted channel estimation is employed in the transceiver designs, because of its low complexity, simplicity and effectiveness. The authors in [27] considered a perfect CSI, which is not a practical scenario, while this work introduces the channel estimation in the design of each sub-optimal FUEs, MUEs, CUEs and RNs pre-coders and decoders. The effect of these channel estimation errors are considered in the simulations.
- The MMSE methodology considered is similar to [27]. However, instead of considering only a joint design for all the pre-coders, we consider decentralised transceiver designs for the MU-MIMO relay systems. We divide the optimisation problem into sub-optimal problems where we consider four different transceiver designs, the FUEs, MUEs, CUEs and RNs. Therefore, decentralised approach is considered in the design of pre-coders and decoders at the FAPs and MBS during the first and second time slots. Furthermore, the transceivers are designed with the estimated channels and are iteratively updated until their optimal values are found. Finding the optimal values for these pre-coders and decoders depends on the Lagrange multipliers.

1.3 Organisation and Notations

Organisation: The remaining sections of the paper are organised as follows: Section II describes the system model, problem formulation, proposed network architecture, uplink training and channel estimation as well as the uplink transmission designs. The decentralised algorithms for the linear transceiver designs with MMSE approach for the FAPs, MUEs and CUEs are presented in Section III. Section IV describes the performance evaluation. Section V presents the conclusion of the paper.

Notations: We use upper-case bold letters for matrices and lower-case bold letters for vectors. $(\cdot)^H$, $(\cdot)^T$, $(\cdot)^*$ and $(\cdot)^{-1}$ denote the Hermitian, transpose, optimal and inverse of matrices respectively. \mathbf{I}_N is a $N \times N$ identity matrix and $\mathbb{E}[\cdot]$ denote the expectation. $\|\cdot\|$ is the norm of a vector or complex scalar and $\text{tr}(\cdot)$ represents the trace of a matrix.

2 System Model and Problem Formulation

2.1 The Network Architecture

The network architecture consists of half-duplex multi-user relay Long Term Evolution-Advanced (LTE-Advanced) femtocell networks deployed into a macrocell network. The CUEs considered are grouped into clusters and communicate to the MBS through a RN. The FUEs and the CUEs transmit during the first time slot while the RNs transmit to the MBS during the second time slot. The MUEs, on the other hand, transmit continuously to the MBS during both first and second time slot. The network architecture is illustrated in Fig. B.1. The RN creates a cooperative communication between the CUEs

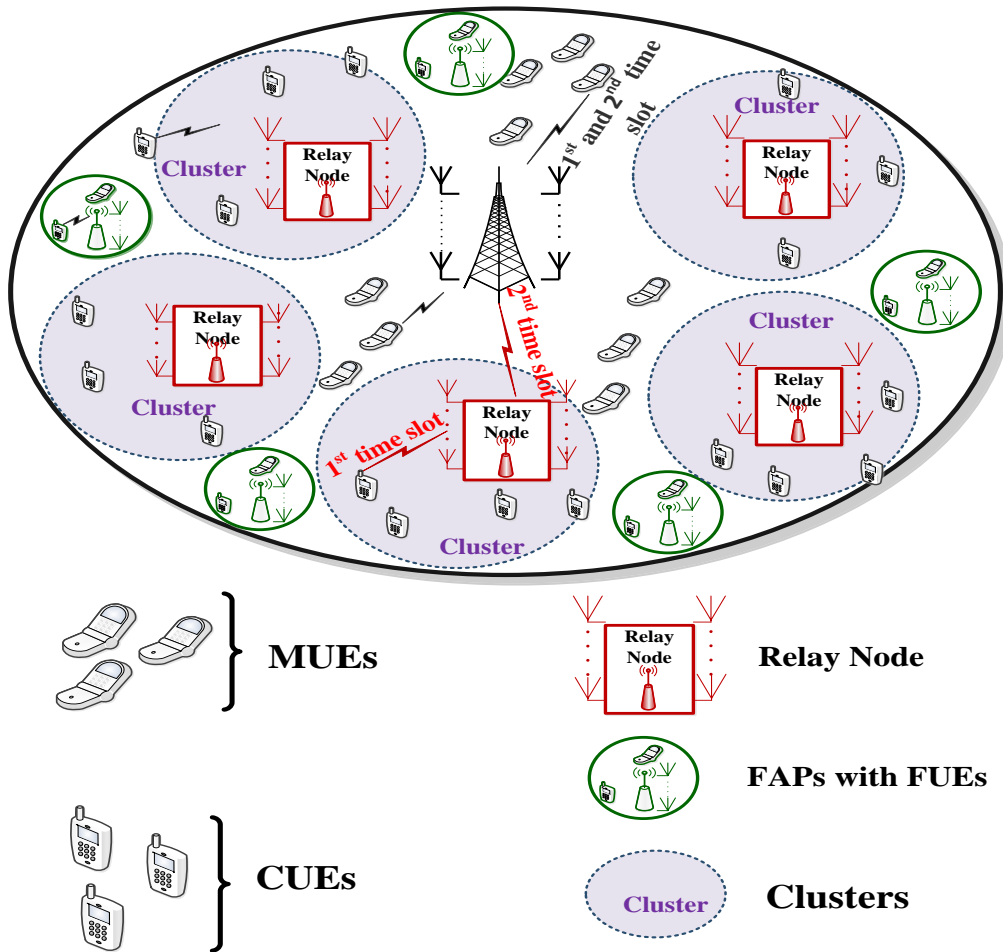


Figure B.1: The network architecture with a single MBS, MUEs, RNs clusters with CUEs, FAPs with FUEs

and the MBS. Furthermore, RNs enable a cross-tier interference management to the neighbouring FAPs.

2.2 Uplink Training and Channel Estimation

We consider an uplink transmission where all users share the same time-frequency resource. To detect the transmitted signal from the users, the base stations use the CSI knowledge acquired through uplink training. We assume that the channel remains constant during the training phase in order to analyse the system performance. For the channel estimation purposes, we use pilot symbols (a set of symbols whose location and values are known to the receiver) multiplexed with the information-bearing data [31]. During the uplink training phase, the users (FUEs, MUEs and CUEs), transmitting to the base stations (FAPs, MBS and RNs), are assigned pilot sequences of length τ symbols.

Let N_s , N_f , N_R and N_B represent the antennas at the users (FUEs, MUEs and CUEs), FAPs, RNs and MBS, respectively. We denote F as the number of FAP and U the number of FUEs in the f^{th} femtocells. Let R be the set of RN in each cluster, K the number of CUEs in the r^{th} RN and M the number of MUEs outside the cluster. Ψ denotes the pilot sequence matrix transmitted from the users to their base stations or access point. The pilot sequence matrix Ψ satisfies $\Psi\Psi^H = \mathbf{I}$. Let U_i be the number of FUEs in the j^{th} FAP. Thus, the received pilot signal \mathbf{y}_j^ψ at the j^{th} FAP is written as

$$\begin{aligned} \mathbf{y}_j^\psi = & \underbrace{\sum_{i=1}^{U_i} \sqrt{P_{ji}^{\text{FAP}} L_{ji}^{\text{FAP}} \mathbf{H}_{ji}^{\text{FAP}} \psi_{ji}^{\text{FAP}}}}_{\text{pilot signal from } j^{\text{th}} \text{ FAP users}} + \underbrace{\sum_{\substack{f=1 \\ f \neq j}}^F \sum_{u=1}^U \sqrt{P_{fu}^{\text{FAP}} L_{fu}^{\text{FAP}} \mathbf{H}_{jfu}^{\text{FAP}} \psi_{fu}^{\text{FAP}}}}_{\text{pilot from other femtocell}} + \underbrace{\sum_{m=1}^M \sqrt{P_{om}^{\text{MUE}} L_{om}^{\text{MUE}} \mathbf{H}_{jm}^{\text{MUE}} \psi_{om}^{\text{MUE}}}}_{\text{pilot from MUE outside the cluster}} \\ & + \underbrace{\sum_{r=1}^R \sum_{k=1}^K \sqrt{P_{rk}^{\text{CUE}} L_{rk}^{\text{CUE}} \mathbf{H}_{jrk}^{\text{CUE}} \psi_{rk}^{\text{CUE}}}}_{\text{pilot from the CUE in the RN}} + \mathbf{n}_j^\psi, \end{aligned} \quad (\text{B.1})$$

where P_{ji}^{FAP} and P_{fu}^{FAP} are the transmit powers of the i^{th} FUE of the j^{th} FAP and the u^{th} FUE of the f^{th} FAP while P_{om}^{MUE} and P_{rk}^{CUE} are the transmit powers of the m^{th} MUE of the MBS and k^{th} CUE of the r^{th} RN. $\mathbf{H}_{ji}^{\text{FAP}}$ denotes the channel matrix of the i^{th} user of the j^{th} FAP. $\mathbf{H}_{jfu}^{\text{FAP}}$ is considered as the channel matrix from the u^{th} user of the f^{th} femtocell to the j^{th} FAP, $\mathbf{H}_{jm}^{\text{MUE}}$ is the channel matrix from m^{th} MUE to the j^{th} FAP and $\mathbf{H}_{jrk}^{\text{CUE}}$ is the channel matrix from k^{th} CUE of the r^{th} RN to the j^{th} FAP. It is worth mentioning that $L_{ji}^{\text{FAP}} \mathbf{H}_{ji}^{\text{FAP}}$ is the propagation loss of the i^{th} FUE of the j^{th} FAPs while $L_{fu}^{\text{FAP}} \mathbf{H}_{jfu}^{\text{FAP}}$ is the propagation loss of the u^{th} FUE of the f^{th} FAP. Similarly, $L_{om}^{\text{MUE}} \mathbf{H}_{jm}^{\text{MUE}}$ is the propagation loss of the m^{th} MUE of the MBS and $L_{rk}^{\text{CUE}} \mathbf{H}_{jrk}^{\text{CUE}}$ is the propagation loss of the k^{th} CUE of the r^{th} RN. However, L_{ji}^{FAP} , L_{fu}^{FAP} , L_{om}^{MUE} and L_{rk}^{CUE} model the distance in slow fading while $\mathbf{H}_{ji}^{\text{FAP}}$, $\mathbf{H}_{jfu}^{\text{FAP}}$, $\mathbf{H}_{jm}^{\text{MUE}}$ and $\mathbf{H}_{jrk}^{\text{CUE}}$ model the fast Rayleigh fading. ψ_{ji}^{FAP} and ψ_{fu}^{FAP} are the pilot symbol of the i^{th} FUE of the j^{th} FAP and u^{th} FUE of the f^{th} FAP, respectively. ψ_{om}^{MUE} and ψ_{rk}^{CUE} are the pilot symbol of the m^{th} MUE of the MBS and k^{th} CUE of the r^{th} RN, respectively. \mathbf{n}_j^ψ is the vector representing additive white Gaussian noise (AWGN) at the j^{th} FAP, where the AWGN vector satisfies

$\mathbb{E}\{\mathbf{n}_j^\psi \mathbf{n}_j^{\psi H}\} = (\sigma_j^{\text{FAP}})^2 \mathbf{I}_{N_f}$ in which $\mathbf{n}_j^{\psi H}$ is the conjugate transpose of \mathbf{n}_j and \mathbf{I}_{N_f} denotes the identity matrix. The received pilot signal \mathbf{y}_r^ψ at the r^{th} RN is written as

$$\begin{aligned} \mathbf{y}_r^\psi = & \underbrace{\sum_{k=1}^K \sqrt{P_{rk}^{\text{CUE}} L_{rk}^{\text{CUE}} \mathbf{H}_{rk}^{\text{CUE}} \psi_{r,k}^{\text{CUE}}}}_{\text{pilot from the } r^{\text{th}} \text{ RN users}} + \underbrace{\sum_{f=1}^F \sum_{u=1}^U \sqrt{P_{fu}^{\text{FAP}} L_{fu}^{\text{FAP}} \mathbf{H}_{rfu}^{\text{FAP}} \psi_{fu}^{\text{FAP}}}}_{\text{pilot from the femtocells}} \\ & + \underbrace{\sum_{m=1}^M \sqrt{P_{om}^{\text{MUE}} L_{om}^{\text{MUE}} \mathbf{H}_{rm}^{\text{MUE}} \psi_{om}^{\text{MUE}}}}_{\text{pilot from the other MUEs}} + \mathbf{n}_r^\psi, \end{aligned} \quad (\text{B.2})$$

where $\mathbf{H}_{rk}^{\text{CUE}}$ is the channel matrix from the k^{th} CUE of the r^{th} RN. $\mathbf{H}_{rfu}^{\text{FAP}}$ is the channel matrix from the u^{th} FUE of the f^{th} femtocell to the r^{th} RN and $\mathbf{H}_{rm}^{\text{MUE}}$ is the channel matrix from m^{th} MUE to the r^{th} RN. \mathbf{n}_r^ψ is the AWGN vector at the r^{th} RN that satisfies $\mathbb{E}\{\mathbf{n}_r^\psi \mathbf{n}_r^{\psi H}\} = (\sigma_r^{\text{CUE}})^2 \mathbf{I}_{N_R}$. The received pilot signal \mathbf{y}_o^ψ at the MBS is written as:

$$\begin{aligned} \mathbf{y}_o^\psi = & \underbrace{\sum_{m=1}^M \sqrt{P_{om}^{\text{MUE}} L_{om}^{\text{MUE}} \mathbf{H}_{om}^{\text{MUE}} \psi_{om}^{\text{MUE}}}}_{\text{pilot from all MUEs}} + \underbrace{\sum_{f=1}^F \sum_{u=1}^U \sqrt{P_{fu}^{\text{FAP}} L_{fu}^{\text{FAP}} \mathbf{H}_{ofu}^{\text{FAP}} \psi_{fu}^{\text{FAP}}}}_{\text{pilot from all femtocells}} \\ & + \underbrace{\sum_{r=1}^R \sum_{k=1}^K \sqrt{P_{rk}^{\text{CUE}} L_{rk}^{\text{CUE}} \mathbf{H}_{ork}^{\text{CUE}} \psi_{rk}^{\text{CUE}}}}_{\text{pilot from all CUEs in the RNs}} + \mathbf{n}_o^\psi, \end{aligned} \quad (\text{B.3})$$

where $\mathbf{H}_{om}^{\text{MUE}}$ is the channel matrix from the m^{th} MUE of the MBS. $\mathbf{H}_{ork}^{\text{CUE}}$ is the channel gain from k^{th} CUE of the r^{th} RN to the MBS and $\mathbf{H}_{ofu}^{\text{FAP}}$ is the channel matrix from the u^{th} user of the f^{th} FAP to the MBS. \mathbf{n}_o^ψ is the AWGN vector at the MBS that satisfies $\mathbb{E}\{\mathbf{n}_o^\psi \mathbf{n}_o^{\psi H}\} = (\sigma_o^{\text{MUE}})^2 \mathbf{I}_{N_B}$.

2.2.1 LS Channel Estimator

The LS channel estimation method finds the channel estimate $\hat{\mathbf{H}}$ by minimizing $\hat{\mathbf{H}} = \underset{\mathbf{H}}{\text{argmin}} \|\mathbf{Y} - \Psi \hat{\mathbf{H}}\|$ which is reduced as $\hat{\mathbf{H}}^{\text{LS}} = \frac{\mathbf{Y}}{\Psi}$. The LS channel estimation $\hat{\mathbf{H}}_{ji}^{\text{FAP-LS}}$ for the j^{th} FAP is given as

$$\hat{\mathbf{H}}_{ji}^{\text{FAP-LS}} = \frac{\mathbf{y}_j^\psi}{\psi_{ji}^{\text{FAP}} \cdot \sqrt{P_{ji}^{\text{FAP}} L_{ji}^{\text{FAP}}}}. \quad (\text{B.4})$$

The LS channel estimate $\hat{\mathbf{H}}_{rk}^{\text{CUE-LS}}$ for r^{th} RN is obtained as follows

$$\hat{\mathbf{H}}_{rk}^{\text{CUE-LS}} = \frac{\mathbf{y}_r^\psi}{\psi_{rk}^{\text{CUE}} \cdot \sqrt{P_{rk}^{\text{CUE}} L_{rk}^{\text{CUE}}}}. \quad (\text{B.5})$$

Similarly, the LS channel estimate $\hat{\mathbf{H}}_{om}^{\text{MUE-LS}}$ for MBS is obtained as

$$\hat{\mathbf{H}}_{om}^{\text{MUE-LS}} = \frac{\mathbf{y}_o^\psi}{\psi_{om}^{\text{MUE}} \cdot \sqrt{P_{om}^{\text{MUE}} L_{om}^{\text{MUE}}}}, \quad (\text{B.6})$$

where we assume that in (B.4, B.5, B.6), P_{ji}^{FAP} , P_{rk}^{CUE} , P_{om}^{MUE} and L_{ji}^{FAP} , L_{rk}^{CUE} , L_{om}^{MUE} are known.

2.2.2 MMSE Channel Estimator

Considering the LS channel estimation equations in (B.4, B.5, B.6), we can formulate the MMSE channel estimations. Hence, the MMSE channel estimator $\hat{\mathbf{H}}_{ji}^{\text{FAP-MMSE}}$ for j^{th} FAP is given as

$$\hat{\mathbf{H}}_{ji}^{\text{FAP-MMSE}} = \hat{\mathbf{H}}_{ji}^{\text{FAP-LS}} \cdot \mathbf{Q}_{ji}^{\text{FAP}} \cdot \mathbf{R}_{\mathbf{H}_{ji}^{\text{FAP}} \hat{\mathbf{H}}_{ji}^{\text{FAP-LS}}}, \quad (\text{B.7})$$

where $\mathbf{R}_{\mathbf{H}_{ji}^{\text{FAP}} \hat{\mathbf{H}}_{ji}^{\text{FAP-LS}}}$ represents the covariance matrix of $N \times N$ matrices $\mathbf{H}_{ji}^{\text{FAP}}$ and $\hat{\mathbf{H}}_{ji}^{\text{FAP-LS}}$, i.e.

$$\mathbf{R}_{\mathbf{H}_{ji}^{\text{FAP}} \hat{\mathbf{H}}_{ji}^{\text{FAP-LS}}} = \mathbb{E} \left\{ (\mathbf{H}_{ji}^{\text{FAP}}) (\hat{\mathbf{H}}_{ji}^{\text{FAP-LS}})^H \right\} \text{ and } \mathbf{Q}_{ji}^{\text{FAP}} = \left(\sum_{i=1}^{U_j} \mathbf{R}_{\mathbf{H}_{ji}^{\text{FAP}} \mathbf{H}_{ji}^{\text{FAP}}} + (\sigma_j^{\text{FAP}})^2 \mathbf{I}_{N_f} \right)^{-1}.$$

The MMSE channel estimator $\hat{\mathbf{H}}_{rk}^{\text{CUE-MMSE}}$ for r^{th} RN is obtained as

$$\hat{\mathbf{H}}_{rk}^{\text{CUE-MMSE}} = \hat{\mathbf{H}}_{rk}^{\text{CUE-LS}} \cdot \mathbf{Q}_{rk}^{\text{CUE}} \cdot \mathbf{R}_{\mathbf{H}_{rk}^{\text{CUE}} \hat{\mathbf{H}}_{rk}^{\text{CUE-LS}}}, \quad (\text{B.8})$$

where $\mathbf{R}_{\mathbf{H}_{rk}^{\text{CUE}} \hat{\mathbf{H}}_{rk}^{\text{CUE-LS}}}$ denotes the covariance matrix of $N \times N$ matrices $\mathbf{H}_{rk}^{\text{CUE}}$ and $\hat{\mathbf{H}}_{rk}^{\text{CUE-LS}}$, i.e.

$$\mathbf{R}_{\mathbf{H}_{rk}^{\text{CUE}} \hat{\mathbf{H}}_{rk}^{\text{CUE-LS}}} = \mathbb{E} \left\{ (\mathbf{H}_{rk}^{\text{CUE}}) (\hat{\mathbf{H}}_{rk}^{\text{CUE-LS}})^H \right\} \text{ and } \mathbf{Q}_{rk}^{\text{CUE}} = \left(\sum_{k=1}^K \mathbf{R}_{\mathbf{H}_{rk}^{\text{CUE}} \mathbf{H}_{rk}^{\text{CUE}}} + (\sigma_r^{\text{CUE}})^2 \mathbf{I}_{N_R} \right)^{-1}.$$

Similarly, the MMSE channel estimation $\hat{\mathbf{H}}_{om}^{\text{MUE-MMSE}}$ for MBS is given as

$$\hat{\mathbf{H}}_{om}^{\text{MUE-MMSE}} = \hat{\mathbf{H}}_{om}^{\text{MUE-LS}} \cdot \mathbf{Q}_{om}^{\text{MUE}} \cdot \mathbf{R}_{\mathbf{H}_{om}^{\text{MUE}} \hat{\mathbf{H}}_{om}^{\text{MUE-LS}}}, \quad (\text{B.9})$$

where $\mathbf{R}_{\mathbf{H}_{om}^{\text{MUE}} \hat{\mathbf{H}}_{om}^{\text{MUE-LS}}}$ represents the covariance matrix of $N \times N$ matrices $\mathbf{H}_{om}^{\text{MUE}}$ and $\hat{\mathbf{H}}_{om}^{\text{MUE-LS}}$, i.e.

$$\mathbf{R}_{\mathbf{H}_{om}^{\text{MUE}} \hat{\mathbf{H}}_{om}^{\text{MUE-LS}}} = \mathbb{E} \left\{ (\mathbf{H}_{om}^{\text{MUE}}) (\hat{\mathbf{H}}_{om}^{\text{MUE-LS}})^H \right\} \text{ and } \mathbf{Q}_{om}^{\text{MUE}} = \left(\sum_{m=1}^M \mathbf{R}_{\mathbf{H}_{om}^{\text{MUE}} \mathbf{H}_{om}^{\text{MUE}}} + (\sigma_o^{\text{MUE}})^2 \mathbf{I}_{N_B} \right)^{-1}.$$

2.3 Uplink Transmission Design

The signals are transmitted from the CUEs to the MBS through the RN during the first time slots. It is assumed that the channels from the CUE to the RN are estimated at the RN. Similarly, the channels from the RN to the MBS are estimated at the MBS and fed back to the RN, which then forwards the estimates back to the MUE. The FUEs also transmit to their respective FAPs during the first time slot while the MUEs transmit to the MBS during both time slots. The relaying operates in a half-duplex mode, in the first time slot, and the CUEs use transmit pre-coding to broadcast to the RN and in the second time slot, the RNs cooperatively forms a distributed relay beam-former to forward the signals to MBS. The Rayleigh flat-fading channel and noise have independent and identically distributed (i.i.d.) complex Gaussian entries with zero mean and unit variance $\mathcal{CN}(0, 1)$.

The complex received signal vector at the j^{th} FAP during the first time slot \mathbf{y}_j is defined as

$$\begin{aligned} \mathbf{y}_j^{\text{FAP}} = & \underbrace{\sum_{i=1}^{U_i} \sqrt{P_{ji}^{\text{FAP}} L_{ji}^{\text{FAP}} \mathbf{H}_{ji}^{\text{FAP}} \mathbf{w}_{ji}^{\text{FAP}} s_{ji}^{\text{FAP}}}}_{\text{FUEs signal of the } j^{\text{th}} \text{ FAP}} + \underbrace{\sum_{m=1}^M \sqrt{P_{om}^{\text{MUE}} L_{om}^{\text{MUE}} \mathbf{H}_{jm}^{\text{MUE}} \mathbf{w}_{om}^{\text{MUE}} s_{om}^{\text{MUE}}}}_{\text{MUEs interference}} \\ & + \underbrace{\sum_{\substack{f=1 \\ f \neq j}}^F \sum_{\substack{u=1 \\ u \neq j}}^U \sqrt{P_{fu}^{\text{FAP}} L_{fu}^{\text{FAP}} \mathbf{H}_{jfu}^{\text{FAP}} \mathbf{w}_{fu}^{\text{FAP}} s_{fu}^{\text{FAP}}}}_{\text{other femtocells interference}} + \underbrace{\sum_{r=1}^R \sum_{k=1}^K \sqrt{P_{rk}^{\text{CUE}} L_{rk}^{\text{CUE}} \mathbf{H}_{jrk}^{\text{CUE}} \mathbf{w}_{rk}^{\text{CUE}} s_{rk}^{\text{CUE}}}}_{\text{CUEs interference}} + \underbrace{\mathbf{n}_j}_{\text{noise}}, \quad (\text{B.10}) \end{aligned}$$

where s_{ji}^{FAP} is the message of the i^{th} user of the j^{th} FAP and $\mathbf{w}_{ji}^{\text{FAP}}$ is the pre-coding vector of the i^{th} FUE of the j^{th} femtocell, while s_{om}^{MUE} and $\mathbf{w}_{om}^{\text{MUE}}$ are the message and pre-coding vector of the m^{th} MUE of the MBS, respectively. s_{fu}^{FAP} is the message of the u^{th} FUE of the f^{th} FAP and $\mathbf{w}_{fu}^{\text{FAP}}$ is the pre-coding vector of the u^{th} FUE of the f^{th} FAP. s_{rk}^{CUE} and $\mathbf{w}_{rk}^{\text{CUE}}$ are the message and the pre-coding vector of the k^{th} CUE of the r^{th} RN, respectively. \mathbf{n}_j is the AWGN vector at the j^{th} FAP and that satisfies $\mathbb{E}\{\mathbf{n}_j \mathbf{n}_j^H\} = (\sigma_j^{\text{FAP}})^2 \mathbf{I}_{N_j}$.

In order to design the pre-coders in (B.10), the knowledge of $\mathbf{w}_{om}^{\text{MUE}}$, $\mathbf{w}_{fu}^{\text{FAP}}$ and $\mathbf{w}_{rk}^{\text{CUE}}$ are required. This can be done by joint design which is computationally complex. To simplify the pre-coder design problem, the design of the pre-coders in (B.10) is divided into four different pre-coder designs where in each design, we assume that the pre-coder variable that is not currently being designed is represented by ZF and is independent of each other. Hence, to find the optimal $\mathbf{w}_{ji}^{\text{FAP}}$ in (B.10) of the i^{th} FUE at the j^{th} FAP, $\mathbf{w}_{om}^{\text{MUE}}$, $\mathbf{w}_{fu}^{\text{FAP}}$ and $\mathbf{w}_{rk}^{\text{CUE}}$ are found using ZF pre-coder assumption and an estimation error as follows

$$\mathbf{w}_{om}^{\text{MUE}'} = \left[(\hat{\mathbf{H}}_{om}^{\text{MUE-Est}})^H \left((\hat{\mathbf{H}}_{om}^{\text{MUE-Est}})^H \hat{\mathbf{H}}_{om}^{\text{MUE-Est}} \right)^{-1} + \varepsilon \right], \quad (\text{B.11})$$

$$\mathbf{w}_{fu}^{\text{FAP}'} = \left[(\hat{\mathbf{H}}_{fu}^{\text{FAP-Est}})^H \left((\hat{\mathbf{H}}_{fu}^{\text{FAP-Est}})^H \hat{\mathbf{H}}_{fu}^{\text{FAP-Est}} \right)^{-1} + \varepsilon \right], \quad (\text{B.12})$$

$$\mathbf{w}_{rk}^{\text{CUE}'} = \left[(\hat{\mathbf{H}}_{rk}^{\text{CUE-Est}})^H \left((\hat{\mathbf{H}}_{rk}^{\text{CUE-Est}})^H \hat{\mathbf{H}}_{rk}^{\text{CUE-Est}} \right)^{-1} + \varepsilon \right], \quad (\text{B.13})$$

where ε represents an estimation error, a Gaussian random number of zero mean and σ_ε^2 . Equation (B.10) is rewritten with the ZF assumption design as

$$\begin{aligned} \mathbf{y}_j^{\text{FAP}'} = & \sum_{i=1}^{U_i} \sqrt{P_{ji}^{\text{FAP}} L_{ji}^{\text{FAP}} \mathbf{H}_{ji}^{\text{FAP}} \mathbf{w}_{ji}^{\text{FAP}} s_{ji}^{\text{FAP}}} + \sum_{\substack{f=1 \\ f \neq j}}^F \sum_{\substack{u=1 \\ u \neq j}}^U \sqrt{P_{fu}^{\text{FAP}} L_{fu}^{\text{FAP}} \mathbf{H}_{jfu}^{\text{FAP}} \mathbf{w}_{fu}^{\text{FAP}'} s_{fu}^{\text{FAP}}} \\ & + \sum_{m=1}^M \sqrt{P_{om}^{\text{MUE}} L_{om}^{\text{MUE}} \mathbf{H}_{jm}^{\text{MUE}} \mathbf{w}_{om}^{\text{MUE}'} s_{om}^{\text{MUE}}} + \sum_{r=1}^R \sum_{k=1}^K \sqrt{P_{rk}^{\text{CUE}} L_{rk}^{\text{CUE}} \mathbf{H}_{jrk}^{\text{CUE}} \mathbf{w}_{rk}^{\text{CUE}'} s_{rk}^{\text{CUE}}} + \mathbf{n}_j. \quad (\text{B.14}) \end{aligned}$$

The received signal $\mathbf{y}_o^{\text{MBS}'}$ of the MBS during the first time slot is assumed to be

$$\begin{aligned} \mathbf{y}_o^{\text{MBS}'} &= \sum_{m=1}^M \sqrt{P_{om}^{\text{MUE}} L_{om}^{\text{MUE}}} \mathbf{H}_{o,m}^{\text{MUE}} \mathbf{w}_{om}^{\text{MUE}} s_{o,m}^{\text{MUE}} + \sum_{r=1}^R \sum_{k=1}^K \sqrt{P_{rk}^{\text{CUE}} L_{rk}^{\text{CUE}}} \mathbf{H}_{ork}^{\text{CUE}} \mathbf{w}_{rk}^{\text{CUE}'} s_{rk}^{\text{CUE}} \\ &+ \sum_{f=1}^F \sum_{u=1}^U \sqrt{P_{fu}^{\text{FAP}} L_{fu}^{\text{FAP}}} \mathbf{H}_{ofu}^{\text{FAP}} \mathbf{w}_{fu}^{\text{FAP}'} s_{fu}^{\text{FAP}} + \mathbf{n}_o, \end{aligned} \quad (\text{B.15})$$

where \mathbf{n}_o is the AWGN vector with variance $(\sigma_o^{\text{MBS}})^2$ distributed according to $\mathcal{CN}(0, (\sigma_o^{\text{MBS}})^2)$.

Similarly, the received signal $\mathbf{y}_r^{\text{RN}'}$ at the RN during the first time slot is

$$\begin{aligned} \mathbf{y}_r^{\text{RN}'} &= \sum_{k=1}^K \sqrt{P_{rk}^{\text{CUE}} L_{rk}^{\text{CUE}}} \mathbf{H}_{rk}^{\text{CUE}} \mathbf{w}_{rk}^{\text{CUE}} s_{rk}^{\text{CUE}} + \sum_{m=1}^M \sqrt{P_{om}^{\text{MUE}} L_{om}^{\text{MUE}}} \mathbf{H}_{rm}^{\text{MUE}} \mathbf{w}_{om}^{\text{MUE}'} s_{om}^{\text{MUE}} \\ &+ \sum_{f=1}^F \sum_{u=1}^U \sqrt{P_{fu}^{\text{FAP}} L_{fu}^{\text{FAP}}} \mathbf{H}_{rfu}^{\text{FAP}} \mathbf{w}_{fu}^{\text{FAP}'} s_{fu}^{\text{FAP}} + \mathbf{n}_r, \quad \forall r = 1, \dots, R \end{aligned} \quad (\text{B.16})$$

where \mathbf{n}_r is the AWGN vector with variance $(\sigma_r^{\text{CUE}})^2$ which is distributed according to $\mathcal{CN}(0, (\sigma_r^{\text{CUE}})^2)$. It is assumed that the channels are i.i.d. complex Gaussian random variables.

The RN receives the signal from the K -CUEs and interference from the FUEs and MUEs. It amplifies and forwards the signal vector multiplied with the RN pre-coder \mathbf{F}_{or} during the second time slot. The amplified r^{th} transmit signal \mathbf{x}_{or} to the MBS during the second time slot is expressed as

$$\mathbf{x}_{or} = \mathbf{F}_{or} \times \mathbf{y}_r^{\text{RN}'}, \quad \forall r = 1, \dots, R. \quad (\text{B.17})$$

The MUEs continuously transmit signals to the MBS in both time slots. The FUEs transmit only during the first time slot. Therefore, the received signal $\mathbf{y}_o^{\text{MBS-nd}'}$ at the MBS is written as:

$$\mathbf{y}_o^{\text{MBS-nd}'} = \sum_{r=1}^R \sqrt{P_r L_r} \mathbf{H}_{or} \mathbf{x}_{or} + \underbrace{\sum_{m=1}^M \sqrt{P_{om}^{\text{MUE}} L_{om}^{\text{MUE}}} \mathbf{H}_{om}^{\text{MUE}} \mathbf{w}_{om}^{\text{MUE}} s_{om}^{\text{MUE}}}_{\text{MUEs signal at the MBS}} + \mathbf{n}_o, \quad (\text{B.18})$$

where \mathbf{H}_{or} is the channel matrix from the r^{th} RN to the MBS and P_r is the transmit power at the RN. L_r is the propagation loss at the r^{th} RN. \mathbf{n}_o is the AWGN vector at the MBS with variance $(\sigma_o^{\text{MBS}})^2$ which is distributed according to $\mathcal{CN}(0, (\sigma_o^{\text{MBS}})^2)$. After substitution and calculation, the received signal at the MBS during the second time signal is written as

$$\begin{aligned} \mathbf{y}_o^{\text{MBS-nd}'} &= \underbrace{\sum_{r=1}^R \sum_{k=1}^K \sqrt{P_r L_r} \mathbf{H}_{or} \mathbf{F}_{or} \mathbf{H}_{rk}^{\text{CUE}} \mathbf{w}_{rk}^{\text{CUE}} s_{rk}^{\text{CUE}}}_{1^{\text{st term}}} \\ &+ \underbrace{\sum_{m=1}^M \sqrt{P_{om}^{\text{MUE}} L_{om}^{\text{MUE}}} \mathbf{H}_{o,m}^{\text{MUE}} \mathbf{w}_{om}^{\text{MUE}} s_{om}^{\text{MUE}}}_{2^{\text{nd term}}} + \mathbf{z}_o, \end{aligned} \quad (\text{B.19})$$

2. SYSTEM MODEL AND PROBLEM FORMULATION

where $\mathbf{z}_o = \sum_{r=1}^R \mathbf{H}_{o,r} \mathbf{F}_{or} \tilde{\mathbf{n}}_r + \mathbf{n}_o$ and $\tilde{\mathbf{n}}_r = \left(\sum_{f=1}^F \sum_{u=1}^U \mathbf{H}_{rfu}^{\text{FAP}} \mathbf{w}_{fu}^{\text{FAP}} s_{fu}^{\text{FAP}} + \mathbf{n}_r \right)$. The femtocell interferences during the first time slot are considered as noise at the MBS. The 1^{st} and 2^{nd} terms of equation (B.19) are the signals to be decoded at the MBS during the second time slot, and need to be combined as one term. *Note:* N_s is the number of antennas for users. N_R is the number of equipped antenna for RNs, N_B is the number of MBS antennas and d_s is the data stream. The following is assumed:

$\hat{d} = \sum_{k=1}^K d_s, \hat{N}_s = \sum_{k=1}^K N_s, N_R \geq \hat{d}$ and $\hat{N}_s > \hat{d}$. We assume that $N_B \geq N_R$. With the above assumptions, the signals, channels matrices and pre-coders for CUEs and MUEs (during the second time slot) are combined as in (B.20, B.21, B.22), respectively.

$$\mathbf{s}^{\text{UE}} = \left[\underbrace{s_{1,1}^{\text{CUE}}, \dots, s_{1,K}^{\text{CUE}} | s_{2,1}^{\text{CUE}}, \dots, s_{2,K}^{\text{CUE}} | \dots | s_{R,1}^{\text{CUE}}, \dots, s_{R,K}^{\text{CUE}}}_{\text{CUE transmit signals}} \underbrace{s_{o,1}^{\text{MUE}}, \dots, s_{o,M}^{\text{MUE}}}_{\substack{\text{MUE transmit signals} \\ \text{at } 2^{\text{nd}} \text{ time slot}}} \right]^T \in \mathbb{C}^{1 \times (RK+M)\hat{d}} \quad (\text{B.20})$$

$$\mathbf{H}^{\text{UE}} = \left[\underbrace{\sqrt{P_{11}^{\text{CUE}} L_{11}^{\text{CUE}}} \mathbf{H}_{11}^{\text{CUE}}, \dots, \sqrt{P_{1K}^{\text{CUE}} L_{1K}^{\text{CUE}}} \mathbf{H}_{1K}^{\text{CUE}} | \dots | \sqrt{P_{R1}^{\text{CUE}} L_{R1}^{\text{CUE}}} \mathbf{H}_{R1}^{\text{CUE}}, \dots, \sqrt{P_{RK}^{\text{CUE}} L_{RK}^{\text{CUE}}} \mathbf{H}_{RK}^{\text{CUE}}}_{\text{CUE channels matrices}} \underbrace{\left| \sqrt{P_{o1}^{\text{MUE}} L_{o1}^{\text{MUE}}} \mathbf{H}_{o1}^{\text{MUE}}, \dots, \sqrt{P_{oM}^{\text{MUE}} L_{oM}^{\text{MUE}}} \mathbf{H}_{oM}^{\text{MUE}} \right|}_{\text{MUE channel matrix}} \right] \in \mathbb{C}^{N_R \times \hat{N}_s (RK+M)} \quad (\text{B.21})$$

$$\mathbf{W}^{\text{UE}} = \begin{pmatrix} \mathbf{w}_{11}^{\text{CUE}} & 0 & \dots & 0 & 0 & \dots & 0 \\ 0 & \mathbf{w}_{22}^{\text{CUE}} & \dots & 0 & 0 & \dots & 0 \\ \vdots & \vdots & \ddots & \vdots & \vdots & \vdots & \vdots \\ 0 & 0 & \dots & \mathbf{w}_{RK}^{\text{CUE}} & 0 & \dots & 0 \\ 0 & 0 & \dots & 0 & \mathbf{w}_{o1}^{\text{MUE}} & \dots & 0 \\ \vdots & \vdots & \vdots & \vdots & \vdots & \ddots & \vdots \\ 0 & 0 & \dots & 0 & 0 & \dots & \mathbf{w}_{oM}^{\text{MUE}} \end{pmatrix} \in \mathbb{C}^{\hat{N}_s (RK+M) \times \hat{d} (RK+M)} \quad (\text{B.22})$$

$$\mathbf{H}_o = [\sqrt{P_1 L_1} \mathbf{H}_{o,1}, \dots, \sqrt{P_R L_R} \mathbf{H}_{o,R}] \in \mathbb{C}^{N_B \times \hat{N}_R (R)} \quad (\text{B.23})$$

$$\mathbf{F}_o = [\mathbf{F}_{o,1}, \dots, \mathbf{F}_{o,R}]^T \in \mathbb{C}^{N_R \times \hat{N}_R (R)} \quad (\text{B.24})$$

The received signal $\mathbf{y}_o^{\text{MBS-nd}}$ of the MBS in (B.19) during the second time slot can be rewritten as

$$\mathbf{y}_o^{\text{MBS-nd}} = \mathbf{H}_o \mathbf{F}_o \mathbf{H}^{\text{UE}} \mathbf{W}^{\text{UE}} \mathbf{s}^{\text{UE}} + \mathbf{z}_o, \quad (\text{B.25})$$

where \mathbf{H}_o and \mathbf{F}_o are as in (B.23) and (B.24), respectively. The combination of CUEs and MUEs will be referred as UEs throughout this article. \mathbf{z}_o is a $\mathbb{C}^{N_B \times 1}$ is the AWGN vector with variance $\sigma_{\mathbf{z}_o}^2$ which is distributed according to $\mathcal{CN}(0, \sigma_{\mathbf{z}_o}^2)$.

3 Decentralised Algorithms for Linear Transceiver Designs

In this section, the decentralised transceiver optimisation algorithms for the FAPs, MUEs and UEs are designed with the coordinated MMSE approach during the first and second time slots.

3.1 Coordinated MMSE Approach for Femtocell and MUEs Pre-coders and Decoders during the First Time Slot

3.1.1 Optimisation of the FAPs Pre-coding and Decoding Vectors

The algorithm starts with initialized random pre-coders and decoders $\mathbf{w}_{jx}^{\text{FAP}}$. In each iteration, the FUE pre-coders and decoders are updated alternatively. Considering the MMSE receiver, we apply the MMSE decoding for j^{th} FAP such that the interference is received from the MUEs and neighbouring femtocells during the first time slot. The decoded information $\hat{s}_{jx}^{\text{FAP}}$ for the x^{th} FUE of the j^{th} FAP can be expressed as

$$\begin{aligned}
 \hat{s}_{jx}^{\text{FAP}} &= (\mathbf{d}_{jx}^{\text{FAP}})^H \cdot \mathbf{y}_{ji}^{\text{FAP}} \\
 &= \sum_{i=1}^{U_i} (\mathbf{d}_{jx}^{\text{FAP}})^H \sqrt{P_{ji}^{\text{FAP}} L_{ji}^{\text{FAP}}} \mathbf{H}_{ji}^{\text{FAP}} \mathbf{w}_{ji}^{\text{FAP}} s_{ji}^{\text{FAP}} + \sum_{m=1}^M (\mathbf{d}_{jx}^{\text{FAP}})^H \sqrt{P_{om}^{\text{MUE}} L_{om}^{\text{MUE}}} \mathbf{H}_{jm}^{\text{MUE}} \mathbf{w}_{om}^{\text{MUE}} s_{om}^{\text{MUE}} \\
 &+ \sum_{\substack{f=1 \\ f \neq j}}^F \sum_{u=1}^U (\mathbf{d}_{jx}^{\text{FAP}})^H \sqrt{P_{fu}^{\text{FAP}} L_{fu}^{\text{FAP}}} \mathbf{H}_{jfu}^{\text{FAP}} \mathbf{w}_{fu}^{\text{FAP}} s_{fu}^{\text{FAP}} + \sum_{r=1}^R \sum_{k=1}^K (\mathbf{d}_{jx}^{\text{FAP}})^H \sqrt{P_{rk}^{\text{CUE}} L_{rk}^{\text{CUE}}} \mathbf{H}_{jrk}^{\text{CUE}} \mathbf{w}_{rk}^{\text{CUE}} s_{rk}^{\text{CUE}} \\
 &+ (\mathbf{d}_{jx}^{\text{FAP}})^H \mathbf{n}_j,
 \end{aligned} \tag{B.26}$$

where $\mathbf{d}_{j,x}^{\text{FAP}}$ is the decoding vector for x^{th} FUE of j^{th} FAP. In order to minimize the power noise component, we employ the coordinated MMSE algorithm that minimizes the sum MSE at the j^{th} FAP estimated as

$$\begin{aligned}
 &\min_{\substack{\mathbf{w}_{j1}^{\text{FAP}}, \dots, \mathbf{w}_{jU_i}^{\text{FAP}} \\ \mathbf{d}_{j1}^{\text{FAP}}, \dots, \mathbf{d}_{jU_i}^{\text{FAP}}}} \sum_{x=1}^{U_i} \mathbb{E} [\|\hat{s}_{j,x}^{\text{FAP}} - s_{j,x}^{\text{FAP}}\|^2] \\
 &\text{subject to } (\mathbf{w}_{jx}^{\text{FAP}})^H (\mathbf{w}_{jx}^{\text{FAP}}) \leq \frac{P_{jx}^{\text{FAP}}}{L_{jx}^{\text{FAP}}}, \quad x = 1, \dots, U_i,
 \end{aligned} \tag{B.28}$$

where P_{jx}^{FAP} is the maximum transmit power of the x^{th} FUE of the j^{th} FAP. We consider the estimated channels to rewrite the minimum sum MSE at the x^{th} FUE of the j^{th} FAP. This is rewritten as

$$\begin{aligned}
 & \min_{\substack{\mathbf{w}_{j1}^{\text{FAP}}, \dots, \mathbf{w}_{jU_i}^{\text{FAP}} \\ \mathbf{d}_{j1}^{\text{FAP}}, \dots, \mathbf{d}_{jU_i}^{\text{FAP}}}} \sum_{x=1}^{U_i} \left[\left\| (\mathbf{d}_{j,x}^{\text{FAP}})^H \sqrt{P_{jx}^{\text{FAP}} L_{jx}^{\text{FAP}}} \hat{\mathbf{H}}_{jx}^{\text{FAP-Est}} \mathbf{w}_{jx}^{\text{FAP}} - 1 \right\|^2 \right. \\
 & + \sum_{\substack{i=1 \\ i \neq x}}^{U_i} \left\| (\mathbf{d}_{j,x}^{\text{FAP}})^H \sqrt{P_{ji}^{\text{FAP}} L_{ji}^{\text{FAP}}} \hat{\mathbf{H}}_{ji}^{\text{FAP-Est}} \mathbf{w}_{ji}^{\text{FAP}'} \right\|^2 \\
 & + \sum_{m=1}^M \left\| (\mathbf{d}_{j,x}^{\text{FAP}})^H \sqrt{P_{om}^{\text{MUE}} L_{om}^{\text{MUE}}} \hat{\mathbf{H}}_{jm}^{\text{MUE-Est}} \mathbf{w}_{om}^{\text{MUE}'} \right\|^2 \\
 & + \sum_{\substack{f=1 \\ f \neq j}}^F \sum_{u=1}^U \left\| (\mathbf{d}_{j,x}^{\text{FAP}})^H \sqrt{P_{fu}^{\text{FAP}} L_{fu}^{\text{FAP}}} \hat{\mathbf{H}}_{jfu}^{\text{FAP-Est}} \mathbf{w}_{fu}^{\text{FAP}'} \right\|^2 \\
 & \left. + \sum_{r=1}^R \sum_{k=1}^K \left\| (\mathbf{d}_{j,x}^{\text{FAP}})^H \sqrt{P_{rk}^{\text{CUE}} L_{rk}^{\text{CUE}}} \hat{\mathbf{H}}_{jrk}^{\text{CUE-Est}} \mathbf{w}_{rk}^{\text{CUE}'} \right\|^2 + \|(\mathbf{d}_{j,x}^{\text{FAP}})\|^2 \sigma^2 \right] \\
 & \text{subject to: } (\mathbf{w}_{jx}^{\text{FAP}})^H (\mathbf{w}_{jx}^{\text{FAP}}) \leq \frac{P_{jx}^{\text{FAP}}}{L_{jx}^{\text{FAP}}}, \quad x = 1, \dots, U_i. \tag{B.29}
 \end{aligned}$$

The minimum sum MSE problem in B.29 is convex in $\mathbf{w}_{j,x}^{\text{FAP}}$, $x = 1, \dots, U_i$, if all $\mathbf{d}_{j,x}^{\text{FAP}}$ are fixed and convex in $\mathbf{d}_{j,x}^{\text{FAP}}$, $x = 1, \dots, U_i$, if all $\mathbf{w}_{j,x}^{\text{FAP}}$ are also fixed. This enables obtaining the FUE pre-coding vectors of the j^{th} FAP when the FUE decoding vectors of the j^{th} FAP are fixed and vice versa [27]. When the $\mathbf{d}_{j,x}^{\text{FAP}}$ are fixed, the sum MSE optimisation problem with respect to the $\mathbf{w}_{j,x}^{\text{FAP}}$ pre-coder can be reformulated as

$$\begin{aligned}
 & \min_{\substack{\mathbf{w}_{j1}^{\text{FAP}}, \dots, \mathbf{w}_{jU_i}^{\text{FAP}}}} \sum_{x=1}^{U_i} \left[\left\| (\mathbf{d}_{j,x}^{\text{FAP}})^H \sqrt{P_{jx}^{\text{FAP}} L_{jx}^{\text{FAP}}} \hat{\mathbf{H}}_{jx}^{\text{FAP-Est}} \mathbf{w}_{jx}^{\text{FAP}} - 1 \right\|^2 \right. \\
 & + \sum_{\substack{i=1 \\ i \neq x}}^{U_i} \left\| (\mathbf{d}_{j,x}^{\text{FAP}})^H \sqrt{P_{ji}^{\text{FAP}} L_{ji}^{\text{FAP}}} \hat{\mathbf{H}}_{ji}^{\text{FAP-Est}} \mathbf{w}_{ji}^{\text{FAP}'} \right\|^2 \\
 & + \sum_{m=1}^M \left\| (\mathbf{d}_{j,x}^{\text{FAP}})^H \sqrt{P_{om}^{\text{MUE}} L_{om}^{\text{MUE}}} \hat{\mathbf{H}}_{jm}^{\text{MUE-Est}} \mathbf{w}_{om}^{\text{MUE}'} \right\|^2 \\
 & + \sum_{\substack{f=1 \\ f \neq j}}^F \sum_{u=1}^U \left\| (\mathbf{d}_{j,x}^{\text{FAP}})^H \sqrt{P_{fu}^{\text{FAP}} L_{fu}^{\text{FAP}}} \hat{\mathbf{H}}_{jfu}^{\text{FAP-Est}} \mathbf{w}_{fu}^{\text{FAP}'} \right\|^2 \\
 & \left. + \sum_{r=1}^R \sum_{k=1}^K \left\| (\mathbf{d}_{j,x}^{\text{FAP}})^H \sqrt{P_{rk}^{\text{CUE}} L_{rk}^{\text{CUE}}} \hat{\mathbf{H}}_{jrk}^{\text{CUE-Est}} \mathbf{w}_{r,k}^{\text{CUE}'} \right\|^2 + \|(\mathbf{d}_{j,x}^{\text{FAP}})\|^2 \sigma^2 \right] \\
 & \text{subject to: } (\mathbf{w}_{jx}^{\text{FAP}})^H (\mathbf{w}_{jx}^{\text{FAP}}) \leq \frac{P_{jx}^{\text{FAP}}}{L_{jx}^{\text{FAP}}}, \quad x = 1, \dots, U_i. \tag{B.30}
 \end{aligned}$$

The Lagrange duality and KKT conditions are employed to efficiently solve the FAP optimisation problem. The KKT conditions are given by

- *Stationarity:*

$$\sum_{i=1}^{U_i} \hat{\mathbf{H}}_{jx}^{\text{FAP-Est}} (\mathbf{d}_{ji}^{\text{FAP}})^H \mathbf{d}_{ji}^{\text{FAP}} (\hat{\mathbf{H}}_{jx}^{\text{FAP-Est}})^H \mathbf{w}_{ji}^{\text{FAP}*} + \mu_{jx} \mathbf{w}_{jx}^{\text{FAP}*} - (\hat{\mathbf{H}}_{jx}^{\text{FAP-Est}})^H \mathbf{d}_{jx}^{\text{FAP}} = 0,$$

- *Primary feasibility:*

$$(\mathbf{w}_{jx}^{\text{FAP}})^H (\mathbf{w}_{jx}^{\text{FAP}}) \leq \frac{P_{jx}^{\text{FAP}}}{L_{jx}^{\text{FAP}}},$$

- *Complementary Slackness:*

$$\mu_{jx} \left((\mathbf{w}_{jx}^{\text{FAP}})^H (\mathbf{w}_{jx}^{\text{FAP}}) - \frac{P_{jx}^{\text{FAP}}}{L_{jx}^{\text{FAP}}} \right) = 0,$$

- *Dual feasibility:*

$$\mu_{jx} \geq 0,$$

where $\mathbf{w}_{jx}^{\text{FAP}*}$ is the optimal value for the FAP pre-coder. Using the KKT conditions the optimal MMSE pre-coding vector $\mathbf{w}_{jx}^{\text{FAP}*}$ is obtained as

$$\mathbf{w}_{jx}^{\text{FAP}*} = \left(\sum_{i=1}^{U_i} (\hat{\mathbf{H}}_{jx}^{\text{FAP-Est}})^H (\mathbf{d}_{ji}^{\text{FAP}}) (\mathbf{d}_{ji}^{\text{FAP}})^H \hat{\mathbf{H}}_{jx}^{\text{FAP-Est}} + \mu_{jx} \mathbf{I}_{U_i} \right)^{-1} \times (\hat{\mathbf{H}}_{jx}^{\text{FAP-Est}})^H \mathbf{d}_{jx}^{\text{FAP}}, \quad (\text{B.31})$$

where μ_{jx} represents the satisfaction of the transmit power constraint $(\mathbf{w}_{jx}^{\text{FAP}})^H (\mathbf{w}_{jx}^{\text{FAP}}) \leq \frac{P_{jx}^{\text{FAP}}}{L_{jx}^{\text{FAP}}}$. Similarly, we fix the pre-coding vectors $\mathbf{w}_{jx}^{\text{FAP}}$ and obtain the KKT conditions for the optimisation problem with respect to the decoder $\mathbf{d}_{jx}^{\text{FAP}}$, from which the optimal decoding matrix $\mathbf{d}_{ji}^{\text{FAP}*}$ can be obtained. The decoding vector $\mathbf{d}_{jx}^{\text{FAP}*}$ can be expressed as

$$\begin{aligned} \mathbf{d}_{jx}^{\text{FAP}*} = & \left(\sum_{m=1}^M (\hat{\mathbf{H}}_{jm}^{\text{MUE-Est}} \mathbf{w}_{om}^{\text{MUE}'}) (\hat{\mathbf{H}}_{jm}^{\text{MUE-Est}} \mathbf{w}_{om}^{\text{MUE}'})^H + \sum_{\substack{f=1 \\ f \neq j}}^F \sum_{u=1}^U (\hat{\mathbf{H}}_{jfu}^{\text{FAP-Est}} \mathbf{w}_{fu}^{\text{FAP}'}) (\hat{\mathbf{H}}_{jfu}^{\text{FAP-Est}} \mathbf{w}_{fu}^{\text{FAP}'})^H \right. \\ & \left. + \sum_{r=1}^R \sum_{k=1}^K (\hat{\mathbf{H}}_{jrk}^{\text{CUE-Est}} \mathbf{w}_{rk}^{\text{CUE}'}) (\hat{\mathbf{H}}_{jrk}^{\text{CUE-Est}} \mathbf{w}_{rk}^{\text{CUE}'})^H + \sigma_j^2 \mathbf{I}_{U_i} \right)^{-1} \times \hat{\mathbf{H}}_{jx}^{\text{FAP-Est}} \mathbf{w}_{jx}^{\text{FAP}}. \end{aligned} \quad (\text{B.32})$$

It is assumed that each pre-coder is updated instantaneously when the decoder is updated. This is accomplished by inserting the resulting pre-coder (B.31) in decoder (B.32). The detailed optimisation process is presented in Algorithm 3.

Algorithm 3 Coordinated MMSE for FAPs during the first time slot

- 1: Initialize and construct the estimated channels using the LS and MMSE channel estimation as (B.4) - (B.9), respectively.
- 2: Initialize the FUEs pre-coders $\mathbf{w}_{jx}^{\text{FAP}}$ with each element drawn i.i.d. from the standard Gaussian distribution $\mathcal{CN}(0, 1)$.
- 3: **for** $j = 1, \dots, F$ **do**
- 4: Initialize the FUEs decoder $\mathbf{d}_{j1}^{\text{FAP}}, \dots, \mathbf{d}_{jx}^{\text{FAP}}$ by $\mathcal{CN}(0, 1)$.
- 5: Compute the $\mathbf{w}_{om}^{\text{MUE}'}, \mathbf{w}_{fu}^{\text{FAP}'}, \mathbf{w}_{rk}^{\text{CUE}'}$ as (B.11) - (B.13)
- 6: Calculate the sum MSE $\epsilon = \sum_{x=1}^{U_i} \mathbb{E} \left[\|\hat{s}_{jx}^{\text{FAP}} - s_{jx}^{\text{FAP}}\|^2 \right]$ in (B.28), (B.29)
- 7: Set $n = 0$ and $\delta_o = \epsilon$
- 8: **repeat**
- 9: Update the decoder $\mathbf{d}_{j1}^{\text{FAP}}, \dots, \mathbf{d}_{jx}^{\text{FAP}}$ as (B.32):
- 10:
$$\mathbf{d}_{jx}^{\text{FAP}(n+1)} = \left(\sum_{m=1}^M \left(\hat{\mathbf{H}}_{jm}^{\text{MUE-Est}} \mathbf{w}_{om}^{\text{MUE}'(n)} \right) \left(\hat{\mathbf{H}}_{jm}^{\text{MUE-Est}} \mathbf{w}_{om}^{\text{MUE}'(n)} \right)^H \right. \\ \left. + \sum_{\substack{f=1 \\ f \neq j}}^F \sum_{u=1}^U \left(\hat{\mathbf{H}}_{jfu}^{\text{FAP-Est}} \mathbf{w}_{fu}^{\text{FAP}'(n)} \right) \left(\hat{\mathbf{H}}_{jfu}^{\text{FAP-Est}} \mathbf{w}_{fu}^{\text{FAP}'(n)} \right)^H \right. \\ \left. + \sum_{r=1}^R \sum_{k=1}^K \left(\hat{\mathbf{H}}_{jrk}^{\text{CUE-Est}} \mathbf{w}_{rk}^{\text{CUE}'(n)} \right) \left(\hat{\mathbf{H}}_{jrk}^{\text{CUE-Est}} \mathbf{w}_{rk}^{\text{CUE}'(n)} \right)^H + \sigma_j^2 \mathbf{I}_{U_i} \right)^{-1} \times \hat{\mathbf{H}}_{jx}^{\text{FAP-Est}} \mathbf{w}_{jx}^{\text{FAP}(n)}$$
- 11: Calculate the FUE pre-coder $\mathbf{w}_{j1}^{\text{FAP}}, \dots, \mathbf{w}_{jx}^{\text{FAP}}$ (B.31) with the updated decoder:
- 12:
$$\mathbf{w}_{jx}^{\text{FAP}(n+1)} = \left(\sum_{i=1}^{U_i} \left(\hat{\mathbf{H}}_{jx}^{\text{FAP-Est}} \right)^H \left(\mathbf{d}_{ji}^{\text{FAP}(n)} \right) \left(\mathbf{d}_{ji}^{\text{FAP}(n)} \right)^H \hat{\mathbf{H}}_{jx}^{\text{FAP-Est}} + \mu_{jx} \mathbf{I}_{U_i} \right)^{-1} \\ \times \left(\hat{\mathbf{H}}_{jx}^{\text{FAP-Est}} \right)^H \mathbf{d}_{jx}^{\text{FAP}(n)}$$
- 13: Calculate ϵ with the new pre-coder and decoder
- 14: set $n = n + 1$
- 15: **until** $\epsilon \approx 0$

3.1.2 Optimisation of the MUEs pre-coding and decoding matrices

Similar to the FAPs algorithm, the MUE algorithm starts with initialized random pre-coders and decoders $\mathbf{w}_{ol}^{\text{MUE}}$. In each iteration, the MUE pre-coders and decoders are updated alternatively. The decoded information $\hat{s}_{ol}^{\text{MUE}}$ is expressed as

$$\hat{s}_{ol}^{\text{MUE}} = (\mathbf{d}_{ol}^{\text{MUE}})^H \cdot \mathbf{y}_o^{\text{MBS}'} \quad (\text{B.33})$$

$$= \sum_{m=1}^M (\mathbf{d}_{ol}^{\text{MUE}})^H \sqrt{P_{om}^{\text{MUE}} L_{om}^{\text{MUE}}} \mathbf{H}_{om}^{\text{MUE}} \mathbf{w}_{om}^{\text{MUE}'} s_{om}^{\text{MUE}} + \sum_{f=1}^F \sum_{u=1}^U (\mathbf{d}_{ol}^{\text{MUE}})^H \sqrt{P_{fu}^{\text{FAP}} L_{fu}^{\text{FAP}}} \mathbf{H}_{ofu}^{\text{FAP}} \mathbf{w}_{fu}^{\text{FAP}'} s_{fu}^{\text{FAP}} \\ + \sum_{r=1}^R \sum_{k=1}^K (\mathbf{d}_{ol}^{\text{MUE}})^H \sqrt{P_{rk}^{\text{CUE}} L_{rk}^{\text{CUE}}} \mathbf{H}_{ork}^{\text{CUE}} \mathbf{w}_{rk}^{\text{CUE}'} s_{rk}^{\text{CUE}} + (\mathbf{d}_{ol}^{\text{MUE}})^H \mathbf{n}_o, \quad (\text{B.34})$$

where $(\mathbf{d}_{ol}^{\text{MUE}})^H$ is the decoding vector for l^{th} MUE of MBS. We describe the minimum sum MSE problem of the l^{th} user at the MBS during the second time slot as follows

$$\begin{aligned} & \min_{\substack{\mathbf{w}_{o1}^{\text{MUE}}, \dots, \mathbf{w}_{oM}^{\text{MUE}} \\ \mathbf{d}_{o1}^{\text{MUE}}, \dots, \mathbf{d}_{oM}^{\text{MUE}}} } \sum_{l=1}^M \mathbb{E}\{\|\hat{s}_{ol}^{\text{MUE}} - s_{ol}^{\text{MUE}}\|^2\} \\ & \text{subject to } \mathbf{w}_{ol}^{\text{MUE}} (\mathbf{w}_{ol}^{\text{MUE}})^H \leq \frac{P_{ol}^{\text{MUE}}}{L_{ol}^{\text{MUE}}}, \quad l = 1, \dots, M, \end{aligned} \quad (\text{B.35})$$

where P_{ol}^{MUE} is the maximum transmit power of the l^{th} MUE of the MBS. We consider the estimated channels to rewrite (B.35), hence the minimum sum MSE for the MUEs during the first time slot is rewritten as

$$\begin{aligned} & \min_{\substack{\mathbf{w}_{o1}^{\text{MUE}}, \dots, \mathbf{w}_{oM}^{\text{MUE}} \\ \mathbf{d}_{o1}^{\text{MUE}}, \dots, \mathbf{d}_{oM}^{\text{MUE}}} } \sum_{l=1}^M \left[\left\| (\mathbf{d}_{ol}^{\text{MUE}})^H \sqrt{P_{ol}^{\text{MUE}} L_{ol}^{\text{MUE}}} \hat{\mathbf{H}}_{ol}^{\text{MUE-Est}} \mathbf{w}_{ol}^{\text{MUE}} \right\|^2 \right. \\ & + \sum_{m=1}^M \left\| (\mathbf{d}_{ol}^{\text{MUE}})^H \sqrt{P_{om}^{\text{MUE}} L_{om}^{\text{MUE}}} \hat{\mathbf{H}}_{om}^{\text{MUE-Est}} \mathbf{w}_{om}^{\text{MUE}'} \right\|^2 \\ & + \sum_{r=1}^R \sum_{k=1}^K \left\| (\mathbf{d}_{o,l}^{\text{MUE}})^H \sqrt{P_{rk}^{\text{CUE}} L_{rk}^{\text{CUE}}} \hat{\mathbf{H}}_{ork}^{\text{CUE-Est}} \mathbf{w}_{rk}^{\text{CUE}'} \right\|^2 \\ & \left. + \sum_{f=1}^F \sum_{u=1}^U \left\| (\mathbf{d}_{ol}^{\text{MUE}})^H \sqrt{P_{fu}^{\text{FAP}} L_{fu}^{\text{FAP}}} \hat{\mathbf{H}}_{ofu}^{\text{FAP-Est}} \mathbf{w}_{fu}^{\text{FAP}'} \right\|^2 + \|\mathbf{d}_{ol}^{\text{MUE}}\|_{\sigma_{ol}^2}^2 \right] \\ & \text{subject to } \mathbf{w}_{ol}^{\text{MUE}} (\mathbf{w}_{ol}^{\text{MUE}})^H \leq \frac{P_{ol}^{\text{MUE}}}{L_{ol}^{\text{MUE}}}, \quad l = 1, \dots, M. \end{aligned} \quad (\text{B.36})$$

The sum MSE problem stated in (B.36) is convex in $\mathbf{w}_{ol}^{\text{MUE}}, l = 1, \dots, M$, if all $\mathbf{d}_{ol}^{\text{MUE}}$ are fixed and convex in $\mathbf{d}_{ol}^{\text{MUE}}, l = 1, \dots, M$, if all $\mathbf{w}_{ol}^{\text{MUE}}$ are also fixed. This enables obtaining the MUE pre-coding vectors when the MUE decoding vectors are fixed and vice versa. When the $\mathbf{d}_{ol}^{\text{MUE}}$ are fixed, the sum MSE optimisation problem with respect to the $\mathbf{w}_{ol}^{\text{MUE}}$ pre-coder can be reformulated as

$$\begin{aligned} & \min_{\mathbf{w}_{o1}^{\text{MUE}}, \dots, \mathbf{w}_{oM}^{\text{MUE}}} \sum_{l=1}^M \left[\left\| (\mathbf{d}_{ol}^{\text{MUE}})^H \sqrt{P_{ol}^{\text{MUE}} L_{ol}^{\text{MUE}}} \hat{\mathbf{H}}_{ol}^{\text{MUE-Est}} \mathbf{w}_{ol}^{\text{MUE}} \right\|^2 \right. \\ & + \sum_{m=1}^M \left\| (\mathbf{d}_{ol}^{\text{MUE}})^H \sqrt{P_{om}^{\text{MUE}} L_{om}^{\text{MUE}}} \hat{\mathbf{H}}_{om}^{\text{MUE-Est}} \mathbf{w}_{om}^{\text{MUE}'} \right\|^2 \\ & + \sum_{r=1}^R \sum_{k=1}^K \left\| (\mathbf{d}_{ol}^{\text{MUE}})^H \sqrt{P_{rk}^{\text{CUE}} L_{rk}^{\text{CUE}}} \hat{\mathbf{H}}_{ork}^{\text{CUE-Est}} \mathbf{w}_{rk}^{\text{CUE}'} \right\|^2 \\ & \left. + \sum_{f=1}^F \sum_{u=1}^U \left\| (\mathbf{d}_{ol}^{\text{MUE}})^H \sqrt{P_{fu}^{\text{FAP}} L_{fu}^{\text{FAP}}} \hat{\mathbf{H}}_{ofu}^{\text{FAP-Est}} \mathbf{w}_{fu}^{\text{FAP}'} \right\|^2 + \|\mathbf{d}_{ol}^{\text{MUE}}\|_{\sigma_{ol}^2}^2 \right] \\ & \text{subject to } \mathbf{w}_{ol}^{\text{MUE}} (\mathbf{w}_{ol}^{\text{MUE}})^H \leq \frac{P_{ol}^{\text{MUE}}}{L_{ol}^{\text{MUE}}}, \quad l = 1, \dots, M. \end{aligned} \quad (\text{B.37})$$

The Lagrange duality and KKT conditions are efficiently used to solve the optimisation problem of the MUEs. The KKT conditions are expressed as

- *Stationarity:*

$$\sum_{m=1}^M \hat{\mathbf{H}}_{ol}^{\text{MUE-Est}} (\mathbf{d}_{om}^{\text{MUE}})^H \mathbf{d}_{om}^{\text{MUE}} (\hat{\mathbf{H}}_{ol}^{\text{MUE-Est}})^H \mathbf{w}_{ol}^{\text{MUE}*} + \mu_{ol} \mathbf{w}_{ol}^{\text{MUE}*} - (\hat{\mathbf{H}}_{ol}^{\text{MUE-Est}})^H \mathbf{d}_{ol}^{\text{MUE}} = 0$$

- *Primary feasibility:*

$$(\mathbf{w}_{ol}^{\text{MUE}})^H (\mathbf{w}_{ol}^{\text{MUE}}) \leq \frac{P_{ol}^{\text{MUE}}}{L_{ol}^{\text{MUE}}}$$

- *Complementary Slackness:*

$$\mu_{ol} \left[(\mathbf{w}_{ol}^{\text{MUE}})^H (\mathbf{w}_{ol}^{\text{MUE}}) - \frac{P_{ol}^{\text{MUE}}}{L_{ol}^{\text{MUE}}} \right] = 0$$

- *Dual feasibility:*

$$\mu_{ol} \geq 0,$$

where $\mathbf{w}_{ol}^{\text{MUE}*}$ is the optimal value for the MUE pre-coder. Using the KKT conditions the optimal MMSE pre-coding vector $\mathbf{w}_{ol}^{\text{MUE}*}$ for l^{th} MUE of the MBS is obtained as

$$\mathbf{w}_{ol}^{\text{MUE}*} = \left(\sum_{m=1}^M (\hat{\mathbf{H}}_{ol}^{\text{MUE-Est}})^H (\mathbf{d}_{om}^{\text{MUE}}) (\mathbf{d}_{om}^{\text{MUE}})^H (\hat{\mathbf{H}}_{ol}^{\text{MUE-Est}}) + \mu_{ol} \mathbf{I}_M \right)^{-1} (\hat{\mathbf{H}}_{ol}^{\text{MUE-Est}})^H \mathbf{d}_{ol}^{\text{MUE}}, \quad (\text{B.38})$$

where μ_{ol} represents the satisfaction of transmit power constraint $(\mathbf{w}_{ol}^{\text{MUE}})^H (\mathbf{w}_{ol}^{\text{MUE}}) \leq P_{ol}^{\text{MUE}}$. Considering the same process of fixing the $\mathbf{w}_{ol}^{\text{MUE}}$ MUE pre-coder and obtaining the KKT conditions of the resulting sum-MSE problem, the optimal decoding vector $\mathbf{d}_{ol}^{\text{MUE}*}$ of the l^{th} MUE of the MBS can be formulated as

$$\begin{aligned} \mathbf{d}_{ol}^{\text{MUE}*} = & \left(\sum_{r=1}^R \sum_{k=1}^K (\hat{\mathbf{H}}_{ork}^{\text{CUE-Est}} \mathbf{w}_{rk}^{\text{CUE}'}) (\hat{\mathbf{H}}_{ork}^{\text{CUE-Est}} \mathbf{w}_{rk}^{\text{CUE}'})^H \right. \\ & \left. + \sum_{f=1}^F \sum_{u=1}^U (\hat{\mathbf{H}}_{ofu}^{\text{FAP-Est}} \mathbf{w}_{fu}^{\text{FAP}'}) (\hat{\mathbf{H}}_{ofu}^{\text{FAP-Est}} \mathbf{w}_{fu}^{\text{FAP}'})^H + \sigma_{ol}^2 \mathbf{I}_M \right)^{-1} \times \hat{\mathbf{H}}_{ol}^{\text{MUE-Est}} \mathbf{w}_{ol}^{\text{MUE}}. \end{aligned} \quad (\text{B.39})$$

The details coordinated MMSE algorithm for the MUEs is presented in Algorithm 4.

3.2 Coordinated MMSE approach for UEs (CUEs and MUEs) during the second time slot

Generally, the transceiver design for cooperative RN system with multiple users is a difficult task since the RN is shared by multiple users and multi-users interference exists at both RN and MBS. In the following, an iterative design algorithm is proposed based on convex quadratic optimisation theory. Specifically, the algorithm iteratively computes the decoder matrices \mathbf{D}_o , relay pre-coder matrices \mathbf{F}_o

Algorithm 4 Coordinated MMSE for MUEs during the first time slot

- 1: Initialize and construct the estimated channels using the LS and MMSE channel estimation as (B.4) - (B.9), respectively.
 - 2: Initialize the MUEs pre-coders $\mathbf{w}_{ol}^{\text{MUE}}$ with each element drawn i.i.d. from the standard Gaussian distribution $\mathcal{CN}(0, 1)$.
 - 3: Initialize the MUEs decoder $\mathbf{d}_{o1}^{\text{MUE}}, \dots, \mathbf{d}_{ol}^{\text{MUE}}$ by $\mathcal{CN}(0, 1)$.
 - 4: Compute the $\mathbf{w}_{fu}^{\text{FAP}'}, \mathbf{w}_{rk}^{\text{CUE}'}$ as (B.12), (B.13)
 - 5: Calculate the sum MSE $\epsilon = \sum_{l=1}^M \mathbb{E} [\|\hat{\mathbf{s}}_{ol}^{\text{MUE}} - \mathbf{s}_{ol}^{\text{MUE}}\|^2]$ as in (B.35), (B.36)
 - 6: Set $n = 0$ and $\delta_o = \epsilon$
 - 7: **repeat**
 - 8: Update the MUE decoder $\mathbf{d}_{o1}^{\text{MUE}}, \dots, \mathbf{d}_{ol}^{\text{MUE}}$ as (B.39):
 - 9:
$$\mathbf{d}_{ol}^{\text{MUE}(n+1)} = \sum_{r=1}^R \sum_{k=1}^K \left(\hat{\mathbf{H}}_{jrk}^{\text{CUE-Est}} \mathbf{w}_{rk}^{\text{CUE}'(n)} \right) \left(\hat{\mathbf{H}}_{jrk}^{\text{CUE-Est}} \mathbf{w}_{r,k}^{\text{CUE}'(n)} \right)^H$$

$$+ \sum_{f=1}^F \sum_{u=1}^U \left(\hat{\mathbf{H}}_{jfu}^{\text{FAP-Est}} \mathbf{w}_{fu}^{\text{FAP}'(n)} \right) \left(\hat{\mathbf{H}}_{jfu}^{\text{FAP-Est}} \mathbf{w}_{fu}^{\text{FAP}'(n)} \right)^H + \sigma_{ol}^2 \mathbf{I}_M \Big)^{-1} \times \hat{\mathbf{H}}_{ol}^{\text{MUE-Est}} \mathbf{w}_{ol}^{\text{MUE}(n)}$$
 - 10: Calculate the MUE pre-coder $\mathbf{w}_{o1}^{\text{MUE}}, \dots, \mathbf{w}_{ol}^{\text{MUE}}$ (B.38) with the updated decoder:
 - 11:
$$\mathbf{w}_{ol}^{\text{MUE}(n+1)} = \left(\sum_{m=1}^M \left(\hat{\mathbf{H}}_{ol}^{\text{MUE-Est}} \right)^H (\mathbf{d}_{om}^{\text{MUE}(n)}) (\mathbf{d}_{om}^{\text{MUE}(n)})^H \left(\hat{\mathbf{H}}_{ol}^{\text{MUE-Est}} \right) + \mu_{ol} \mathbf{I}_M \right)^{-1}$$

$$\times \left(\hat{\mathbf{H}}_{ol}^{\text{MUE-Est}} \right)^H \mathbf{d}_{ol}^{\text{MUE}(n)}$$
 - 12: Calculate ϵ with the new pre-coder and decoder
 - 13: set $n = n + 1$
 - 14: **until** $\epsilon \approx 0$
-

and UE pre-coder matrices \mathbf{W}^{UE} , starting with initial values for \mathbf{W}^{UE} and \mathbf{F}_o . The decoded information $\hat{\mathbf{s}}^{\text{UE}}$ of the UE through the RN is expressed as

$$\hat{\mathbf{s}} = (\mathbf{D}_o)^H \cdot \mathbf{y}_o^{\text{MBS-nd}} \quad (\text{B.40})$$

$$= (\mathbf{D}_o)^H \mathbf{H}_o \mathbf{F}_o \mathbf{H}^{\text{UE}} \mathbf{W}^{\text{UE}} \mathbf{s}^{\text{UE}} + (\mathbf{D}_o)^H \mathbf{z}_o, \quad (\text{B.41})$$

where \mathbf{D}_o is the decoding matrix for UEs. The same process of minimizing the sum MSE for the UEs to the MBS during the second time slot is applied and estimated as

$$\begin{aligned} & \min_{\mathbf{W}^{\text{UE}}, \mathbf{D}_o} \mathbb{E} \{ \|\hat{\mathbf{s}}^{\text{UE}} - \mathbf{s}^{\text{UE}}\|^2 \} \\ & \text{s. t. } (\mathbf{W}^{\text{UE}})(\mathbf{W}^{\text{UE}})^H \leq \frac{\mathbf{P}^{\text{UE}}}{L^{\text{UE}}}, \\ & \left(\mathbf{F}_o \left(\hat{\mathbf{H}}^{\text{UE-Est}} \mathbf{W}^{\text{UE}} (\mathbf{W}^{\text{UE}})^H \left(\hat{\mathbf{H}}^{\text{UE-Est}} \right)^H + \sigma_{\text{UE}}^2 \mathbf{I}_{N_B} \right) \mathbf{F}_o^H \right) \leq \frac{\mathbf{P}_R}{L_R}, \end{aligned} \quad (\text{B.42})$$

where P_{max}^{UE} is the maximum transmit power of the UE and P_R is the maximum transmit power at the RN. The sum MSE problem for UE in (B.42) can be rewritten as

$$\begin{aligned} \min_{\mathbf{W}^{UE}, \mathbf{D}_o} & \left[\|(\mathbf{D}_o)^H \hat{\mathbf{H}}_o^{\text{Est}} \mathbf{F}_o \hat{\mathbf{H}}^{\text{UE-Est}} \mathbf{W}^{UE} - 1\|^2 + \|(\mathbf{D}_o)^H\|^2 C_{\mathbf{z}_o} \right] \\ \text{s. t. } & (\mathbf{W}^{UE})(\mathbf{W}^{UE})^H \leq \frac{P^{UE}}{L^{UE}}, \\ & \left(\mathbf{F}_o \left(\hat{\mathbf{H}}^{\text{UE-Est}} \mathbf{W}^{UE} (\mathbf{W}^{UE})^H (\hat{\mathbf{H}}^{\text{UE-Est}})^H + \sigma_{\text{UE}}^2 \mathbf{I}_{N_B} \right) \mathbf{F}_o^H \right) \leq \frac{P_R}{L_R}, \end{aligned} \quad (\text{B.43})$$

where $C_{\mathbf{z}_o}$ is the equivalent noise covariance matrix given by

$$\begin{aligned} C_{\mathbf{z}_o} &= \mathbb{E} \left[\mathbf{z}_o \mathbf{z}_o^H \right] \\ &= \sum_{r=1}^R \mathbb{E} \left[\left(\hat{\mathbf{H}}_{o,r}^{\text{Est}} \mathbf{F}_{o,r} \tilde{\mathbf{n}}_r + \mathbf{n}_o \right) \left(\hat{\mathbf{H}}_{o,r}^{\text{Est}} \mathbf{F}_{o,r} \tilde{\mathbf{n}}_r + \mathbf{n}_o \right)^H \right] \\ &= \sum_{r=1}^R \hat{\mathbf{H}}_{o,r}^{\text{Est}} \mathbf{F}_{o,r} (\hat{\mathbf{H}}_{o,r}^{\text{Est}})^H (\mathbf{F}_{o,r})^H + \mathbf{I}_{N_B}. \end{aligned} \quad (\text{B.44})$$

3.2.1 Design of the RN pre-coding matrix

In order to evaluate the RN pre-coder \mathbf{F}_o , we consider the fixed MMSE decoder \mathbf{D}_o and pre-coder \mathbf{W}^{UE} , the sum-MSE optimisation pre-coder with respect to the RN pre-coder can be formulated as

$$\begin{aligned} \min_{\mathbf{F}_o} & \|(\mathbf{D}_o)^H \hat{\mathbf{H}}_o^{\text{Est}} \mathbf{F}_o \hat{\mathbf{H}}^{\text{UE}} \mathbf{W}^{UE} - 1\|^2 + \|(\mathbf{D}_o)^H\|^2 C_{\mathbf{z}_o} \\ \text{s. t. } & \left(\mathbf{F}_o \left(\hat{\mathbf{H}}^{\text{UE-Est}} \mathbf{W}^{UE} (\mathbf{W}^{UE})^H (\hat{\mathbf{H}}^{\text{UE-Est}})^H + \sigma_{\text{UE}}^2 \mathbf{I}_{N_B} \right) \mathbf{F}_o^H \right) \leq \frac{P_R}{L_R}. \end{aligned} \quad (\text{B.45})$$

The sum-MSE optimisation problem is solve with the Lagrange function and the KKT conditions. The Lagrange function is written as

$$\begin{aligned} \mathcal{L}^{\text{RN}}(\lambda, \mathbf{F}_o) &= \left[\|(\mathbf{D}_o)^H \hat{\mathbf{H}}_o^{\text{Est}} \mathbf{F}_o \hat{\mathbf{H}}^{\text{UE-Est}} \mathbf{W}^{UE} - 1\|^2 + \|(\mathbf{D}_o)^H\|^2 C_{\mathbf{z}_o} \right] \\ &+ \lambda \left[\mathbf{F}_o \left(\hat{\mathbf{H}}^{\text{UE-Est}} \mathbf{W}^{UE} (\mathbf{W}^{UE})^H (\hat{\mathbf{H}}^{\text{UE-Est}})^H + \sigma_{\text{UE}}^2 \mathbf{I}_{N_B} \right) \mathbf{F}_o^H - \frac{P_R}{L_R} \right], \end{aligned} \quad (\text{B.46})$$

where λ is the non-negative Lagrange multiplier, $\lambda \geq 0$. The KKT conditions are given as

- *Stationarity:*

$$\frac{\partial \mathcal{L}^{\text{RN}}(\lambda, \mathbf{F}_o)}{\partial \mathbf{F}_o} = 0,$$

- *Primary feasibility:*

$$\left[\mathbf{F}_o \left(\hat{\mathbf{H}}^{\text{UE-Est}} \mathbf{W}^{UE} (\mathbf{W}^{UE})^H (\hat{\mathbf{H}}^{\text{UE-Est}})^H + \sigma_{\text{UE}}^2 \mathbf{I}_{N_B} \right) \mathbf{F}_o^H \right] \leq \frac{P_R}{L_R},$$

- *Complementary Slackness:*

$$\lambda \left[\left(\mathbf{F}_o \left(\hat{\mathbf{H}}^{\text{UE-Est}} \mathbf{W}^{\text{UE}} (\mathbf{W}^{\text{UE}})^H (\hat{\mathbf{H}}^{\text{UE-Est}})^H + \sigma_{\text{UE}}^2 \mathbf{I} \right) \mathbf{F}_o^H \right) - P_R \right] = 0,$$

- *Dual feasibility:*

$$\lambda \geq 0.$$

Through the mathematical manipulation, we can derive the optimal RN pre-coder as

$$\begin{aligned} \mathbf{F}_o &= \left(\mathbf{D}_o^H \hat{\mathbf{H}}_o^{\text{Est}} \mathbf{F}_o \hat{\mathbf{H}}^{\text{UE-Est}} \mathbf{W}^{\text{UE}} \mathbf{D}_o (\hat{\mathbf{H}}_o^{\text{Est}})^H \mathbf{F}_o^H (\hat{\mathbf{H}}^{\text{UE-Est}})^H (\mathbf{W}^{\text{UE}})^H + \lambda \phi \right)^{-1} \\ &\quad \times \mathbf{D}_o (\hat{\mathbf{H}}_o^{\text{Est}})^H \mathbf{F}_o^H (\hat{\mathbf{H}}^{\text{UE-Est}})^H (\mathbf{W}^{\text{UE}})^H, \end{aligned} \quad (\text{B.47})$$

where $\phi = \left((\hat{\mathbf{H}}^{\text{UE-Est}})^H \mathbf{W}^{\text{UE}} (\mathbf{W}^{\text{UE}})^H \hat{\mathbf{H}}^{\text{UE-Est}} + \sigma_{\text{UE}}^2 \mathbf{I}_{N_B} \right)$.

3.2.2 Design of the pre-coding and decoding matrices

To solve the optimisation problem in (B.43), we consider the Lagrange duality and KKT conditions.

The Lagrange function is formulated as

$$\begin{aligned} \mathcal{L}^{\text{UE}}(\mu_1, \mu_2, \mathbf{D}_o, \mathbf{W}^{\text{UE}}) &= \left[\left\| (\mathbf{D}_o)^H \hat{\mathbf{H}}_o^{\text{Est}} \mathbf{F}_o \hat{\mathbf{H}}^{\text{UE-Est}} \mathbf{W}^{\text{UE}} - 1 \right\|^2 + \left\| (\mathbf{D}_o)^H \right\|^2 C_{z_o} \right] \\ &\quad + \mu_2 \left[\left(\mathbf{F}_o \left(\hat{\mathbf{H}}^{\text{UE-Est}} \mathbf{W}^{\text{UE}} (\mathbf{W}^{\text{UE}})^H (\hat{\mathbf{H}}^{\text{UE-Est}})^H + \sigma_{\text{UE}}^2 \mathbf{I}_{N_B} \right) \mathbf{F}_o^H \right) - \frac{P_R}{L_R} \right] \\ &\quad + \mu_1 \left[(\mathbf{W}^{\text{UE}})(\mathbf{W}^{\text{UE}})^H - \frac{P^{\text{UE}}}{L^{\text{UE}}} \right], \end{aligned} \quad (\text{B.48})$$

where μ_1, μ_2 are the non-negative Lagrange multipliers, $\mu_1, \mu_2 \geq 0$. The KKT conditions for UEs pre-coders are given as

- *Stationarity:*

$$\frac{\partial \mathcal{L}^{\text{UE}}(\mu_1, \mu_2, \mathbf{D}_o, \mathbf{W}^{\text{UE}})}{\partial \mathbf{W}^{\text{UE}}} = 0,$$

- *Primary feasibility:*

$$\begin{aligned} (\mathbf{W}^{\text{UE}})(\mathbf{W}^{\text{UE}})^H &\leq \frac{P^{\text{UE}}}{L^{\text{UE}}}, \\ \left[\mathbf{F}_o \left(\hat{\mathbf{H}}^{\text{UE-Est}} \mathbf{W}^{\text{UE}} (\mathbf{W}^{\text{UE}})^H (\hat{\mathbf{H}}^{\text{UE-Est}})^H + \sigma_{\text{UE}}^2 \mathbf{I}_{N_B} \right) \mathbf{F}_o^H \right] &\leq \frac{P_R}{L_R}, \end{aligned}$$

- *Complementary Slackness:*

$$\begin{aligned} \mu_1 \left[(\mathbf{W}^{\text{UE}})(\mathbf{W}^{\text{UE}})^H - \frac{P^{\text{UE}}}{L^{\text{UE}}} \right] &= 0, \\ \mu_2 \left[\mathbf{F}_o \left(\hat{\mathbf{H}}^{\text{UE-Est}} \mathbf{W}^{\text{UE}} (\mathbf{W}^{\text{UE}})^H (\hat{\mathbf{H}}^{\text{UE-Est}})^H + \sigma_{\text{UE}}^2 \mathbf{I}_{N_B} \right) \mathbf{F}_o^H - \frac{P_R}{L_R} \right] &= 0, \end{aligned}$$

- *Dual feasibility:*

$$\mu_1, \mu_2 \geq 0.$$

To evaluate the derivation of the Lagrange function given in (B.46) the matrices \mathbf{D}_o and \mathbf{D}_o^H are treated independently. This is also applied to \mathbf{W}^{UE} and $(\mathbf{W}^{\text{UE}})^H$. Furthermore, it can be seen that the optimisation problem in (B.43) is convex with respect to \mathbf{W}^{UE} . The Lagrange duality function can be defined as

$$f(\mu_1, \mu_2) = \min_{\mathbf{W}^{\text{UE}}} \mathcal{L}^{\text{UE}}(\mu_1, \mu_2, \mathbf{D}_o, \mathbf{W}^{\text{UE}}). \quad (\text{B.49})$$

Moreover, the dual problem is defined as

$$\max_{\mu_1, \mu_2 \geq 0} f(\mu_1, \mu_2). \quad (\text{B.50})$$

Using the KKT conditions for the resulting problem, the optimal decoder \mathbf{D}_o^* is obtained with the fixed pre-coders as

$$\mathbf{D}_o^* = \left(\hat{\mathbf{H}}_o^{\text{Est}} \mathbf{F}_o \hat{\mathbf{H}}^{\text{UE-Est}} \mathbf{W}^{\text{UE}} (\hat{\mathbf{H}}_o^{\text{Est}})^H \mathbf{F}_o^H (\hat{\mathbf{H}}^{\text{UE-Est}})^H (\mathbf{W}^{\text{UE}})^H + C_{\mathbf{z}_o} \right)^{-1} \hat{\mathbf{H}}_o^{\text{Est}} \mathbf{F}_o \hat{\mathbf{H}}^{\text{UE-Est}} \mathbf{W}^{\text{UE}}. \quad (\text{B.51})$$

Hence, the MMSE pre-coding vector \mathbf{W}^{UE} for UE during the second time slot is obtained as

$$\mathbf{W}^{\text{UE}*} = \left(\mu_1 \mathbf{I}_{\text{UE}} + \mu_2 \left((\hat{\mathbf{H}}^{\text{UE-Est}})^H \mathbf{F}_o \mathbf{F}_o^H \hat{\mathbf{H}}^{\text{UE-Est}} \right) \right)^{-1} \times \mathbf{D}_o (\hat{\mathbf{H}}_o^{\text{Est}})^H (\hat{\mathbf{H}}^{\text{UE-Est}})^H \mathbf{F}_o^H, \quad (\text{B.52})$$

where μ_1 represents the satisfaction of UE transmit power constraint $(\mathbf{W}^{\text{UE}})^H (\mathbf{W}^{\text{UE}}) \leq \frac{P_{\text{UE}}^{\text{UE}}}{L_{\text{UE}}}$ and μ_2 represents the satisfaction of the RN transmit power $\left[\left(\mathbf{F}_o (\hat{\mathbf{H}}^{\text{UE-Est}} \mathbf{W}^{\text{UE}} (\mathbf{W}^{\text{UE}})^H (\hat{\mathbf{H}}^{\text{UE-Est}})^H + \sigma_{\text{UE}}^2 \mathbf{I}_{N_B}) \mathbf{F}_o^H \right) - \frac{P_R}{L_R} \right]$. The details of the proposed decentralised algorithm for the UEs is presented in Algorithm 5.

Algorithm 5 Coordinated MMSE for CUEs and MUEs (during the second time slot)

- 1: Initialize and construct the estimated channels $\hat{\mathbf{H}}_o^{\text{Est}}$ and $\hat{\mathbf{H}}^{\text{UE-Est}}$ using the LS and MMSE channel estimators.
 - 2: Initialize the UEs and RN pre-coders \mathbf{W}^{UE} and \mathbf{F}_o with each element drawn i.i.d. from the standard Gaussian distribution $\mathcal{CN}(0, 1)$.
 - 3: Compute the $\mathbf{w}_{om}^{\text{MUE}'}$, $\mathbf{w}_{fu}^{\text{FAP}'}$ as (B.11), (B.12)
 - 4: Initialize the UEs decoder \mathbf{D}_o by $\mathcal{CN}(0, 1)$.
 - 5: Calculate the sum MSE $\epsilon = \mathbb{E} [\|\hat{\mathbf{s}}^{\text{UE}} - \mathbf{s}^{\text{UE}}\|^2]$ in (B.42), (B.43)
 - 6: Set $n = 0$ and $\delta_o = \epsilon$
 - 7: **repeat**
 - 8: Update the UE decoder \mathbf{D}_o as (B.51)
 - 9:
$$\mathbf{D}_o^{(n+1)} = \left(\hat{\mathbf{H}}_o^{\text{Est}} \mathbf{F}_o^{(n)} \hat{\mathbf{H}}^{\text{UE-Est}} \mathbf{W}^{\text{UE}(n)} (\hat{\mathbf{H}}_o^{\text{Est}})^H (\mathbf{F}_o^{(n)})^H (\hat{\mathbf{H}}^{\text{UE-Est}})^H (\mathbf{W}^{\text{UE}(n)})^H + C_{\mathbf{z}_o} \right)^{-1} \\ \times \hat{\mathbf{H}}_o^{\text{Est}} \mathbf{F}_o^{(n)} \hat{\mathbf{H}}^{\text{UE-Est}} \mathbf{W}^{\text{UE}(n)}$$
 - 10: Calculate the RN pre-coder \mathbf{F}_o (B.47) with the updated decoder as
 - 11:
$$\mathbf{F}_o^{(n+1)} = \left((\mathbf{D}_o^{(n+1)})^H \hat{\mathbf{H}}_o^{\text{Est}} \mathbf{F}_o^{(n)} \hat{\mathbf{H}}^{\text{UE-Est}} \mathbf{W}^{\text{UE}(n)} \mathbf{D}_o^{(n)} (\hat{\mathbf{H}}_o^{\text{Est}})^H (\mathbf{F}_o^{(n)})^H (\hat{\mathbf{H}}^{\text{UE-Est}})^H (\mathbf{W}^{\text{UE}(n)})^H \right. \\ \left. + \lambda \phi \right)^{-1} \mathbf{D}_o^{(n+1)} \hat{\mathbf{H}}_o^{\text{Est}} (\mathbf{F}_o^{(n)})^H (\hat{\mathbf{H}}^{\text{UE-Est}})^H (\mathbf{W}^{\text{UE}(n)})^H$$
 - 12: Obtain the UE pre-coder with the updated decoder and RN pre-coder as (B.52)
 - 13:
$$\mathbf{W}^{\text{UE}(n+1)} = \left(\mu_1 \mathbf{I}_{\text{UE}} + \mu_2 ((\hat{\mathbf{H}}^{\text{UE-Est}})^H \mathbf{F}_o^{(n+1)} (\mathbf{F}_o^{(n+1)})^H \hat{\mathbf{H}}^{\text{UE-Est}}) \right)^{-1} \\ \times \mathbf{D}_o^{(n+1)} (\hat{\mathbf{H}}_o^{\text{Est}})^H (\hat{\mathbf{H}}^{\text{UE-Est}})^H (\mathbf{F}_o^{(n+1)})^H$$
 - 14: Calculate ϵ with the new UE, RN pre-coder and decoder
 - 15: set $n = n + 1$
 - 16: **until** $\epsilon \approx 0$
-

4 Performance Evaluation

In this section, we present the performance evaluation of the proposed schemes for FAPs, MUEs and UEs in the MU-MIMO relay system through numerical simulations. The simulated model is illustrated in Fig. B.2. This figure shows a macrocell of dimension $2km \times 2km$ with a MBS placed at the center of the area at coordinates $(1km, 1km)$. There are 12 MUEs distributed near the cell edge, considered as the CUEs. The CUEs are grouped into clusters where each cluster has 1 RN and 3 CUEs. The RNs are strategically placed at the coordinates detailed in the Table B.1. The CUEs are located at distance d^{CUE} from their respective RN. The RNs are located at d^{RN} from the MBS. The users (CUEs, FUEs and

MUEs) are randomly placed in the area at the coordinated detailed in Table B.1. There are 10 MUEs deployed in the macrocell area located at a distance d^{MUE} from the MBS. We consider 3 FAPs with 2 FUEs each uniformly distributed with the distance d^{FAP} . All the channel coefficients are assumed to be Rayleigh fading channels complex Gaussian random variables with zero mean and variance one. The propagation loss is modelled for each FUEs, MUEs and UEs based on their respective distance. All the simulation parameters are given in Table B.2.

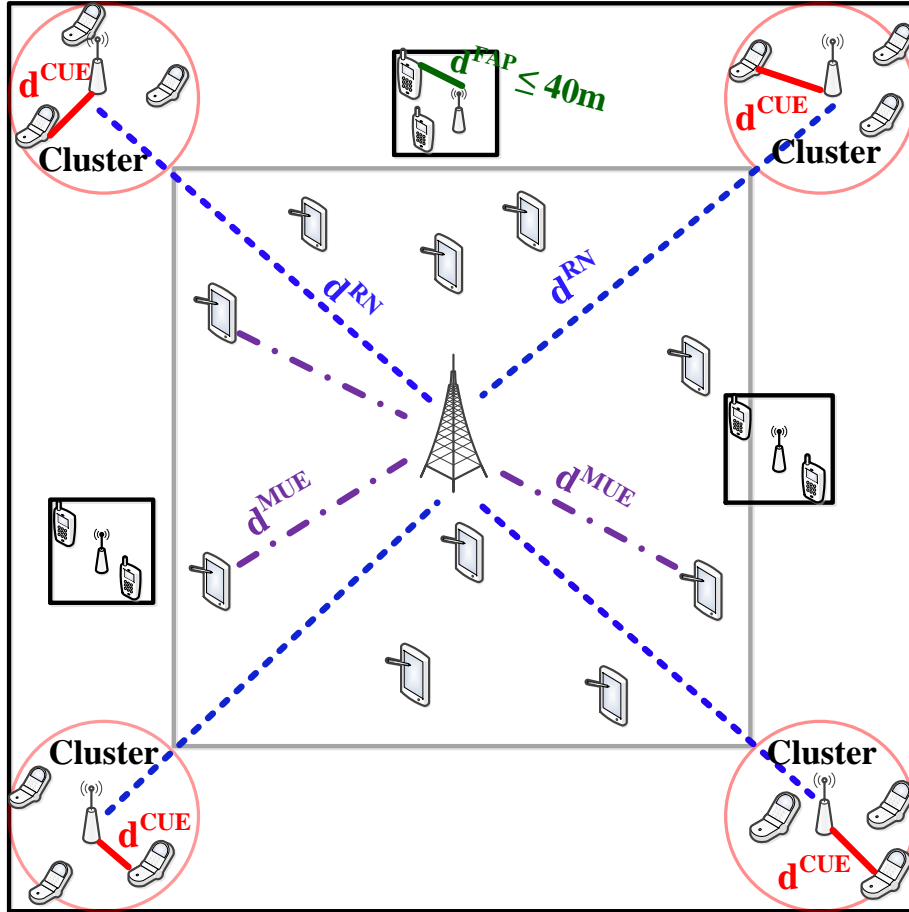


Figure B.2: Simulation scenario with fixed MBS, FAPs with their FUEs, MUEs and CUEs randomly distributed with a certain distance.

In several cases, the users and RN pre-coders are derived by assuming that all channel matrices are perfectly known at each node. In practical systems, such assumption may not always be realistic. In this regard, the BER evaluation of the channel estimation errors effect is further conducted for the proposed schemes for the FAPs, MUEs and UEs at both time slots. We consider different cases for CSI scenarios such as the proposed scheme with perfect CSI, the proposed scheme with LS and MMSE channel estimators.

Table B.1: Coordinate Parameters

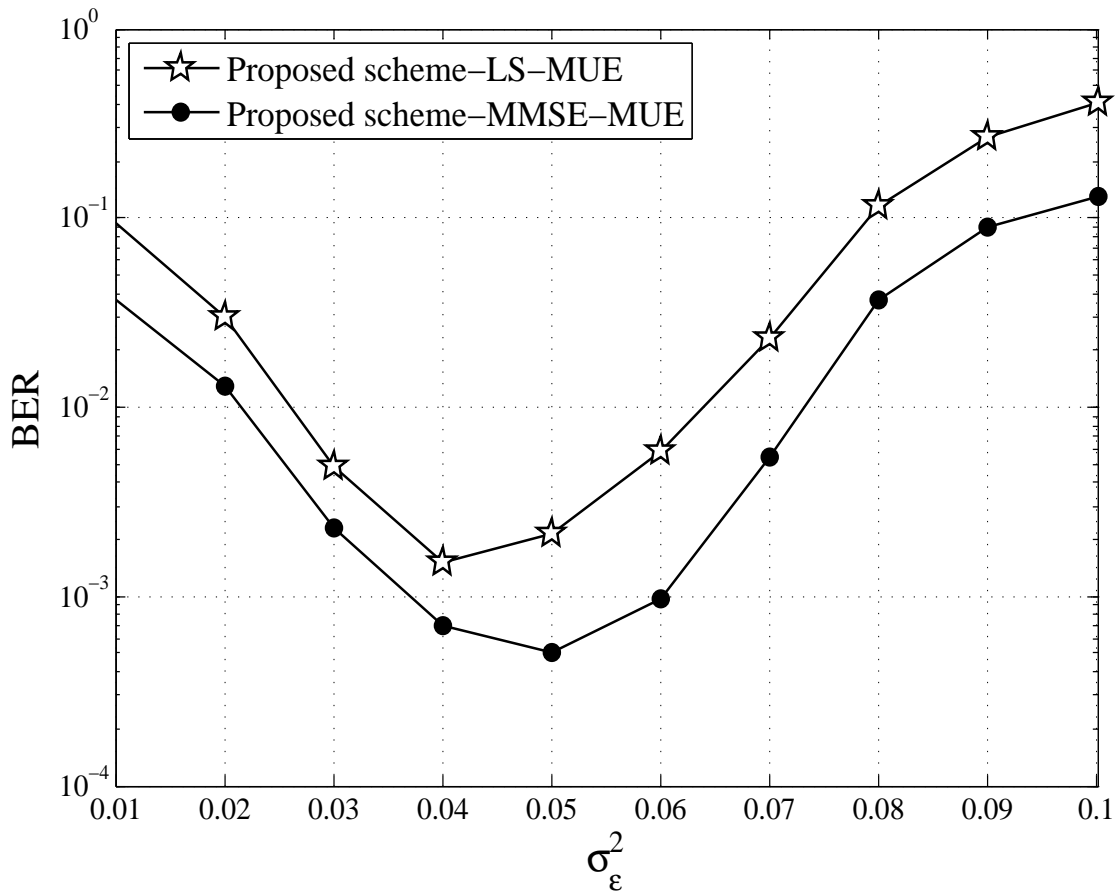
| Parameters | Values |
|-------------------------------|--|
| MBS | (1km, 1km) |
| MUEs | MUEs are uniformly distributed within the following interval range $x = [> 0.25\text{km} - < 1.75\text{km}]$, $y = [> 0.25\text{km} - < 1.75\text{km}]$ |
| 1. Cluster 1: | CUEs are randomly distributed with the following interval range in RN 1 for (x,y) |
| • RN 1 for R=1 | (0.125 km \times 0.125 km) |
| • CUE 1, CUE 2, CUE 3 in RN 1 | $x = [0 - \leq 0.25\text{km}]$, $y = [0 - \leq 0.25\text{km}]$ |
| 2. Cluster 2: | CUEs are randomly distributed with the following interval range in RN 2 for (x,y) |
| • RN 2 for R=2 | (0.125 km \times 1.875 km) |
| • CUE 1, CUE 2, CUE 3 in RN 2 | $x = [0 - \leq 0.25\text{km}]$, $y = [1.75\text{km} - \leq 2\text{km}]$ |
| 3. Cluster 3: | CUEs are randomly distributed with the following interval range in RN 3 for (x,y) |
| • RN 3 for R=3 | (1.875 km \times 0.125 km) |
| • CUE 1, CUE 2, CUE 3 in RN 3 | $x = [\geq 1.75\text{km} - 2\text{km}]$, $y = [0 - \leq 0.25\text{km}]$ |
| 4. Cluster 4: | CUEs are randomly distributed with the following interval range in RN 4 for (x,y) |
| • RN 4 for R=4 | (1.875 km \times 1.875 km) |
| • CUE 1, CUE 2, CUE 3 in RN 4 | $x = [\geq 1.75\text{km} - 2\text{km}]$, $y = [\geq 1.75\text{km} - 2\text{km}]$ |

The BER performance evaluation versus different value of σ_{ε}^2 for the MUEs during the first time slot is shown in Fig. B.3. The effect of the LS and MMSE channel estimators is considered and compared. It can be observed that for a chosen value of SNR, as the estimation value of σ_{ε}^2 increases, the BER performance increases as well until a maximum estimation value is achieved. It then starts

Table B.2: Simulation Parameters

| Parameters | Values |
|--|--------------------------------|
| - Number of MUEs, M | 10 |
| - Number of RNs, R | 4 |
| - Number of CUEs, K | 12 with 3 per RN |
| - Number of FAPs, F | 3 |
| - Number of FUEs per FAP, U | 2 per FAP |
| - Propagation Loss for distance $d \geq 0.75\text{km}$ | $148.1 + 37.6 \log_{10}(d)$ dB |
| - Propagation Loss for distance $d \leq 0.75\text{km}$ | $127 + 30 \log_{10}(d)$ dB |

decreasing as the estimation value decreases. This indicates that the maximum estimation value σ_ε^2 improves the performance of the MUEs in terms of BER evaluation versus the SNR and can achieve the optimal performance. For the LS and MMSE channel estimators, the maximum estimation value is achieved at $\sigma_\varepsilon^2 = 0.04$ and $\sigma_\varepsilon^2 = 0.05$, respectively.

Figure B.3: BER performance of the proposed schemes for MUEs with different values of σ_ε^2 , SNR= 15 dB

The BER performance versus the different values of σ_ε^2 is illustrated in Fig. B.4 for FAPs with SNR= 15dB. Although, the effect of the channel estimation errors is considered, the proposed scheme for FAP still performed well. As observed, the BER performance increases when σ_ε^2 increases and decreases after a certain value of σ_ε^2 . For the proposed scheme with LS estimator, the maximum value for σ_ε^2 to achieve an optimal BER performance is $\sigma_\varepsilon^2 = 0.06$ while for the proposed scheme with MMSE estimator is $\sigma_\varepsilon^2 = 0.05$.

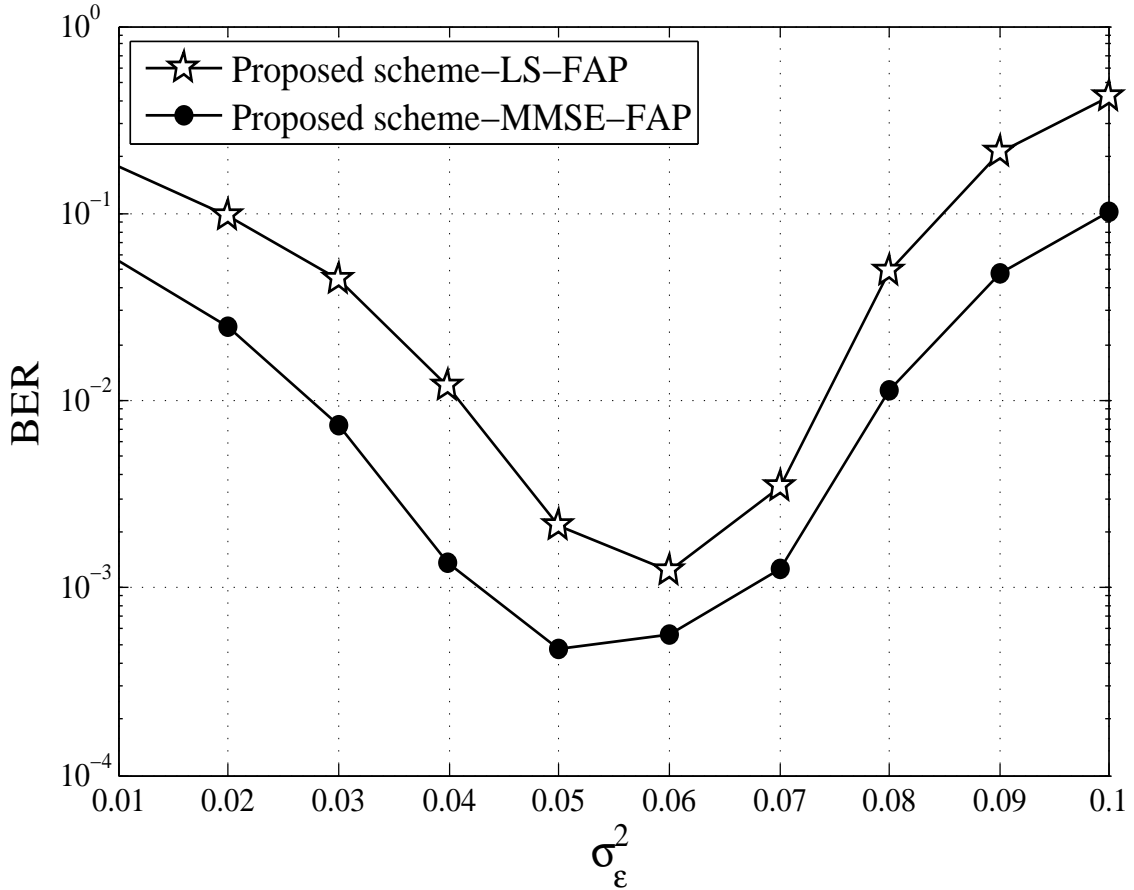


Figure B.4: BER performance of the proposed schemes for FAP with different values of σ_ε^2 , SNR= 15 dB

The BER performance as a function of SNR for FAPs is illustrated in Fig. B.5, for the LS and MMSE channel estimators with $\sigma_\varepsilon^2 = 0$ and $\sigma_\varepsilon^2 = 0.04$. It can be observed that, the proposed scheme with MMSE channel estimator outperforms the BER performance with the LS estimator effect regardless the value of σ_ε^2 . Another interesting observation is that the value of σ_ε^2 affects the BER of the proposed schemes such that it can increase the performance at the maximum value and decrease after the maximum value. With the value of $\sigma_\varepsilon^2 = 0.04$ for LS and MMSE estimators at SNR = 15dB, it can be seen that the achieved BER performances in Fig. B.5 are similar to the ones in Fig. B.4.

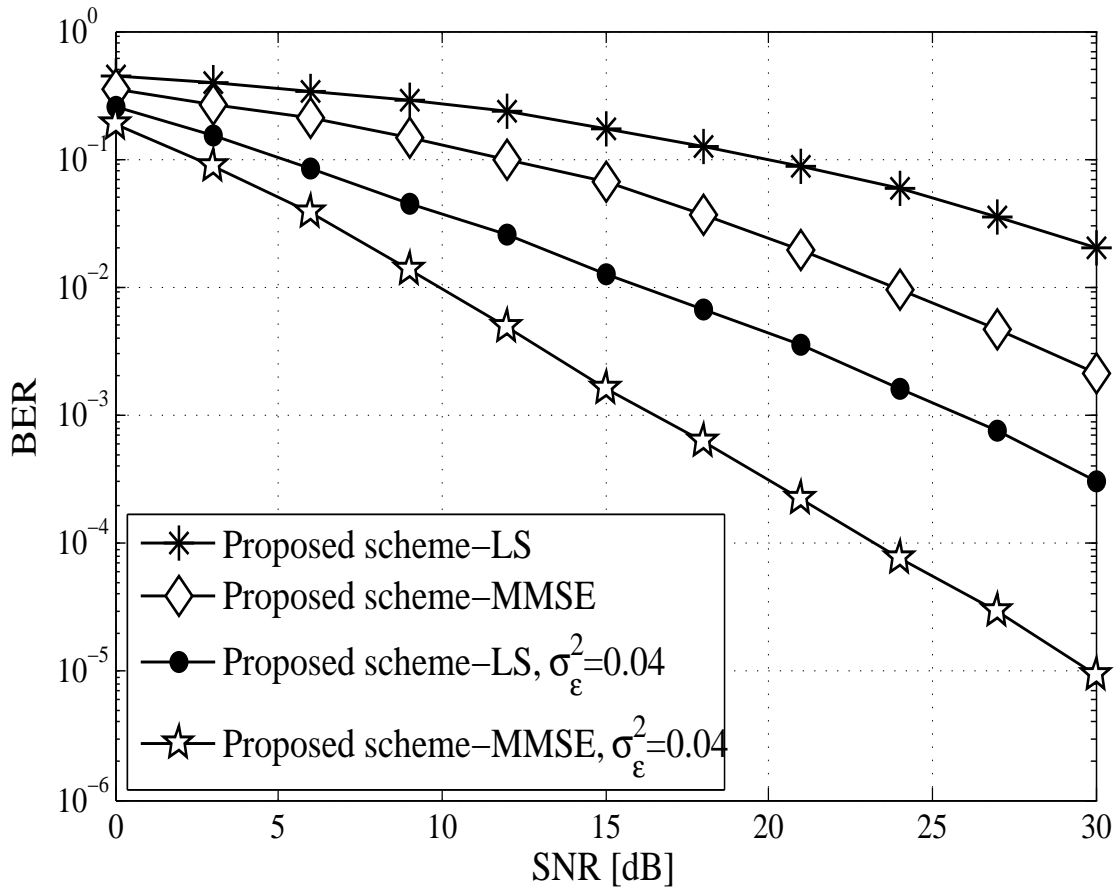


Figure B.5: BER performance versus SNR for the FAP during the first time slot

Figure B.6 illustrates the BER performance as a function of σ_ε^2 for the CUE with and without cooperative RN during the first time slot with SNR = 20dB. It can be observed that, the BER performance of a system without cooperative RNs is not as good as a system with cooperative RNs. However, the performance of the proposed scheme with "No RN" is improved when adding estimation values to the ZF assumptions. For LS and MMSE estimators of the proposed scheme with "No RN", the maximum σ_ε^2 is achieved between 0.05 and 0.06, respectively. Note that the "No RN" performance with channel estimation are based on the model proposed in [27]. The proposed scheme, on the other hand, achieves far better BER performance when $\sigma_\varepsilon^2 = 0.06$ for LS estimator and $\sigma_\varepsilon^2 = 0.05$ for the MMSE estimator. Therefore, with the parameters considered, we showed that very significant performances are obtained by adding estimation values to the ZF assumptions.

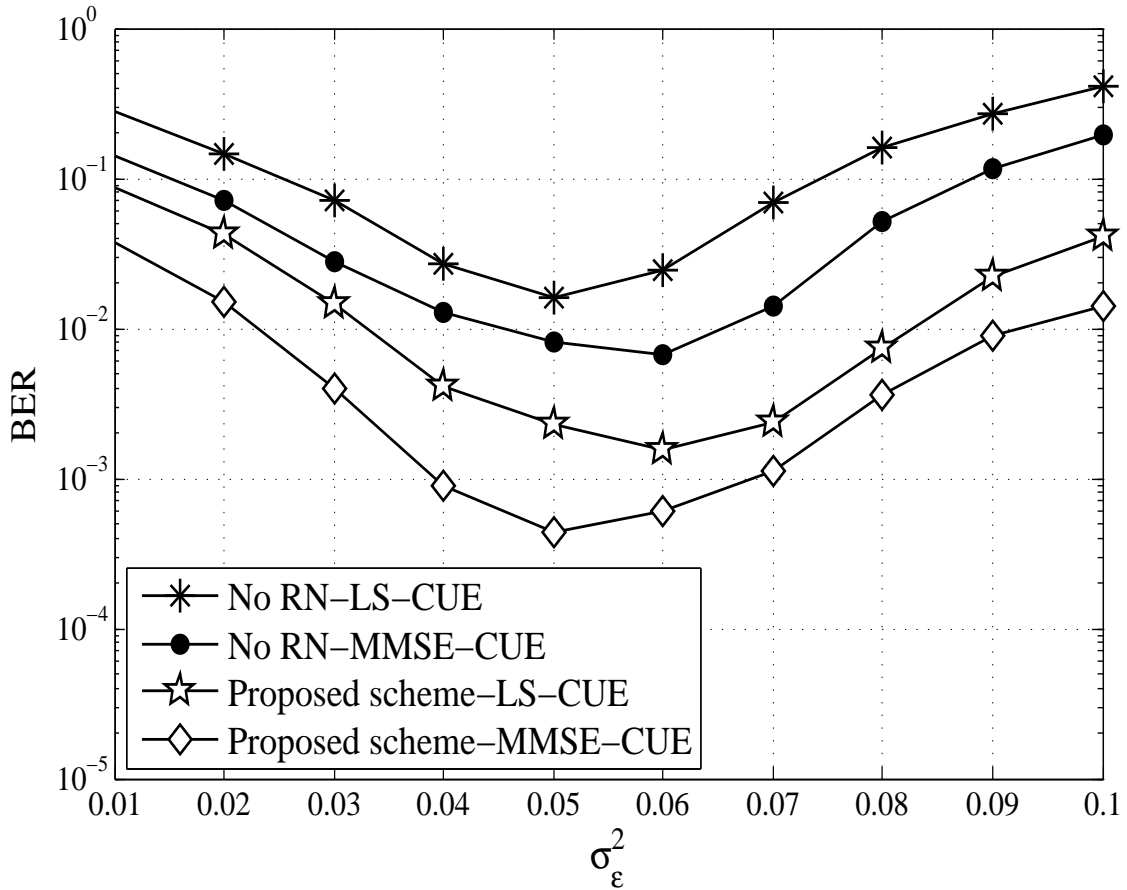


Figure B.6: BER performance versus different values σ_ε^2 for the CUEs with and without the RN

In Fig. B.7, we consider the maximum σ_ε^2 in the case of CUEs with and without RN. For the LS $\sigma_\varepsilon^2 = 0.05$ and MMSE estimators $\sigma_\varepsilon^2 = 0.06$ for "No RN", the same σ_ε^2 are considered for the proposed scheme. We can observe that the proposed schemes for the CUEs still provide significant improvement with the effect of MMSE and LS channel estimators than when a RN is not considered.

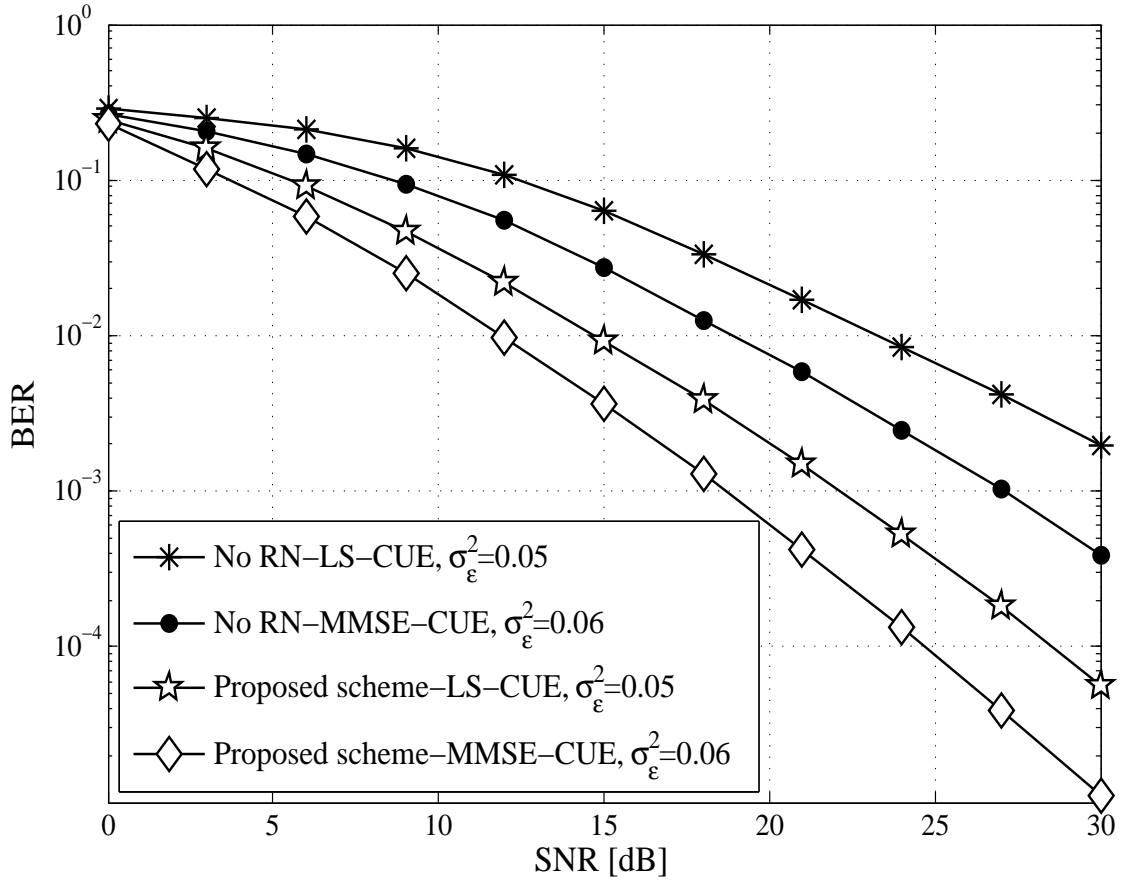


Figure B.7: BER evaluation as function of the SNR for the CUEs with and without the RN during the first time slot, for $\sigma_\varepsilon^2 = 0.05$ and $\sigma_\varepsilon^2 = 0.06$

Fig. B.8 shows the BER evaluation versus different values of σ_ε^2 for the UEs during the second time slot with the effect of the LS and MMSE channel estimators. As observed, the proposed scheme with the MMSE channel estimator is better than the LS estimator performance. Interestingly, the maximum value of σ_ε^2 to achieve an optimal BER performance for the proposed scheme with LS estimator is $\sigma_\varepsilon^2 = 0.05$ while $\sigma_\varepsilon^2 = 0.06$ for the proposed scheme with MMSE estimator.

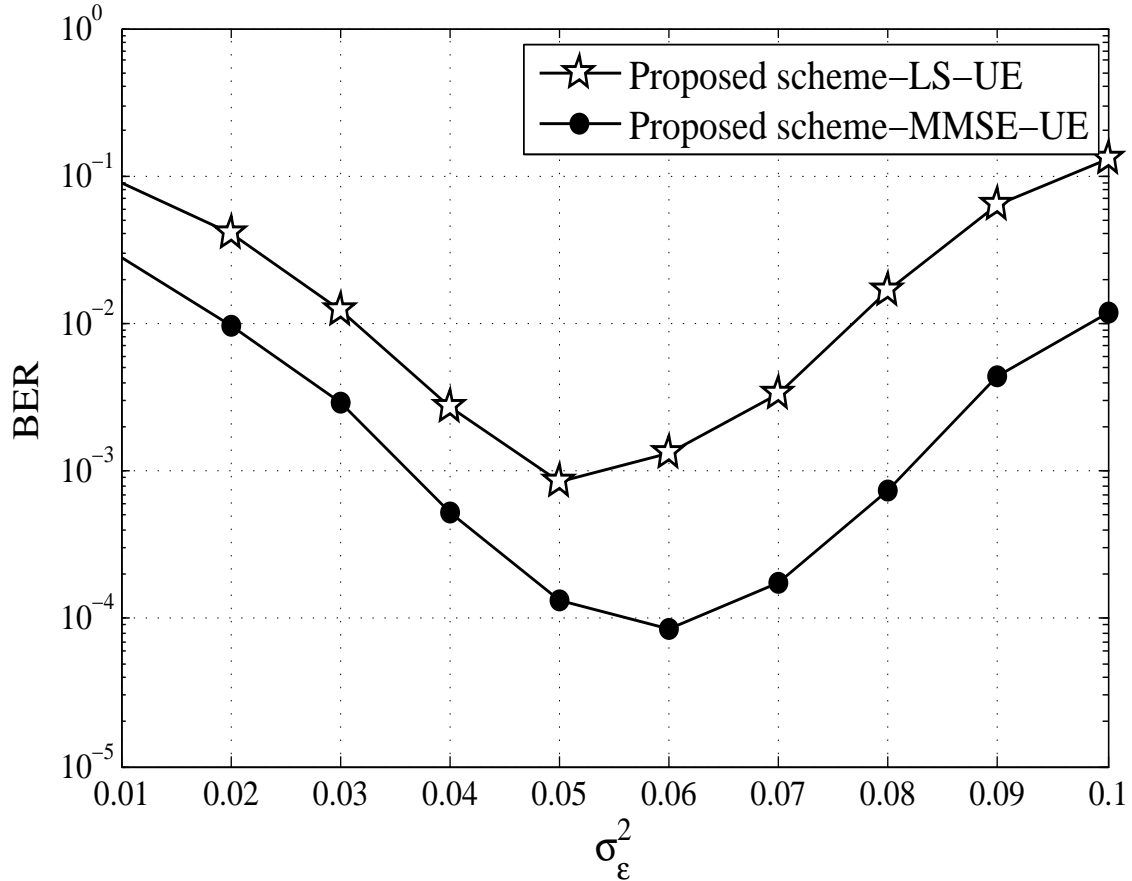


Figure B.8: BER performance of the proposed schemes for UEs with different values of σ_ε^2 , SNR= 15 dB

Fig. B.9 illustrates the BER performance as a function of the SNR for the UEs during the second time slot. This considers the UEs, which the signal coming from the RN and the MUEs during the second time slot to the MBS. As observed in the figure, the proposed scheme with the effect channel estimator still perform well. The reason is that, the proposed schemes update the Lagrange multiplier at each iteration in addition to the UEs and RN matrices. Interestingly, the BER performance of the proposed scheme with the MMSE estimator is better than the LS channel estimator. Furthermore, the proposed scheme with $\sigma_\varepsilon^2 = 0.03$, obviously outperforms the proposed schemes with channel estimators when only the ZF $\sigma_\varepsilon^2 = 0$ is considered without adding the estimation error σ_ε^2 .

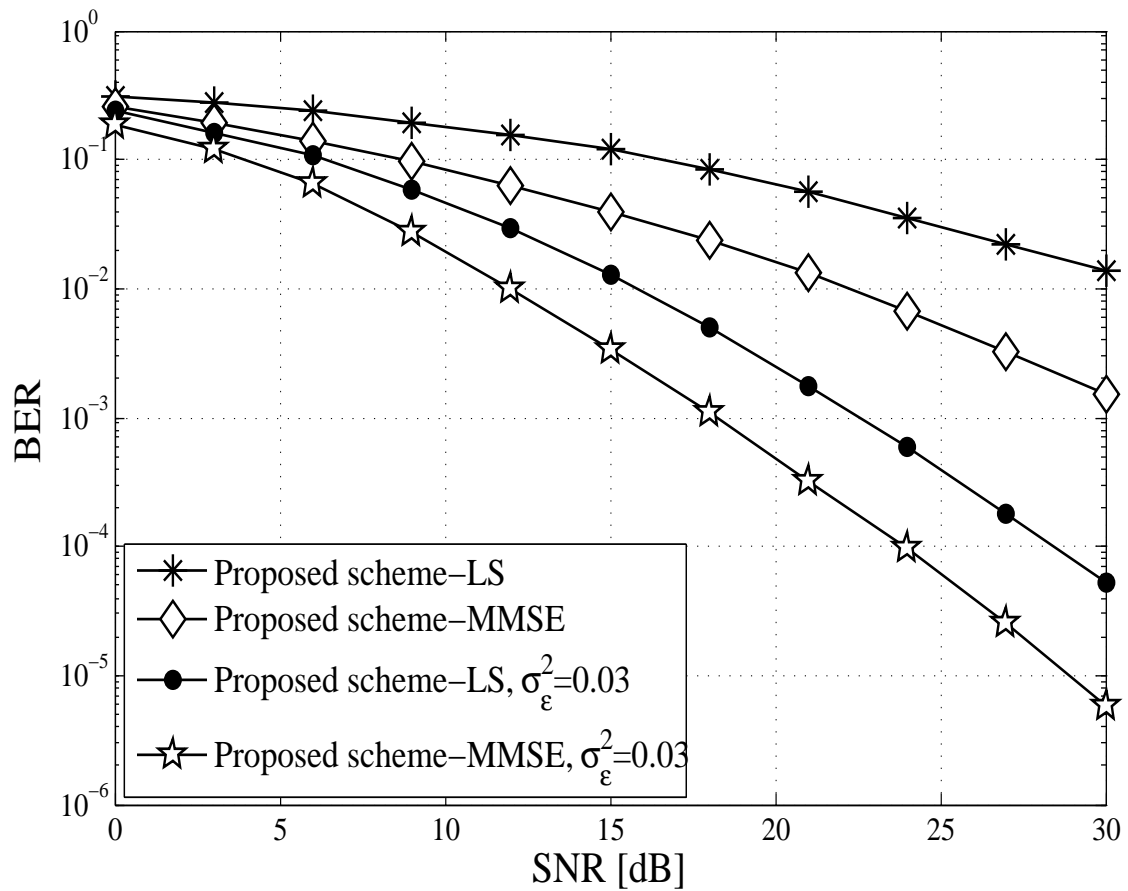


Figure B.9: BER performance of the proposed schemes for the UEs during the second time slot, for $\sigma_\varepsilon^2 = 0.03$

5 Conclusion

In this paper, optimal transceivers for the FUEs, MUEs, CUEs and RN (amplifying matrix) with channel estimators in the MU-MIMO relay systems have been designed for interference management. We considered a decentralised transceiver design instead of a centralised design which essentially is computationally impossible to do in this MU-MIMO relay system due to the unknown interfering terms. The interfering terms have been assumed to be generated as ZF solutions. Due to the inaccuracy of the ZF solutions, estimation values were added to the ZF assumptions in order to achieve better performance. The simulation results demonstrate a much better performance of the proposed schemes in terms of BER when estimation values are added to the ZF assumptions. The proposed decentralised schemes further enhance performance with respect to non-cooperative MU-MIMO systems. This confirms the importance of including cooperative RNs into MU-MIMO systems. Future lines of research could consider the application of the proposed algorithms in a massive MIMO system.

References

- [1] N. Saquib, E. Hossain, L. B. Le, and D. I. Kim, "Interference management in OFDMA femtocell networks: Issues and approaches," *IEEE Wireless Commun.*, vol. 19, no. 3, pp. 86–95, 2012.
- [2] N. Zhao, F. R. Yu, M. Jin, Q. Yan, and V. C. Leung, "Interference alignment and its applications: A survey, research issues, and challenges," *IEEE Commun. Surveys & Tutorials*, vol. 18, no. 3, pp. 1779–1803, 2016.
- [3] A. S. Hamza, S. S. Khalifa, H. S. Hamza, and K. Elsayed, "A survey on inter-cell interference coordination techniques in OFDMA-based cellular networks," *IEEE Commun. Surveys Tuts*, vol. 15, no. 4, pp. 1642–1670, 2013.
- [4] N. I. Miridakis and D. D. Vergados, "A survey on the successive interference cancellation performance for single-antenna and multiple-antenna OFDM systems," *IEEE Commun. Surveys & Tutorials*, vol. 15, no. 1, pp. 312–335, 2013.
- [5] S. Serbetli and A. Yener, "Iterative transceiver optimization for multiuser MIMO systems," in *Proc. of the annual allerton conf. commun., control and computing*, vol. 40, no. 2. The University; 1998, 2002, pp. 926–935.
- [6] C.-T. Lin, F.-S. Tseng, and W.-R. Wu, "MMSE transceiver design for full-duplex MIMO relay systems," *IEEE Trans. Veh. Technol.*, vol. 66, no. 8, pp. 6849 – 6861, 2017.
- [7] N. I. Miridakis and T. A. Tsiftsis, "On the joint impact of hardware impairments and imperfect CSI on successive decoding," *IEEE Trans. Veh. Technol.*, vol. 66, no. 6, pp. 4810–4822, 2017.
- [8] N. Khaled, G. Leus, C. Desset, and H. De Man, "A robust joint linear precoder and decoder MMSE design for slowly time-varying MIMO channels," in *Proc. IEEE International Conf. Acoustics, Speech, and Signal Process.(ICASSP'04)*, vol. 4, 2004, pp. iv–iv.
- [9] P. Sure and C. M. Bhuma, "A survey on OFDM channel estimation techniques based on denoising strategies," *Engineering Science and Technology, an International Journal*, vol. 20, no. 2, pp. 629–636, 2017.
- [10] C. Bouras, G. Kavourgiyas, V. Kokkinos, and A. Papazois, "Interference management in LTE femtocell systems using an adaptive frequency reuse scheme," in *Proc. IEEE Wireless Telecommun. Symposium (WTS)*, 2012, pp. 1–7.

- [11] A. Hatoum, R. Langar, N. Aitsaadi, R. Boutaba, and G. Pujolle, "Cluster-based resource management in OFDMA femtocell networks with QoS guarantees," *IEEE Trans. Veh. Technol.*, vol. 63, no. 5, pp. 2378–2391, 2014.
- [12] M. Ndong and T. Fujii, "Cross-tier interference management with a distributed antenna system for multi-tier cellular networks," *EURASIP Journal on Wireless Communications and Networking*, vol. 2014, no. 1, pp. 1–12, 2014.
- [13] —, "Joint femtocell clustering and cross-tier interference mitigation with distributed antenna system in small cell networks," in *Proc. 9th IEEE International Symposium on Commun Systems, Netw. & Digital Signal Process. (CSNDSP)*, 2014, pp. 652–657.
- [14] L. Li, Y. Jing, and H. Jafarkhani, "Interference cancellation at the relay for multi-user wireless cooperative networks," *IEEE Trans. Wireless Commun.*, vol. 10, no. 3, pp. 930–939, 2011.
- [15] C.-B. Chae, T. Tang, R. W. Heath Jr, and S. Cho, "MIMO relaying with linear processing for multiuser transmission in fixed relay networks," *IEEE Trans. Signal Process.*, vol. 56, no. 2, pp. 727–738, 2008.
- [16] S. Malik, S. Moon, B. Kim, C. You, H. Liu, and I. Hwang, "Design and analysis of an interference cancellation algorithm for AF, DF and DMF relay protocol in multiuser MIMO scenario based on the LTE-Advanced system," *Wireless personal communications*, vol. 75, no. 1, pp. 775–797, 2014.
- [17] J.-C. Shen, J. Zhang, and K. B. Letaief, "Downlink user capacity of massive MIMO under pilot contamination," *IEEE Trans. Wireless Commun.*, vol. 14, no. 6, pp. 3183–3193, 2015.
- [18] A. Khansefid and H. Minn, "On channel estimation for massive MIMO with pilot contamination," *IEEE Commun. Lett.*, vol. 19, no. 9, pp. 1660–1663, 2015.
- [19] Y. Huang, W. Tang, H. Wei, J. Li, D. Wang, and X. Su, "On the performance of iterative receivers in massive mimo systems with pilot contamination," in *Proc. 9th IEEE Conf. Industrial Electronics and Applications (ICIEA)*, 2014, pp. 52–57.
- [20] L. Li, A. Ashikhmin, and T. Marzetta, "Pilot contamination precoding for interference reduction in large scale antenna systems," in *Proc. 51st IEEE Annual Allerton Conf. Commun., Control, and Computing (Allerton)*, 2013, pp. 226–232.
- [21] J. Liu, F. Gao, and Z. Qiu, "Robust transceiver design for downlink multiuser MIMO AF relay systems," *IEEE Trans. Wireless Commun.*, vol. 14, no. 4, pp. 2218–2231, 2015.

- [22] A. C. Cirik, S. Biswas, S. Vuppala, and T. Ratnarajah, "Robust transceiver design for full duplex multiuser MIMO systems," *IEEE Wireless Commun. Lett.*, vol. 5, no. 3, pp. 260–263, 2016.
- [23] M. R. Khandaker and Y. Rong, "Joint transceiver optimization for multiuser MIMO relay communication systems," *IEEE Trans. Signal Process.*, vol. 60, no. 11, pp. 5977–5986, 2012.
- [24] J. Yang and B. Champagne, "Joint transceiver optimization for MIMO multiuser relaying networks with channel uncertainties," in *Proc. 80th IEEE Veh. Technol. Conf. (VTC Fall)*, 2014, pp. 1–6.
- [25] M. Raja and P. Muthuchidambaranathan, "Multiuser MIMO transceiver design for uplink and downlink with imperfect CSI," *Springer Wireless pers. commun.*, vol. 75, no. 2, pp. 1215–1234, 2014.
- [26] S. Serbetli and A. Yener, "Transceiver optimization for multiuser MIMO systems," *IEEE Trans. Signal Process.*, vol. 52, no. 1, pp. 214–226, 2004.
- [27] B. Guler and A. Yener, "Uplink interference management for coexisting MIMO femtocell and macrocell networks: An interference alignment approach," *IEEE Trans. Wireless Commun.*, vol. 13, no. 4, pp. 2246–2257, 2014.
- [28] A. Dong, H. Zhang, D. Yuan, and X. Zhou, "Interference alignment transceiver design by minimizing the maximum mean square error for MIMO interfering broadcast channel," *IEEE Trans. Veh. Technol.*, vol. 65, no. 8, pp. 6024–6037, 2016.
- [29] B. D. Antwi-Boasiako, C. Song, and K.-J. Lee, "Transceiver designs for mimo relaying systems with imperfect channel state information," *Hindawi, Mobile Information Systems*, vol. 2018, pp. 1–12, 2018.
- [30] Z. He, W. Jiang, and Y. Rong, "Robust design for amplify-and-forward MIMO relay systems with direct link and imperfect channel information," *IEEE Trans. Wireless Commun.*, vol. 14, no. 1, pp. 353–363, 2015.
- [31] C. Qi, G. Yue, L. Wu, Y. Huang, and A. Nallanathan, "Pilot design schemes for sparse channel estimation in OFDM systems," *IEEE Trans. Veh. Technol.*, vol. 64, no. 4, pp. 1493–1505, 2015.

Paper C

Energy Efficient Transceiver Design for Cooperative Multi-User MIMO Systems

Armeline Dembo Mafuta, Tom M. Walingo and Fambirai Takawira

The paper is under review at the
IEEE Transactions on Communications Journal, 2018

© 2018 IEEE

The layout has been revised.

Abstract

This work undertakes an efficient transceivers design that optimises energy efficiency (EE) in multi-user multiple-input multiple-output (MU-MIMO) relay systems. In this system, cell-edge macrocell user equipments (CUEs) are grouped into clusters and communicate with the macrocell base station (MBS) through a relay node (RN). The macrocell UEs (MUEs), on the other hand, communicate directly with the MBS. The femtocell UEs (FUEs) communicate with their respective femtocell access points (FAPs). The centralised transceiver design for such a system is not trivial. This work proposes decentralised algorithms with perfect channel state information (CSI) to optimise the linear transceivers for the multi-users and the RN. This is done under the quality of service (QoS) and transmit power constraints to achieve the EE maximisation. The weighted minimum mean square error (WMMSE) is employed in the design of the decentralised algorithms. Parameter subtractive functions are introduced into each proposed schemes to surmount the non-convexity of the formulated EE optimisation problem. These parameters are updated by the Dinkelbach's algorithm. The performance investigation demonstrates the superiority of the proposed over existing scheme in terms of the average EE and convergence.

1 Introduction and Related Works

Recently, energy efficiency (EE) has attracted huge attention in the research community. It is a key performance criterion considered by the international telecommunication union (ITU) in the design of next generation of communication networks while guaranteeing sustainable evolution [1], [2]. In fourth generation (4G) and fifth generation (5G) cellular networks, energy saving is commonly done by minimising the transmit power subject to quality of service (QoS) constraint or by optimising the achievable sum rate and the consumed energy ratio, i.e., the bit/Joule. The multi-user multiple input multiple output (MU-MIMO) used in Long Term Evolution Advanced (LTE-Advanced) employs features for achieving high spectral efficiency (SE) and EE gains. Moreover, it combines the high capacity of MIMO processing with space division multiple access (SDMA) to increase capacity by facilitating multiplexing data streams across multiple users in the networks [3]. To further improve the connectivity and performance of cell edge users, cooperative relay nodes (RNs) have been added in the MU-MIMO system to form the MU-MIMO relay networks, an integral part of the existing wireless communication standards [4]. The additional RNs retransmit the received signal from sources to their respective destinations to reduce the communication cost and to enhance reliability [5]. In the MU-MIMO relay networks, RNs provide a high throughput and reliable communication coverage between

the sources and destinations when the direct link experiences deep fading [6], [7]. Furthermore, small cells have been introduced to keep up with the exponential increase in data rate demand foreseen for the 4G/5G networks. These, however, generate intra and inter-cell interferences when small-cells share the same spectrum with the macrocell networks fitted with RN. The inter and intra-cell interference is a key limiting factor for improving the EE of full frequency reuse cellular networks.

Due to the high-energy consumption in MU-MIMO relay communications, different scenarios such as single-cell scenario, cooperative relaying system or cognitive radio, have been investigated. Maximising the EE in MU-MIMO relay systems has been addressed in [8]. The EE and SE on the uplink of a large multi-cell and single-cell MU-MIMO systems is considered. However, the authors did not consider transceiver technique for energy consumption minimisation, one of the good approach for energy management for such networks. Transceivers, known as pre-coder and decoder schemes [9], are employed to manage the interferences and to optimise the EE performance in MU-MIMO networks [10] [11]. Hence, transceiver design based on the EE maximisation and weighted minimum mean square error (WMMSE) approach is considered in maximising EE performance mitigating interferences in MU-MIMO relay systems. Different performance measurements such as average minimum bit error rate (BER), WMMSE or joint design [12], can be considered in obtaining optimum linear transceiver structure. In addition to these measurements, convex optimisation [13] needs to be adopted in order to get optimum pre-coder and decoder design and achieve superior performance [14]. For instance, a low complexity iterative method based on fractional programming is proposed in [15], to solve the pseudo-concave problem and optimise the transmit power. The authors in [16], on the other hand, considered total transmit power minimisation in multicell MU-MIMO systems where an optimal linear pre-coder has been designed. The authors in [17] investigated and analysed the energy consumption in a very large MU-MIMO system and considered the impact of user equipment's (UEs) mobility. The authors in [18] developed an iterative joint transceiver algorithm to maximise the weighted sum-rate for downlink MU-MIMO relay network. Moreover, an iterative algorithm to jointly optimise the multi-user and relay pre-coder in MU-MIMO relay channel with perfect and imperfect channel state information (CSI) is proposed in [19], maximising EE. Optimal energy efficient source and relay pre-coders are designed by [20] in a cooperative MIMO amplify-and-forward (A-F) system. The EE is investigated in [21] with SE as one of the constraints. This is modelled as a cube inequality to maximise the EE and satisfy the SE requirement. In [22], an EE-SE trade-off under non-ideal power amplifier models is investigated in a MU-MIMO system where the EE maximisation problem is solved by considering different SE values. However, all these works do not consider a system with multiple femtocells networks, RNs and network performance at the cell edges, this is not trivial.

In this work, we go beyond the system considered in [20], [23], [24] by considering a more realistic MU-MIMO relay systems with RNs and multiple femtocells deployed in a macrocell coverage. The work in [20] is extended further by deriving not only the source and RN pre-coder but the destination decoder and investigating the system performance of the cell edge users. In contrast to aforementioned researches, a joint linear transceiver design could not be appropriate for the system considered. Therefore, decentralised transceivers design is proposed in the MU-MIMO systems. Furthermore, in the formulation of EE optimisation problem, different constraints are considered depending on the performance requirement that needs to be satisfied. These constraints are the transmit power and the QoS constraints that are used to optimise the EE and design the decentralised energy efficient transceivers in the MU-MIMO relay systems.

The main contributions of this paper are summarized as follows. Firstly, the transceiver design for a complete MU-MIMO relay network consisting of FUEs, MUEs CUEs is done. These UE's transmit to the FAPs, MBS and RNs during the first and second time slot while the RNs and MUEs transmit to the MBS during the second time slot. The clustered CUEs transmit to the MBS through the RNs. Simple network transceiver design is currently done in literature [19], [20]. In [19] a simple network architecture with K-users simultaneously transmitting to the same BS through a RN is employed. A similar architecture is investigated in [20], however, a single source node transmits through a RN and directly to the destination node. Unlike these works, a more complex network architecture for femtocells, RNs and MBS is considered. Moreover, the cell-edges users are investigated. Secondly, we consider a decentralised approach for the design of pre-coders and decoders at the FAP and MBS where each FAPs and MBS determine its own pre-coder and decoder while assuming the knowledge of the channel state. The decentralised transceiver design is considered for this MU-MIMO relay systems since the global CSI is not available at each base stations (FAPs, RNs and MBS). This approach differs from [20] which consider centralised approach in the pre-coders and decoders design. In both approaches, the optimal solution is found by alternating optimisation in which the pre-coders and decoders are updated consecutively. However, in this work, the unknown neighbouring pre-coders are determined using the zero-forcing (ZF) approach and an estimation error parameter Δ_e . The obtained neighbouring pre-coders facilitate the decentralised implementation and the design of optimal FUEs, MUEs and CUEs pre-coders. Furthermore, when considering the estimation error Δ_e , the average EE performance increases for the FAPs users, MUEs and CUEs. The formulation of EE maximisation problem is based on the same approach used in [19].

The remaining sections of the paper are organised as follows: The system model and problem formulation are addressed in Section II. Section III gives the details on the EE maximisation and transceiver optimisation for the FUEs and MUEs during the first time slot. Section IV describes the

EE maximisation formulation and transceiver optimisation for CUEs through RN and MUEs during the second time slot. Section V addresses the performance evaluation of the proposed scheme while section VI gives the conclusion of the paper.

Notation: The following notations are used in this paper. Upper-case and lower-case bold-faced letters are used to denote matrices and column vectors, respectively. The superscripts $(\cdot)^*$, $(\cdot)^H$, and $(\cdot)^{-1}$ represent optimality, Hermitian and inverse operators, respectively. $\mathbf{I}_{N \times N}$ denotes an N by N identity matrix. $\|\cdot\|$ is the Frobenius norm, and $|\cdot|$ represents the absolute value of a scalar. $\mathbb{E}[\cdot]$ and $\text{Tr}(\cdot)$ are the expectation and the trace respectively.

2 System Model

2.1 Network architecture

We consider uplink MU-MIMO relay communications composed of macrocell, femtocells and RNs. The MUEs, which are far from the MBS, are grouped into clusters and transmit to the MBS through a RN, are called CUEs. It is assumed that the RNs are placed at the optimal locations to avoid interference to femtocell networks. Let K be the number of CUEs in a cluster and F the total number of FAPs in the whole network. M denotes the MUE outside the clusters which transmit directly to MBS. R represents the number of RN in the network, equivalent to the number of clusters. The CUEs and FUEs transmit during the first time slot while the RNs transmit to the MBS during the second time slot. The MUEs, on the other hand, transmit continuously during both time slots to the MBS. This is illustrated in Figure C.1. The UEs, FAPs, RNs and MBS are equipped with N_s , N_f , N_R and N_B antennas, respectively. Let d_s be the data streams of the information transmitted from the k^{th} CUE. The intended signal from the k^{th} CUE to the RN at the first time slot is given as

$$\mathbf{x}_{r,k} = \mathbf{w}_{r,k} s_{r,k}, \quad k = 1, \dots, K \quad (\text{C.1})$$

where $\mathbf{w}_{r,k}$ is the linear transmit pre-coder vector of the CUE with $\mathbf{w}_{r,k} \in \mathbb{C}^{N_s \times 1}$ and corresponds to the data symbol $s_{r,k}$ with the unity norm constraint $\|\mathbf{w}_{r,k}\| = 1$. $\mathbf{x}_{r,k}$ is the signal transmitted from the k^{th} CUE to the r^{th} RN. The linear transmit pre-coder matrix for K -CUE to the r^{th} RN can be written $\mathbf{W}_r = [\mathbf{w}_{r,1}, \mathbf{w}_{r,2}, \dots, \mathbf{w}_{r,K}] \in \mathbb{C}^{N_s \times d_s}$, its corresponding data symbol matrix is $\mathbf{s}_r = [s_{r,1}, s_{r,2}, \dots, s_{r,K}] \in \mathbb{C}^{d_s \times 1}$.

It is assumed that the node in the MU-MIMO relay system operates in the half-duplex mode and the communication between the K -CUEs and the MBS is completed within two consecutive time slots

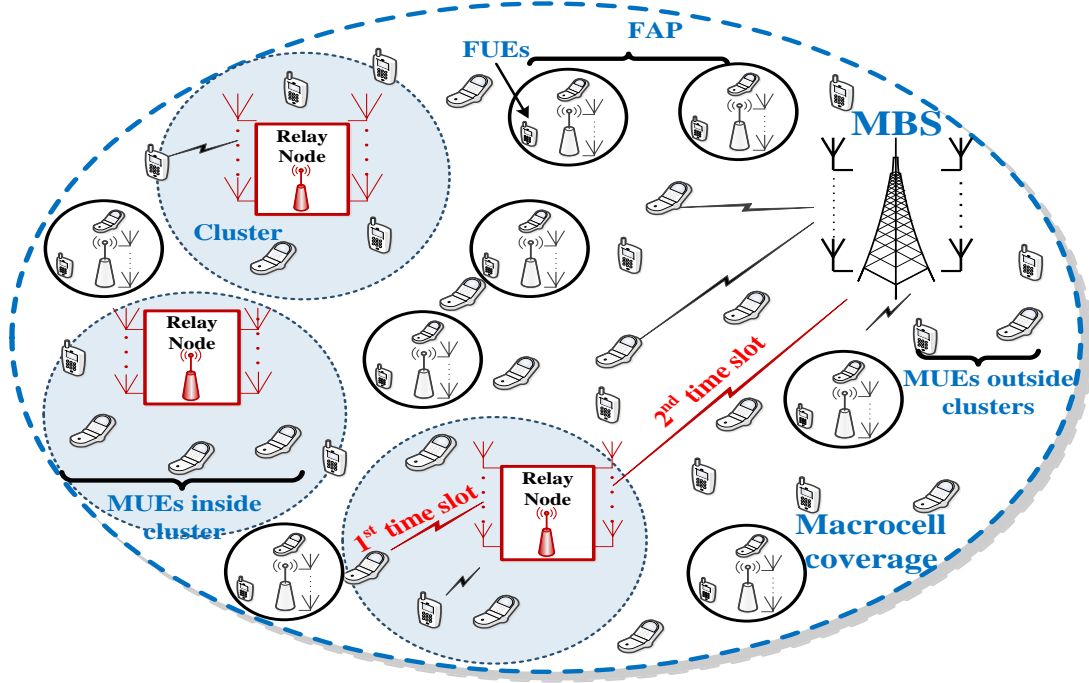


Figure C.1: Illustration of an uplink MU-MIMO relay system with several CUEs, MUEs, RN and femtocells under MBS coverage.

through the RN. The j^{th} FAP received signal \mathbf{y}_j^{st} in the first time slot is given as

$$\begin{aligned}
 \mathbf{y}_j^{st} = & \underbrace{\sum_{i=1}^{U_i} \mathbf{H}_{j,i}^{\text{FAP}} \mathbf{w}_{j,i}^{\text{FAP}} s_{j,i}^{\text{FAP}}}_{\text{desired FUE signals at the } j^{\text{th}} \text{ FAP}} + \underbrace{\sum_{m=1}^M \mathbf{H}_{j,m}^{\text{MUE}} \mathbf{w}_{o,m}^{\text{MUE}} s_{o,m}^{\text{MUE}}}_{\text{macrocell interference outside the cluster to the } j^{\text{th}} \text{ FAP}} + \underbrace{\sum_{\substack{f=1 \\ f \neq j}}^F \sum_{u=1}^U \mathbf{H}_{j,f,u}^{\text{FAP}} \mathbf{w}_{f,u}^{\text{FAP}} s_{f,u}^{\text{FAP}}}_{\text{Other femtocells interference to the } j^{\text{th}} \text{ FAP}} \\
 & + \underbrace{\sum_{r=1}^R \sum_{k=1}^K \mathbf{H}_{j,r,k}^{\text{CUE}} \mathbf{w}_{r,k}^{\text{CUE}} s_{r,k}^{\text{CUE}}}_{\text{interference from CUEs transmission to RN}} + \underbrace{\mathbf{n}_j}_{\text{noise}}, \tag{C.2}
 \end{aligned}$$

where $\mathbf{H}_{j,i}^{\text{FAP}}$ is channel matrix from i^{th} FUE to j^{th} FAP and $\mathbf{H}_{j,m}^{\text{MUE}}$ is the channel matrix from m^{th} MUE to j^{th} FAP. $\mathbf{H}_{j,f,u}^{\text{FAP}}$ is channel matrix from the u^{th} FUE of the f^{th} FAP to the j^{th} FAP while $\mathbf{H}_{j,r,k}^{\text{CUE}}$ is channel matrix from the k^{th} CUE of the r^{th} RN to the j^{th} FAP. $\mathbf{w}_{j,i}^{\text{FAP}}$ and $s_{j,i}^{\text{FAP}}$ are the pre-coding matrix and its corresponding data symbol for the i^{th} FUE of the j^{th} FAP. $\mathbf{w}_{o,m}^{\text{MUE}}$ and $s_{o,m}^{\text{MUE}}$ are the pre-coding matrix and its corresponding data symbol for the m^{th} MUE of the MBS. $\mathbf{w}_{f,u}^{\text{FAP}}$ and $s_{f,u}^{\text{FAP}}$ are the pre-coding matrix and its corresponding data symbol for the u^{th} FUE of the f^{th} FAP. $\mathbf{w}_{r,k}^{\text{CUE}}$ and $s_{r,k}^{\text{CUE}}$ are the pre-coding matrix and its corresponding data symbol for the k^{th} CUE of the r^{th} RN. \mathbf{n}_j denotes the additive white Gaussian noise (AWGN) vector with variance $(\sigma_j^{\text{FAP}})^2$ distributed according to $\mathcal{CN}(0, (\sigma_j^{\text{FAP}})^2)$.

We assume that the design of the pre-coders and decoders at each FAPs and MBS are independent of one another. Hence, to find the optimal $\mathbf{w}_{j,i}^{\text{FAP}}$ in (C.2) at the j^{th} FAP, we use the estimated $\mathbf{w}_{o,m}^{\text{MUE}'}$, $\mathbf{w}_{f,u}^{\text{FAP}'}$ and $\mathbf{w}_{r,k}^{\text{CUE}'}$, found using ZF pre-coder with an estimation error Δ_e ,

$$\mathbf{w}_{o,m}^{\text{MUE}'} = [\mathbf{H}_{o,m}^{\text{MUE}H} (\mathbf{H}_{o,m}^{\text{MUE}H} \mathbf{H}_{o,m}^{\text{MUE}})^{-1} + \Delta_e], \quad \forall m = 1 \quad (\text{C.3})$$

$$\mathbf{w}_{f,u}^{\text{FAP}'} = [\mathbf{H}_{f,u}^{\text{FAP}H} (\mathbf{H}_{f,u}^{\text{FAP}H} \mathbf{H}_{f,u}^{\text{FAP}})^{-1} + \Delta_e], \quad \forall u = 1 \quad (\text{C.4})$$

$$\mathbf{w}_{r,k}^{\text{CUE}'} = [\mathbf{H}_{r,k}^{\text{CUE}H} (\mathbf{H}_{r,k}^{\text{CUE}H} \mathbf{H}_{r,k}^{\text{CUE}})^{-1} + \Delta_e], \quad \forall k = 1, \quad (\text{C.5})$$

where Δ_e is a Gaussian random number of zero mean and variance of $\sigma_{\Delta_e}^2$. The received signal \mathbf{y}_j^{st} at the j^{th} FAP becomes,

$$\begin{aligned} \tilde{\mathbf{y}}_j^{\text{st}} = & \underbrace{\sum_{i=1}^{U_j} \mathbf{H}_{j,i}^{\text{FAP}} \mathbf{w}_{j,i}^{\text{FAP}} s_{j,i}^{\text{FAP}}}_{\text{desired FUE signal}} + \underbrace{\sum_{m=1}^M \mathbf{H}_{j,m}^{\text{MUE}} \mathbf{w}_{o,m}^{\text{MUE}' } s_{o,m}^{\text{MUE}}}_{\text{MUE Inteference denoted } I_m} + \underbrace{\sum_{\substack{f=1 \\ f \neq j}}^F \sum_{u=1}^U \mathbf{H}_{j,f,u}^{\text{FAP}} \mathbf{w}_{f,u}^{\text{FAP}' } s_{f,u}^{\text{FAP}}}_{\text{FUE inteference denoted } I_u} \\ & + \underbrace{\sum_{r=1}^R \sum_{k=1}^K \mathbf{H}_{j,r,k}^{\text{CUE}} \mathbf{w}_{r,k}^{\text{CUE}' } s_{r,k}^{\text{CUE}}}_{\text{CUE interference denoted } I_k} + \mathbf{n}_j. \end{aligned} \quad (\text{C.6})$$

The transmit power $P_{j,i}$ of the i^{th} FUE at the j^{th} FAP must satisfy $P_{j,i} = \text{Tr}(\mathbf{w}_{j,i}^{\text{FAP}} (\mathbf{w}_{j,i}^{\text{FAP}})^H) \leq P_{i,max}^j$ where $P_{i,max}^j$ is the maximum transmit power for each FUE. An acceptable QoS needs to be provided by the system to serve as many users as possible. It is expressed in form of lower threshold on the received signal to interference plus noise ratio (SINR) at each user [25]. Due to the ZF precoders assumed for the interference, $\text{SINR}_j^{\text{FAP}}$ is given by (C.7).

$$\text{SINR}_j^{\text{FAP}} = \frac{\|\mathbf{H}_{j,i}^{\text{FAP}} \mathbf{w}_{j,i}^{\text{FAP}}\|^2}{\sum_{m=1}^M \|\mathbf{H}_{j,m}^{\text{MUE}} \mathbf{w}_{o,m}^{\text{MUE}'}\|^2 + \sum_{\substack{f=1 \\ f \neq j}}^F \sum_{u=1}^U \|\mathbf{H}_{j,f,u}^{\text{FAP}} \mathbf{w}_{f,u}^{\text{FAP}'}\|^2 + \sum_{r=1}^R \sum_{k=1}^K \|\mathbf{H}_{j,r,k}^{\text{CUE}} \mathbf{w}_{r,k}^{\text{CUE}'}\|^2 + (\sigma_j^{\text{FAP}})^2 \mathbf{I}_{N_s}}. \quad (\text{C.7})$$

The achievable sum rate of the FAP communication $\mathcal{R}_{sum}^{\text{FAP}}$, is formulated as

$$\mathcal{R}_{sum}^{\text{FAP}} = \frac{1}{2} \log_2(1 + \text{SINR}_j^{\text{FAP}}). \quad (\text{C.8})$$

The received signal \mathbf{y}_o^{st} at the MBS during the first time slot is given as

$$\mathbf{y}_o^{\text{st}} = \underbrace{\sum_{m=1}^M \mathbf{H}_{o,m}^{\text{MUE}} \mathbf{w}_{o,m}^{\text{MUE}' } s_{o,m}^{\text{MUE}}}_{\text{desired signal from the MUEs to the MBS}} + \underbrace{\sum_{r=1}^R \sum_{k=1}^K \mathbf{H}_{o,r,k}^{\text{CUE}} \mathbf{w}_{r,k}^{\text{CUE}' } s_{r,k}^{\text{CUE}}}_{\text{Interference from the CUEs to the MBS}} + \underbrace{\sum_{f=1}^F \sum_{u=1}^U \mathbf{H}_{o,f,u}^{\text{FAP}} \mathbf{w}_{f,u}^{\text{FAP}' } s_{f,u}^{\text{FAP}}}_{\text{femtocells inteference to the MBS}} + \underbrace{\mathbf{n}_o}_{\text{noise}}, \quad (\text{C.9})$$

where $\mathbf{H}_{o,m}^{\text{MUE}}$ is the channel matrix of m^{th} MUE of the MBS, $\mathbf{H}_{o,r,k}^{\text{CUE}}$ is the channel matrix from k^{th} CUE of the r^{th} RN to the MBS and $\mathbf{H}_{o,f,u}^{\text{FAP}}$ is the channel matrix from the u^{th} FUE of the f^{th} FAP to the MBS. \mathbf{n}_o is the AWGN vector with variance $(\sigma_o^{\text{MBS}})^2$ distributed according to $\mathcal{CN}(0, (\sigma_o^{\text{MBS}})^2)$. Similar to the FAP, the received signal \mathbf{y}_o^{st} of MBS at the first time slot becomes

$$\tilde{\mathbf{y}}_o^{\text{st}} = \underbrace{\sum_{m=1}^M \mathbf{H}_{o,m}^{\text{MUE}} \mathbf{w}_{o,m}^{\text{MUE}} s_{o,m}^{\text{MUE}}}_{\text{desired MUE signal}} + \underbrace{\sum_{r=1}^R \sum_{k=1}^K \mathbf{H}_{o,r,k}^{\text{CUE}} \mathbf{w}_{r,k}^{\text{CUE}'} s_{r,k}^{\text{CUE}}}_{\text{CUE Interference}} + \underbrace{\sum_{f=1}^F \sum_{u=1}^U \mathbf{H}_{o,f,u}^{\text{FAP}} \mathbf{w}_{f,u}^{\text{FAP}'} s_{f,u}^{\text{FAP}}}_{\text{FUE interference}} + \mathbf{n}_o. \quad (\text{C.10})$$

The transmit power $P_{o,m}$ of the m^{th} MUE at the MBS in the first time slot must satisfy $P_{o,m} = \text{Tr}(\mathbf{w}_{o,m}^{\text{MUE}} (\mathbf{w}_{o,m}^{\text{MUE}})^H) \leq P_{o,m}^{\text{max}}$, where $P_{o,m}^{\text{max}}$ is the maximum transmit power for each MUE at the MBS. The SINR $_o^{\text{MBS}}$ is given by (C.11).

$$\text{SINR}_o^{\text{MBS}} = \frac{\|\mathbf{H}_{o,m}^{\text{MUE}} \mathbf{w}_{o,m}^{\text{MUE}}\|^2}{\sum_{f=1}^F \sum_{u=1}^U \|\mathbf{H}_{j,f,u}^{\text{FAP}} \mathbf{w}_{f,u}^{\text{FAP}'}\|^2 + \sum_{r=1}^R \sum_{k=1}^K \|\mathbf{H}_{j,r,k}^{\text{CUE}} \mathbf{w}_{r,k}^{\text{CUE}'}\|^2 + (\sigma_o^{\text{MBS}})^2 \mathbf{I}_{N_s}}. \quad (\text{C.11})$$

The achievable sum rate of the MUE communication to the MBS, denoted $\mathcal{R}_{\text{sum}}^{\text{MUE}}$ is formulated as

$$\mathcal{R}_{\text{sum}}^{\text{MUE}} = \frac{1}{2} \log_2(1 + \text{SINR}_o^{\text{MBS}}). \quad (\text{C.12})$$

The received signal \mathbf{y}_r^{st} during the first time slot at the r^{th} RN is given as

$$\begin{aligned} \tilde{\mathbf{y}}_r^{\text{st}} = & \underbrace{\sum_{k=1}^K \mathbf{H}_{r,k}^{\text{CUE}} \mathbf{w}_{r,k}^{\text{CUE}} s_{r,k}^{\text{CUE}}}_{\substack{\text{desired CUE signals} \\ \text{through the RN}}} + \underbrace{\sum_{m=1}^M \mathbf{H}_{r,m}^{\text{MUE}} \mathbf{w}_{o,m}^{\text{MUE}'} s_{o,m}^{\text{MUE}}}_{\substack{\text{macrocell interference} \\ \text{outside the cluster to the RN}}} \\ & + \underbrace{\sum_{f=1}^F \sum_{u=1}^U \mathbf{H}_{r,f,u}^{\text{FAP}} \mathbf{w}_{f,u}^{\text{FAP}'} s_{f,u}^{\text{FAP}}}_{\substack{\text{femtocells interference} \\ \text{to the RN}}} + \underbrace{\mathbf{n}_r}_{\text{noise}}, \quad \forall r = 1, \dots, R \end{aligned} \quad (\text{C.13})$$

where $\mathbf{H}_{r,k}^{\text{CUE}}$ is $\mathbb{C}^{N_R \times N_s}$ channel matrix from k^{th} CUE to r^{th} RN and $\mathbf{H}_{r,m}^{\text{MUE}}$ is the channel matrix from the m^{th} MUE to the r^{th} RN. $\mathbf{H}_{r,f,u}^{\text{FAP}}$ is the channel matrix from the u^{th} FUE of the f^{th} FAP to the r^{th} RN. \mathbf{n}_r is the AWGN vector with variance $(\sigma_r^{\text{CUE}})^2$ which is distributed according to $\mathcal{CN}(0, (\sigma_r^{\text{CUE}})^2)$. We assume a perfect CSI at all the base stations and their users. It is also assumed that the channels are independent and identically distributed (i.i.d.) complex Gaussian random variables.

The RN receives the signal from the K -CUEs and the interferences from the FUEs and MUEs. The signal is amplified with the RN pre-coder $\mathbf{F}_{o,r}$ and forwarded to the MBS during the second time slot. The amplified r^{th} transmit signal $\mathbf{x}_{o,r}$ to the MBS during the second time slot is given as

$$\mathbf{x}_{o,r} = \mathbf{F}_{o,r} \times \tilde{\mathbf{y}}_r^{\text{st}}, \quad \forall r = 1, \dots, R. \quad (\text{C.14})$$

During the second time slot, the MUEs continuously transmit signals to the MBS while the FUEs assume to be transmitting only during the first time slot. Therefore, the received signal \mathbf{y}_o^{nd} at the MBS during the second time slot is written as

$$\mathbf{y}_o^{nd} = \sum_{r=1}^R \mathbf{H}_{o,r} \mathbf{x}_{o,r} + \underbrace{\sum_{m=1}^M \mathbf{H}_{o,m}^{\text{MUE}} \mathbf{w}_{o,m}^{\text{MUE}} s_{o,m}^{\text{MUE}}}_{\text{MUEs signal at the MBS}} + \mathbf{n}_o, \quad (\text{C.15})$$

where $\mathbf{H}_{o,r}$ is $\mathbb{C}^{N_B \times N_R}$ the channel matrix from the r^{th} RN to the MBS and \mathbf{n}_o is the AWGN vector at the MBS with variance $(\sigma_o^{\text{MBS}})^2$ which is distributed according to $\mathcal{CN}(0, (\sigma_o^{\text{MBS}})^2)$. The interference and noise are also amplified and forwarded to the MBS, so (C.15) becomes

$$\begin{aligned} \mathbf{y}_o^{nd} = & \underbrace{\sum_{r=1}^R \mathbf{H}_{o,r} \mathbf{F}_{o,r} \left(\sum_{k=1}^K \mathbf{H}_{r,k}^{\text{CUE}} \mathbf{w}_{r,k}^{\text{CUE}} s_{r,k}^{\text{CUE}} \right)}_{1^{\text{st}} \text{ term}} + \underbrace{\sum_{r=1}^R \mathbf{H}_{o,r} \mathbf{F}_{o,r} \left(\sum_{m=1}^M \mathbf{H}_{r,m}^{\text{MUE}} \mathbf{w}_{o,m}^{\text{MUE}} s_{o,m}^{\text{MUE}} \right)}_{2^{\text{nd}} \text{ term}} \\ & + \underbrace{\sum_{r=1}^R \mathbf{H}_{o,r} \mathbf{F}_{o,r} \tilde{\mathbf{n}}_r}_{3^{\text{rd}} \text{ term}} + \underbrace{\sum_{m=1}^M \mathbf{H}_{o,m}^{\text{MUE}} \mathbf{w}_{o,m}^{\text{MUE}} s_{o,m}^{\text{MUE}}}_{4^{\text{th}} \text{ term}} + \underbrace{\mathbf{n}_o}_{5^{\text{th}} \text{ term}}, \end{aligned} \quad (\text{C.16})$$

where $\tilde{\mathbf{n}}_r = \left(\sum_{f=1}^F \sum_{u=1}^U \mathbf{H}_{r,f,u}^{\text{FAP}} \mathbf{w}_{f,u}^{\text{FAP}} s_{f,u}^{\text{FAP}} + \mathbf{n}_r \right)$, such that the femtocell interferences at the first time slot are considered as noise at the MBS. From (C.16), the 2^{nd} term is the MUE transmit signal during the first time slot which is amplified at the RN and forwarded to the MBS during the second time slot. This term can be cancelled at the MBS since it is known. The 3^{rd} and 5^{th} terms in (C.16), on the other hand, are considered as noise and interference. The 1^{st} and 4^{th} are the signals to be decoded at the MBS during the second time slot, and need to be combined to one term. With this understanding, (C.16) can be reformulated as

$$\mathbf{y}_o^{nd} = \sum_{r=1}^R \sum_{k=1}^K \mathbf{H}_{o,r} \mathbf{F}_{o,r} \mathbf{H}_{r,k}^{\text{CUE}} \mathbf{w}_{r,k}^{\text{CUE}} s_{r,k}^{\text{CUE}} + \sum_{m=1}^M \mathbf{H}_{o,m}^{\text{MUE}} \mathbf{w}_{o,m}^{\text{MUE}} s_{o,m}^{\text{MUE}} + \mathbf{z}_o, \quad (\text{C.17})$$

where $\mathbf{z}_o = \sum_{r=1}^R \mathbf{H}_{o,r} \mathbf{F}_{o,r} \tilde{\mathbf{n}}_r + \mathbf{n}_o$. Note that during the second time slot the CUEs and MUEs are combined into a single signal and are referred as UEs throughout this article. Moreover, the pre-coder and decoder design at the MBS during the second time slot involves determining multiple unknown parameters (variables) such as the UEs \mathbf{W} and RN pre-coder \mathbf{F}_o , the decoder \mathbf{D}_o . The following are assumed: $\hat{d} = \sum_{k=1}^K d_s$, $\hat{N}_s = \sum_{k=1}^K N_s$, $N_R \geq \hat{d}$ and $\hat{N}_s > \hat{d}$. We assume that $N_B \geq N_R$. Defining CUEs $\mathbf{H}_{R,K}^{\text{CUE}}$ and MUEs $\mathbf{H}_{o,M}^{\text{MUE}}$ channel matrices and their required antennas as follows

$$\mathbf{H}_{R,K}^{\text{CUE}} = [\mathbf{H}_{1,1}^{\text{CUE}}, \dots, \mathbf{H}_{R,K}^{\text{CUE}}], \quad (\text{C.18})$$

$$\mathbf{H}_{o,M}^{\text{MUE}} = [\mathbf{H}_{1,1}^{\text{MUE}}, \dots, \mathbf{H}_{o,M}^{\text{MUE}}] \quad (\text{C.19})$$

$$\mathbf{H}_{r,k}^{\text{CUE}} \in \mathbb{C}^{N_R \times N_s} \Rightarrow \mathbf{H}_{R,K}^{\text{CUE}} \in \mathbb{C}^{N_R \times \hat{N}_s},$$

$$\mathbf{H}_{o,m}^{\text{MUE}} \in \mathbb{C}^{N_B \times N_s} \Rightarrow \mathbf{H}_{o,M}^{\text{MUE}} \in \mathbb{C}^{N_B \times \hat{N}_s}.$$

The CUEs $\mathbf{w}_{R,K}^{\text{CUE}}$ and MUEs $\mathbf{w}_{o,M}^{\text{MUE}}$ pre-coders matrices and their required number of antennas are defined as follows

$$\mathbf{w}_{R,K}^{\text{CUE}} = \begin{pmatrix} \mathbf{w}_{1,1}^{\text{CUE}} & \cdots & 0 \\ \vdots & \ddots & \vdots \\ 0 & \cdots & \mathbf{w}_{R,K}^{\text{CUE}} \end{pmatrix}, \quad (\text{C.20})$$

$$\mathbf{w}_{o,M}^{\text{MUE}} = \begin{pmatrix} \mathbf{w}_{o,1}^{\text{MUE}} & \cdots & 0 \\ \vdots & \ddots & \vdots \\ 0 & \cdots & \mathbf{w}_{o,M}^{\text{MUE}} \end{pmatrix} \quad (\text{C.21})$$

$$\mathbf{w}_{r,k}^{\text{CUE}} \in \mathbb{C}^{N_s \times d_s} \Rightarrow \mathbf{w}_{R,K}^{\text{CUE}} \in \mathbb{C}^{\hat{N}_s \times \hat{d}},$$

$$\mathbf{w}_{o,m}^{\text{MUE}} \in \mathbb{C}^{N_s \times d_s} \Rightarrow \mathbf{w}_{o,M}^{\text{MUE}} \in \mathbb{C}^{\hat{N}_s \times \hat{d}},$$

with the above assumptions, the signals, channels matrices and pre-coders for CUEs and MUEs (during the second time slot) combined are given by (C.22, C.23, C.24), respectively,

$$\mathbf{s} = \left[\underbrace{s_{1,1}^{\text{CUE}}, \dots, s_{1,K}^{\text{CUE}} | s_{2,1}^{\text{CUE}}, \dots, s_{2,K}^{\text{CUE}} | \dots | s_{R,1}^{\text{CUE}}, \dots, s_{R,K}^{\text{CUE}}}_{\text{CUE transmit signals}} \mid \underbrace{s_{o,1}^{\text{MUE}}, \dots, s_{o,M}^{\text{MUE}}}_{\substack{\text{MUE transmit signals} \\ \text{at } 2^{nd} \text{ time slot}}} \right]^T \in \mathbb{C}^{1 \times (RK+M)\hat{d}} \quad (\text{C.22})$$

$$\mathbf{H} = \left[\underbrace{\mathbf{H}_{1,1}^{\text{CUE}}, \dots, \mathbf{H}_{1,K}^{\text{CUE}} | \mathbf{H}_{2,1}^{\text{CUE}}, \dots, \mathbf{H}_{2,K}^{\text{CUE}} | \dots | \mathbf{H}_{R,1}^{\text{CUE}}, \dots, \mathbf{H}_{R,K}^{\text{CUE}}}_{\text{CUE channels matrices}} \mid \underbrace{\mathbf{H}_{o,1}^{\text{MUE}}, \dots, \mathbf{H}_{o,M}^{\text{MUE}}}_{\text{MUE channel matrix}} \right] \in \mathbb{C}^{N_R \times \hat{N}_s (RK+M)} \quad (\text{C.23})$$

$$\mathbf{W} = \begin{pmatrix} \mathbf{w}_{1,1}^{\text{CUE}} & 0 & 0 & 0 & \dots & 0 & 0 & \dots & 0 \\ 0 & \mathbf{w}_{2,2}^{\text{CUE}} & 0 & 0 & \dots & 0 & 0 & \dots & 0 \\ 0 & 0 & \mathbf{w}_{3,3}^{\text{CUE}} & 0 & \dots & 0 & 0 & \dots & 0 \\ 0 & 0 & 0 & \mathbf{w}_{4,4}^{\text{CUE}} & \dots & 0 & 0 & \dots & 0 \\ \vdots & \vdots & \vdots & \vdots & \ddots & \vdots & \vdots & \vdots & \vdots \\ 0 & 0 & 0 & 0 & \dots & \mathbf{w}_{R,K}^{\text{CUE}} & 0 & \dots & 0 \\ 0 & 0 & 0 & 0 & \dots & 0 & \mathbf{w}_{o,1}^{\text{MUE}} & \dots & 0 \\ \vdots & \ddots & \vdots \\ 0 & 0 & 0 & 0 & \dots & 0 & 0 & \dots & \mathbf{w}_{o,M}^{\text{MUE}} \end{pmatrix} \in \mathbb{C}^{\hat{N}_s (RK+M) \times \hat{d} (RK+M)} \quad (\text{C.24})$$

$$\mathbf{H}_o = [\mathbf{H}_{o,1}, \dots, \mathbf{H}_{o,R}] \in \mathbb{C}^{N_B \times \hat{N}_R(R)} \quad (\text{C.25})$$

$$\mathbf{F}_o = [\mathbf{F}_{o,1}, \dots, \mathbf{F}_{o,R}]^T \in \mathbb{C}^{N_R \times \hat{N}_R(R)}. \quad (\text{C.26})$$

The received signal \mathbf{y}_o^{nd} of the MBS in (C.17) during the second time slot is rewritten as

$$\mathbf{y}_o^{nd} = \mathbf{H}_o \mathbf{F}_o \mathbf{H} \mathbf{W} \mathbf{s} + \mathbf{z}_o, \quad (\text{C.27})$$

where \mathbf{H}_o and \mathbf{F}_o are described in (C.25) and (C.26), respectively. $\mathbf{z}_o \in \mathbb{C}^{N_B \times 1}$ is the AWGN vector with variance $\sigma_{\mathbf{z}_o}^2$ which is distributed according to $\mathcal{CN}(0, \sigma_{\mathbf{z}_o}^2)$.

The achievable sum rate of the UEs through to the MBS, denoted $\mathcal{R}_{sum}^{\text{UEs}}$ is formulated as:

$$\mathcal{R}_{sum}^{\text{UEs}}(\mathbf{W}, \mathbf{F}_o) = \log_2(1 + \text{SINR}_o^{\text{MBS-nd}}), \quad (\text{C.28})$$

where the $\text{SINR}_o^{\text{MBS-nd}}$ is expressed as follows:

$$\text{SINR}_o^{\text{MBS-nd}} = \frac{\|\mathbf{H}_o \mathbf{F}_o \mathbf{H} \mathbf{W}\|^2}{\sigma_{\mathbf{z}_o}^2 \mathbf{I}_{N_B}}. \quad (\text{C.29})$$

2.2 The total power consumption design

Considering each FAP, the power consumption is composed of two different parts, the dynamic P_d^{FAP} and static P_s^{FAP} power consumption [26]. The total power consumption at the j^{th} FAP, denoted P_j^{FAP} , is written as:

$$P_j^{\text{FAP}} = \frac{1}{2} \left(\underbrace{\left(\sum_{i=1}^{U_i} P_{j,i} \right)}_{P_d^{\text{FAP}}} + P_s^{\text{FAP}} \right). \quad (\text{C.30})$$

P_s^{FAP} describes ordinary operations of the MBS and FAPs whereas, the P_d^{FAP} depends on the group of load variations. The factor $\frac{1}{2}$ arises due to the communication process over the entire channel being done within two consecutive time slots. The P_d^{FAP} term is known as the aggregation of the emitted powers and is given as:

$$P_d^{\text{FAP}} = \rho_i \sum_{i=1}^{U_i} \|\mathbf{w}_{j,i}^{\text{FAP}}\|^2, \quad (\text{C.31})$$

where ρ_i is the power amplifier efficiency of the i^{th} FUE of the j^{th} FAP. The total power consumption P_j^{FAP} at the j^{th} is rewritten as

$$P_j^{\text{FAP}} = \frac{1}{2} \left(\rho_i \sum_{i=1}^{U_i} \|\mathbf{w}_{j,i}^{\text{FAP}}\|^2 + P_s \right). \quad (\text{C.32})$$

Similarly, the total power consumption P_o^{MUE} of MUE at the MBS during the first time slot is expressed as follows:

$$P_o^{\text{MUE}} = \frac{1}{2} \left(\rho_m \sum_{m=1}^M \|\mathbf{w}_{o,m}^{\text{MUE}}\|^2 + P_s \right), \quad (\text{C.33})$$

where ρ_m is the power amplifier efficiency of the m^{th} MUE of the MBS. In this paper, $\rho_i, \rho_m = 1$ for brevity. The transmit power P_r^{CUE} of the RN during the second time slot is given by

$$P_r^{\text{CUE}} = \sum_{k=1}^K \text{Tr} \left(\mathbf{F}_{o,r} \left(\mathbf{H}_{r,k}^{\text{CUE}} \mathbf{w}_{r,k}^{\text{CUE}} (\mathbf{w}_{r,k}^{\text{CUE}})^H (\mathbf{H}_{r,k}^{\text{CUE}})^H + (\sigma_r^{\text{CUE}})^2 \mathbf{I}_{N_r} \right) \mathbf{F}_{o,r}^H \right). \quad (\text{C.34})$$

From C.18, C.20 and C.26, the transmit power of the RN during the second time slot can be rewritten as

$$P_r^{\text{CUE}} = \mathbf{F}_o \left(\mathbf{H}_{R,K}^{\text{CUE}} \mathbf{W}_{R,K}^{\text{CUE}} (\mathbf{W}_{R,K}^{\text{CUE}})^H (\mathbf{H}_{R,K}^{\text{CUE}})^H + (\sigma_R^{\text{CUE}})^2 \mathbf{I}_{N_R} \right) \mathbf{F}_o^H. \quad (\text{C.35})$$

The total power consumption $P_o^{\text{MBS-nd}}$ at the MBS during the second time slot is:

$$P_o^{\text{MBS-nd}} = \frac{1}{2} \left(P_r^{\text{CUE}} + \underbrace{\rho_m \sum_{m=1}^M \|\mathbf{w}_{o,m}^{\text{MUE}}\|^2}_{P_d^{\text{MUE}} \text{ during the second time slot}} + P_s \right). \quad (\text{C.36})$$

3 EE Maximisation and Transceiver Optimisation for FUEs and MUEs

EE has become an important design criterion in wireless communications due to rapidly rising energy consumption in information and communication technology. The EE maximisation is subject to the QoS and power constraints. The available power resource for transmission is constrained and needs to be limited to a threshold.

3.1 EE problem formulation for FUEs and MUEs

The total power consumption is mainly related to the transmit power at the FAPs or MUE, dynamic power P_d , static power P_s . The objective function is also subject to the QoS constraint, the achievable rate constraint. The EE problem denoted $\varphi_{\text{FAP}}^{\text{EE}} = \frac{\mathcal{R}_{\text{FAP}}^{\text{sum}}}{P_{\text{FAP}}^{\text{sum}}}$ at the FAP is then formulated as follows:

$$\begin{aligned} & \max_{\mathbf{w}_{j,i}^{\text{FAP}}} \frac{\log_2 \left(1 + \frac{\|\mathbf{H}_{j,i}^{\text{FAP}} \mathbf{w}_{j,i}^{\text{FAP}}\|^2}{(\tilde{\sigma}_j^{\text{FAP}})^2 \mathbf{I}_{N_s}} \right)}{\left(\rho_i \sum_{i=1}^{U_i} \|\mathbf{w}_{j,i}^{\text{FAP}}\|^2 + P_s \right)}, \\ & \text{s. t. } \frac{1}{2} \log_2 \left(1 + \frac{\|\mathbf{H}_{j,i}^{\text{FAP}} \mathbf{w}_{j,i}^{\text{FAP}}\|^2}{(\tilde{\sigma}_j^{\text{FAP}})^2 \mathbf{I}_{N_s}} \right) \geq \gamma_i^{\min} \\ & \sum_{i=1}^{U_i} \text{Tr} \left(\mathbf{w}_{j,i}^{\text{FAP}} (\mathbf{w}_{j,i}^{\text{FAP}})^H \right) \leq P_{i,\max}^j, \quad \forall i \in U_i. \end{aligned} \quad (\text{C.37})$$

$$\text{Let } \tilde{\mathbf{n}}_j = \sum_{m=1}^M \left\| \mathbf{H}_{j,m}^{\text{MUE}} \mathbf{w}_{o,m}^{\text{MUE}'} \right\|^2 + \sum_{\substack{f=1 \\ f \neq j}}^F \sum_{u=1}^U \left\| \mathbf{H}_{j,f,u}^{\text{FAP}} \mathbf{w}_{f,u}^{\text{FAP}'} \right\|^2 + \sum_{r=1}^R \sum_{k=1}^K \left\| \mathbf{H}_{j,r,k}^{\text{CUE}} \mathbf{w}_{r,k}^{\text{CUE}'} \right\|^2 + (\sigma_j^{\text{FAP}})^2 \mathbf{I}_{N_s},$$

the denominator in (C.7) with variance $(\tilde{\sigma}_j^{\text{FAP}})^2$ of equation (C.37), distributed according to $\mathcal{CN}(0, (\tilde{\sigma}_j^{\text{FAP}})^2)$ and γ_i^{\min} is a fixed QoS threshold. In order to maximise the EE of the FAP, the received signal is multiplied by a decoder $\mathbf{d}_{j,i}^{\text{FAP}}$ to recover the transmit data. Thus, the EE optimisation problem $\varphi_{\text{FAP}}^{\text{EE}}$ is solved by optimising the $\mathbf{w}_{j,i}^{\text{FAP}}$ and the decoder $\mathbf{d}_{j,i}^{\text{FAP}}$ iteratively. The estimated signal $\hat{s}_{j,i}^{\text{FAP}}$ is expressed as:

$$\begin{aligned} \hat{s}_{j,i}^{\text{FAP}} &= \sum_{i=1}^{U_i} (\mathbf{d}_{j,i}^{\text{FAP}})^H \mathbf{H}_{j,i}^{\text{FAP}} \mathbf{w}_{j,i}^{\text{FAP}} s_{j,i}^{\text{FAP}} + \sum_{m=1}^M (\mathbf{d}_{j,i}^{\text{FAP}})^H \mathbf{H}_{j,m}^{\text{MUE}} \mathbf{w}_{o,m}^{\text{MUE}'} s_{o,m}^{\text{MUE}} \\ &+ \sum_{\substack{f=1 \\ f \neq j}}^F \sum_{u=1}^U (\mathbf{d}_{j,i}^{\text{FAP}})^H \mathbf{H}_{j,f,u}^{\text{FAP}} \mathbf{w}_{f,u}^{\text{FAP}'} s_{f,u}^{\text{FAP}} + \sum_{r=1}^R \sum_{k=1}^K (\mathbf{d}_{j,i}^{\text{FAP}})^H \mathbf{H}_{j,r,k}^{\text{CUE}} \mathbf{w}_{r,k}^{\text{CUE}'} s_{r,k}^{\text{CUE}} + (\mathbf{d}_{j,i}^{\text{FAP}})^H \mathbf{n}_j, \end{aligned} \quad (\text{C.38})$$

Similarly, the EE problem $\varphi_{\text{MUE}}^{\text{EE}} = \frac{\mathcal{R}_{\text{sum}}^{\text{MUE}}}{P_t^{\text{MUE}}}$ for the MUEs at the MBS during the first time slot is expressed as follows:

$$\begin{aligned} & \max_{\mathbf{w}_{o,m}^{\text{MUE}}} \frac{\log_2 \left(1 + \frac{\|\mathbf{H}_{o,m}^{\text{MUE}} \mathbf{w}_{o,m}^{\text{MUE}}\|^2}{(\tilde{\sigma}_o^{\text{MBS}})^2 \mathbf{I}_{N_s}} \right)}{\left(\rho_m \sum_{m=1}^M \|\mathbf{w}_{o,m}^{\text{FAP}}\|^2 + P_s \right)}, \\ & \text{s. t. } \frac{1}{2} \log_2 \left(1 + \frac{\|\mathbf{H}_{o,m}^{\text{MUE}} \mathbf{w}_{o,m}^{\text{MUE}}\|^2}{(\tilde{\sigma}_o^{\text{MBS}})^2 \mathbf{I}_{N_s}} \right) \geq \gamma_m^{\min} \\ & \sum_{m=1}^M \text{Tr}(\mathbf{w}_{o,m}^{\text{MUE}}, (\mathbf{w}_{o,m}^{\text{MUE}})^H) \leq P_{m,\max}^o. \end{aligned} \quad (\text{C.39})$$

Let $\tilde{\mathbf{n}}_o = \sum_{f=1}^F \sum_{u=1}^U \|\mathbf{H}_{j,f,u}^{\text{FAP}} \mathbf{w}_{f,u}^{\text{FAP}}\|^2 + \sum_{r=1}^R \sum_{k=1}^K \|\mathbf{H}_{j,r,k}^{\text{CUE}} \mathbf{w}_{r,k}^{\text{CUE}}\|^2 + (\sigma_o^{\text{MBS}})^2 \mathbf{I}_{N_s}$, the denominator in (C.11) with variance $(\tilde{\sigma}_o^{\text{MBS}})^2$ of equation (C.39), distributed according to $\mathcal{CN}(0, (\tilde{\sigma}_o^{\text{MBS}})^2)$ and γ_m^{\min} is a fixed QoS threshold. The received signal is also multiplied by a decoder $\mathbf{d}_{o,m}^{\text{MUE}}$ to recover the transmit MUEs data. Thus, the EE problem $\varphi_{\text{MUE}}^{\text{EE}}$ is solved by optimising the $\mathbf{w}_{o,m}^{\text{MUE}}$ and the decoder $\mathbf{d}_{o,m}^{\text{MUE}}$ iteratively. The estimated signal $\hat{s}_{o,m}^{\text{MUE}}$ is formulated as

$$\begin{aligned} \hat{s}_{o,m}^{\text{MUE}} &= \underbrace{\sum_{m=1}^M (\mathbf{d}_{o,m}^{\text{MUE}})^H \mathbf{H}_{o,m}^{\text{MUE}} \mathbf{w}_{o,m}^{\text{MUE}} s_{o,m}^{\text{MUE}}}_{\text{desired MUE signal}} + \underbrace{\sum_{r=1}^R \sum_{k=1}^K (\mathbf{d}_{o,m}^{\text{MUE}})^H \mathbf{H}_{o,r,k}^{\text{CUE}} \mathbf{w}_{r,k}^{\text{CUE}} s_{r,k}^{\text{CUE}}}_{\text{CUE Interference}} \\ &+ \underbrace{\sum_{f=1}^F \sum_{u=1}^U (\mathbf{d}_{o,m}^{\text{MUE}})^H \mathbf{H}_{o,f,u}^{\text{FAP}} \mathbf{w}_{f,u}^{\text{FAP}} s_{f,u}^{\text{FAP}}}_{\text{FUE interference}} + (\mathbf{d}_{o,m}^{\text{MUE}})^H \mathbf{n}_o. \end{aligned} \quad (\text{C.40})$$

As observed, the two fractional EE objective function problems in (C.37) and (C.39) are non-convex problem where the achievable sum-rate terms $\mathcal{R}_{\text{sum}}^{\text{FAP}}$ and $\mathcal{R}_{\text{sum}}^{\text{MUE}}$ are non-concave. As a result, the QoS rate constraints are non-convex as well. Due to the non-linear fractional objective function and some optimisation variable in the QoS constraint, these EE objective function problems and the optimum solutions are hard to solve and derive directly. Therefore, we address this by optimising each transceiver component iteratively such as finding the optimal pre-coders for the FUEs and MUEs during the first time slot and their respective decoding matrices.

3.2 Optimisation of the pre-coders $\mathbf{w}_{j,i}^{\text{FAP}}$, $\mathbf{w}_{o,m}^{\text{MUE}}$ and decoders $\mathbf{d}_{j,i}^{\text{FAP}}$, $\mathbf{d}_{o,m}^{\text{MUE}}$

The WMMSE approach is employed to optimise the pre-coders $\mathbf{w}_{j,i}^{\text{FAP}}$, $\mathbf{w}_{o,m}^{\text{MUE}}$ and decoders $\mathbf{d}_{j,i}^{\text{FAP}}$, $\mathbf{d}_{o,m}^{\text{MUE}}$. This method depends on the relation between the SINR and the weighted MSE, to weaken the non-linearity of the expression of the achievable rate. The sum rate is transformed into a WMMSE

problem by introducing some auxiliary variables. It is known that the WMMSE is considered to be a distributed linear pre-coder/decoder design method and converges to at least a local optimal solution of the optimisation problem with low computational complexity [27]. By considering the estimated signal of FAP $\hat{s}_{j,i}^{\text{FAP}}$, let the MSE \mathbf{E}_i of the signal waveform estimation be given as

$$\begin{aligned}
 \mathbf{E}_i &= \mathbb{E} \left[(\hat{s}_{j,i}^{\text{FAP}} - s_{j,i}^{\text{FAP}})(\hat{s}_{j,i}^{\text{FAP}} - s_{j,i}^{\text{FAP}})^H \right] \\
 &= \left[\left(\sum_{i=1}^{U_i} (\mathbf{d}_{j,i}^{\text{FAP}})^H \mathbf{H}_{j,i}^{\text{FAP}} \mathbf{w}_{j,i}^{\text{FAP}} - \mathbf{I}_{N_s} \right) \left(\sum_{i=1}^{U_i} (\mathbf{d}_{j,i}^{\text{FAP}})^H \mathbf{H}_{j,i}^{\text{FAP}} \mathbf{w}_{j,i}^{\text{FAP}} - \mathbf{I}_{N_s} \right)^H \right. \\
 &\quad + \sum_{m=1}^M (\mathbf{d}_{j,i}^{\text{FAP}})^H \mathbf{H}_{j,m}^{\text{MUE}} \mathbf{w}_{o,m}^{\text{MUE}'} \mathbf{d}_{j,i}^{\text{FAP}} (\mathbf{H}_{j,m}^{\text{MUE}})^H (\mathbf{w}_{o,m}^{\text{MUE}'})^H \\
 &\quad + \sum_{\substack{f=1 \\ f \neq j}}^F \sum_{u=1}^U (\mathbf{d}_{j,i}^{\text{FAP}})^H \mathbf{H}_{j,f,u}^{\text{FAP}} \mathbf{w}_{f,u}^{\text{FAP}'} \mathbf{d}_{j,i}^{\text{FAP}} (\mathbf{H}_{j,f,u}^{\text{FAP}})^H (\mathbf{w}_{f,u}^{\text{FAP}'})^H \\
 &\quad \left. + \sum_{r=1}^R \sum_{k=1}^K (\mathbf{d}_{j,i}^{\text{FAP}})^H \mathbf{H}_{j,r,k}^{\text{CUE}} \mathbf{w}_{r,k}^{\text{CUE}'} \mathbf{d}_{j,i}^{\text{FAP}} (\mathbf{H}_{j,r,k}^{\text{CUE}})^H (\mathbf{w}_{r,k}^{\text{CUE}'})^H + (\mathbf{d}_{j,i}^{\text{FAP}})^H (\sigma_j^{\text{FAP}})^2 \mathbf{d}_{j,i}^{\text{FAP}} \right]. \quad (\text{C.41})
 \end{aligned}$$

According to [27] [28], the achievable sum rate $\mathcal{R}_{sum}^{\text{FAP}}$ in (C.37) can be rewritten as a weighted sum-MSE problem as

$$\max_{\mathbf{v}_i^{\text{FAP}}, \mathbf{d}_{j,i}^{\text{FAP}}} \sum_{i=1}^{U_i} \log_2 (\mathbf{v}_i^{\text{FAP}}) - \text{Tr}(\mathbf{v}_i^{\text{FAP}} \mathbf{E}_i) + \text{Tr}(\mathbf{I}_{N_s}), \quad (\text{C.42})$$

where $\mathbf{v}_i^{\text{FAP}}$ is a weighting matrix.

The EE $\varphi_{\text{FAP}}^{\text{EE}}$ optimisation problem can be reformulated by substituting the weighted sum-MSE problem from (C.42) into (C.37). The EE optimisation problem $\varphi_{\text{FAP}}^{\text{EE}}$ is now expressed as

$$\begin{aligned}
 &\max_{\mathbf{w}_{j,i}^{\text{FAP}}, \mathbf{v}_i^{\text{FAP}}, \mathbf{d}_{j,i}^{\text{FAP}}} \left(\frac{\sum_{i=1}^{U_i} \log_2 (\mathbf{v}_i^{\text{FAP}}) - \text{Tr}(\mathbf{v}_i^{\text{FAP}} \mathbf{E}_i) + \text{Tr}(\mathbf{I}_{N_s})}{\left(\rho_i \sum_{i=1}^{U_i} \|\mathbf{w}_{j,i}^{\text{FAP}}\|^2 + P_s \right)} \right), \\
 &\text{s.t.} \quad \sum_{i=1}^{U_i} \log_2 (\mathbf{v}_i^{\text{FAP}}) - \text{Tr}(\mathbf{v}_i^{\text{FAP}} \mathbf{E}_i) + \text{Tr}(\mathbf{I}_{N_s}) \geq R_i^{\min}, \\
 &\quad \sum_{i=1}^{U_i} \text{Tr}(\mathbf{w}_{j,i}^{\text{FAP}} (\mathbf{w}_{j,i}^{\text{FAP}})^H) \leq P_{i,\max}^j. \quad (\text{C.43})
 \end{aligned}$$

As noticed in (C.43), the problem is still a non-convex in terms of joint $\mathbf{w}_{j,i}^{\text{FAP}}$, $\mathbf{v}_i^{\text{FAP}}$ and $\mathbf{d}_{j,i}^{\text{FAP}}$. This is due to the non-linear fractional EE objective function. An iterative optimisation algorithm to find $\mathbf{w}_{j,i}^{\text{FAP}}$, $\mathbf{v}_i^{\text{FAP}}$ and $\mathbf{d}_{j,i}^{\text{FAP}}$ is necessary to tackle this non-convexity. By fixing the $\mathbf{w}_{j,i}^{\text{FAP}}$ and $\mathbf{v}_i^{\text{FAP}}$, then

minimising the MSE, we can obtain the optimal linear decoder $\mathbf{d}_{j,i}^{\text{FAP}^*}$ as [27] [28]

$$\begin{aligned} \mathbf{d}_{j,i}^{\text{FAP}^*} = & \mathbf{H}_{j,i}^{\text{FAP}} \mathbf{w}_{j,i}^{\text{FAP}} \left(\sum_{\substack{f=1 \\ f \neq j}}^F \sum_{u=1}^U (\mathbf{H}_{j,f,u}^{\text{FAP}} \mathbf{w}_{f,u}^{\text{FAP}'}) (\mathbf{H}_{j,f,u}^{\text{FAP}} \mathbf{w}_{f,u}^{\text{FAP}'})^H + \sum_{r=1}^R \sum_{k=1}^K (\mathbf{H}_{j,r,k}^{\text{CUE}} \mathbf{w}_{r,k}^{\text{CUE}'}) (\mathbf{H}_{j,r,k}^{\text{CUE}} \mathbf{w}_{r,k}^{\text{CUE}'})^H \right. \\ & \left. + \sum_{m=1}^M (\mathbf{H}_{j,m}^{\text{MUE}} \mathbf{w}_{o,m}^{\text{CUE}'}) (\mathbf{H}_{j,m}^{\text{CUE}} \mathbf{w}_{o,m}^{\text{CUE}'})^H + (\sigma_j^{\text{FAP}})^2 \mathbf{I}_{N_s} \right)^{-1}. \end{aligned} \quad (\text{C.44})$$

Using the optimal linear decoder, the corresponding MSE \mathbf{E}_i matrix becomes

$$\mathbf{E}_i^* = \mathbf{I}_{N_s} - \mathbf{H}_{j,i}^{\text{FAP}} \mathbf{w}_{j,i}^{\text{FAP}} \mathbf{d}_{j,i}^{\text{FAP}^*} (\mathbf{H}_{j,i}^{\text{FAP}})^H (\mathbf{w}_{j,i}^{\text{FAP}})^H. \quad (\text{C.45})$$

The weighting vector $\mathbf{v}_i^{\text{FAP}}$ is found from the achievable sum-rate $\mathcal{R}_{sum}^{\text{FAP}}$ of the objective function in the EE optimisation problem. This can easily be handle by optimising each variable while holding the others fixed. Then, the update of the optimal weighting matrix $\mathbf{v}_i^{\text{FAP}^*}$ is in closed-form and is given by

$$\mathbf{v}_i^{\text{FAP}^*} = (\mathbf{E}_i^*)^{-1}. \quad (\text{C.46})$$

Once the decoder $\mathbf{d}_{j,i}^{\text{FAP}}$ and the MMSE weight matrix $\mathbf{v}_i^{\text{FAP}}$ have been fixed, we consider the sum MSE optimisation problem with respect to the pre-coder $\mathbf{w}_{j,i}^{\text{FAP}}$ according to (C.42) and (C.43).

Theorem 1: A fractional function $f(\mathbf{X}) = \frac{M(\mathbf{X})}{N(\mathbf{X})}$ is a quasi-concave function if $M(\mathbf{X})$ is a concave function and $N(\mathbf{X})$ is a linear function with respect to the matrix variable \mathbf{X} , respectively. Moreover, by defining the parametric subtractive function

$$F(q) = \max\{M(\mathbf{X}) - qN(\mathbf{X})\}$$

where q is an arbitrary scalar, we confirm that $F(q)$ is a convex and monotonically decreasing function. For determined q , we can calculate $F(q)$ via the standard convex optimisation method. In fact, the problem of maximising the quasi-concave fractional function $f(\mathbf{X})$ is equivalent to finding the zero point of the $F(q)$ with positive q [29].

Considering **Theorem 1**, the $\varphi_{\text{FAP}}^{\text{EE}}$ optimisation problem in (C.43) is transformed into a linear programming problem by introducing a parameter η that cause the zero output of the corresponding subtractive function. It is also the optimal solution to the objective optimisation problem in (C.43).

This parametric subtractive function is as given by (C.47)

$$\begin{aligned}
 g_j(\eta, \mathbf{v}_i^{\text{FAP}}, \mathbf{d}_{j,i}^{\text{FAP}}) &= \max_{\mathbf{w}_{j,i}^{\text{FAP}}} \sum_{i=1}^{U_i} \log_2(\mathbf{v}_i^{\text{FAP}}) - \text{Tr}(\mathbf{v}_i^{\text{FAP}} \mathbf{E}_i) + \text{Tr}(\mathbf{I}_{N_s}) - \eta \left(\rho_i \sum_{i=1}^{U_i} \text{Tr} \left(\mathbf{w}_{j,i}^{\text{FAP}} (\mathbf{w}_{j,i}^{\text{FAP}})^H \right) + P_s \right) \\
 \text{s.t. } & \sum_{i=1}^{U_i} \log_2(\mathbf{v}_i^{\text{FAP}}) - \text{Tr}(\mathbf{v}_i^{\text{FAP}} \mathbf{E}_i) + \text{Tr}(\mathbf{I}_{N_s}) \geq R_i^{\text{min}} \\
 & \sum_{i=1}^{U_i} \text{Tr}(\mathbf{w}_{j,i}^{\text{FAP}}, (\mathbf{w}_{j,i}^{\text{FAP}})^H) \leq P_{i,\text{max}}^j
 \end{aligned} \tag{C.47}$$

where η is updated using the Dinkelbach's algorithm [30] [31]. Thus, we derive the Lagrange multipliers method $\mu_1, \mu_2 \geq 0$ into the QoS and power constraints of (C.47) resulting in the Lagrangian function expressed in (C.48)

$$\begin{aligned}
 \mathcal{L}(\mathbf{w}_{j,i}^{\text{FAP}}, \eta, \mu_1, \mu_2) &= \log_2(\mathbf{v}_i^{\text{FAP}}) - \text{Tr}(\mathbf{v}_i^{\text{FAP}} \mathbf{E}_i) + \text{Tr}(\mathbf{I}_{N_s}) - \eta \left(\rho_i \sum_{i=1}^{U_i} \text{Tr} \left(\mathbf{w}_{j,i}^{\text{FAP}} (\mathbf{w}_{j,i}^{\text{FAP}})^H \right) + P_s \right) \\
 & - \mu_1 \left(\sum_{i=1}^{U_i} \log_2(\mathbf{v}_i^{\text{FAP}}) - \text{Tr}(\mathbf{v}_i^{\text{FAP}} \mathbf{E}_i) + \text{Tr}(\mathbf{I}_{N_s}) - R_i^{\text{min}} \right) \\
 & - \mu_2 \left(\sum_{i=1}^{U_i} \text{Tr}(\mathbf{w}_{j,i}^{\text{FAP}}, (\mathbf{w}_{j,i}^{\text{FAP}})^H) - P_{i,\text{max}}^j \right).
 \end{aligned} \tag{C.48}$$

From (C.48), the Lagrange dual function is defined as [18]

$$g(\mu_1, \mu_2) = \max_{\mathbf{w}_{j,i}^{\text{FAP}}} \mathcal{L}(\mathbf{w}_{j,i}^{\text{FAP}}, \eta, \mu_1, \mu_2) \tag{C.49}$$

Moreover, the dual problem is described as

$$\min_{\mu_1, \mu_2 \geq 0} g(\mu_1, \mu_2). \tag{C.50}$$

For any μ_1 and μ_2 , we can obtain the dual function by solving the maximisation problem in (C.49).

The maximisation problem can be solved by setting the gradient of the Lagrange dual function to zero,

$\frac{\partial \mathcal{L}(\mathbf{w}_{j,i}^{\text{FAP}}, \eta, \mu_1, \mu_2)}{\partial \mathbf{w}_{j,i}^{\text{FAP}}} = 0$. With $\mu_1, \mu_2 \geq 0$, as the Lagrange multipliers corresponding to the QoS and power constraints respectively. After mathematical manipulation, the optimal FAP pre-coder $\mathbf{w}_{j,i}^{\text{FAP}*}$ is

obtained as

$$\begin{aligned}
 \mathbf{w}_{j,i}^{\text{FAP}*} &= \left((1 + \mu_1) \sum_{i=1}^{U_i} \mathbf{H}_{j,i}^{\text{FAP}} \mathbf{d}_{j,i}^{\text{FAP}'} \mathbf{v}_i^{\text{FAP}} (\mathbf{H}_{j,i}^{\text{FAP}})^H (\mathbf{d}_{j,i}^{\text{FAP}'})^H + (\eta + \mu_2) \mathbf{I}_{N_s} \right)^{-1} \\
 & \times (\mathbf{H}_{j,i}^{\text{FAP}})^H \mathbf{v}_i^{\text{FAP}} \mathbf{d}_{j,i}^{\text{FAP}}.
 \end{aligned} \tag{C.51}$$

The Lagrange multipliers μ_1 and μ_2 are updated as follows [9], [18]

$$\mu_1^{(n+1)} = \left[\mu_1^{(n)} - \sum_{i=1}^{U_i} \log_2(\mathbf{v}_i^{\text{FAP}}) - \text{Tr}(\mathbf{v}_i^{\text{FAP}} \mathbf{E}_i) + \text{Tr}(\mathbf{I}_{N_s}) - R_i^{\text{min}} \right]^+, \tag{C.52}$$

$$\mu_2^{(n+1)} = \left[\mu_2^{(n)} - \left(\sum_{i=1}^{U_i} \text{Tr} \left((\mathbf{w}_{j,i}^{\text{FAP}})^{(n+1)}, ((\mathbf{w}_{j,i}^{\text{FAP}})^{(n+1)})^H \right) - P_{i,\text{max}}^j \right) \right]^+. \tag{C.53}$$

They are updated until $\mathcal{L}(\eta, \mu_1, \mu_2, \mathbf{w}_{j,i}^{\text{FAP}}) \approx g_j(\eta, \mathbf{v}_i^{\text{FAP}}, \mathbf{d}_{j,i}^{\text{FAP}}) \approx 0$.

Similarly, by considering the estimated signal $\hat{s}_{o,m}^{\text{MUE}}$, let the MSE \mathbf{E}_m of the signal waveform estimation be expressed as

$$\begin{aligned} \mathbf{E}_m &= \mathbb{E} \left[(\hat{s}_{o,m}^{\text{MUE}} - s_{o,m}^{\text{MUE}})(\hat{s}_{o,m}^{\text{MUE}} - s_{o,m}^{\text{MUE}})^H \right] \\ &= \left[\left(\sum_{m=1}^M (\mathbf{d}_{o,m}^{\text{MUE}})^H \mathbf{H}_{o,m}^{\text{MUE}} \mathbf{w}_{o,m}^{\text{MUE}} - \mathbf{I}_{N_s} \right) \left(\sum_{m=1}^M (\mathbf{d}_{o,m}^{\text{MUE}})^H \mathbf{H}_{o,m}^{\text{MUE}} \mathbf{w}_{o,m}^{\text{MUE}} - \mathbf{I}_{N_s} \right)^H \right. \\ &\quad + \sum_{f=1}^F \sum_{u=1}^U (\mathbf{d}_{o,m}^{\text{MUE}})^H \mathbf{H}_{o,f,u}^{\text{FAP}} \mathbf{w}_{f,u}^{\text{FAP}'} \mathbf{d}_{o,m}^{\text{MUE}} (\mathbf{H}_{o,f,u}^{\text{FAP}})^H (\mathbf{w}_{f,u}^{\text{FAP}'})^H \\ &\quad \left. + \sum_{r=1}^R \sum_{k=1}^K (\mathbf{d}_{o,m}^{\text{MUE}})^H \mathbf{H}_{o,r,k}^{\text{CUE}} \mathbf{w}_{r,k}^{\text{CUE}'} \mathbf{d}_{o,m}^{\text{MUE}} (\mathbf{H}_{o,r,k}^{\text{CUE}})^H (\mathbf{w}_{r,k}^{\text{CUE}'})^H + (\mathbf{d}_{o,m}^{\text{MUE}})^H (\sigma_o^{\text{MBS}})^2 \mathbf{d}_{o,m}^{\text{MUE}} \right]. \quad (\text{C.54}) \end{aligned}$$

The weighted sum-MSE problem for the MUE is formulated using (C.54) and the $\mathcal{R}_{sum}^{\text{MUE}}$ in (C.39) as [27], [28]

$$\max_{\mathbf{v}_m^{\text{MUE}}, \mathbf{d}_{o,m}^{\text{MUE}}} \sum_{m=1}^M \log_2(\mathbf{v}_m^{\text{MUE}}) - \text{Tr}(\mathbf{v}_m^{\text{MUE}} \mathbf{E}_m) + \text{Tr}(\mathbf{I}_{N_s}), \quad (\text{C.55})$$

where $\mathbf{v}_m^{\text{MUE}}$ is a MUE weighting vector.

Thus, the EE $\varphi_{\text{MUE}}^{\text{EE}}$ optimisation problem is reformulated by substituting the weighted sum-MSE problem in (C.55) into (C.39). The EE optimisation problem $\varphi_{\text{MUE}}^{\text{EE}}$ is rewritten as

$$\begin{aligned} &\max_{\mathbf{w}_{o,m}^{\text{MUE}}, \mathbf{v}_m^{\text{MUE}}, \mathbf{d}_{o,m}^{\text{MUE}}} \left(\frac{\sum_{m=1}^M \log_2(\mathbf{v}_m^{\text{MUE}}) - \text{Tr}(\mathbf{v}_m^{\text{MUE}} \mathbf{E}_m) + \text{Tr}(\mathbf{I}_{N_s})}{\left(\rho_m \sum_{m=1}^M \|\mathbf{w}_{o,m}^{\text{FAP}}\|^2 + P_s \right)} \right), \\ &\text{s.t.} \quad \sum_{m=1}^M \log_2(\mathbf{v}_m^{\text{MUE}}) - \text{Tr}(\mathbf{v}_m^{\text{MUE}} \mathbf{E}_m) + \text{Tr}(\mathbf{I}_{N_s}) \geq R_m^{\min} \\ &\quad \sum_{m=1}^M \text{Tr}(\mathbf{w}_{o,m}^{\text{MUE}}, (\mathbf{w}_{o,m}^{\text{MUE}})^H) \leq P_{m,max}^o. \quad (\text{C.56}) \end{aligned}$$

The problem in (C.56) is non-convex due to the non-linear fractional EE objective function. To find the $\mathbf{w}_{o,m}^{\text{MUE}}$, $\mathbf{v}_m^{\text{MUE}}$ and $\mathbf{d}_{o,m}^{\text{MUE}}$, an iterative algorithm is necessary to tackle the non-convexity of this problem.

After fixing $\mathbf{w}_{o,m}^{\text{MUE}}$ and $\mathbf{v}_m^{\text{MUE}}$, the optimal linear decoder $\mathbf{d}_{o,m}^{\text{MUE}*}$ is found as [27]

$$\begin{aligned} \mathbf{d}_{o,m}^{\text{MUE}*} &= \mathbf{H}_{o,m}^{\text{MUE}} \mathbf{w}_{o,m}^{\text{MUE}} \left(\sum_{f=1}^F \sum_{u=1}^U (\mathbf{H}_{o,f,u}^{\text{FAP}} \mathbf{w}_{f,u}^{\text{FAP}'}) (\mathbf{H}_{o,f,u}^{\text{FAP}} \mathbf{w}_{f,u}^{\text{FAP}'})^H \right. \\ &\quad \left. + \sum_{r=1}^R \sum_{k=1}^K (\mathbf{H}_{o,r,k}^{\text{CUE}} \mathbf{w}_{r,k}^{\text{CUE}'}) (\mathbf{H}_{o,r,k}^{\text{CUE}} \mathbf{w}_{r,k}^{\text{CUE}'})^H + (\sigma_o^{\text{MBS}})^2 \mathbf{I}_{N_s} \right)^{-1}. \quad (\text{C.57}) \end{aligned}$$

Using the optimal linear decoder $\mathbf{d}_{o,m}^{\text{MUE}^*}$, the corresponding MSE \mathbf{E}_m matrix becomes

$$\mathbf{E}_m^* = \mathbf{I}_{N_s} - \mathbf{H}_{o,m}^{\text{MUE}} \mathbf{w}_{o,m}^{\text{MUE}} \mathbf{d}_{o,m}^{\text{MUE}^*} (\mathbf{H}_{o,m}^{\text{MUE}})^H (\mathbf{w}_{o,m}^{\text{MUE}})^H. \quad (\text{C.58})$$

Then, the MUE weighting matrix $\mathbf{v}_m^{\text{MUE}}$ is designed using the achievable sum-rate $\mathcal{R}_{sum}^{\text{MUE}}$ from the objective function of the EE optimisation problem. This can easily be handle by optimising each variable while holding the others fixed. The update of the optimal weighting matrix $\mathbf{v}_m^{\text{MUE}^*}$ is in a closed-form given by

$$\mathbf{v}_m^{\text{MUE}^*} = (\mathbf{E}_m^*)^{-1}. \quad (\text{C.59})$$

With the fixed decoder $\mathbf{d}_{o,m}^{\text{MUE}}$ and the MUE weighting matrix $\mathbf{v}_m^{\text{MUE}}$, we consider the sum MSE optimisation problem with respect to MUE pre-coder $\mathbf{w}_{o,m}^{\text{MUE}}$ according to (C.55) and (C.56) which can be formulated as a linear programming problem.

Similarly to the problem transformation of $\varphi_{\text{FAP}}^{\text{EE}}$, the EE objective optimisation problem $\varphi_{\text{MUE}}^{\text{EE}}$ in (C.56) is transformed into a linear programming problem by introducing the parameter τ that causes the zero output of the corresponding subtractive function. This parameter is also the optimal solution to the objective optimisation problem in (C.56). This parametric subtractive function is formulated as given in (C.60)

$$\begin{aligned} g_o(\tau, \mathbf{v}_m^{\text{MUE}}, \mathbf{d}_{o,m}^{\text{MUE}}) &= \max_{\mathbf{w}_{o,m}^{\text{MUE}}} \sum_{m=1}^M \log_2 (\mathbf{v}_m^{\text{MUE}}) - \text{Tr}(\mathbf{v}_m^{\text{MUE}} \mathbf{E}_m) + \text{Tr}(\mathbf{I}_{N_s}) \\ &\quad - \tau \left(\rho_m \sum_{m=1}^M \text{Tr} \left(\mathbf{w}_{o,m}^{\text{MUE}} (\mathbf{w}_{o,m}^{\text{MUE}})^H \right) + P_s \right) \\ \text{s.t.} \quad &\sum_{m=1}^M \log_2 (\mathbf{v}_m^{\text{MUE}}) - \text{Tr}(\mathbf{v}_m^{\text{MUE}} \mathbf{E}_m) + \text{Tr}(\mathbf{I}_{N_s}) \geq R_m^{\min} \\ &\sum_{m=1}^M \text{Tr}(\mathbf{w}_{o,m}^{\text{MUE}} (\mathbf{w}_{o,m}^{\text{MUE}})^H) \leq P_{m,max}^o. \end{aligned} \quad (\text{C.60})$$

The optimal pre-coder $\mathbf{w}_{o,m}^{\text{MUE}}$ is obtained by fixing the parameter τ using the Dinkelbach's algorithm, the problem in (C.60) becomes a standard convex optimisation problem. Thus, we derive the Lagrange multiplier method $\lambda_1, \lambda_2 \geq 0$ into the QoS and power constraints of (C.60) resulting in the Lagrange

function expressed as in (C.61).

$$\begin{aligned}
 \mathcal{L}(\tau, \lambda_1, \lambda_2, \mathbf{w}_{o,m}^{\text{MUE}}) &= \sum_{m=1}^M \log_2(\mathbf{v}_m^{\text{MUE}}) - \text{Tr}(\mathbf{v}_m^{\text{MUE}} \mathbf{E}_m) + \text{Tr}(\mathbf{I}_{N_s}) \\
 &\quad - \tau \left(\rho_m \sum_{m=1}^M \text{Tr}(\mathbf{w}_{o,m}^{\text{MUE}} (\mathbf{w}_{o,m}^{\text{MUE}})^H) + P_s \right) \\
 &\quad - \lambda_1 \left(\sum_{m=1}^M \log_2(\mathbf{v}_m^{\text{MUE}}) - \text{Tr}(\mathbf{v}_m^{\text{MUE}} \mathbf{E}_m) + \text{Tr}(\mathbf{I}_{N_s}) - R_m^{\text{min}} \right) \\
 &\quad - \lambda_2 \left(\sum_{m=1}^M \text{Tr}(\mathbf{w}_{o,m}^{\text{MUE}}, (\mathbf{w}_{o,m}^{\text{MUE}})^H) - P_{m,\text{max}}^o \right)
 \end{aligned} \tag{C.61}$$

From (C.61), the Lagrange dual function is defined as follows [18]:

$$g(\lambda_1, \lambda_2) = \max_{\mathbf{w}_{o,m}^{\text{MUE}}} \mathcal{L}(\mathbf{w}_{o,m}^{\text{MUE}}, \tau, \lambda_1, \lambda_2). \tag{C.62}$$

Moreover, the dual problem is described as

$$\min_{\lambda_1, \lambda_2 \geq 0} g(\lambda_1, \lambda_2). \tag{C.63}$$

For any λ_1 and λ_2 , we can obtain the dual function by solving the maximisation problem in (C.62).

The maximisation problem can be solved by setting the gradient of the Lagrange dual function to zero as $\frac{\partial \mathcal{L}(\mathbf{w}_{o,m}^{\text{MUE}}, \tau, \lambda_1, \lambda_2)}{\partial \mathbf{w}_{o,m}^{\text{MUE}*}} = 0$. With $\lambda_1, \lambda_2 \geq 0$, as the Lagrange multiplier corresponding to the power constraint, the first order optimality condition of the Lagrange function with respect to each $\mathbf{w}_{o,m}^{\text{MUE}*}$ yield

$$\begin{aligned}
 \mathbf{w}_{o,m}^{\text{MUE}*} &= \left((1 + \lambda_1) \sum_{m=1}^M \mathbf{H}_{o,m}^{\text{MUE}} \mathbf{d}_{o,m}^{\text{MUE}'} \mathbf{v}_m^{\text{MUE}} (\mathbf{H}_{o,m}^{\text{MUE}})^H (\mathbf{d}_{o,m}^{\text{MUE}'})^H + (\tau + \lambda_2) \mathbf{I}_{N_s} \right)^{-1} \\
 &\quad \times (\mathbf{H}_{o,m}^{\text{MUE}})^H \mathbf{v}_m^{\text{MUE}} \mathbf{d}_{o,m}^{\text{MUE}}.
 \end{aligned} \tag{C.64}$$

The Lagrange multipliers λ_1 and λ_2 are updated as [9], [18]

$$\lambda_1^{(n+1)} = \left[\lambda_1^{(n)} - \sum_{m=1}^M \log_2(\mathbf{v}_m^{\text{MUE}}) - \text{Tr}(\mathbf{v}_m^{\text{MUE}} \mathbf{E}_m) + \text{Tr}(\mathbf{I}_{N_s}) - R_m^{\text{min}} \right]^+, \tag{C.65}$$

$$\lambda_2^{(n+1)} = \left[\lambda_2^{(n)} - \left(\sum_{m=1}^M \text{Tr} \left((\mathbf{w}_{o,m}^{\text{MUE}})^{(n+1)}, ((\mathbf{w}_{o,m}^{\text{MUE}})^{(n+1)})^H \right) - P_{m,\text{max}}^o \right) \right]^+. \tag{C.66}$$

The Lagrange multipliers are updated until $\mathcal{L}(\tau, \lambda_1, \lambda_2, \mathbf{w}_{o,m}^{\text{MUE}}) \approx g_o(\tau, \mathbf{v}_m^{\text{MUE}}, \mathbf{d}_{o,m}^{\text{MUE}}) \approx 0$.

3.3 EE Maximisation Algorithms

The convergence of the proposed schemes in section 3.2 depends on the Lagrange multipliers. Both the pre-coder and decoder matrices are fixed with initial values, then update at each iteration in order

4. EE MAXIMISATION AND TRANSCIEVER OPTIMISATION FOR CUES THROUGH RN AND MUES DURING THE SECOND TIME SLOT

to find their optimal values. The Lagrange multipliers are also updated at each iteration until the algorithm converges. Algorithm 6 describes the iterative EE maximisation of the FAP networks while Algorithm 7 gives the details of the EE maximisation of the MUEs at the first time slot.

Algorithm 6 Iterative EE maximisation of the FAP networks during the first time slot

- 1: Initialize and construct the channel matrix \mathbf{H}
 - 2: Initialize the FUE pre-coders with each element drawn i.i.d. from the standard Gaussian distribution $\mathcal{CN}(0, 1)$
 - 3: Initialize the weighted vector $\mathbf{v}_i^{\text{FAP}(0)}$ as Gaussian distribution
 - 4: Set $n = 0, \mu^{(0)} = 0$
 - 5: **for** $j = 1, \dots, F$ **do**
 - 6: **Repeat**
 - 7: Calculate $\mathbf{d}_{j,i}^{\text{FAP}(n+1)}$ by eq. (C.44) for given $\mathbf{v}_i^{\text{FAP}(n)}, \mathbf{w}_{j,i}^{\text{FAP}(n)}, \mu_1^{(n)}$ and $\mu_2^{(n)}$.
 - 8: Update $\mathbf{v}_i^{\text{FAP}(n+1)}$ by eq. (C.46) and $\mathbf{w}_{j,i}^{\text{FAP}(n+1)}$ by solving eq. (C.47) and (C.51) using the WMMSE method with $\mathbf{d}_{j,i}^{\text{FAP}(n+1)}, \mu_1^{(n)}$ and $\mu_2^{(n)}$.
 - 9: Update $\mu_1^{(n+1)}$ and $\mu_2^{(n+1)}$ by eq. (C.52) and (C.53) for the given $\mathbf{d}_{j,i}^{\text{FAP}(n+1)}$ and $\mathbf{w}_{j,i}^{\text{FAP}(n+1)}$
 - 10: set $n = n + 1$
 - 11: **Until** $g_j(\mu_1^{(n)}, \mu_2^{(n)}, \mathbf{w}_{j,i}^{\text{FAP}(n)}) \approx 0$
 - 12: **Return:** the optimal $\mathbf{w}_{j,i}^{\text{FAP}*}, \mathbf{d}_{j,i}^{\text{FAP}*}, \mu_1$ and μ_2
-

4 EE Maximisation and Transceiver Optimisation for CUEs through RN and MUEs during the second time slot

The fractional programming method and the parameter subtractive function is applied to determine the RN pre-coder. The weighted sum MSE approach is used to simplify the EE optimisation problem and to determine the RN pre-coder by solving a standard convex optimisation problem. With the obtained optimal RN pre-coder, the parameter subtractive function, Lagrange multipliers and WMMSE technique are employed to jointly obtained the optimal UEs pre-coders. Then the parameters in the parameter subtractive function are updated with the Dinkelbach's algorithm.

4. EE MAXIMISATION AND TRANSCIEVER OPTIMISATION FOR CUES THROUGH RN AND MUES DURING THE SECOND TIME SLOT

Algorithm 7 Iterative EE maximisation of the MUEs during the first time slot

- 1: Initialize and construct the channel matrix \mathbf{H}
 - 2: Initialize the MUE pre-coders with each element drawn i.i.d. from the standard Gaussian distribution $\mathcal{CN}(0, 1)$
 - 3: Initialize the weighted vector $\mathbf{v}_m^{\text{MUE}(0)}$ as Gaussian distribution
 - 4: Set $n = 0, \lambda^{(0)} = 0$
 - 5: **for** $m = 1, \dots, M$ **do**
 - 6: **Repeat**
 - 7: Calculate $\mathbf{d}_{o,m}^{\text{MUE}(n+1)}$ by eq. (C.57) for given $\mathbf{v}_m^{\text{MUE}(n)}, \mathbf{w}_{o,m}^{\text{MUE}(n)}, \lambda_1^{(n)}$ and $\lambda_2^{(n)}$.
 - 8: Update $\mathbf{v}_m^{\text{MUE}(n+1)}$ by eq. (C.55) and $\mathbf{w}_{o,m}^{\text{MUE}(n+1)}$ by solving eq. (C.60) and (C.64) using the WMMSE method with $\mathbf{d}_{o,m}^{\text{MUE}(n+1)}, \lambda_1^{(n)}$ and $\lambda_2^{(n)}$.
 - 9: Update $\lambda_1^{(n+1)}$ and $\lambda_2^{(n+1)}$ by eq. (C.65) and (C.66), respectively for the given $\mathbf{d}_{o,m}^{\text{MUE}(n+1)}$ and $\mathbf{w}_{o,m}^{\text{MUE}(n+1)}$
 - 10: set $n = n + 1$
 - 11: **Until** $g_j(\lambda_1^{(n)}, \lambda_2^{(n)}, \mathbf{w}_{o,m}^{\text{MUE}(n)}) \approx 0$
 - 12: **Return:** the optimal $\mathbf{w}_{o,m}^{\text{MUE}*}, \mathbf{d}_{o,m}^{\text{MUE}*}, \lambda_1$ and λ_2
-

4.1 EE problem formulation for UEs

The EE problem denoted $\varphi_{\text{UEs}}^{\text{EE}} = \frac{\mathcal{R}_{\text{UEs}}^{\text{sum}}}{P_{\text{MBS}}^{\text{sum}}}$ at the MBS during the second time slot is formulated as in (C.67).

$$\begin{aligned}
 & \log_2 \left(1 + \frac{\|\mathbf{H}_o \mathbf{F}_o \mathbf{H} \mathbf{W}\|^2}{\tilde{\sigma}_{\mathbf{z}_o}^2 \mathbf{I}_{N_B}} \right) \\
 \max_{\mathbf{W}} & \frac{\left(\text{Tr} \left(\mathbf{F}_o \left(\mathbf{H}_{R,K}^{\text{CUE}} \mathbf{W}_{R,K}^{\text{CUE}} (\mathbf{W}_{R,K}^{\text{CUE}})^H (\mathbf{H}_{R,K}^{\text{CUE}})^H + \sigma_R^2 \mathbf{I}_{N_R} \right) \mathbf{F}_o^H \right) + \text{Tr}(\mathbf{W}_{o,M}, (\mathbf{W}_{o,M})^H) + P_s \right)}{\left(\text{Tr} \left(\mathbf{F}_o \left(\mathbf{H}_{R,K}^{\text{CUE}} \mathbf{W}_{R,K}^{\text{CUE}} (\mathbf{W}_{R,K}^{\text{CUE}})^H (\mathbf{H}_{R,K}^{\text{CUE}})^H + \sigma_R^2 \mathbf{I}_{N_R} \right) \mathbf{F}_o^H \right) \right)} \\
 \text{s. t. } & \frac{1}{2} \log_2 \left(1 + \frac{\|\mathbf{H}_o \mathbf{F}_o \mathbf{H} \mathbf{W}\|^2}{\tilde{\sigma}_{\mathbf{z}_o}^2 \mathbf{I}_{N_B}} \right) \geq \gamma_o^{\min} \\
 & \text{Tr} \left(\mathbf{F}_o \left(\mathbf{H}_{R,K}^{\text{CUE}} \mathbf{W}_{R,K}^{\text{CUE}} (\mathbf{W}_{R,K}^{\text{CUE}})^H (\mathbf{H}_{R,K}^{\text{CUE}})^H + \sigma_R^2 \mathbf{I}_{N_R} \right) \mathbf{F}_o^H \right) \leq P_R^{\max} \\
 & \text{Tr}(\mathbf{W}_{o,M}, (\mathbf{W}_{o,M})^H) \leq P_o^{\max} \tag{C.67}
 \end{aligned}$$

As observed, the objective function in (C.67) is not convex due to the non-linear fractional optimisation as well as the QoS constraint. Thus, identifying a solution of this problem directly is quite complicated. To address this non-convexity problem, an iterative optimisation approach to design the transceiver is done in the next subsection.

4.2 Optimisation of RN pre-coder and Receiver decoder

We describe the method to optimally design pre-coders for the UEs (CUEs and MUEs) \mathbf{W} , the RN pre-coding matrix \mathbf{F}_o and the decoders \mathbf{D}_o at the MBS during the second time slot to maximise the EE optimisation problem $\varphi_{\text{UES}}^{\text{EE}}$ in MU-MIMO relay networks. This maximises the UEs data rate under the maximum transmit power $P_{k,max}^r$ and QoS constraints. The WMMSE and achievable sum-rate is considered for \mathbf{W} , \mathbf{F}_o and \mathbf{D}_o design. Hence, the received signal in (C.27) is multiplied by the decoder $(\mathbf{D}_o)^H$ and used to write the WMMSE optimisation problem by introducing some auxiliary variables.

To obtain the desired signal from the RN and UEs at the MBS, the estimated received signal $\hat{\mathbf{s}}_o$ is multiplied by the decoder matrix $(\mathbf{D}_o)^H$ becoming

$$\hat{\mathbf{s}}_o = (\mathbf{D}_o)^H \mathbf{y}_o^{nd}, \quad (\text{C.68})$$

where $\mathbf{D}_o \in \mathbb{C}^{N_B \times \hat{d}}$ is the decoder matrix used at the MBS to retrieve the transmitted CUE signal through the RN and the MUEs at the second time slot. After substitution of the \mathbf{y}_o^{nd} in (C.68), the estimated received signal $\hat{\mathbf{s}}_o$ is

$$\hat{\mathbf{s}}_o = (\mathbf{D}_o)^H \mathbf{H}_o \mathbf{F}_o \mathbf{H} \mathbf{W} \mathbf{s} + (\mathbf{D}_o)^H \mathbf{z}_o. \quad (\text{C.69})$$

The MSE covariance matrix \mathbf{E}_o is designed as

$$\begin{aligned} \mathbf{E}_o &= \mathbb{E} \left[(\hat{\mathbf{s}}_o - \mathbf{s})(\hat{\mathbf{s}}_o - \mathbf{s})^H \right] \\ &= \left[\left((\mathbf{D}_o)^H \mathbf{H}_o \mathbf{F}_o \mathbf{H} \mathbf{W} - \mathbf{I}_{N_B} \right) \left((\mathbf{D}_o)^H \mathbf{H}_o \mathbf{F}_o \mathbf{H} \mathbf{W} - \mathbf{I}_{N_B} \right)^H + (\mathbf{D}_o)^H \sigma_{\mathbf{z}_o}^2 \mathbf{D}_o \right]. \end{aligned} \quad (\text{C.70})$$

From (C.70), the weighted sum MSE problem can be formulated as [27]

$$\max_{\mathbf{V}_o, \mathbf{D}_o} \log_2 (\mathbf{V}_o) - \text{Tr}(\mathbf{V}_o \mathbf{E}_o) + \text{Tr}(\mathbf{I}_{N_B}), \quad (\text{C.71})$$

where \mathbf{V}_o is a weighting matrix. After substituting the MSE covariance matrix into (C.67), the EE optimisation problem $\varphi_{\text{UES}}^{\text{EE}}$ is given by (C.72).

$$\begin{aligned} &\max_{\mathbf{W}, \mathbf{F}_o, \mathbf{V}_o, \mathbf{D}_o} \frac{\log_2 (\mathbf{V}_o) - \text{Tr}(\mathbf{V}_o \mathbf{E}_o) + \text{Tr}(\mathbf{I}_{N_B})}{\left(\text{Tr} \left(\mathbf{F}_o \left(\mathbf{H}_{R,K}^{\text{CUE}} \mathbf{W}_{R,K}^{\text{CUE}} (\mathbf{W}_{R,K}^{\text{CUE}})^H (\mathbf{H}_{R,K}^{\text{CUE}})^H + \sigma_R^2 \mathbf{I}_{N_R} \right) \mathbf{F}_o^H \right) + \text{Tr}(\mathbf{W}_{o,M}, \mathbf{W}_{o,M}^H) + P_s \right)} \\ &\text{s. t. } \log_2 (\mathbf{V}_o) - \text{Tr}(\mathbf{V}_o \mathbf{E}_o) + \text{Tr}(\mathbf{I}_{N_B}) \geq R_B^{\text{min}} \\ &\quad \text{Tr} \left(\mathbf{F}_o \left(\mathbf{H}_{R,K}^{\text{CUE}} \mathbf{W}_{R,K}^{\text{CUE}} (\mathbf{W}_{R,K}^{\text{CUE}})^H (\mathbf{H}_{R,K}^{\text{CUE}})^H + \sigma_R^2 \mathbf{I}_{N_R} \right) \mathbf{F}_o^H \right) \leq P_R^{\text{max}} \\ &\quad \text{Tr}(\mathbf{W}_{o,M}, \mathbf{W}_{o,M}^H) \leq P_o^{\text{max}}. \end{aligned} \quad (\text{C.72})$$

4. EE MAXIMISATION AND TRANSCEIVER OPTIMISATION FOR CUES THROUGH RN AND MUES DURING THE SECOND TIME SLOT

This problem can be solved by fixing any three of the four variables $\mathbf{W}, \mathbf{F}_o, \mathbf{V}_o, \mathbf{D}_o$. These variables become convex with respect to each other. So an iterative algorithm can be employed to solve (C.72) by sequentially fixing three of the four variables and updating the fourth. The MMSE decoder \mathbf{D}_o is written as [27]

$$\mathbf{D}_o^* = \operatorname{argmin}_{\mathbf{D}_o} \operatorname{Tr}(\mathbf{E}_o), \quad (\text{C.73})$$

with $\frac{\partial \operatorname{Tr}(\mathbf{E}_o)}{\partial \mathbf{D}_o} = 0$, the optimal MMSE decoder is obtained as

$$\mathbf{D}_o^* = \mathbf{H}_o^H \mathbf{F}_o^H \mathbf{H}^H \mathbf{W}^H \left(\mathbf{H}_o \mathbf{F}_o \mathbf{H} \mathbf{W} \mathbf{H}_o^H \mathbf{F}_o^H \mathbf{H}^H \mathbf{W}^H + \sigma_{z_o}^2 \mathbf{I}_{N_B} \right)^{-1}. \quad (\text{C.74})$$

Hence, the MSE covariance matrix \mathbf{E}_o^* is given by

$$\mathbf{E}_o^* = \mathbf{I}_{N_B} - \mathbf{D}_o^* \mathbf{H}_o \mathbf{F}_o \mathbf{H} \mathbf{W}. \quad (\text{C.75})$$

Since the weighted matrix \mathbf{V}_o exists only in the numerator in problem (C.72), with the fixed \mathbf{W}, \mathbf{F}_o and \mathbf{D}_o , the optimal weighted matrix \mathbf{V}_o^* is obtained as

$$\mathbf{V}_o^* = (\mathbf{E}_o)^{-1}. \quad (\text{C.76})$$

For the fixed UEs pre-coder \mathbf{W} and relay pre-coder \mathbf{F}_o , the decoder at the MBS \mathbf{D}_o is updated as given in (C.74) and the weighted matrix \mathbf{V}_o is updated as given in (C.76). Therefore, to obtain the relay pre-coder \mathbf{F}_o , the EE optimisation $\varphi_{\text{UES}}^{\text{EE}}$ is reformulated as given in (C.77).

$$\begin{aligned} \max_{\mathbf{F}_o} \log_2(\mathbf{V}_o) - \operatorname{Tr}(\mathbf{V}_o \mathbf{E}_o) + \operatorname{Tr}(\mathbf{I}_{N_B}) - \omega \left(\operatorname{Tr} \left(\mathbf{F}_o \left(\mathbf{H}_{R,K}^{\text{CUE}} \mathbf{W}_{R,K}^{\text{CUE}} (\mathbf{W}_{R,K}^{\text{CUE}})^H (\mathbf{H}_{R,K}^{\text{CUE}})^H + \sigma_R^2 \mathbf{I}_{N_R} \right) \mathbf{F}_o^H \right) \right. \\ \left. + \operatorname{Tr}(\mathbf{W}_{o,M}, \mathbf{W}_{o,M}^H) + P_s \right) \end{aligned}$$

$$\text{s. t. } \log_2(\mathbf{V}_o) - \operatorname{Tr}(\mathbf{V}_o \mathbf{E}_o) + \operatorname{Tr}(\mathbf{I}_{N_B}) \geq R_B^{\min}$$

$$\operatorname{Tr} \left(\mathbf{F}_o \left(\mathbf{H}_{R,K}^{\text{CUE}} \mathbf{W}_{R,K}^{\text{CUE}} (\mathbf{W}_{R,K}^{\text{CUE}})^H (\mathbf{H}_{R,K}^{\text{CUE}})^H + \sigma_R^2 \mathbf{I}_{N_R} \right) \mathbf{F}_o^H \right) \leq P_R^{\max}. \quad (\text{C.77})$$

The Lagrangian function is written as given in (C.78).

$$\begin{aligned} \mathcal{L}(\mathbf{F}_o, \omega, \gamma_1, \gamma_2) = \log_2(\mathbf{V}_o) - \operatorname{Tr}(\mathbf{V}_o \mathbf{E}_o) + \operatorname{Tr}(\mathbf{I}_{N_B}) \\ - \omega \left(\operatorname{Tr} \left(\mathbf{F}_o \left(\mathbf{H}_{R,K}^{\text{CUE}} \mathbf{W}_{R,K}^{\text{CUE}} (\mathbf{W}_{R,K}^{\text{CUE}})^H (\mathbf{H}_{R,K}^{\text{CUE}})^H + \sigma_R^2 \mathbf{I}_{N_R} \right) \mathbf{F}_o^H \right) \right. \\ \left. + \operatorname{Tr}(\mathbf{W}_{o,M}, \mathbf{W}_{o,M}^H) + P_s \right) + \gamma_1 \left(\log_2(\mathbf{V}_o) - \operatorname{Tr}(\mathbf{V}_o \mathbf{E}_o) + \operatorname{Tr}(\mathbf{I}_{N_B}) - R_B^{\min} \right) \\ - \gamma_2 \left(\operatorname{Tr} \left(\mathbf{F}_o \left(\mathbf{H}_{R,K}^{\text{CUE}} \mathbf{W}_{R,K}^{\text{CUE}} (\mathbf{W}_{R,K}^{\text{CUE}})^H (\mathbf{H}_{R,K}^{\text{CUE}})^H + \sigma_R^2 \mathbf{I}_{N_R} \right) \mathbf{F}_o^H \right) - P_R^{\max} \right). \quad (\text{C.78}) \end{aligned}$$

The KKT conditions are employed to solve the problem in (C.77) and are given by [18]

$$\frac{\partial \mathcal{L}(\mathbf{F}_o, \omega, \gamma_1, \gamma_2)}{\partial \mathbf{F}_o} = 0, \quad (\text{C.79})$$

$$\log_2(\mathbf{V}_o) - \text{Tr}(\mathbf{V}_o \mathbf{E}_o) + \text{Tr}(\mathbf{I}_{N_B}) \geq R_B^{min}, \quad (\text{C.80})$$

$$\gamma_1 \left[\log_2(\mathbf{V}_o) - \text{Tr}(\mathbf{V}_o \mathbf{E}_o) + \text{Tr}(\mathbf{I}_{N_B}) - R_B^{min} \right], \quad (\text{C.81})$$

$$\left[\text{Tr} \left(\mathbf{F}_o \left(\mathbf{H}_{R,K}^{\text{CUE}} \mathbf{W}_{R,K}^{\text{CUE}} (\mathbf{W}_{R,K}^{\text{CUE}})^H (\mathbf{H}_{R,K}^{\text{CUE}})^H + \sigma_R^2 \mathbf{I}_{N_R} \right) \mathbf{F}_o^H \right) \leq P_R^{max} \right], \quad (\text{C.82})$$

$$\gamma_2 \left[\text{Tr} \left(\mathbf{F}_o \left(\mathbf{H}_{R,K}^{\text{CUE}} \mathbf{W}_{R,K}^{\text{CUE}} (\mathbf{W}_{R,K}^{\text{CUE}})^H (\mathbf{H}_{R,K}^{\text{CUE}})^H + \sigma_R^2 \mathbf{I}_{N_R} \right) \mathbf{F}_o^H \right) - P_R^{max} \right], \quad (\text{C.83})$$

$$\gamma_1, \gamma_2 \geq 0. \quad (\text{C.84})$$

After mathematical calculation, we can derive the relay pre-coder \mathbf{F}_o as

$$\mathbf{F}_o^* = \left((1 + \gamma_1) \mathbf{D}_o \mathbf{H}_o \mathbf{H} \mathbf{W} \mathbf{V}_o (\mathbf{D}_o)^H \mathbf{H}_o^H \mathbf{H}^H \mathbf{W}^H + (\omega + \gamma_2) \phi \right)^{-1} \mathbf{V}_o (\mathbf{D}_o)^H \mathbf{H}_o \mathbf{H}^H \mathbf{W}^H, \quad (\text{C.85})$$

where $\phi = (\mathbf{H}_{R,K}^{\text{CUE}} \mathbf{W}_{R,K}^{\text{CUE}} (\mathbf{W}_{R,K}^{\text{CUE}})^H (\mathbf{H}_{R,K}^{\text{CUE}})^H + \sigma_R^2 \mathbf{I}_{N_R})$, ω is updated using the Dinkelbach's algorithm [31], and γ_2 is determined from (C.83) and (C.84) by a bisection search with respect to the relay power constraint only. Assuming $\gamma_2 = 0$, we can test if the relay transmit power constraints in (C.82) is met, then $\gamma_2 = 0$. Otherwise, γ_2 can be solved by substituting (C.85) into the equation of $\left[\text{Tr} \left(\mathbf{F}_o(\gamma_2) \left(\mathbf{H}_{R,K}^{\text{CUE}} \mathbf{W}_{R,K}^{\text{CUE}} (\mathbf{W}_{R,K}^{\text{CUE}})^H (\mathbf{H}_{R,K}^{\text{CUE}})^H + \sigma_R^2 \mathbf{I}_{N_R} \right) \mathbf{F}_o^H(\gamma_2) \right) = P_R^{max} \right]$ [18]. The Lagrange multiplier γ_1 , on the other hand, is similarly updated as in (C.97). For the fixed decoder \mathbf{D}_o , weighted matrix \mathbf{V}_o and the relay pre-coder \mathbf{F}_o , the UEs pre-coder \mathbf{W} can be updated by solving the EE optimisation problem for the UEs where the MUEs and relay transmit power constraints during the second time slot must be included as well. Therefore, the EE optimisation problem $\varphi_{\text{UEs}}^{\text{EE}}$ is reformulated as given in (C.86).

$$\begin{aligned} f(\eta, \mathbf{W}, \mathbf{F}_o, \mathbf{D}_o) = \max_{\mathbf{W}} & \log_2(\mathbf{V}_o) - \text{Tr}(\mathbf{V}_o \mathbf{E}_o) + \text{Tr}(\mathbf{I}_{N_B}) \\ & - \tau \left(\text{Tr} \left(\mathbf{F}_o \left(\mathbf{H} \mathbf{W} \mathbf{W}^H \mathbf{H}^H + \sigma_{z_o}^2 \mathbf{I}_{N_B} \right) \mathbf{F}_o^H \right) + P_s \right) \\ \text{s. t. } & \log_2(\mathbf{V}_o) - \text{Tr}(\mathbf{V}_o \mathbf{E}_o) + \text{Tr}(\mathbf{I}_{N_B}) \geq R_B^{min} \\ & \text{Tr} \left(\mathbf{F}_o \left(\mathbf{H} \mathbf{W} \mathbf{W}^H \mathbf{H}^H + \sigma_{z_o}^2 \mathbf{I}_{N_B} \right) \mathbf{F}_o^H \right) \leq P_R^{max}. \end{aligned} \quad (\text{C.86})$$

The Lagrangian function is written as given in (C.87).

$$\begin{aligned} \mathcal{L}(\mathbf{W}, \alpha, \delta_1, \delta_2) = & \log_2(\mathbf{V}_o) - \text{Tr}(\mathbf{V}_o \mathbf{E}_o) + \text{Tr}(\mathbf{I}_{N_B}) \\ & - \alpha \left(\text{Tr} \left(\mathbf{F}_o \left(\mathbf{H} \mathbf{W} \mathbf{W}^H \mathbf{H}^H + \sigma_{\mathbf{z}_o}^2 \mathbf{I}_{N_B} \right) \mathbf{F}_o^H \right) + P_s \right) \\ & - \delta_1 \left(\log_2(\mathbf{V}_o) - \text{Tr}(\mathbf{V}_o \mathbf{E}_o) + \text{Tr}(\mathbf{I}_{N_B}) - R_B^{\min} \right) \\ & - \delta_2 \left(\text{Tr} \left(\mathbf{F}_o \left(\mathbf{H} \mathbf{W} \mathbf{W}^H \mathbf{H}^H + \sigma_{\mathbf{z}_o}^2 \mathbf{I}_{N_B} \right) \mathbf{F}_o^H \right) - P_R^{\max} \right). \end{aligned} \quad (\text{C.87})$$

From (C.87), the Lagrange dual function can be defined as

$$f(\delta_1, \delta_2) = \max_{\mathbf{W}} \mathcal{L}(\mathbf{W}, \alpha, \delta_1, \delta_2). \quad (\text{C.88})$$

Moreover, the dual problem is described as

$$\min_{\delta_1, \delta_2 \geq 0} f(\delta_1, \delta_2). \quad (\text{C.89})$$

For any δ_1 and δ_2 , we can obtain the dual function by solving the maximisation problem in (C.88).

The maximisation problem can be solved by setting the gradient of the Lagrange dual function to zero as $\frac{\partial \mathcal{L}(\mathbf{W}, \alpha, \delta_1, \delta_2)}{\partial \mathbf{W}^*} = 0$. The KKT conditions are employed to solve the problem in (C.86) and are given by

$$\frac{\partial \mathcal{L}(\mathbf{W}, \alpha, \delta_1, \delta_2)}{\partial \mathbf{W}} = 0, \quad (\text{C.90})$$

$$\log_2(\mathbf{V}_o) - \text{Tr}(\mathbf{V}_o \mathbf{E}_o) + \text{Tr}(\mathbf{I}_{N_B}) \geq R_B^{\min}, \quad (\text{C.91})$$

$$\delta_1 \left(\log_2(\mathbf{V}_o) - \text{Tr}(\mathbf{V}_o \mathbf{E}_o) + \text{Tr}(\mathbf{I}_{N_B}) - R_B^{\min} \right), \quad (\text{C.92})$$

$$\text{Tr} \left(\mathbf{F}_o \left(\mathbf{H} \mathbf{W} \mathbf{W}^H \mathbf{H}^H + \sigma_{\mathbf{z}_o}^2 \mathbf{I}_{N_B} \right) \mathbf{F}_o^H \right) \leq P_R^{\max}, \quad (\text{C.93})$$

$$\delta_2 \left[\text{Tr} \left(\mathbf{F}_o \left(\mathbf{H} \mathbf{W} \mathbf{W}^H \mathbf{H}^H + \sigma_{\mathbf{z}_o}^2 \mathbf{I}_{N_B} \right) \mathbf{F}_o^H \right) - P_R^{\max} \right], \quad (\text{C.94})$$

$$\delta_1, \delta_2 \geq 0. \quad (\text{C.95})$$

After mathematical calculation, we can derive the UEs pre-coder \mathbf{W} as

$$\begin{aligned} \mathbf{W}^* = & \left((1 + \delta_1) \mathbf{D}_o \mathbf{H}_o \mathbf{H} \mathbf{F}_o \mathbf{V}_o (\mathbf{D}_o)^H \mathbf{H}_o^H \mathbf{H}^H \mathbf{F}_o^H + (\alpha + \delta_2) (\mathbf{H} \mathbf{F}_o \mathbf{F}_o^H \mathbf{H}^H) \right)^{-1} \\ & \times \mathbf{V}_o (\mathbf{D}_o) \mathbf{H}_o \mathbf{H}^H \mathbf{F}_o^H, \end{aligned} \quad (\text{C.96})$$

where the update of the Lagrange multiplier is given by

$$\delta_1^{(n+1)} = \left[\delta_1^{(n)} - \log_2(\mathbf{V}_o) - \text{Tr}(\mathbf{V}_o \mathbf{E}_o) + \text{Tr}(\mathbf{I}_{N_B}) \right]^+, \quad (\text{C.97})$$

$$\delta_2^{(n+1)} = \left[\delta_2^{(n)} - \left(\text{Tr} \left(\mathbf{F}_o \left(\mathbf{H} \mathbf{W}^{(n+1)} (\mathbf{W}^{(n+1)})^H \mathbf{H}^H + \sigma_{\mathbf{z}_o}^2 \mathbf{I}_{N_B} \right) \mathbf{F}_o^H \right) - P_R^{\max} \right) \right]^+. \quad (\text{C.98})$$

4.3 EE Maximisation Algorithm for the UEs

Algorithm 8 describes the iterative EE maximisation of the the UEs at the second time slot

Algorithm 8 Iterative EE maximisation of the UEs (CUEs through RN and MUEs during the second time slot)

- 1: Initialize and construct the channel matrices \mathbf{H} and \mathbf{H}_o according to (C.23) and (C.25), respectively.
 - 2: Initialize the UEs pre-coders $\mathbf{W}^{(0)}$ with each element drawn i.i.d. from the standard Gaussian distribution $\mathcal{CN}(0, 1)$, based to the dimension in (C.24).
 - 3: Initialize the weighted matrix $\mathbf{V}^{(0)}$ as Gaussian distribution $\mathcal{CN}(0, 1)$
 - 4: Set $n = 0, \delta_1^{(0)}, \delta_2^{(0)} = 0$
 - 5: **Repeat**
 - 6: Calculate $\mathbf{D}_o^{(n+1)}$ by (C.74) for given $\mathbf{V}_o^{(n)}, \mathbf{F}_o^{(n)}, \mathbf{W}^{(n)}$
 - 7: Update $\mathbf{V}_o^{(n+1)}$ by (C.76) for given $\mathbf{D}_o^{(n+1)}, \mathbf{F}_o^{(n)}, \mathbf{W}^{(n)}$ by solving (C.47) using the WMMSE method
 - 8: Solve (C.77) for given $\mathbf{D}_o^{(n+1)}, \mathbf{V}_o^{(n+1)}, \mathbf{W}^{(n)}, \delta_1^{(n)}, \delta_2^{(n)}$ and update $\mathbf{F}_o^{(n+1)}$ by (C.85).
 - 9: Calculate $\mathbf{W}^{(n+1)}$ by (C.96) after solving (C.86)
 - 10: Update $\delta_1^{(n+1)}$ and $\delta_2^{(n+1)}$ by (C.97) and (C.98) respectively after solving (C.87) for the given $\mathbf{W}^{(n+1)}$ and $\mathbf{F}_o^{(n+1)}$
 - 11: set $n = n + 1$
 - 12: **Until** $f(\eta, \mathbf{W}, \mathbf{F}_o, \mathbf{D}_o) \approx 0$
 - 13: **Return:** the optimal $\mathbf{W}_*, \mathbf{F}_o^*, \mathbf{D}_o^*$
-

5 Performance Evaluation

In this section, we present the performance of the proposed algorithms to maximise the EE in MU-MIMO relay systems. The simulation results are provided to validate and demonstrate the effectiveness of proposed schemes. The following simulation parameters are considered: $F = 5$ FAPs each having $U = 2$ FUEs, $M = 10$ MUEs, $R = 3$ clusters, each having $K = 5$ CUEs with $N_s = 2, N_R = \{2, 4\}, N_B = 10, d_s = 2$. All users are uniformly distributed into the macrocell coverage area. The channel coefficients for the FAPs, MUEs and CUEs are i.i.d complex Gaussian variables with zero mean and unit variance (they are generated as $\mathcal{CN}(0, 1)$ i.e. Rayleigh fading). It is assumed that the circuit power consumption $P_c = 7$ (dB) [32]. We assume the message $s_{j,i}^{\text{FAP}}, s_{o,m}^{\text{MUE}}$ and $s_{r,k}^{\text{CUE}} = \pm 1$ each with equal probability. The perfect CSI of the uplink MU-MIMO relay channel is considered where the average EE achieved by the proposed schemes for the FAPs and the MUEs during the first time slot and the UEs (CUEs through RN and MUEs) during the second time slot are compared with that achieved by another scheme. It is worth mentioning that the CUEs distance d_k to the RN and the RN distance d_r to the MBS are generated as specified in [33] such that the RN helps the CUEs to experience a better QoS. The "proposed scheme" for UEs is compared with the algorithm described in [34] and hereby referred to as "EE based DAM".

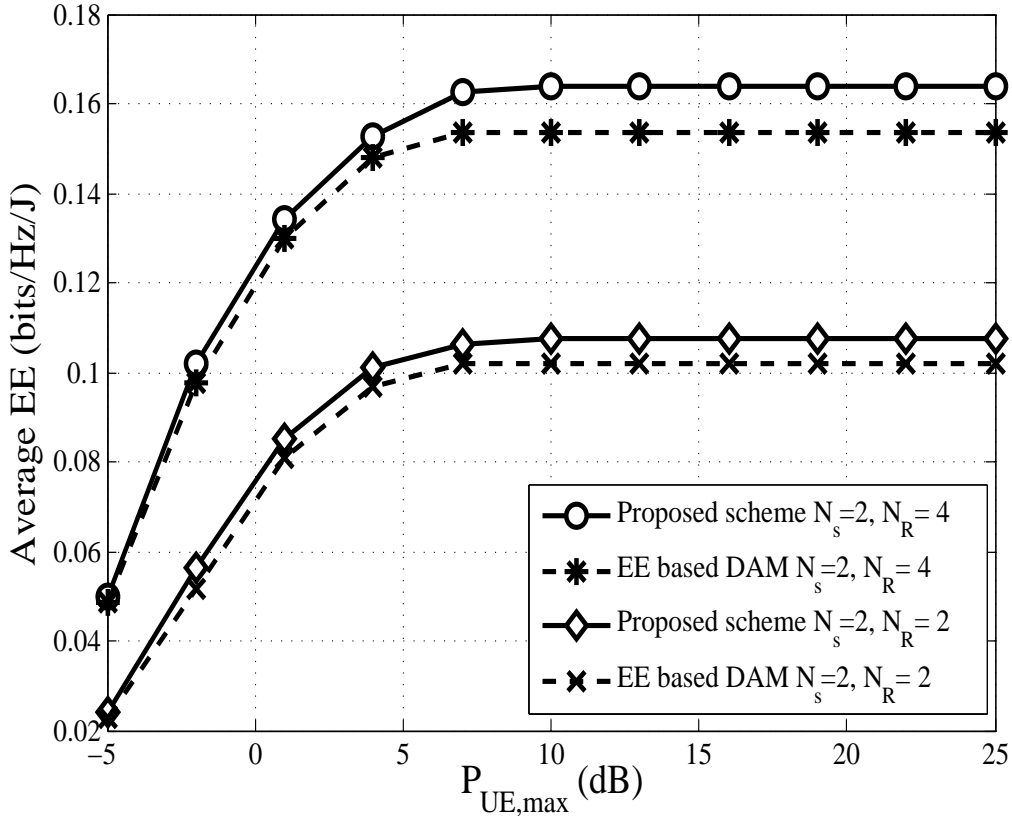


Figure C.2: Average EE versus the maximum UEs transmit powers for $N_s = 2, N_R = 2, 4$.

Fig. C.2 illustrates the average EE performance as function of the $P_{\text{UEs,max}}(\text{dB})$ of the "proposed scheme" for the UEs and the "EE based DAM" when $N_R = \{2, 4\}$ with $N_s = 2$. It can be observed that the achievable average EE for the UEs increases as the N_R increases for both algorithms. However, the "proposed scheme" for the UEs achieves a higher EE performance when compared to the "EE based DAM", specifically when the N_R increases. This is due to the fact that the "proposed scheme" explores the multiplexing gain at each node while the "EE based DAM" is only based on the scalarized SINR formulation.

Fig. C.3 shows the average EE performance of the UEs for different values of $\sigma_{\Delta_e}^2$, varying between 0.01 and 0.11. The simulation considered $N_R = 2$ and $N_s = 2$ for $P_{\text{UEs}}^{\text{max}} = 15(\text{dB})$. It is observed that the average EE performance for maximum UEs transmit power keep increasing when $\sigma_{\Delta_e}^2$ increases until $\sigma_{\Delta_e}^2 = 0.05$. This shows that adding an estimation error to the ZF assumption considered in section 2, improves the average EE performance for the UEs to a maximum value of $\sigma_{\Delta_e}^2$, where the optimum EE performance for the UEs is achieved, after which, it deteriorates.

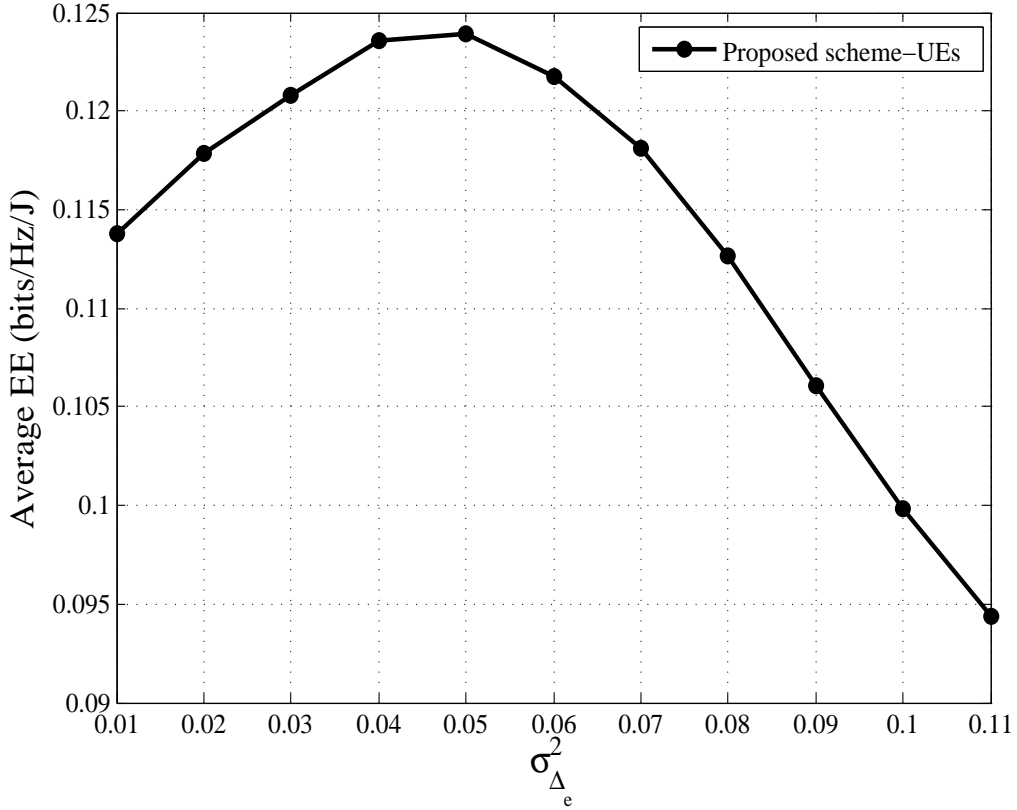


Figure C.3: Average EE versus the different value of $\sigma_{\Delta_e}^2$ for the UEs with $N_s = 2, N_R = 2$.

The numerical result of the average EE versus the maximum relay transmit power P_R^{\max} (dB) is illustrated in Fig. C.4. Similarly to Fig. C.2, the "proposed scheme" outperforms the "EE based DAM". It is worth mentioning that in the algorithms, the intended signal and the noise are amplified at the RN and forwarded to the MBS. It can be seen that both algorithms saturate at a certain value due to the A-F technique used at the RN.

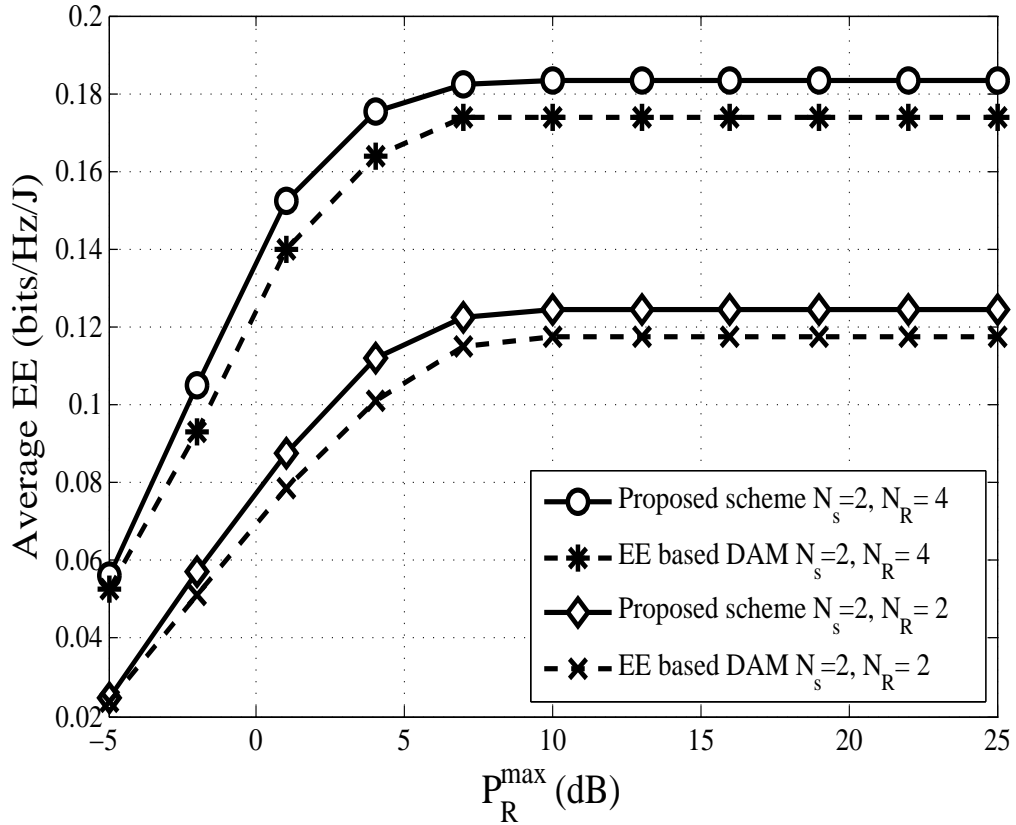


Figure C.4: Average EE versus the maximum RN transmit power for $N_s = 2, N_R = 2, 4$.

The average EE performance versus the number of iteration for the "*proposed scheme-UEs*" and the "*EE based DAM*" in Fig. C.5. As observed, both schemes have good convergence rate regardless the number of antennas. However, the higher EE performance is achieved by the "*proposed scheme-UE*" for different set of value of N_s and N_R . Moreover, increasing N_R , also improves the achievable EE performance which is attributed to the increasing multi-antenna multiplexing gain.

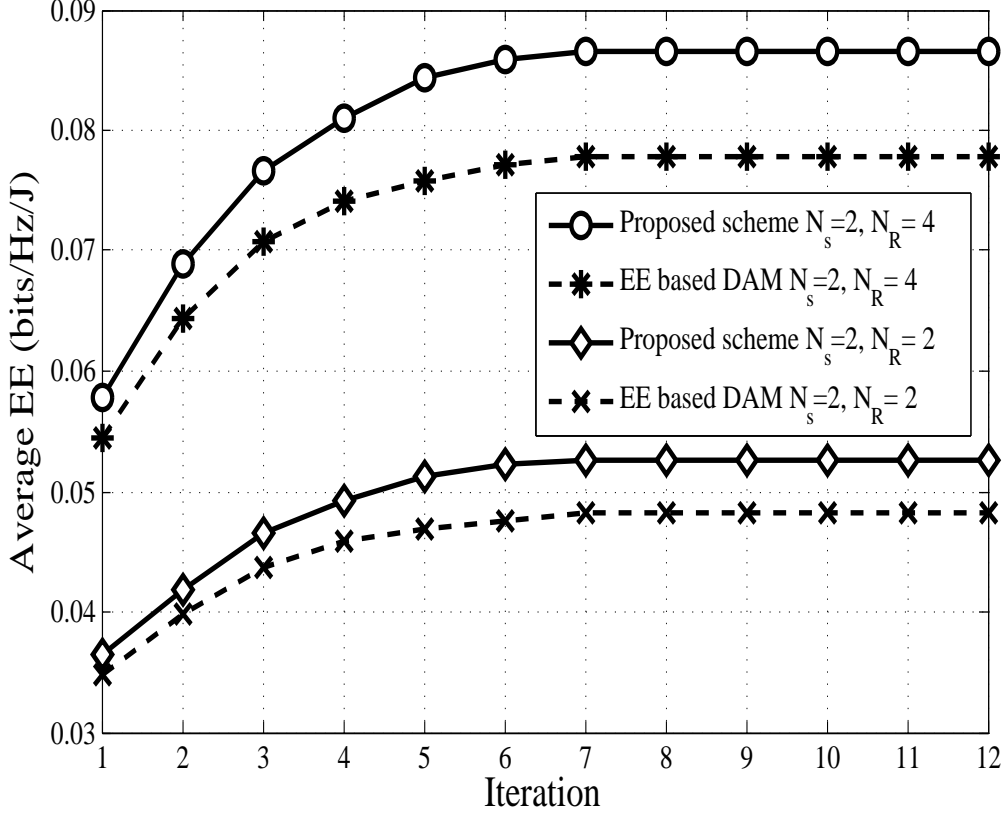


Figure C.5: Average EE versus the number of iteration for $N_s = 2, N_R = 2, 4$.

Fig. C.6 demonstrates the average EE performance of the MUEs and FAPs as a function of different values of $\sigma_{\Delta_e}^2$ during the first time slot. It is observed that the maximum average EE for the both, MUEs and FAPs is achieved at $\sigma_{\Delta_e}^2 = 0.06$ with the transmit power 15dB. This confirms the high performance of the proposed schemes in terms of the average maximum EE versus the transmit power for MUEs and FAPs when $\sigma_{\Delta_e}^2 = 0.06$. Besides, it can be seen that the "*proposed scheme for MUE*" performs higher than the "*proposed scheme for FAP*" in terms of average EE at all values of $\sigma_{\Delta_e}^2$. This is due to the multi-antenna diversity exploited by the MUEs. Due to the space consideration, we omitted the performance of the EE maximisation versus the maximum transmit powers for the MUEs and FAPs during the first time slot.

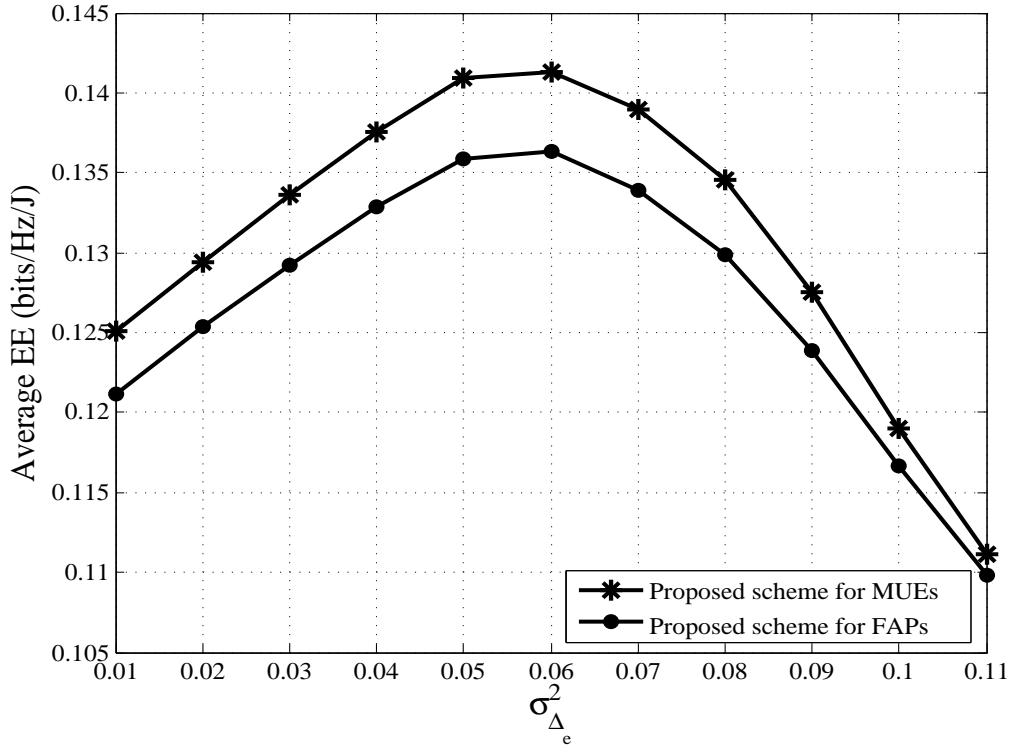


Figure C.6: Average EE versus the different value of $\sigma_{\Delta_e}^2$ for the MUEs and FAPs.

6 Conclusion

In this article, we proposed EE maximisation algorithm in the MU-MIMO relay networks. The decentralised approach was considered for the FAPs, MUEs and UEs transceiver designs while the ZF solution with estimation values helped to design the unknown interfering terms. The non-convexity of the formulated EE maximisation problems were addressed by designing iterative algorithms and the corresponding parametric subtractive function to optimise the different transceivers. Moreover, the FAPs, MUE and UEs transceivers were designed based on the WMMSE and Lagrange duality approach in order to achieve optimality and better performance. The performance evaluation demonstrated the higher achievable maximum EE performance when compared to other scheme. The EE maximisation performance of the proposed schemes was shown to increase by use of estimation value. Future lines of research could consider an EE optimisation in a massive MU-MIMO relay system with a robust transceiver design.

References

- [1] “IMT vision framework and overall objectives of the future development of IMT for 2020 and beyond,” *International Telecommunication Union, Geneva, Switzerland, ITU-R Recommendations M.2083-0*, Sep. 2015.
- [2] G. Y. Li, Z. Xu, C. Xiong, C. Yang, S. Zhang, Y. Chen, and S. Xu, “Energy-efficient wireless communications: tutorial, survey, and open issues,” *IEEE Wireless Commun.*, vol. 18, no. 6, 2011.
- [3] G. Miao, “Energy-efficient uplink multi-user MIMO,” *IEEE Trans. Wireless Commun.*, vol. 12, no. 5, pp. 2302–2313, 2013.
- [4] Z. Hasan, H. Boostanimehr, and V. K. Bhargava, “Green cellular networks: A survey, some research issues and challenges,” *IEEE Commun. Surveys Tuts*, vol. 13, no. 4, pp. 524–540, 2011.
- [5] T. Luan, F. Gao, X.-D. Zhang, J. C. F. Li, and M. Lei, “Robust beam-forming for relay-aided multiuser MIMO cognitive radio networks,” *Proc. IEEE Wireless Commun. Netw. Conf. (WCNC)*, pp. 2473–2477, 2013.
- [6] N. Yang, M. ElKashlan, and J. Yuan, “Impact of opportunistic scheduling on cooperative dual-hop relay networks,” *IEEE Trans. Commun.*, vol. 59, no. 3, pp. 689–694, 2011.
- [7] M. ElKashlan, P. Yeoh, N. Yang, T. Duong, and C. Leung, “A comparison of two MIMO relaying protocols in nakagami- m fading,” *IEEE Trans. Veh. Technol.*, vol. 61, no. 3, pp. 1416–1422, 2012.
- [8] H. Q. Ngo, E. G. Larsson, and T. L. Marzetta, “Energy and spectral efficiency of very large multiuser MIMO systems,” *IEEE Trans. Commun.*, vol. 61, no. 4, pp. 1436–1449, 2013.
- [9] T. T. Vu, H. H. Kha, and H. D. Tuan, “Transceiver design for optimizing the energy efficiency in multiuser MIMO channels,” *IEEE Commun. Lett.*, vol. 20, no. 8, pp. 1507–1510, 2016.
- [10] L. Sanguinetti, E. Björnson, M. Debbah, and A. L. Moustakas, “Optimal linear precoding in multi-user MIMO systems: A large system analysis,” in *Proc. IEEE GLOBECOM*, 2014, pp. 3922–3927.
- [11] C. Masouros, M. Sellathurai, and T. Ratnarajah, “Maximizing energy efficiency in the vector precoded MU-MISO downlink by selective perturbation,” *IEEE Trans. Wireless Commun.*, vol. 13, no. 9, pp. 4974–4984, 2014.

- [12] C. Manikandan, P. Neelamegam, A. Srivishnu, and K. G. Raj, "A survey of MIMO transceiver designs in wireless communication systems," *Int. J. of Applied Engineering Research*, vol. 10, no. 5, pp. 12 073–12 078, 2015.
- [13] D. P. Palomar and Y. C. Eldar, *Convex optimization in signal processing and communications*. Cambridge university press, 2010.
- [14] S. Boyd and L. Vandenberghe, *Convex optimization*. Cambridge university press, 2004.
- [15] X. Zhou, B. Bai, and W. Chen, "A low complexity energy efficiency maximization method for multiuser amplify-and-forward MIMO relay systems with a holistic power model," *IEEE Commun. Lett.*, vol. 18, no. 8, pp. 1371–1374, 2014.
- [16] L. Sanguinetti, R. Couillet, and M. Debbah, "Base station cooperation for power minimization in the downlink: Large system analysis," in *Proc. IEEE GLOBECOM*, 2015, pp. 1–6.
- [17] L. Sanguinetti, A. L. Moustakas, E. Björnson, and M. Debbah, "Large system analysis of the energy consumption distribution in multi-user MIMO systems with mobility," *IEEE Trans. Wireless Commun.*, vol. 14, no. 3, pp. 1730–1745, 2015.
- [18] Q. Sun and L. Li, "Weighted sum rate maximization for downlink multiuser relay network with direct link," *Springer Wireless Pers. Commun.*, vol. 75, no. 1, pp. 369–384, 2014.
- [19] S. Gong, C. Xing, N. Yang, Y.-C. Wu, and Z. Fei, "Energy efficient transmission in multi-user MIMO relay channels with perfect and imperfect channel state information," *IEEE Trans. Wireless Commun.*, vol. 16, no. 6, pp. 3885–3898, 2017.
- [20] F. Heliot and R. Tafazolli, "Optimal energy-efficient source and relay precoder design for cooperative MIMO-AF systems," *IEEE Trans. Signal Process.*, vol. 66, no. 3, pp. 573–588, 2018.
- [21] K. M. S. Huq, S. Mumtaz, J. Rodriguez, and R. L. Aguiar, "Energy efficiency optimization in MU-MIMO system with spectral efficiency constraint," in *Proc. IEEE Symposium Computers Commun. (ISCC)*, 2014, pp. 1–5.
- [22] Y. Dong, Y. Huang, and L. Qiu, "Energy-efficient sparse beamforming for multiuser MIMO systems with nonideal power amplifiers," *IEEE Trans. Veh. Technol.*, vol. 66, no. 1, pp. 134–145, 2017.

- [23] L. Sboui, H. Ghazzai, Z. Rezki, and M.-S. Alouini, "Precoder design and power allocation for MIMO cognitive radio two-way relaying systems," *IEEE Trans. Commun.*, vol. 64, no. 10, pp. 4111–4120, 2016.
- [24] Z. Wang, L. Li, X. Li, H. Wang, and H. Tian, "Precoding designs in non-regenerative mimo two-way relay systems for maximizing weighted sum energy efficiencies," in *Proc. 84th IEEE Veh. Technol. Conf. (VTC-Fall)*, 2016, pp. 1–5.
- [25] M. Bengtsson and B. Ottersten, "Optimal and suboptimal transmit beamforming," in *Handbook of Antennas in Wireless Commun.*, L. C. Godara, Ed. CRC Press, 2001.
- [26] D. W. K. Ng, E. S. Lo, and R. Schober, "Energy-efficient resource allocation in OFDMA systems with large numbers of base station antennas," *IEEE Trans. Wireless Commun.*, vol. 11, no. 9, pp. 3292–3304, 2012.
- [27] Q. Shi, M. Razaviyayn, Z.-Q. Luo, and C. He, "An iteratively weighted MMSE approach to distributed sum-utility maximization for a MIMO interfering broadcast channel," *IEEE Trans. Signal Process.*, vol. 59, no. 9, pp. 4331–4340, 2011.
- [28] S.-R. Lee, J. Jung, H. Park, and I. Lee, "A new energy-efficient beamforming strategy for MISO interfering broadcast channels based on large systems analysis," *IEEE Trans. Wireless Commun.*, vol. 15, no. 4, pp. 2872–2882, 2016.
- [29] W. Dinkelbach, "On nonlinear fractional programming," *INFORMS Management science*, vol. 13, no. 7, pp. 492–498, 1967.
- [30] Q. Wu, M. Tao, D. W. K. Ng, W. Chen, and R. Schober, "Energy-efficient resource allocation for wireless powered communication networks," *IEEE Trans. Wireless Commun.*, vol. 15, no. 3, pp. 2312–2327, 2016.
- [31] S. Schaible, "Fractional programming. II, on dinkelbach's algorithm," *INFORMS Management science*, vol. 22, no. 8, pp. 868–873, 1976.
- [32] X. Chen and L. Lei, "Energy-efficient optimization for physical layer security in multi-antenna downlink networks with QoS guarantee," *IEEE Commun. Lett.*, vol. 17, no. 4, pp. 637–640, 2013.
- [33] A. Zappone, P. Cao, and E. A. Jorswieck, "Energy efficiency optimization in multiuser relay-assisted MIMO systems," in *Proc. IEEE Asilomar Conf. Signals, Systems and Computers*, 2013, pp. 778–782.

REFERENCES

- [34] J. Zhang and M. Haardt, "Energy efficient two-way non-regenerative relaying for relays with multiple antennas," *IEEE Signal Process. Lett.*, vol. 22, no. 8, pp. 1079–1083, 2015.

Part III

Thesis Conclusion

Conclusion and Future Works

This thesis addressed three different challenges in the LTE-Advanced femtocell networks namely, the efficient coverage extension, interference management and EE optimisation. The details of the cellular network evolution and background informations on the LTE-Advanced network are widely investigated in the introduction part of this thesis. Despite the significant benefits of deploying LTE-Advanced femtocells and RNs into a macrocell coverage to increase the network capacity or to extend the coverage in a cost-effective way, interference and EE were identified as the largest challenges in such networks resulting from the transmit power disparity in cells of different classes. These challenges are among the major obstacles to future capacity improvement and coverage enhancements. Thus, the investigation for efficient management solutions to achieve promising performance gains being paramount to this research. The different mitigation approaches and research methodology are studied towards designing appropriate algorithms to assure an efficient and optimal coverage extension, interference management and EE optimisation in a case of imperfect and perfect CSI. The next sections summarise the research contribution of this thesis and give direction for the future works.

1 Summary of the Research Contributions

In the first article, paper A, the energy efficient RN placement in the LTE-Advanced femtocell system was investigated to maximise the coverage extension subject to the energy cost constraint. The EEORNP algorithm based on the greedy algorithm was designed using the sub-modularity and monotonicity optimisation satisfying the Matroid rank function constraint for an effective and optimal RNs deployment. The presented simulation results proved the out-performance of the proposed algorithm over the other schemes.

In the second article, paper B, the performance of CUEs was investigated by considering half-duplex communication of the CUEs to the MBS through RNs and the interference management in the resulting MU-MIMO relay systems. Due to the distributed architecture of MU-MIMO relay systems, we designed decentralised transceivers for each sub-optimal minimum sum MSE problems to manage

the interferences. The ZF solutions were assumed in the design of the unknown interference terms. Moreover, channel estimation errors and MMSE approach were employed to design the transceivers for MUEs, CUEs, RNs and femtocells to achieve better performance in a more realistic scenario. The results have shown the performance of the proposed decentralised schemes based channel estimation when estimation values are added to the ZF assumption, in terms of BER evaluation.

In the last article, paper C, the EE optimisation was investigated in MU-MIMO relay systems. We proposed decentralised pre-coder and decoder schemes using WMMSE approach and Lagrange duality to achieve optimality. The unknown interference terms were designed with the ZF assumption and the estimation values were added to the ZF solutions in order to improve the performance of the proposed decentralised schemes. The simulation results were presented to show the performance of the proposed decentralised algorithms with the ZF solutions. The average EE as a function of different estimation values was also presented. These results shown that adding estimation values to the ZF solutions improves the average EE evaluation until the maximum estimation value is achieved and decreases after then. In the main, the research objectives listed in this thesis were successfully achieved.

2 Future Works

This section provides some insight into possible future lines of research that could extend to this and other contributions on the topic of EE and interference management in future cooperative mobile networks. While the models presented within this thesis are not extensively complex, further refinement and upgrades are still expected to provide the same overall results, conclusions, and recommendations. Following the lines of this thesis, a minor upgrade could be that of considering a wider network with multiple antennas such as massive MIMO, providing a richer comparison between the potential energy saving and applicability of different features. In the light of the conclusion, future research items, with respect to the articles of the thesis on the LTE-Advanced femtocell network aforementioned include:

- On the interference management issue, the proposed decentralised algorithms could consider the interference alignment approach to align the interference terms instead of the ZF assumption in order to get better network performance in a massive MIMO network. In addition, when considering pilot-channel estimation, the pilot contamination transceiver will need to be designed in order to manage the pilot contamination challenges.
- On the EE optimisation challenge, the decentralised transceivers are based on the assumption of the perfect CSI. Future work could considered the effect of imperfect CSI in the

2. FUTURE WORKS

decentralised transceivers designs in massive MIMO network. The imperfect CSI in the EE optimisation problem is a practical consideration that degrades the performance of the network and thus should be examined. Moreover, channel estimation errors could also be considered in the channel model.